STRATHCLYDE INSTITUTE OF PHARMACY & BIOMEDICAL SCIENCES

University of Strathclyde Science

A Study of the Metabolic Immune Responses produced by some Natural Products

By

Abdulmalik M. H. Alqarni

A Thesis Submitted in Fulfillment of the Requirements for the Award of Degree of Doctor of Philosophy in Strathclyde Institute of Pharmacy and Biomedical Sciences at the University of Strathclyde

2020

Declaration

'I declare that, except where specifically indicated, all the work presented in this report is my own and I am the sole author of all parts.'

Signed: _____

Date: _____

Acknowledgements

First and foremost, I thank God Almighty for giving me the strength, knowledge, ability and opportunity to undertake this research study and to persevere and complete it satisfactorily.

I also extend a very big thank you to my supervisor Professor David Watson for all the support and encouragement he gave me, during the long months I spent with him. Without his guidance and constant feedback, this PhD would not have been achievable.

I also to offer my heartfelt appreciation to my supervisor Dr Valerie Ferro, who regularly reviewed my research. I would like also to express my gratitude to my academic assessor, Dr Christine Dufes, who regularly reviewed my research progress through mini-vivas.

I also express my gratitude to the entire research team in Dave's lab, consisting of Adel, Mohammed, Abdulwahab, Mansour, Ahmed and Abdullah. It was such a rewarding experience working with such a wonderful group of people.

I extend a heartfelt thank you to my wife Rahaf, my daughter Rose and my son Mohammed for their love and for always believing in me and encouraging me to follow my dreams. I also express my gratitude to my father, my mother and my brothers and sisters for their love, support and understanding during my study.

I also thank the Saudi government, represented in Imam Abdulrahman bin Faisal University, for sponsoring my PhD study.

Table of contents:

List of tables

List of figures

3PG	3-Phospho-D-glycerate
4-GB	4-Guanidinobutanoate
5'TOP	5'-terminal oligopyrimidine
5-Hydroxy-L-tryp.	5-Hydroxy-L-tryptophan
ADP	Adenosine Diphosphate
AMP	Adenosine monophosphate
AMPK	Adenosine monophosphate-activated protein kinase
ATP	Adenosine Triphosphate
BV	Bee venom
CV-ANOVA	Cross validated ANOVA
TCA	Cycle Tricarboxylic Acid cycle
CDP	Cytidine diphosphate
CTP	Cytidine Triphosphate
Glu-1,6-L-6-P	D-Glucono-1,5-lactone 6-phosphate
G6S	D-Glucose 6-sulfate
EI	Electron impact
ESI	Electrospray ionisation
ELISAs	Enzyme-linked immunosorbent assay
FAO	Fatty acids oxidation
FAS	Fatty acids synthesis
F-2,6-BP	Fructose-2,6-bisphosphate
F6P	Fructose-6-phosphate
G6P	Glucose-6-phosphate
G3P	glyceraldehyde-3-phosphate
GLP	Glycerone phosphate
Gyp	Gypenoside
HPLC	High Performance Liquid Chromatography
HILIC	Hydrophilic Interaction Liquid Chromatography
HIF-1α	Hypoxia inducible factor-1α
IMP	Inosine monophosphate
KEGG	Kyoto Encyclopedia of Genes and Genomes
LPS	Lipopolysaccharide
LC-MS	Liquid chromatography-mass spectrometry
mTOR	Mammalian target of rapamycin
m/z	Mass to charge ratio
MCD	Mast cell degranulating
Mel	Melittin

Arg. Succ.	N-(L-Arginino)succinate
NAD+	Nicotinamide Adenine Dinucleotide (oxidised)
NADH	Nicotinamide Adenine Dinucleotide (reduced)
NADP+	Nicotinamide Adenine Dinucleotide phosphate (oxidised)
NADPH	Nicotinamide Adenine Dinucleotide phosphate (reduced)
NO	Nitric oxide
iNOS	Nitric oxide synthase
NP	Normal phase
NF-κB	Nuclear factor kappa B
NMR	Nuclear Magnetic Resonance
OPLS-DA	Orthogonal Partial Least Squares Discriminant Analysis
OXPHOS	Oxidative phosphorylation
PAMPs	Pathogen-associated molecular patterns
PRRs	Pattern Recognition Receptors
PMA	Phorbol 12-myristate 13-acetate
PBS	Phosphate Buffered Saline
PC	Phosphocholines
PFK2	Phosphofructokinase-2
PG	Phosphoglycerols
PI	Phosphoinositol
PLA2	Phospholipase A2
PS	Phosphoserines
PCA	Principal Component Analysis
PGE2	Prostaglandin E2
Q	Quadrupoles
QC	Quality control
ROS	Reactive oxygen species
RT	Retention Time
RP	Reversed Phase
S7P	Sedoheptulose 7-phosphate
SIMCA	Soft-Independent Modelling of Class Analogy
TLRs	Toll-like receptors
UPLC-MS	Ultra-Performance Liquid Chromatograph-Mass Spectrometry
UDP	Uridine diphosphate
UMP	Uridine monophosphate
UTP	Uridine-5'-triphosphate
ZIC	Zwitterionic

Paper Published

Chapter 3

- Alqarni, A., Ferro, V., Parkinson, J., Dufton, M. and Watson, D., 2018. Effect of melittin on metabolomic profile and cytokine production in PMA-differentiated THP-1 cells. *Vaccines*, *6*(4), p.72.

Chapter 4

- Alqarni, A.M., Niwasabutra, K., Sahlan, M., Fearnley, H., Fearnley, J., Ferro, V.A. and Watson, D.G., 2019. Propolis exerts an anti-inflammatory effect on PMA-differentiated THP-1 cells via inhibition of purine nucleoside phosphorylase. *Metabolites*, *9*(4), p.75.

Chapter 5

- Alqarni, A. M., Dissanayake, T., Nelson, D. J., Parkinson, J. A., Dufton, M. J., Ferro, V. A., & Watson, D. G. (2019). Metabolomic profiling of the immune stimulatory effect of eicosenoids on PMA-differentiated THP-1 cells. *Vaccines*, *7*(4), 142.

Poster presented:

- Alqarni, A. and Watson, D., editors. 2018. Metabolomic Profiling of the Effects of Melittin in combination with LPS on Bone Marrow Macrophages Cells Using Mass Spectrometry. Scottish Metabolomics network meeting; Glasgow.

- Alqarni, A. and Watson, D., editors. 2018. Effect of bees products on Metabolomic Profile and Cytokine Production in PMA-Differentiated THP-1 Cells. Scottish Metabolomics network meeting; Dundee.

Abstract

Macrophages play a crucial role in inflammatory conditions by producing a range of pro-inflammatory molecules, including cytokines, nitric oxide and reactive oxygen species (ROS). Several studies have demonstrated the physiological and inflammatory responses of macrophages to different stimuli, such as lipopolysaccharide (LPS), the Gram-negative–derived bacterial cell wall component. However, research is lacking on the metabolic responses of macrophages to these stimuli. Recently, the involvement of metabolic pathways in the regulation of LPS signalling and macrophage activation has become a focus of research in inflammation. The aim of the present study was to assess and characterise cytokine production and the metabolic profiles of THP-1 monocyte-derived macrophage cells following stimulation with LPS, alone or in combination with different natural products. Some of these natural products, such as melittin and eicosanoids, were considered to act as vaccine adjuvants and to enhance the LPS-stimulated release of cytokines and inflammatory metabolite signalling, while others, such as propolis and gypenoside (Gyp), were suggested to antagonise LPS action, thereby modulating immune responses. Macrophages were therefore viewed as having the potential to undergo different reprogrammed pathways once activated by LPS.

In this study, THP-1 cells were differentiated using phorbol 12-myristate 13-acetate (PMA) for 48 hours and then rested for 24 hours by replacing the PMA-containing culture medium with normal medium. The cells were then treated with LPS alone, a natural product alone or a combination of the natural product and LPS for another 24

hours. The THP-1 macrophages were then evaluated for the release of tumour necrosis factor-α (TNF-α) and the cytokines interleukin-1β (IL-1β), IL-6 and IL-10 using enzyme-linked immunosorbent assay (ELISA) methods. The cells were extracted and their metabolites were characterised by liquid chromatography-mass spectrometry (LC-MS).

LPS treatment of THP-1 cells mainly increased glycolysis and the pentose phosphate pathway and decreased the TCA cycle activity. Several biomarker metabolites were altered significantly by LPS, including NADPH, glutathione, oxidised glutathione, L-citrulline, L-arginine, L-ornithine, hypoxanthine, xanthine and urate. The addition of melittin enhanced the LPS effects on the cellular metabolome and cytokine secretion. Several fatty acids, including arachidonic acid, were substantially affected by melittin. Similar responses were found for eicosenoid compounds, which were able to stimulate the immune response and enhance the LPS inflammatory activities. By contrast, propolis (samples obtained from different geographic regions) and Gyp were able to trigger anti-inflammatory actions and inhibit the LPS-induced cytokine release, while also antagonising LPS effects on the cellular metabolome.

These findings point to a need to evaluate the possible anti-inflammatory actions of some reported natural products as a strategy for identifying new therapies and confirming the targeted pathways and/or metabolites affected by inflammatory conditions. Understanding the metabolic pathways in reprogrammed macrophages is critical for planning further investigations of immune adjuvants for vaccines. The immunomodulatory effects observed in THP-1 cells highlight the potential use of natural products in clinical therapies.

Chapter One

General Introduction

1 General Introduction

Compounds isolated from natural sources have established their therapeutic effectiveness in different areas, such as in treating inflammation and metabolic disorders. The main traditional sources for natural products that cure disease are plants [1], but venoms in the animal kingdom have also been a subject of interest throughout human history, largely due to their inherent associated threat to life. A wide range of animal kingdom species produce venom as a defence tool or for capturing prey [2]; the best example is snake venom, which is the most widespread and most frequently fatal venom in humans [3]. Generally, venom can be defined as a "secretion, produced in a specialised gland in one animal and delivered to a target animal through the infliction of a wound-regardless of how tiny-which contains molecules that disrupt normal physiological or biochemical processes so as to facilitate feeding or defence by the producing animal" [4]. Animal venoms consist of complex mixtures of peptides, fatty acids, proteins and small molecules. Several studies have shown the pharmacological properties of these molecules and particularly the venom peptides [2].

Some animal venoms contain novel compounds with pharmacological activity that can play essential roles in the treatment of diseases. In fact, many peptide compounds are now used clinically or are in pre-clinical stages. However, most of the animal venoms remain chemically uncharacterised, despite the development of a number of technological instruments for identification and characterisation purposes [5]. Nevertheless, a number of bioactive molecules derived from natural products have

shown particular immune modulatory or immune-stimulatory activities. Venom and propolis from bees are natural products that have been extensively studied with regards to immune responses [6, 7].

1.1 Introduction to the venom of *Apis mellifera* (honey bee)

Honey bee (*Apis mellifera*) venom from social hymenoptera [8] is a complex mixture of substances produced in the abdominal cavity, where the bee's venom gland is located [9]. The venom is used as an important and effective chemical weapon for the defence of the colony or individuals [8]. In honey bee species, a secretory filament is joined to the reservoir, which opens to the collector apparatus of the stinger [4]. The development cycle of the *Apis* venom gland includes active (containing active substances) and regression stages, similar to the stages found in other exocrine glands [10].

A large number of studies have been carried out to determine the composition of honey bee venom. The biochemical composition of bee venom consists of a variety of active peptides, including melittin, adolapin, apamin and mast cell degranulation peptide. The bee venom also contains histamine, glycerol, sinkaline, noradrenaline, amino acids and various enzymes, including phospholipase A2 and hyaluronidase [11]. Melittin and phospholipase A2 are two major components of bee venom [9, 12].

The use of bee products in the treatment and prevention of diseases is termed apitherapy [13]. The use of natural products, including their active compounds, is

based on epidemiological observations as well as on the experience of traditional medical practice [14]. The use of bee venom as a folk remedy treatment is well known and has been documented as a treatment for various biological disorders, including back pain, angiocardiopathy, cancerous tumours and multiple sclerosis [15-17]. The composition of bee venom and the percentages of the different components are presented in **Table 1-1**.

Honey bee venom contains a very complex mixture of compounds that have yet to be analysed sufficiently. It also contains some volatile compounds which are rapidly lost during the collection process [8]. Bee venom has been analysed by several analytical techniques to identify its component amino acids, proteins, peptides and enzymes. High performance liquid chromatography (HPLC) was able to identify and separate most of the bee venom components [18, 19], and reversed phase (RP)-HPLC is generally used for bee venom analysis. Haghi *et al.* (2013) were able to analyse honey bee venom using RP-HPLC coupled with a photodiode array (PDA) detector [20]. A method using capillary electrophoresis (CE) with a UV detector was developed for analysis and separation of honey bee venom components [19]. Recently, mass spectrometry coupled with HPLC has become powerful instrumentation for quantification of components from bee venom and other complex biological samples [21].

Table 1-1: Important compounds in honey bee venom [13]

Molecule classes	*Components*	*% of dry bee venom*	*Description of major active compounds*
Proteins and peptides	Melittin	40–50	**Melittin:** A 26 amino acid peptide. Classified as a cytolytic toxin and minor allergen [22].
	Apamin	1–3	**Apamin:** An 18 amino acid peptide. Smallest known neurotoxin [23].
	Mast cell degranulating peptide (MCD)	1–2	**MCD:** A 22 amino acid peptide. It causes a massive breakdown of mast cells to cause release of histamine during an allergic reaction [24].
	Secapin	0.5–2	**Secapin:** A 25 amino acid, newly discovered peptide. Protease inhibitor: Unspecified [25].
	Procamine	1–2	
	Adolapin	1.0	
	Protease inhibitor	0.8	
	Tertiapin	0.1	**Tertiapin:** Has a high-affinity binding sites in rat brain; inhibits the enzyme-activating ability of calmodulin; inhibits activity of soluble phosphodiesterases [26].
	Other small peptides (<5 amino acids)	13–15	
Enzymes	Phospholipase A2	10–12	**Phospholipase A2:** A protein allergen. Acts in synergy with melittin to cause cell cytotoxicity [27].

	Hyaluronidase	1–3	**Hyaluronidase:** Large protein allergen. Acts to disrupts hyaluron-ic acid intracellular matrix [28]
	Acid phosphomonoesterase	1	**Acid phosphomonoesterase:** Protein allergen. Act like other high molecular weight phosphatases by hydrolysing phosphoesters.
	Lysophopholipase	1	
	α-Glucosidase	0.6	
Physiologically active amines	Histamine	0.5–2.0	**Histamine:** low molecular weight amine with known pharmacological activities [29].
	Dopamine	0.2–1.0	
	Noradrenaline	0.1–0.7	
Amino acids	Aminobutyric acid	0.5	
	α-Amino acids	1	
Sugars	Glucose and fructose	2	
Phospholipids		5	
Volatile compounds		4–8	

1.2 Major components of honey bee venom

1.2.1 Melittin: a major peptide of bee venom

Several active compounds have been identified in honey bee venom, including peptides such as melittin, a major toxic polypeptide component of bee venom [9]. The melittin structure contains 26 amino acid residues of both lipophilic and hydrophilic types. The carboxyl terminal consists of 6 hydrophilic amino acids, whereas the amino terminal contains the remaining 20 residues and imparts the peptide's hydrophobic properties; the end result is an amphipathic character for melittin [22]. This water-soluble peptide contains six positive charges: four amino acid residues with positive charges found in the C-terminal end (Lys-Arg-Lys-Arg) and the two remaining positively charged amino acids are situated in the N-terminal end (Gly-1 and Lys-7) [30, 31]. The melittin charge is mostly concentrated close to the C-terminal. The amino acid sequence of melittin was identified as the following [32]:

GIGAVLKVLTTGLPALISWIKRKRQQ

Despite the high proportion of non-polar amino acids in the melittin structure, the peptide is highly soluble in water and moderately soluble in methanol. Melittin is considered to be a monomeric molecule at low concentrations, where it adopts a random coil conformation in aqueous solution [33]. Terwilliger and Eisenberg [34] described the three-dimensional structure of tetrameric polypeptide melittin using X-ray crystallography. Each of the four melittin monomers is composed of two 'α-helical' segments. The overall shape of melittin, as shown in **Figure 1-1**, is a bent

rod. The bend is due to the presence of a proline residue at the 14 position, which gives an angle of about 120° between residues 1–10 and 16–26 through the helix axes. As a result, the melittin chain can be divided in to three main regions: the hydrophobic NH_2 terminal, the hydrophilic C-terminal and a central section with both hydrophilic and hydrophobic properties [34].

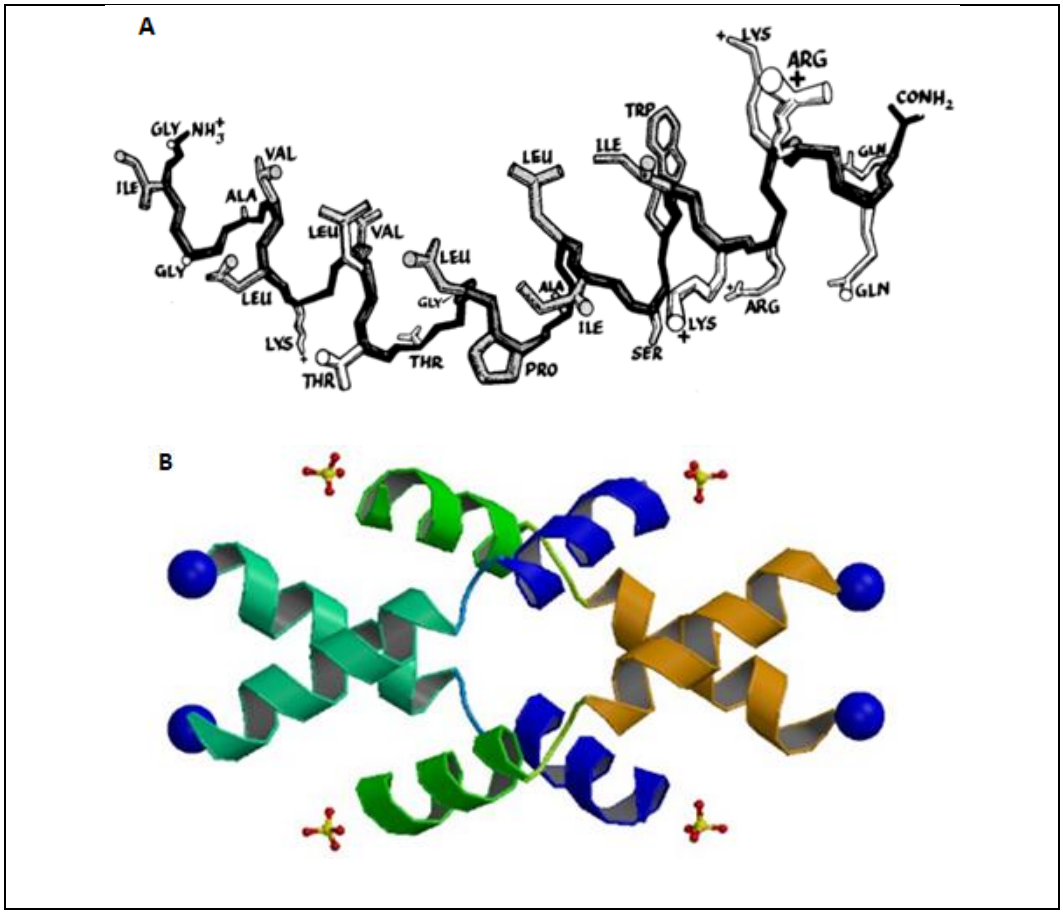

Figure 1-1: The structure of melittin.
A) Melittin single chain conformation from the tetramer. Figure adapted from [34]. **B)** Melittin chain conformation from the tetramer as obtained from the Protein Data Bank.

The 3D structure of melittin in aqueous solution was analysed using X-ray crystallography, and the four monomers of melittin were determined to be identical. The melittin monomeric and tetrameric structures were confirmed by nuclear

magnetic resonance (NMR) spectroscopy in aqueous solution [35], and its monomeric structure was further confirmed in methanol [36].

The aggregation behaviour of melittin in solution is very complex and depends on both the properties of the solution in which it is dissolved (i.e., the pH and ionic strength) and the concentration of melittin. These factors strongly affect the electrostatic interaction, hydrophobicity and interactions of the helix-dipole at the N-terminal. The monomeric structure of melittin combines to form a tetramer (aggregate) in aqueous solution in the presence of high melittin concentration, high pH and high salt. These conditions suppress the high charge density on melittin and decrease the electrostatic repulsion between the monomers [33]. The presence of the aromatic group in the tryptophan amino acid in the melittin structure makes the peptide fluorescent, which allows an easier interpretation of the fluorescence data and the study of melittin membrane interactions [37].

The melittin peptide is one of the most extensively studied peptides in terms of the interaction with cell membranes. The amphipathic property of melittin gives it the ability to bind directly to a lipid bilayer by forming an α-helical conformation. The orientation of melittin has been observed in two ways and confirmed to cause pore formation; at low concentrations, melittin binds in a parallel manner with the membrane and is shifted towards its perpendicular orientation at high concentration [38]. This was supported by another study showing that melittin at low concentration binds to the surface of the membrane in an inactive parallel conformation, thereby

preventing other melittin molecules from inserting into and binding within the membrane [39].

The aggregation of an α-helical synthetic peptide (PEP1) on a solid supported lipid membrane was characterised by Wang *et al*. [40] using microcantilevers. The interactions between PEP1 peptides and the lipid bilayer were concentration dependent, as the membrane surface stress was altered at a critical calculated peptide concentration (4μM) and the peptides started to aggregate and form membrane pores. However, at peptide concentrations ≥ 20μM, the surface stress decreased and membrane damage developed [40]. The effects of melittin on membrane permeability could be the basis for its therapeutic effects.

1.2.2 Other active components of bee venom

Crude bee venom contains several other molecules that have uses in different therapies. These compounds differ in their molecular weight (MW), ranging from large-sized proteins to lower MW amines. The latter include histamine (MW ~16 kDa), a low molecular weight amine, and hyaluronidase enzymes (MW~54 kDa) which are relatively larger [29]. Much of the toxicity of bee venom arises from the enzymes phospholipase A_2 (PLA_2) and hyaluronidase. Phospholipase A_2 (PLA_2), a major enzyme in bee venom, belongs to a class of esterase enzymes which release arachidonic acid from the sn-2 position of membrane phospholipids [27]. Steinem *et al*. investigated the influence of PLA_2 on the interaction of melittin with a solid support membrane in the presence and absence of ethylenediaminetetraacetic acid (EDTA). EDTA at a 5mM concentration is known to inhibit the phospholipase. The

results showed that melittin had a more pronounced impact on the membrane electrical parameters in the absence of EDTA, revealing its synergistic effect with PLA_2. This observation was believed to reflect the ability of melittin to expand the lipid membrane headgroups, which increases the PLA_2 binding sites and allows an increased attack on the lipid bilayer by PLA_2 [41].

Kemeny *et al.* (1984) were able to purify and characterise the hyaluronidase from bee venom using several chromatographic steps [42]. This enzyme is a single polypeptide with 350 residues and is secreted as a glycoprotein that contains carbohydrate and two disulphide bonds. Hyaluronidase facilitates the spread of bee venom in the body by degrading the hyaluronic acid present in the extracellular skin matrix. Hyaluronidase and PLA2 have been identified as major allergens within bee venom and are responsible for the allergic reactions in the majority of patients allergic to bee venom [28].

The small apamin peptide in bee venom is a neurotoxin with 18 amino acid residues, four of which are cysteines that form two disulphide bridges [43]. Apamin (MW 2027 Da) accounts for 1–3% of dry bee venom [44]. Apamin has the ability to reach the liver, adrenal cortex and brain grey matter to affect the central nervous system [45]. Mourre *et al.* showed that apamin inactivates and blocks calcium-activated potassium channels, thereby inducing neurodegeneration of Purkinje cells [46]. Apamin has been patented as a therapeutic agent to overcome the side effects of treatments used for Parkinson's disease (e.g. L-Dopa), as it can protect neurons from damage and restore the function of other silent neurons. In addition, apamin is used for the treatment of degenerative brain diseases [44].

Mast cell degranulating (MCD) peptide has proved to be pharmacologically interesting. It is a 22 amino acid peptide with a MW of approximately 2.5 kDa. It has a similar structure to apamin, as it also contains four cysteine residues that form cross linked disulphide bonds [24]. However, MCD has different cellular receptors from apamin and therefore gives completely different responses. The MCD peptide is considered to be an anti-inflammatory agent, as it triggers the degranulation of mast cells and the release of histamine at low concentrations [47].

Shkenderov and Koburova (1982) were able to isolate adolapin, another important peptide in bee venom. Adolapin was reported to have a COX inhibitory effect, as well as anti-inflammatory and analgesic effects [48]. Another peptide, tertiapin, is composed of 21 amino acids with six positive charge residues. It also contains disulphide bridges between four cysteine residues, and it blocks certain types of 'inwardly rectifying potassium channels' (K_{ir} channels) [49].

1.3 Other compounds and extracts investigated for immunomodulatory activity

1.3.1 Propolis

Propolis, also called bee glue, is a natural resin and wax-like substance collected by *Apis mellifera* from different tree buds. It is mainly used as a cementing material to seal cracks and protect the hive from infections [50]. Propolis has been used as a traditional medicine since 300 BC [51] and is recognised as an anti-bacterial in Europe [52]. During the 17th century, it was recognised as a wound-healing treatment in England [53]. It is also used as an anti-cancer and anti-infection

medicine in China [54] and for treatment of wounds in Egypt [55]. Currently, propolis is used to treat inflammation and bacterial and viral infections [56]. It is also used as an antioxidant, anti-protozoal and anti-fungal treatment [57]. The medical applications of propolis have increased interest in its biological activities and chemical compositions. It consists mainly of about 50% resin and balsam, 30% wax, 10% essential and aromatic oils and 5% pollen [58]. Its chemical composition varies depending on its botanical origin due to variability of plant species around the hive [59], as well as seasonality, altitude, food availability and collector type [60]. However, the main chemical classes detected in propolis are flavonoid, aromatic and phenolic compounds, in addition to terpenoids and volatile oils [61].

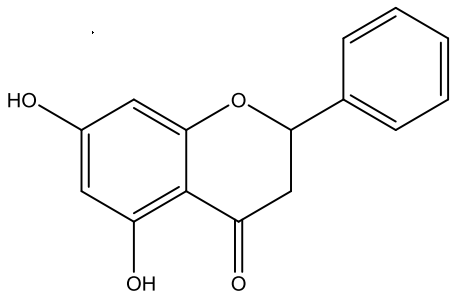

Pinocembrin

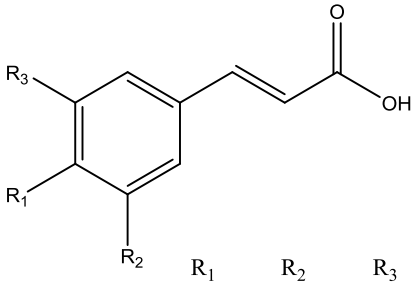

	R_1	R_2	R_3
Cinnamic acid	H	H	H
p-Coumaric acid	OH	H	H
Caffeic acid	OH	OH	H

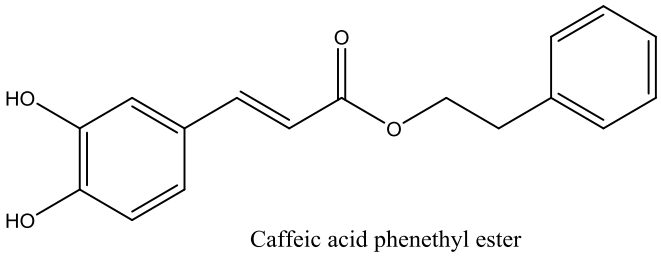

Caffeic acid phenethyl ester

Figure 1-2: Some typical flavonoids and phenolics present in propolis.

1.3.2 Gypenoside

Gypenoside (Gyp), a dammarane saponin, is believed to be the main active component of *Gynostemma pentaphyllum* (Thunb.) Makino, a traditional Chinese medicinal plant that belongs to the Cucurbitaceae family that includes melon and cucumber [62]. The reported clinical responses of Gyp include lipid-lowering effects [63]. Further investigations have shown that Gyp improves cardiovascular disease, cancer management and immune system functions [64, 65]

1.4 Immunometabolism

1.4.1 An overview of ATP production

Understanding the metabolic abnormalities underlying disease requires a knowledge of normal cell metabolism. Generally, metabolic pathways can be categorised as an anabolic, catabolic and amphibolic, where the amphibolic pathways, such as the tricarboxylic acid (TCA) cycle, act as a link between catabolic and anabolic pathways. Compounds synthesised in the anabolic pathways use endergonic reactions, while exergonic reactions occur during the breakdown of macromolecules in catabolic pathways. Dietary proteins, lipids and carbohydrates undergo the digestion process in order to produce amino acids, fatty acids and glycerol, and glucose, respectively (**Figure 1-3**). These small molecules are then

metabolised to a major product, acetyl-CoA, which is further oxidised by the TCA cycle to produce energy [66].

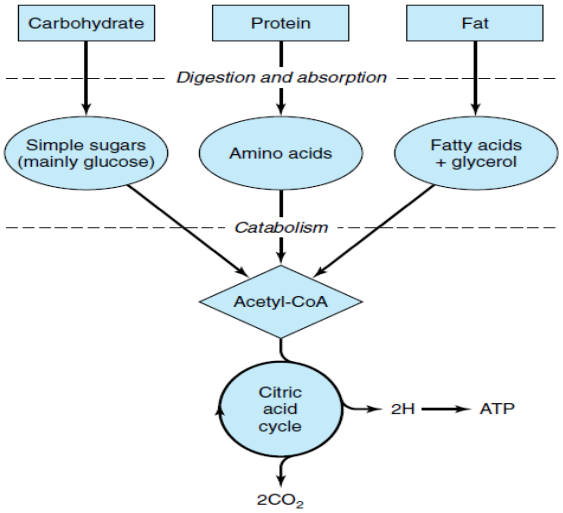

Figure 1-3: Illustration of the major catabolic pathways of carbohydrates, proteins and fats. Acetyl CoA is the main product and enters the citric acid (tricarboxylic acid) cycle to generate ATP. Figure adapted from [66].

Understanding the differences in biological systems between normal and inflammatory cells is essential for the design and development of anti-inflammatory drugs with selective mechanisms of action. This can also help to understand the differences in metabolism and in achieving high drug therapeutic efficiency and selectivity.

Glycolysis involves a series of metabolic processes that convert one molecule of glucose into two pyruvate molecules, with a net gain of two molecules of adenosine triphosphate (ATP) and two molecules of reduced nicotinamide adenine dinucleotide (NADH). In the first half of the pathway, two ATP molecules are consumed to produce fructose-1,6-biphosphate. The latter is then converted stepwise into pyruvate, with the production of two molecules of NADH and four molecules of

ATP [67]. Under aerobic conditions, the end product of glycolysis is the three-carbon (C3) pyruvic acid, which enters the mitochondrion and is oxidised to produce an acetyl group (acetyl CoA), with the release of a molecule of CO_2. Acetyl CoA is the starting point for the TCA cycle and combines with the four-carbon acid oxaloacetate to produce citrate. This is followed by oxidative phosphorylation (OXPHOS) to produce 36 ATPs (via formation of NADH) from one glucose molecule and this is termed mitochondrial respiration. Under anaerobic conditions, pyruvic acid is instead reduced to lactate in the cytoplasm by lactate dehydrogenase (LDH) and the lactate is excreted into the extracellular space. Anaerobic respiration produces only a limited amount of energy when compared to aerobic respiration [68].

At the beginning of the TCA cycle, the production of citrate is followed by seven sequential reactions that regenerate the oxaloacetate molecule while releasing CO_2. In one complete cycle, one acetyl CoA is oxidised to give three molecules of reduced nicotinamide adenine dinucleotide (NADH) by the reduction of 3 NAD^+, one molecule of reduced flavin adenine dinucleotide ($FADH_2$) and one molecule of ATP. The regulatory enzymes in the cycle are citrate synthase, iso-citrate dehydrogenase and α-ketoglutarate dehydrogenase and the pyruvate–acetyl CoA conversion rates which maintain the overall regulation. TCA is considered an amphibolic pathway, as it has other metabolic roles besides oxidation [69, 70].

The electron transport chain (ETC) process follows the TCA cycle in aerobic respiration and produces most of the ATP molecules. The electron transport process takes place on the inner mitochondria membrane. The respiratory chain consists of an association of five complexes whose spatial organisation favours a rapid exchange of

electrons. The first four enzyme complexes form the ETC, while the fifth complex is responsible for ATP synthesis [71]. Two different pathways exist for electron transfer through the respiratory chain: a high energy electron transport pathway from NADH via complexes I, III, and IV and a second electron transport pathway from $FADH_2$ via complexes II, III and IV [69]. Each of I/III/IV complexes act as a proton pump which creates a proton flux outward across the membrane. This causes an accumulation of protons (H^+) outside the membrane and creates an electrochemical potential difference across the membrane (by differences in pH and electrical potential). This potential difference leads to a flow of H^+ into the mitochondrial matrix via complex V, with a concurrent synthesis of ATP from ADP+P via the ATP synthase enzyme. This process is called chemiosmosis, as ATP production is coupled to the transport of hydrogen ions [66]

1.4.2 Metabolic pathways in immunity

Intrinsic and extrinsic cellular signalling regulate metabolic activities to generate key products to maintain cellular survival and needs. However, the production of distinct sets of inflammatory signals has been connected to alterations in metabolic pathways and immune effector functions. Generally, immune cells use several metabolic pathways to produce numerous biosynthetic intermediates and adequate levels of energy that allow cellular growth and proliferation. This is connected mainly with the activity of six key metabolic pathways: the glycolytic, TCA cycle, pentose phosphate (PPP), fatty acid oxidation (FAO), fatty acid synthesis (FAS) and amino acid pathways.

1.4.2.1 Glycolysis in immunity

An involvement of glycolysis in several immune process has been established. In immune cells, glycolysis is rapidly activated via the stimulation of the enzymes involved in this pathway. By contrast, OXPHOS is more complex and very slow as it needs a mitochondrial biogenesis. Glycolysis is able to generate biosynthetic intermediates required for cell growth, such as intermediates for the PPP, activators of the TCA cycle and metabolites required for the synthesis of key biomass molecules, including glycine, serine, and alanine, as well as acetyl-CoA for lipid biosynthesis [72]. Several previous studies have reported an enhancement of glycolysis in different activated immune cells, such as lipopolysaccharide (LPS)-activated macrophages [73] and dendritic cells (DCs) [74], activated T and B cells [75, 76] and activated natural killer cells (NK) [77]. This leads to reprogramming of the cells to produce their immune effector functions (e.g. phagocytosis and release of inflammatory cytokines by macrophages and antigen presentation by DCs) [78].

1.4.2.2 Pentose phosphate pathway in immunity

The oxidative and non-oxidative arms of the PPP have two important outcomes: the production of nucleotides and the generation of NADPH (reduced form of nicotinamide adenine dinucleotide phosphate-NADP+). NADPH in immune cells has crucial functions that balance the generation of reactive oxygen species (ROS) and antioxidant compounds like glutathione. During infections, ROS are used to clear infectious agents, but subsequent tissue damage is prevented by the release of antioxidants. The PPP is activated in LPS-induced macrophages and is considered important for M1 macrophage function [79].

1.4.2.3 The TCA cycle in immunity

The TCA cycle has been studied extensively in immune cells, as it is suppressed in these cells, which shift towards glycolysis and away from the TCA cycle [80]. In M1 macrophages, the cycle is disrupted after the citrate and succinate steps and these two products accumulate. Citrate is exported to the cytoplasm to generate fatty acids, nitric oxide and itaconate [81], whereas succinate contributes to cytokine production and to electron transport chain (ETC) inactivation, which promotes ROS production [82].

1.4.2.4 Fatty acid oxidation (FAO) and fatty acid synthesis (FAS) in immunity

The metabolic pathways begin with the glycolysis of glucose taken up from outside the cells into the cytoplasm to produce pyruvate and several other products. Two molecules of adenosine triphosphate (ATP) are generated during glycolysis, but this conversion is relatively inefficient for general cell metabolism. However, glycolysis has a dominant and essential role in rapidly proliferating cells, as it allows the reduction of NAD+ to NADH. NADH, in turn, is used as an enzyme cofactor and enables the diversion of glycolytic intermediates to biosynthetic growth pathways (anabolic growth), for example, the synthesis of nucleotides (substrate for ribose biosynthesis), amino acids (through serine biosynthesis), and fatty acids (through pyruvate entry into the TCA cycle to produce citrate) [72].

The FAO process starts with the conversion of the fatty acid into fatty acid acyl-CoA for entry into the mitochondrion. Short-chain fatty acids can diffuse directly into the mitochondrion, while medium- to long-chain fatty acids can enter by conjugating with carnitine. Fatty acid acyl-CoA undergoes β-oxidation to yield large amounts of

acetyl-CoA, NADH and $FADH_2$ to generate energy. By contrast, FAS is required to generate lipids for cellular growth and proliferation. The FAS process uses components derived from different metabolic pathways, including glycolysis (e.g. glycerol), the TCA cycle (e.g. citrate) and the PPP (e.g. NADPH) [72].

In M1 macrophages activated by LPS or IFN-γ, citrate accumulates in the cytoplasm, where it is used for FAS, for supporting inflammatory signalling and for increasing the production of cytokines and nitric oxide (NO) [81, 83]. Succinate is an integral part of the macrophage inflammatory program, as confirmed by LPS experiments that demonstrated an increase in succinate accumulation and a resulting stabilisation of hypoxia-inducible factor 1 alpha (HIFα1) and secretion of IL-1β [82]. FAS was upregulated during DC activation and stimulation of T-cell responses [78]. FAS was also suggested to fuel FAO in M2 macrophages [84].

FAO is required for inflammasome activation in M1 macrophages [85] and for M2 polarisation [84]. Overall, FAO seems to promote the activity and development of non-inflammatory immune cells and to support the anti-inflammatory responses. By contrast, FAS was a positive regulator of the function and generation of pro-inflammatory immune cells, thereby playing an opposing role in the immune system.

1.4.3 Immuno-adjuvant effects

The aim of vaccination is to induce a protective immunity, and this can be enhanced by the addition of adjuvants. Adjuvants are defined as “substances used in combination with a specific antigen that produce a more robust immune response than the antigen alone”. Different classes of compounds have been evaluated as

adjuvants, including microbial products, cytokines, saponins, emulsions and liposomes [86]. One or more mechanisms can explain the effects of adjuvants, including antigen release at the injection site, cytokine and chemokine upregulation, immune cell recruitment at the injection site, activation of inflammasomes, activation of antigen-presenting cells (APC) and activation of B and/or T cell responses [87]. A combination of different adjuvants can trigger potent activities that stimulate the immune responses against vaccine antigens.

1.4.4 Lipopolysaccharide (LPS)

LPS has been extensively studied as an immune stimulatory component of Gram-negative bacteria which induces systemic inflammation [88]. It mainly consists of three parts: lipid A, a core oligosaccharide and an O side chain [89]. Lipid A of LPS is the main pathogen-associated molecular pattern (PAMP) and can stimulate Toll-like receptor 4 (TLR4) to trigger further release of pro-inflammatory cytokines [90]. Regulation of toll-like receptor (TLR) signalling has the potential to link innate and adaptive immunity, making LPS a powerful adjuvant [91].

1.5 Chromatography

1.5.1 Theory and introduction to chromatography

Chromatography is a technique used to separate and quantify a mixture of substances according to differences in their physical properties. The separations rely on the different affinity of the constituents of a mixture (called analytes or solutes) between two chromatographic phases (stationary and mobile phases). Chromatographic techniques are generally specified and named by the mobile phase

physical state. Thus, liquid chromatography (LC) indicates the use of a liquid mobile phase, while gas chromatography (GC) indicates the use of a gas mobile phase (the analytes are also volatile). The state of the stationary phase can also be used to further sub-classify the chromatographic processes; for example, liquid-solid chromatography (LSC) occurs on a solid stationary phase, while liquid-liquid chromatography (LLQ) occurs on a liquid stationary phase.

Elution chromatography is a separation process that involves the flow of a mobile phase along or through the chromatographic bed (stationary phase) in a definite direction (**Figure 1-4**). The tendency of analytes within the same compound to be attracted to the stationary phase is expressed as an equilibrium (distribution) constant or partition coefficient. In chromatography, the greater the attraction to stationary phase, the greater the value of the distribution constant [92].

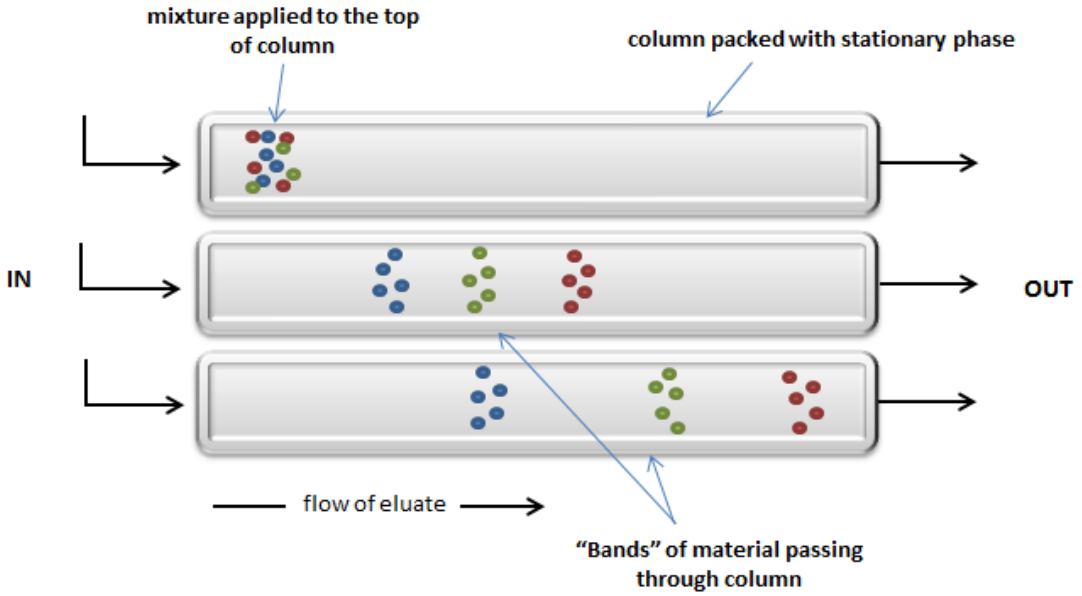

Figure 1-4: The separation process in column chromatography.
Small differences in the interaction of the components in a mixture with stationary phase cause different rates of migration.

The retention time (t_R) for each analyte can be defined as the time period from the point of injection of the sample to the time of elution of the maximum concentration (i.e. highest peak point in the chromatogram) of the analyte. As the analyte flows through the column, it can be described as more retained if it migrates more slowly than the other components (migration rate). This rate is affected by different factors, including the structure of the analyte, the chemical compositions of the stationary phase (column) and the mobile phase, and the temperature [93]. The time taken by an unretained compound to flow through the column (i.e. while travelling at the same rate as the solvent) is determined by the void volume (V_0) of the column [94]. Several methods can be used to achieve or optimise the separation, including sample pre-treatment, selection of chromatographic modes (e.g. reversed phase and normal phase chromatography), choice of separation conditions (e.g. mobile phase strength, run time and pH) and selection of an appropriate detector (e.g. UV and mass spectrometry).

1.5.2 Classification based on mechanism of retardation

The relative retardation of a solute between two phases (mobile and stationary phase) is determined by its chemical and physical proprieties. The analyte undergoes a series of interactions between the two phases; therefore, selectivity can be achieved by varying either the mobile or stationary phases, or both.

Table 1-2: Type of chromatography according to the molecular forces exploited.

Chromatography						
Stationary phase	Adsorption (solid)		Partition (Liquid)		Ion exchange (Solid)	Permeation (Polymer)
Mobile phase	Gas (GSC)	Liquid (LSC)	Gas (GLC)	Liquid (LLC)	Liquid (IEC)	Liquid (GPC)

1.5.2.1 Adsorption chromatography

Also known as normal phase chromatography (NP), adsorption chromatography uses a relatively polar solid stationary phase. The mobile phase can be a liquid (liquid-solid, most common) or a gas (gas-solid chromatography). The mobile phase is usually a nonpolar organic solvent, which can contain a small amount of a relatively polar organic solvent to adjust the polarity (e.g. hexane with chloroform). The more polar solutes will be preferentially adsorbed or retained by binding at onto the polar surface of the column (stationary phase), while the less polar analytes will be eluted first from the column as they have more affinity for the less polar mobile phase [93]. Retention in NP chromatography is characteristically a reversible process (or *displacement process*). As the solvent molecules are adsorbed onto the silica surface of the column from the mobile phase, they need to be removed and displaced from the surface in order to make room for adsorption of new molecules. The competition between the analyte and solvent molecules for the stationary phase is also affected by the interaction of each compound between the two phases [95].

Silica is the most often used column material in NP chromatography and is usually covered with silanol groups (≡Si-OH). Other types of column widely used in NP chromatography have polar groups, such as amino, diol and cyano groups, bonded to the silica. The polar interactions of a solute with the polar stationary phase

(particularly silica columns) are localised and highly directional, so NP is better than other types of chromatographic separation at separating isomers. The mechanism of isomer selectivity on a silica column can be characterised as electron withdrawal or donation from a polar group, steric hindrance of a polar group and the planarity of the solute and the position of different polar groups within the compound [93].

1.5.2.2 Partition chromatography

The mechanism of retardation in partition chromatography depends on the overall lipophilicity of the compound (i.e. log P). The lipophilicity can be used to measure a compound's polarity, as a polar group will decrease the lipophilicity of the compound [94]. The underlying mechanism of partition chromatography involves the partitioning of more lipophilic (less polar) molecules between a non-polar stationary phase and a polar mobile phase. That is, solutes are eluted from the column in order of increasing lipophilicity, i.e. polar analytes (less lipophilic) are eluted first. Therefore, the partitioning process generally depends on the natures of the stationary and mobile phases and the molecular structure of the analyte.

The most commonly used column of this type is the *reversed phase* (RP) column, which has a chemically modified silica gel surface. RP partitioning involve less polar stationary phase to a more polar mobile phase. The chemical interaction between the solutes and an RP column affects the column selectivity, which is determined by several mechanisms, including hydrophobic interaction, steric exclusion of large molecules and electrostatic interaction with the ionised silanol (SiO-H) groups of the silica gel support. In addition, there is a possibility for the formation of hydrogen bonds between the solute and the free silanol groups on the surface of stationary

phase [93, 96]. The chemical composition of the functional groups in an RP column can vary, but the C_{18} octadecylsilyl (ODS) ligand is the most common. The maximum effect of steric interactions have been exhibited for C_{18} columns when compared with C_1 and C_{30} columns [97].

RP chromatography is still widely used and applicable; however, the separation quality still has some limitations, particularly for polar substances. Similarly, NP columns have low efficiency for separating some polar molecules as the use of only organic solvents as a mobile phase can cause asymmetrical peaks. Therefore, *hydrophilic interaction liquid chromatography* (HILIC) is now considered an alternative method for separating polar compounds (i.e. this column type shows very little retention of non-polar and many neutral solutes). The HILIC method is a combination of a normal stationary phase and a RP mobile phase. The stationary phase is highly hydrophilic and is used with an aqueous organic mobile phase (e.g. acetonitrile or methanol with water) [98]. The mobile phase in most HILIC separations ranges from 3% up to 30% water, which forms a layer on the surface around the silica particles (by polar interactions). The mechanism of retardation was suggested to be as normal phase with the involvement of hydrogen bond formation. However, the retardation appears to occur mostly by partitioning of solutes between the organic solvent and the partially immobilised water on the surface of the stationary phase [99]. The HILIC column is often created from silica particles, which can be bonded with different coatings (e.g. amino, cyano, amide and zwitterion) to provide different selectivity (**Figure 1-5**).

Generally, HILIC separation has several advantages; for example, it can increase the sensitivity of a mass spectrometry detector (i.e. organic solvents with greater volatility can be used, which are better for electrospray ionisation) and allow the use of a high flow rates and produce lower column pressures (due to lower viscosity of the organic solvents, mobile phase) [93].

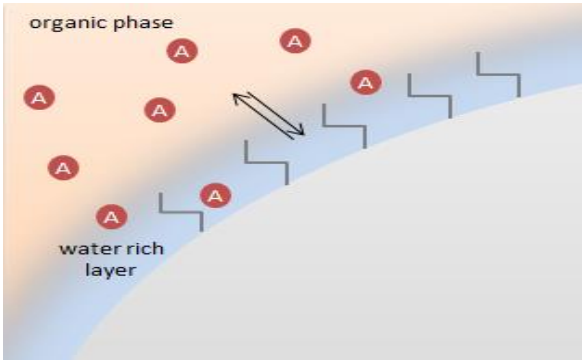

Figure 1-5: HILIC column. Separation of solutes by partitioning between the organic phase and the water layer; A:analytes

1.5.2.3 Ion exchange chromatography

Ion exchange chromatography (IEC) is carried out on columns that have ionisable groups attached to the surface of the stationary phase. Cations, such as quaternary ammonium groups ($-N(CH_3)_3^+$), or anions, such as sulfonate groups ($-SO_3^-$) are attached covalently to the surface of the solid stationary phase. Oppositely charged solutes can then be retained by electrostatic interactions. In the case of cation exchange columns, protonated base solutes (BH^+) are retained from the liquid mobile phase, whereas ionised acidic solutes (A^-) in case of using anionic exchange columns [100]. The mobile phase counter ions and sample ions will compete to interact with the oppositely charged stationary phase to result in the final retention. Therefore, the IEC mobile phase mainly consists of buffer (to adjust the pH), water and counter ions

(salt) to control the retention. Sample retention is reduced by increasing the charge of the counter ions. The pH of the mobile phase is a crucial factor for the ionisation process, as only the ionised ions are retained on the IEC column. For instance, acidic molecules become more ionised (are retained more) if the pH of the mobile phase is increased, whereas the base ionisation is increased by reducing the pH of the mobile phase. Depending on the kind of ionic group on the stationary phase, an IEC column can be categorised as a weak or strong cation exchanger (WCX and SCX, respectively) or a weak or strong anion exchanger (WAX and SAX, respectively) [93].

1.5.2.4 Size exclusion chromatography

Size exclusion chromatography (SEC) is one of the most commonly used techniques to detect differences in molecular size of any type of polymer. The SEC stationary phase contains a rigid carrier bonded to polymers, which are considered to be more stable media. The mechanism of separation relies on the shape and size of both the stationary phase pores and the sample molecules (size exclusion effect). Therefore, larger molecules pass through the column without entering the pores and are eluted first. However, small solutes can enter the pores and therefore take a longer time to elute. This mechanism of separation by SEC allows information to be obtained regarding the shape, size and aggregation state of the investigated compounds [101]. It is also called molecular exclusion chromatography, gel permeation chromatography and gel filtration chromatography; these all have the same separation mechanism but use different mobile phases and samples [102].

1.5.2.5 Affinity chromatography

Affinity chromatography was described by Harris (2010) [100] as the most selective type of chromatographic separation. It is performed by exploiting the specific interactions between the investigated solutes and molecules that are attached covalently to the stationary phase (e.g. a specific antibody that interacts with a particular protein from a mixture). The attached protein can ultimately be removed from the column by changing the pH or the ionic strength [100].

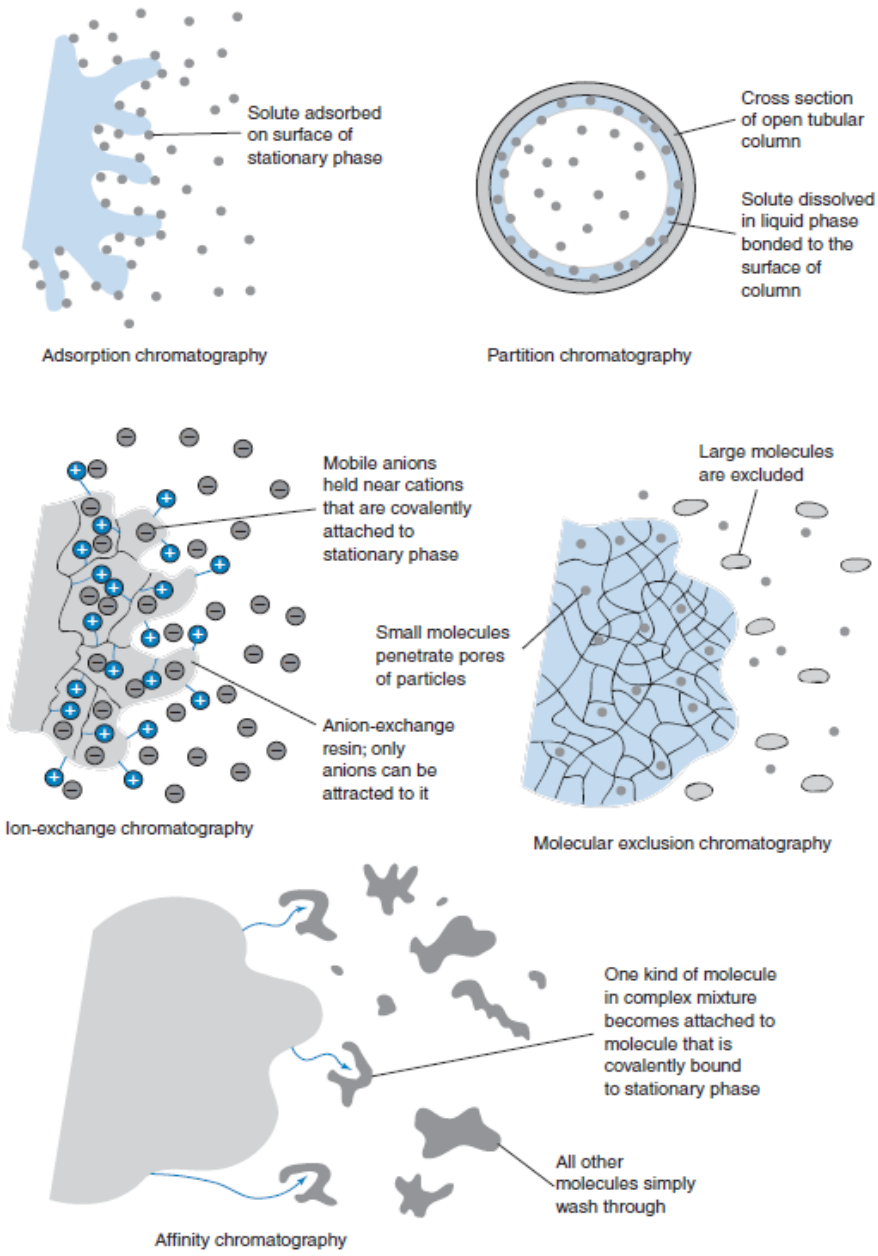

Figure 1-6: Major types of chromatographic separation based on the mechanism of retardation. Figure adapted from [100].

Silica is the most commonly used material used as a support in HPLC column packing. It has a high mechanical strength, which allows the silica packing beds to retain stability for long periods under high pressure conditions. In addition, silica gives a higher plate number (*N*) value compared to other column support materials.

Silica can be fabricated with a wide range of pore and particle sizes and in different particle configurations (regular and irregular) [103].

Silica interaction properties are influenced strongly by the chemical nature of the unmodified silica surface. Generally, this is a network of (-Si-O) bonds on the surface of the stationary phase. Different types of silica surfaces, such as free silanol groups (-Si-OH), geminal silanols, associated silanols, surface metals and internal metals (M^+), give multiple interaction sites The purity of the silica support plays a crucial role in determining the acidity of the silanol and therefore the column performance [103].

1.5.3 Elution profiles in chromatography

Samples can be separated by HPLC with or without changes in the mobile phase composition during the run. Isocratic elution is performed without changing the mobile phase composition, whereas gradient elution is performed by changing the composition of the mobile phase with time. The changes in the mobile phase composition can include changes in ionic strength, pH, percentages of mobile phase solvents and levels of specific additives, or combinations of these changes. Gradient elution is the most commonly used particularly with RP-HPLC, NP chromatography, HILIC and ion pair chromatography (**Figure 1-7**) [104].

Gradient elution is essentially used for four major purposes. It is used to reduce the total separation run time, to modify the retention time to achieve and optimise a good separation between specific molecules, to decrease band broadening (narrow the peaks) and to clean the column. The capacity factor or retention factor (k') is widely

used to describe the extent of the retention and evaluates the quality of the separation and the retention of compounds in a mixture. In a typical HPLC separation, the values of k' for solutes should be in the range $1 \leq k' \geq 10$, to allow shortening of the retention time. The k' values can be adjusted by altering the composition of the mobile phase [105].

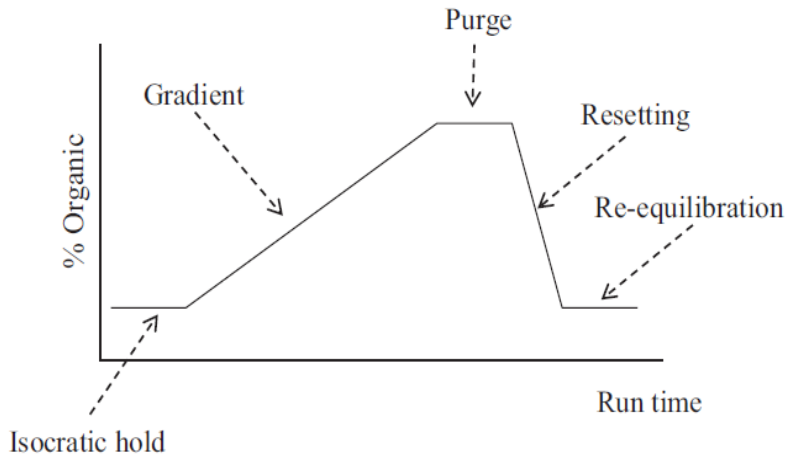

Figure 1-7: Schematic diagram illustrates a simple gradient elution profile in an HPLC system. Obtained from [105]

The percent of organic solvent (%B) is usually varied from 0% to 100% during a gradient elution. At the end of the run, re-equilibration is important for restoring the column stationary phase to its initial conditions before a new run is started. The mobile phase composition is normally varied for each solute, taking into consideration the variation in special additives for a particular detector to enhance the separations.

1.5.4 High performance liquid chromatography

High performance liquid chromatography (HPLC) is the most powerful chromatographic system used to achieve analysis and separation of chemical mixtures that would be difficult to be separated using other chromatographic techniques. It is a technique that applies high pressure on a liquid solvent containing a mixture of compounds that is pumped through a column. The components of the sample mixtures spend different times interacting with the stationary phase, thereby leading to efficient separations. The column effluent can be monitored using a variety of detectors. HPLC provides an accurate and precise method for quantitative analysis of pharmaceutical compounds, for conducting stability and degradation tests of drug substances, and for measuring drugs metabolites in biological samples. The selectivity of the method can be adjusted by using different column and detector types [106].

HPLC systems are specially designed for low flow rate, high flow rate, or for high pressure applications. The instrument system generally consists of the following components: a solvent reservoir, a pump (capable of pressure up to 4000 psi and control of the flow rate), a sample injection valve (or auto-sampler), a column (where the separation take place), a detector (responds to changes in solute concentration) and a data capturing system (monitors the detector output and processes the chromatographic data) (**Figure 1-8**) [94].

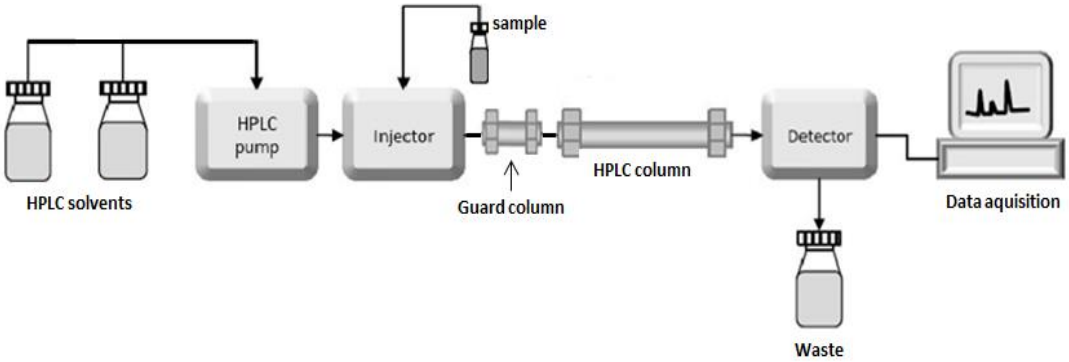

Figure 1-8: Typical diagram of a high performance liquid chromatography (HPLC) system. The use of a pre-column (Guard column) is optional.

Many types of detectors have been joined successfully to HPLC systems and used for general and specific applications. Generally, the ideal HPLC detector should have high sensitivity and specificity for all solutes while providing qualitative information about the detected peaks. The commonly used HPLC detectors are summarised in **Error! Not a valid bookmark self-reference.**.

Table 1-3: Detectors in common use with HPLC system [93, 94]

Detector	***Description***
Variable wavelength ultraviolet /Visible (UV/Vis) detector	Samples must absorb UV light; detection is based on the absorption of the UV light at different wavelengths. Sensitive to temperature and flow changes. Range of 0.01-100 µg of a sample provide robust detection and good sensitivity. The detector sensitivity depends on the specific absorbance (A) of the analysed compound.
Diode-array detector (DAD)	Array of photodiodes used to detect light dispersion over a range of wavelengths using a fixed monochromator. It is a type of UV detector and can be operated to collect the data

	at one or more wavelengths, or collect full spectra of one or more analytes with widely different absorbance ranges, offering a resolution of about 1 nm. This could help to identify unknown compounds.
Evaporative light-scattering detector (ELSD)	A beam of light is scattered by particles of non-volatile compounds remaining after mobile phase evaporation. It differs from UV detection as it does not require a chromophore in the compound for detection. Applications include analysis of lipids, surfactants and sugars. However, it cannot be used to detect very volatile solutes or non-volatile materials.
Fluorescence detector	Fluorescence detectors have high sensitivity and selectivity for analytes that exhibit fluorescence. Detection is based on fluorescence emission and excitation of fluorescent substances. It is sensitive to below the 'ng' level for highly fluorescent compounds.
Electrochemical detector	In the presence of an electrical potential between electrodes, compounds can be oxidised (produce electrons) and reduced (consume electrons) allowing their detection at very low concentrations. The mobile phase should be electrically conductive. Electrochemical detection is widely applicable to bioanalysis, such as analysis of drugs in biological fluids.
Refractive index detector (RI)	The refractive index detector responds to changes in the refractive index of the solutes relative to the solvent as passes through sample cell in the detector. RI detection is very sensitive to the temperature and to the composition of the mobile phase. If the RI of the solute differs from that of the mobile phase, the solute can give a response and be detected.

1.5.5 Ultra-Performance Liquid Chromatography

In HPLC, the choice of particle size should be a compromise. Where, the smaller is the particle size, the higher column back-pressure. This could be a limitation from using normal HPLC column. Thus, using ultra-performance Liquid chromatography (UPLC) would accomplish these problems with a higher resolution by using smaller column packed with smaller particles size, usually < 2 µm in diameter. It is a relatively new technique with a new possibilities in liquid chromatography, particularly concerning shorter running time and decreasing solvent consumption [107, 108].

1.5.6 Medium pressure liquid chromatography

Medium pressure liquid chromatography (MPLC) is a preparative column chromatography separation technique which allows purification of large quantities of compounds (**Figure 1-9**). MPLC has become widely used for the isolation and purification of natural products. The instrument setup consists of a pump for solvent delivery and the sample is injected through an injection system. The sample passes through a self-packed or commercially-packed column and is collected with a fraction collector. The product separation is followed with detectors or it can be monitored manually using thin layer chromatography (TLC). The column dimensions are selected based on the sample amount to be isolated. The separated compounds are usually detected using UV/Vis and ELSD detectors, as these allow the detection of both chromophoric and non-chromophoric compounds [109].

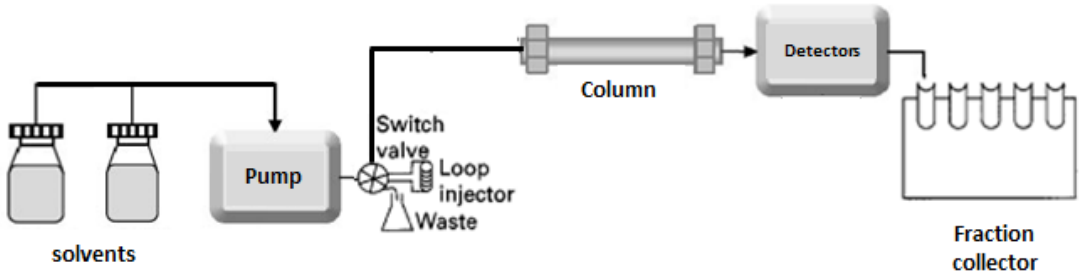

Figure 1-9: Typical diagram of a medium pressure liquid chromatography (MPLC) system.

1.6 Ultraviolet/visible spectroscopy (UV/Vis)

UV and visible light absorption detectors are both widely used in modern HPLC protocols. The UV detector is very sensitive for many analytes if the samples absorb in the UV wavelength region (200–700 nm). Light is passed through the sample cell and the portion of the transmitted light that is absorbed is related to the sample concentration. The absorption of UV/Vis radiation occurs as molecules and atoms pass from lower to higher (excited) states. As a molecule absorbs energy, an electron is excited from the highest occupied molecular orbital (HOMO) to the lowest unoccupied molecular orbital (LUMO). Every molecule has many states of vibration, rotation and electronic excitation, and UV absorption normally occurs over a wide range of wavelengths to give a broad band spectrum (band spectra). Three different types of orbital electrons can provide rise to electron: transition sigma bond electrons (σ), non-bonding electrons (n) and pi electrons (π) in conjugated double bonds. Double bond systems extend to form chromophores (e.g. the benzene ring) which are responsible for the absorption in UV/Vis region. In addition, the presence of 'auxochrome' groups can change the light absorption of a chromophore (i.e. change

the wavelength and the absorption intensity). Typically, the UV/Vis spectrophotometer consists of light source, a monochromator to disperse the light into component wavelengths and a detector to record the transmitted light intensity [110].

1.7 Evaporative light scattering detector (ELSD) spectroscopy

An evaporative light scattering detector (ELSD) detects any solute that is less volatile than the mobile phase in which it is analysed. Eluates enter into a nebuliser in the detector and are mixed with an inert gas, such as nitrogen, and then passed through a small bore needle to form tiny droplets. In a heated drift tube, the solvent is evaporated from the droplets, leaving tiny solid particles which pass through the detection zone and are detected by the light they scatter. The detector response does not relate to the structural properties, but merely to the masses of the analytes present. Volatile buffers, such as trifluoroacetic acid and triethylamine, should be used as these are easily evaporated [111].

1.8 Mass spectrometry

Mass spectrometry (MS) is a micro-analytical technique that can be used for selective detection and determination of the amount of a given solute. It is a technique used to determine the exact masses of atoms or molecules or molecular fragments. A high vacuum region generates charged molecules or molecular fragments. A mass spectrum is obtained by ionising molecular species in a gaseous phase. The charged molecules are then accelerated by the application of magnetic

fields or electric fields which allow the separation of molecules or any further fragments according to their mass to charge ratio (*m*/*z*, the mass of the ion on the atomic scale divided by the number of charges that the ion possesses) (**Figure 1-10**) [112]. MS is the most common method used to determine and confirm the structure or identity of raw materials and drugs. In addition, it is widely used in drug discovery and for characterisation of impurities in drugs and excipients during the manufacturing processes. LC-MS and GC-MS are the methods of choice for highly sensitive and specific determinations of pharmaceutical compounds and metabolites within biological systems [94].

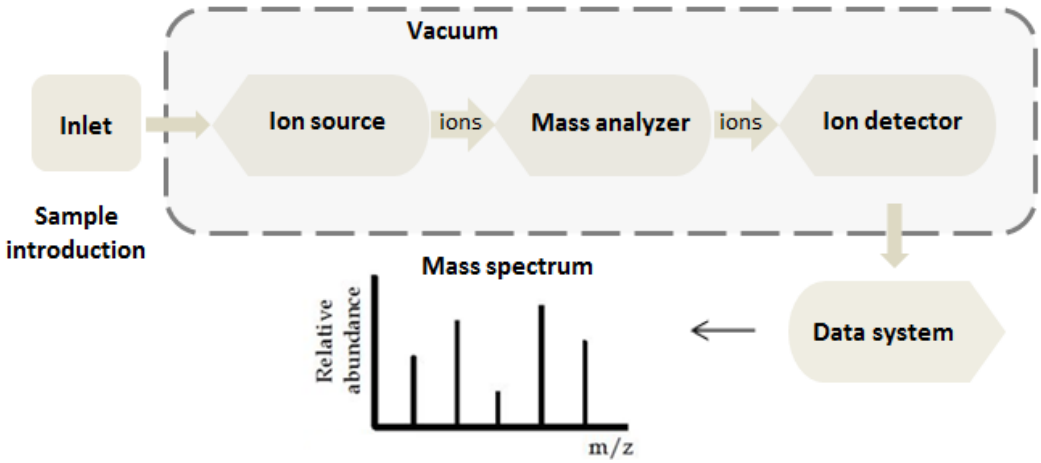

Figure 1-10: Illustration of the three major components of a mass spectrometry system. The sample is introduced into the ion source for the ionisation process, and then the ions are separated in the mass analyser according to their *m/z* ratio. Ions emerging from the analyser are converted into electrical signals in the detector for detection.

Figure 1-10 shows the five components of a mass spectrometer system: the sample inlet brings the sample from atmospheric pressure to a lower pressure. The sample is then transferred into the gas phase in the ion source part of instrument and the ions

are accelerated by an electrical or magnetic field. The sample ions separate according to their *m/z* ratios in the mass analyser and are counted by the detector. The ion signals are processed and recorded by the data system to provide a graph of the ions detected versus their *m/z* ratios (mass spectrum).

In terms of ion generation, three methods are commonly used: electrospray ionisation (ESI), atmospheric pressure chemical ionisation (APCI) and electron impact ionisation (EI). Other forms of ion generation include desorption ionisation (DI) techniques, which are used to analyse non-volatile and large molecules and can be categorised into three methods: fast atom bombardment (FAB), secondary ion mass spectrometry (SIMS) and matrix assisted laser desorption ionisation (MALDI) [110].

1.8.1 Electron impact ionisation (EI)

Electron impact ionisation (EI) was one of the first ionisation methods used before the development of ESI. EI techniques are not compatible with the use of HPLC as it has to operate under high vacuum. EI can only be used when the molecules can be introduced in the gas phase via gas chromatography or by a direct-heated probe. In EI, the sample is introduced to the ion source by heating it with a beam of high energy electrons (70 eV) from a filament until it evaporates and causes molecule ionisation (M^+). Extensive fragmentation of molecules occurs due to the large potential difference between the electrons used and the strengths of the bonds within the molecules (4–7 eV). A positively charged repeller plate directs the newly created positive ions towards the ion separation device or mass analyser (**Figure 1-11**). EI has advantages for routine applications and is considered a robust

and reproducible method. The complex fragmentation patterns of compounds produced by EI can be used as a fingerprint, which simplifies the process of confirming or determining the molecule identity [94].

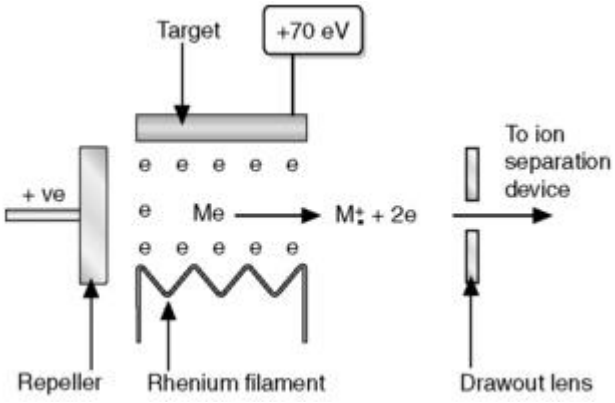

Figure 1-11: Ionisation process in an electron impact source. Figure adapted from [94]

1.8.2 Electrospray ionisation (ESI)

The phenomenon of electrospray of liquids is presented from the perspective of the electrical chemistry involved. ESI was first introduced and began to be popularised around 25 years ago, since most drug molecules can be ionised by this technique. It is currently the most widely applied method for ion generation because of its ready compatibility with HPLC [94]. ESI is used for quantitative and qualitative studies of simple organic and inorganic compounds, as well as complex biological fluids. It is conducted at a low flow rate under atmospheric pressure, with samples dissolved in polar solvents passed to the ionisation source through a metal or quartz needle (**Figure 1-12**).

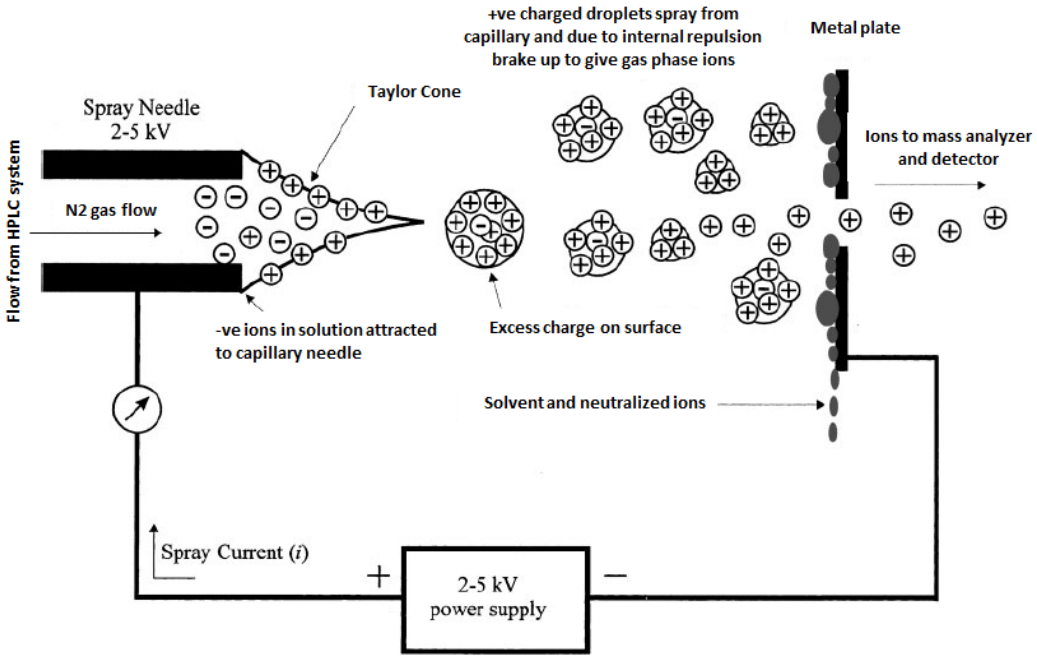

Figure 1-12: Schematic of the ESI process, as modified from [113].
The ESI solution is pumped through a capillary needle to which a high voltage is applied. Negative ions in the solution are stripped away by being attracted to the positively (+ve) charged needle, forming a 'Taylor cone'. Charged droplets are formed and the process repeats until gaseous ions are formed and move towards the mass analyser.

An electrical potential, which can be either negative or positive depending on the nature of the solute, is applied at the needle to form highly charged droplets (i.e. nebulisation) that are sprayed into the atmosphere. Under the influence of a neutral gas (e.g. nitrogen), the gaseous droplets are formed and driven electrically away from the needle. The droplets continue to break up due to internal charge repulsion, termed coulombic forces, where the repulsive force at the drop's surface become very high and exceeds the solvent surface tension, resulting in the formation of gas phase ions [114].

1.8.3 Atmospheric pressure chemical ionisation (APCI)

APCI is closely related to ESI, which is conducted under atmospheric pressure using a heated tube instead of passing the solvent through a charged needle. Gaseous molecules form by solvent evaporation in the presence of a heated drying gas. Ionisation of the gas phase molecules of the solute and solvent occur as they pass through a corona discharge electrode. Ionisation of the solvent molecules generates a reactive species which reacts with the analyte molecules to form a cluster and promotes their ionisation. APCI is mainly used for low to medium polarity compounds and can be applied at high flow rates. The mechanism of ionisation in APCI does not involve the formation of droplets, thereby reducing the matrix effects (ion suppression) [115].

1.8.4 Mass analysers

After ion generation, the mass analyser part of the instrument separates the charged ions generated in the ion source. A **magnetic sector,** a traditional analyser, separates the ions by employing a magnetic field. Ions pass through the electrostatic field region to narrow the range of their kinetic energy and then enter the magnetic field region [94].

Greater sensitivity and higher resolution are obtained with quadrupole mass analysers, which are set essentially as mass filters. This type of analyser is composed of four solid rods arranged parallel to the direction of the ion beam. In quadrupole instruments, two electric fields (+ve and -ve) are applied to the rods at right angles to

each other, creating a fluctuating electrostatic field. One of the fields is direct current (DC) and the other is alternating current (AC) at radiofrequency. Ions oscillate within this electrostatic field depending on the ratio between the two currents. The resonance frequency for each ion continues to increase until some ions strike one of the rods, while others undergo a stable oscillation and are detected. Ions which resonate at the frequency of the quadrupole are selected (**Figure 1-13**). The separation of ions depends on their *m/z* ratios and these can be selected to scan from low to high values [110].

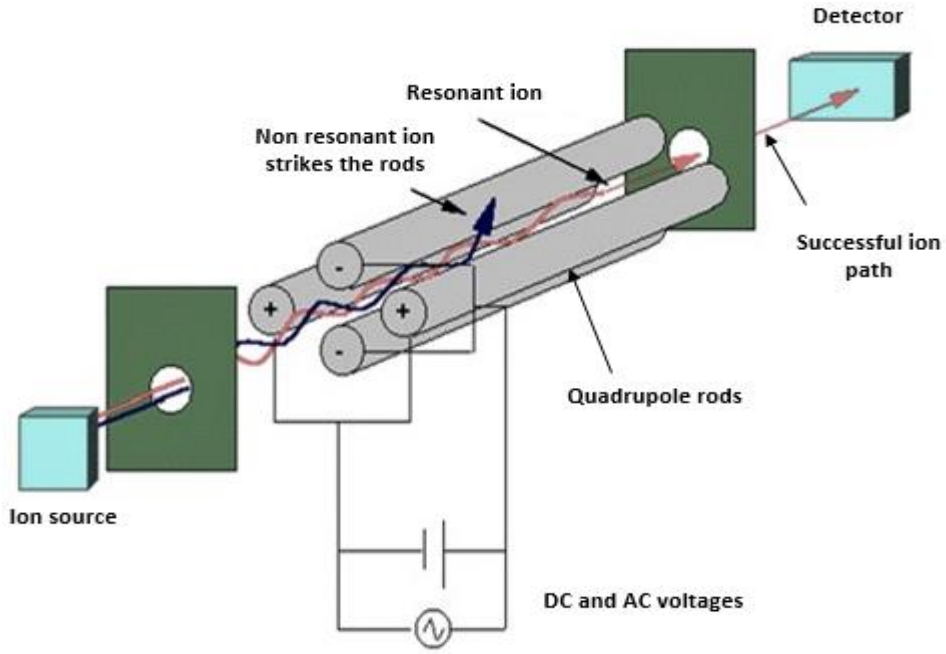

Figure 1-13: Separation of ions using a quadrupole mass analyser.
Resonant ions with specific *m/z* values pass into the detector. Obtained and modified from [116]

Ions can be separated using a high resolution mass analyser called a **Time-of-Flight (TOF)** analyser, where the ions generated by MALDI, ESI or APCI ion sources. Ions are filtered through quadrupole rods before entering the TOF separation stage, which

simply depends on the free flight of ions in a tube. The basis of the separation is that larger fragments will take longer and smaller fragments will reach the detector first. In order to avoid spectral overlap, a 'reflectron' device is used to focus the kinetic energy of the ions and send the ions back in the opposite direction. This increases the length of the flight tube and increases the instrument resolution [117].

Quadrupole ion trap (QIT) mass analysers produce a pure quadrupole electric field for trapping and analysing ions. A QIT instrument contains of a ring electrode, where the radiofrequency (RF) potential is applied, and two endcap electrodes, which are mainly used for ion injection from the ion source and ejection towards the detector by applying a DC potential. A light bath and gas (usually helium) is modulated in the ion traps to quench the ion energy and increase the instrument resolution and accuracy. The most common advantage of this device is the selectivity for a particular ion and the amount of control that can be exerted by changing the RF potential, increasing the numbers of ion fragments [118].

The **Orbitrap mass analyser** has the same principle of an ion trap, where the ions are introduced between a central and outer electrode. An electrostatic field is used to trap the ions and electrostatic attraction forces them to orbit around the central spindle electrode. The ion oscillations are independent of the initial energy, position and angles and are detected as an image current. A Fourier transform is employed to convert the frequencies of oscillation into highly accurate mass (*m/z* ratio) [119]. The Orbitrap mass analyser has several advantages, including high mass accuracy, high mass resolution and a high *m/z* range [120].

Tandem mass spectrometry (MS/MS), a multiple-step mass selection, relies on the separation of a specific *m/z* as a precursor ion in the first quadrupole, followed by a fragmentation process that can then be detected in the last quadrupole as a product ion. Tandem in space is a commonly used method that uses a triple quadrupole mass analyser (QqQ). The first quadrupole works as a mass filter (isolation process) to scan across a range of masses or to select a specific mass, followed by fragmentation of ions with a gas in a collision cell. After formation of the product ions, they can be selected as one or a few masses in the last quadrupole (second mass filter). Ions (which have some kinetic energy) collide with a neutral gas, causing the ions to fragment (in a process called Collision Induced Dissociation, or CID). Fragment ions can also be induced by alternative processes, such as electron-capture-induced dissociation and surface-induced dissociation [114]. Selected ion monitoring (SIM) is mainly used for structural studies in which the instrument is set to monitor a few *m/z* ratios. The selectivity is increased by selected reaction monitoring, which includes CID, as shown in **Figure 1-14** for a triple quadrupole mass spectrometer [100].

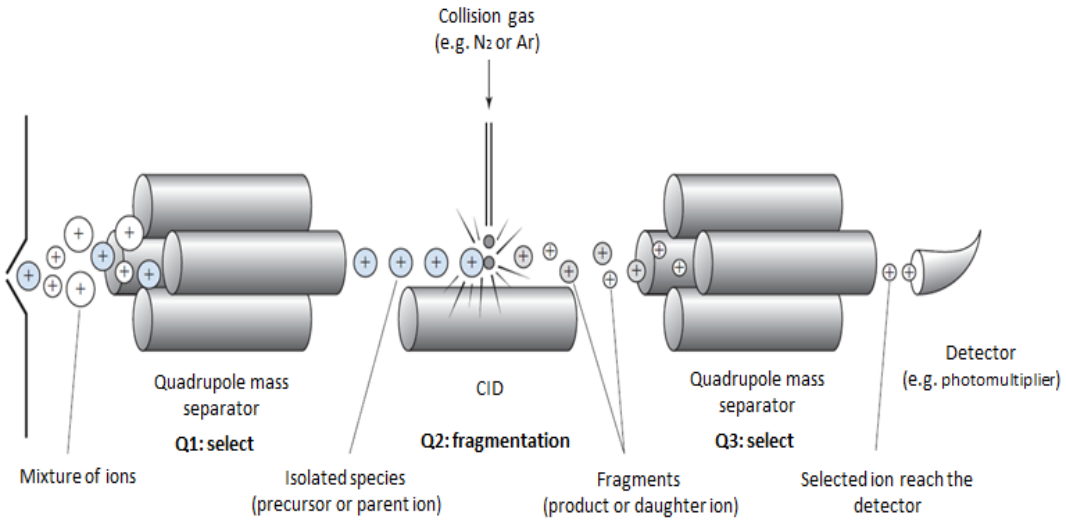

Figure 1-14: A schematic showing the principle of selected reaction monitoring in a tandem mass spectrometer, as modified from [100].
A specific ion is selected in Q1 and then subjected to collision in Q2, followed by the separation of the product ion before it reaches the detector.

1.9 Metabolomics

The word metabolomics can be defined in different ways, as no universal and agreed upon definition yet exists. However, it can be defined as the unbiased global survey of small MW molecules or metabolites in a biofluid, organism, organ, tissue or cell with the aim of characterising, understanding and measuring the chemical processing of metabolites and evaluating the changes in metabolites resulting from treatments or different diseases. Metabolites are the basic downstream products of transcriptomic, genomic and proteomic perturbations; therefore, changes in a biological system would be reflected in the changes in metabolite fluxes or concentrations [121]. One area where metabolomics is playing a key role is in drug metabolism investigations, which have become an essential part of drug development, toxicity studies and clinical therapies. Drugs are eliminated from the body by transforming the drug into, most often, inactive products with greater polarity than the parent drug. These metabolites can sometimes be reactive and cause toxicity by binding covalently to RNA, DNA or proteins [122].

Several instruments can be effectively used for metabolomics studies. NMR-based metabolomics studies are abundant. However, instruments with high sensitivity and resolution are required for the identification of small molecular weight metabolites. This can be achieved with mass spectrometry (MS) analysis which is now increasingly being used. Liquid chromatography coupled with MS (LC-MS) is the prevailing method used for metabolomics analysis, as LC-MS has the advantages of faster run times and an absence of the chemical derivatisations required for gas chromatography-MS (GC-MS) [10, 123].

Metabolomics experiments are designed using either targeted or untargeted approaches. In a targeted approach, a specific list of metabolites of known identity is measured. This method is used to investigate one or more pathways of interest and is widely used in pharmacokinetic studies of drug metabolism, as well as for detection of specific enzymes influenced by therapeutic or genetic modifications. Generally, a highly sensitive and robust method (e.g. QqQ-MS) is used extensively to quantify low-concentration metabolites with high throughput. Untargeted metabolomics provides an untargeted profile of the metabolome within biological fluids. LC-MS is the method of choice for this type of measurement, as it gives numerous peaks for the detected ions.

Interpreting untargeted profiling data is difficult and complicated, due to possible small deviations in retention time from sample to sample due to column degradation or fluctuations in the mobile phase pH and temperature, which need manual inspection. However, data analysis has been made possible by the advances in informatics tools and software, such as MzMine and Mzmatch [124]. The ultimate objective of metabolomics is to determine as many metabolites from the samples as possible and then to link the expressed metabolites with different experimental factors.

Table 1-4: Definitions of terms related to metabolomics [125, 126]

Term	Definition
Metabolite	A small molecule produced from enzyme-catalysed reactions that occur naturally within the cells to support growth, maintenance and normal function of the cells.
Metabolome	The complete set of metabolites present within an organism.
Metabolomics	Scientific study of all metabolites for identification and quantification purpose.
Metabolic profiling	Quantitative analysis of low molecular weight metabolites and their intermediates within biological system. This varies from a wide range of metabolites (untargeted) to a very limited number of metabolites (targeted).
Metabolic fingerprinting	A global, high-throughput screening approach to classify samples from different biological status (i.e. treatment/control or disease/healthy) based on metabolite patterns.
Metabolic footprinting	Analysis of extracellular metabolites excreted/uptake by cells into the cell culture medium.

1.9.1 Metabolomics data analysis

Data generation generally includes sample collection, pre-treatment and analytical measurements. Data acquisition should aim to minimise the variation of nuisance to optimise the quantification process, such as analytical measurement variations and sample handling. The variations in measurement can come from different lab processes, such as differences in the efficiency of derivatisation as well as instrumental drifts. However, control of the biological samples is more important during the analysis of large sets of metabolites to minimise the matrix effect. The

variability within the analytical measurements is corrected and controlled using a number of strategies, such as the use of internal standards and pooled or quality control (QC) samples [127] .

Several important steps, such as data pre-processing and data pre-treatment, should be performed prior to statistical analysis. For LC-MS metabolomics, raw data are reduced in complexity by subjecting them to a *pre-processing* step, such as spectral deconvolution, alignment and normalisation, using several available software programs. Peak deconvolution and detection are crucial steps that detect and quantify each measured ion in the sample and assign a feature of *m/z*-t_R pair. In this step, peak deconvolutions are obtained from the extracted ion chromatogram, taking into account the baseline noise. In data *pre-treatment*, centering the data is able to remove the offset from the data and focus on biological variation. Consequently, scaling is needed to consider the low abundance metabolites apart from the large contributions of high abundance metabolites to the model. In addition, data transformations, such as log and power transformations, might be necessary before applying centering or scaling the data [128]. Several software tools, such as mzMine and mzMatch, are available for LC-MS metabolomics data analysis and spectral processing. Once the metabolic features, such as spectral peak area and metabolite concentrations, are robustly quantified, multiple chemometric methods can be used to perform the study analysis. The design of the classification models needs to be validated to estimate the performance of the models when applied to new samples. Permutation tests are one of the most widely used tests for the validation purposes. These tests can be

conducted using several software programs; however, SIMCA-P software is commonly used for multivariate analysis.

1.9.2 Data modelling

Univariate methods analyse metabolomics data independently and are very common and easy methods for statistical analysis. However, the main drawback is that they do not take into account the interactions between metabolites, as occurs in most biological samples. In addition, univariate analysis does not take into account the confounding variables, such as gender, age and diet, so it increases the possibility of obtaining false results. By contrast, multivariate analysis considers all metabolomics features and works simultaneously to identify the patterns of the relationship between them. In biological samples, data modelling is used to explore valuable information and to identify the metabolomics groups. Various multivariate analysis methods are described below and can be classified into supervised (i.e. identification of treatment differences) and unsupervised (i.e. discovering the sample patterns) methods [129].

1.9.2.1 Unsupervised methods

The similarity patterns within the metabolomics data can be identified using unsupervised methods, where the types and classes of the metabolites are not taken into account. An unsupervised method is normally used to represent the complex metabolomics data and identify the clusters in the data. Principle Component Analysis (PCA) and Hierarchical Cluster Analysis (HCA) are the most common statistical methods used in an unsupervised model which aims to categorise the samples into groups of similar characteristics [130].

PCA is the fundamental method used for multivariate data analysis. It is a non-supervised method and is based on the linear transformations of metabolic data into a set of linear uncorrelated variables. PCA transforms the high dimensional variables of metabolomics datasets into a small number of orthogonal factors, with the aim of providing them as lower dimensionality output data. PCA analysis is applied to ensure that the data are reduced to a few underlying components (principle components) [131]. PCA is normally employed to explore and visualise the sample distribution at the start of an analysis, in order to detect groups, trends and outliers. It is the method of choice for examining instrument reproducibility, which can be achieved by analysing QC samples.

Hierarchical Cluster Analysis (HCA), a non-supervised clustering method, is used to set a natural clustering of samples and variables. The result is usually visualised in a dendrogram, with the clustering procedure of the samples provided according to a predefined distance measure. Thus, each single object is considered as part of a cluster, and the minimal distance between clusters is found again, and they are clustered again. In general, HCA is a suitable method for detecting non-linear parameters and visualising metabolic phenotypes [129].

1.9.2.2 Supervised methods

Supervised methods are those used to determine the metabolic patterns that are correlated with the phenotypic variable of interest while suppressing other variance sources. Partial least squares (PLS) is the most widely used supervised multivariate linear regression method and it has a similar concept to PCA. It finds the relationships between the data and their response (data X & response Y); however,

and unlike PCA, PLS maximises the covariance of the latent variables but does not maximise the explained dataset variance [129]. PLS is also used as a binary classifier by PLS Discriminant Analysis (PLS-DA), which has the ability to handle highly collinear data and effectively discover a biomarker. However, the disadvantages of PLS is that some metabolic features that are not correlated with the variable of interest can affect the results. Orthogonal PLS (O-PLS) was developed to address this problem [131].

OPLS is a modification of the PLS method, but it provides a better interpretation of the variables with the same predictive power. It decomposes the data into information related to a response Y "predictive" and that is not related to the Y "orthogonal". OPLS Discriminant Analysis (OPLS-DA) has been widely used in the metabolomics field, and it is now the method of choice for multivariate linear models for classification (i.e. classifying new objects into one of the classes) and class discrimination (i.e. separating two classes and investigate the reasons for the class separation), such as biomarker discovery and lower and higher concentrations of metabolites (**Figure 1-15A**) [128].

1.9.3 Model validation

An OPLS-DS model is usually validated using cross-validation-ANOVA (CV-ANOVA), which compares the size of the residuals of two models applied to the same data. CV-ANOVA corresponds to the H0 hypothesis of an equal cross-validated predictive residual of the supervised model around the mean. It is considered easy to evaluate since it provides a *p*-value (where $p < 0.05$ denotes a significant model) [132]. The model can also be validated by a permutation test, which repeatedly permutes the responses/labels of samples to estimate the distribution under the null hypothesis of the test [133]. The permutation test consists of comparing the R2 and Q2 obtained for the original dataset with the permuted R2 and Q2 values. These new permuted responses should be lower than the original ones, or the predictive model regression line should cross the horizontal zero line (**Figure 1-15B**) [134].

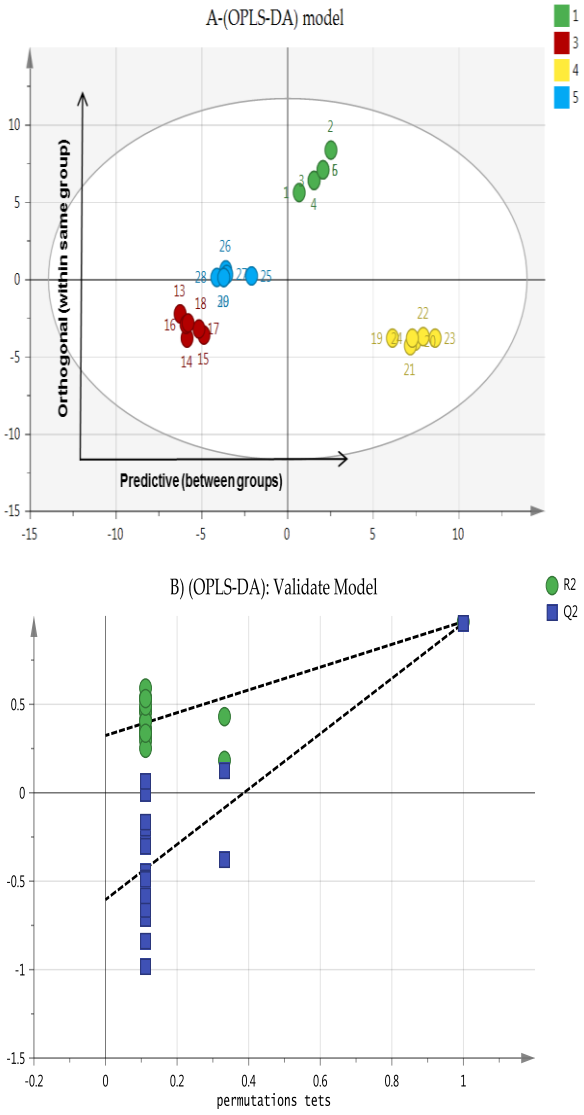

Figure 1-15: (A) OPLS-DA score plot versus **(B)** Permutation test.
A) The OPLS-DA score plot shows four groups of treatments, which are clearly separated horizontally (t-predictive) and vertically (orthogonal). The model was significantly validated with *p* value associated with the cross-validation (CV)-ANOVA = 1.188×10^{-24}. **B)** The plot shows that the vertical axis gives the R2Y and Q2Y values of each model. The horizontal axis represents the correlation coefficient between the original Y (= 1.0), and the permuted Y. If the supervised model has valid predictive ability, the R2Y and Q2Y of the original model are always higher than the corresponding values of the models fitted to the permuted responses.

1.10 Hypothesis, aims and objectives:

General hypothesis: Natural compounds contain useful biologically active compounds which can be used in medical treatment.

In the current study, the general aim was to assess the changes in the metabolic profiling of THP-1 derived-macrophages cells in response to different natural compounds as following:

Aim 1: To assess the synergistic effects of melittin on phorbol-12-myristate-13-acetate (PMA)-differentiated THP-1 cells induced by lipopolysaccharide (LPS).

Specific objectives:

- To repeat and confirm the previous developed method [135] used to isolate and fractionate melittin from whole bee venom sample.
- To measure the viability of THP-1 monocytes and PMA-differentiated THP-1 macrophages after exposure to melittin.
- To determine the pro-inflammatory (TNF-α, IL-1β, and IL-6) and anti-inflammatory (IL-10) cytokine levels in response to melittin in the presence and absence of LPS.
- To characterise the metabolomic effects induced by melittin in THP-1 derived-macrophages in the presence or absence of LPS.
- To carry out lipidomic analysis of the effects of melittin in THP-1 derived-macrophages in the presence or absence of LPS.

Aim 2: To assess the anti-inflammatory effects of propolis extracts on PMA-differentiated THP-1 cells induced by LPS.

Specific objectives:

- To measure the viability of PMA-differentiated THP-1 after exposure to propolis ethanolic extracts from different regions.
- To determine the pro-inflammatory (TNF-α, IL-1β, and IL-6) and anti-inflammatory (IL-10) cytokines levels by the effect of propolis samples in the presence and absence of LPS.
- To characterise the metabolomic effects of Cameroonian propolis extract in THP-1 derived-macrophages cells in the presence and absence of LPS.

Aim 3: To assess the synergistic effects of (Z)-11-eicosenol with its derivations methyl cis-11-eicosenoate and cis-11-eicosenoic acid on PMA-differentiated THP-1 cells induced by LPS.

Specific objectives:

- To synthesise (Z)-11-eicosenol, elucidate the structure and confirm the structure with the one compound isolated previously from bee venom [136].
- To measure the viability of PMA-differentiated THP-1 after exposure to eicosenoid compounds.

- To determine the pro-inflammatory (TNF-α, IL-1β, and IL-6) and anti-inflammatory (IL-10) cytokine levels in response to eicosenoid compounds in the presence and absence of LPS.
- To characterise the metabolomic effects induced by eicosenoid compounds in THP-1 derived-macrophages cells in the presence and absence of LPS.
- To carry out lipidomic analysis of the effects of eicosenoid compounds in THP-1 derived-macrophages in the presence and absence of LPS.

Aim 4: To assess the anti-inflammatory effects of Gypenoside on PMA-differentiated THP-1 cells induced by LPS.

Specific objectives:

- To measure the viability of PMA-differentiated THP-1 after exposure to gypenoside.
- To determine the pro-inflammatory (TNF-α, IL-1β, and IL-6) and anti-inflammatory (IL-10) cytokines levels in response to gypenoside in the presence and absence of LPS.
- To characterise the metabolomic effects of gypenoside in THP-1 derived macrophages cells in the presence and absence of LPS.

Chapter Two

Material and Methods

2.1 Chemicals and solvents

HPLC grade methanol, acetonitrile, ethanol, acetic acid and water were purchased from Sigma- Aldrich (Dorset, UK). Sulfuric acid solution obtained from Fluka® analytical (Munich, Germany) Ammonium carbonate, sodium chloride, sodium phosphate, potassium chloride, potassium phosphate and all the analytical standards used for evaluation or development were purchased from Sigma-Aldrich, UK. Dimethyl sulfoxide (DMSO) was obtained from Sigma- Aldrich (Dorset, UK).

2.2 Cell culture methods

2.2.1 Cell Culture and Differentiation

The THP-1 human cell line was obtained from American Type Culture Collection-ATCC® (Porton Down, Salisbury, UK) and maintained at a 1×10^5 cells/mL seeding density in Roswell Park Memorial Institute (RPMI) 1640 (Thermo Fisher Scientific, Loughborough, UK) containing 10% (*v*/*v*) foetal calf serum (FCS) (Life Tech, Paisley, UK), 2 mmol/L L-glutamine (LifeTech, Paisley, UK) and 100 IU/100 µg/mL penicillin/streptomycin (Life Tech, Paisley, UK). Cells were sub-cultured using fresh media every 2–4 days and maintained in an incubator (37 °C, 5% CO_2, 100% humidity). THP-1 cells were differentiated using PMA (Sigma-Aldrich, Dorest, UK) at a final concentration of 60 ng/mL and incubated for 48 h. THP-1 differentiated cell was rested for a further 24 h by removing the PMA-containing media and adding fresh media. Cells were checked under a light microscope for the evidence of differentiation.

2.2.2 Cell Viability Assay

THP-1 cells were seeded at a density of 1×10^5 cells/well in 96-well plates and incubated for 24 h at 37 °C in a humidified atmosphere of 5% CO_2. After 24 h, the cells were treated with different concentrations of investigated samples and incubated for a further 24 h. Controls included cells alone (no treatment), medium alone (background) and dimethyl sulphoxide (DMSO, positive) were added. Resazurin salt solution (0.1 mg/mL) was added at a final concentration of 10% (*v*/*v*) and the plates were incubated for a further 24 h. Fluorescence readings were taken using a SpectraMax M5 plate reader (Molecular Devices, Sunnyvale, CA, USA) at λEx of 560 nm and λEm of 590 nm. After background correction, cell viability for each concentration was calculated relative to the mean value of negative control (*n* = 3). GraphPad Prism for Windows (version 5.00, GraphPad Software, San Diego, CA, USA) was used to obtain dose–response curves and mean inhibitory concentration (IC50) values.

2.3 Cytokine Production

Following differentiation, the cells were incubated with final concentrations of investigated samples with and without LPS (Sigma-Aldrich) (0.5 µg/mL) for an additional 24 h. Conditioned medium was collected and frozen until required for Enzyme-Linked Immunosorbent Assay (ELISA) (*n* = 3).

2.4 Enzyme-Linked Immunosorbent Assay (ELISA).

ELISA Ready-Set-Go kits were purchased from Thermo Fisher Scientific (Loughborough, UK). The assays were performed according to the manufacturer's instructions to quantify the release of inflammatory cytokines (TNF-α, IL-1β, IL-6

and IL-10). The reaction was stopped using acid solution (1 M sulphuric acid). The plates were read using a SpectraMax M5 plate reader (Molecular Devices, Sunnyvale, CA, USA) at 560 nm and the absorbance values were corrected by subtracting readings taken at 570 nm.

Standard calibration curves were plotted by fitting the optical density (OD) data of TNF-α, IL-1β, IL-6 and IL-10 to 4-parameter logistic (4-PL) regression curves. Each of these standards were prepared in duplicate at each of the concentrations in the ranges recommended by the manufacturer. The regression analysis also computes the R2 value which gives an indication of how best the fitted curve agrees with the data. the concentrations of TNF-α, IL-1β and IL-6 induced by each of the samples assayed (with and without LPS) were calculated and expressed as ratios of the mean cytokine level induced by LPS (positive control), assayed in triplicate (n=3). The resulting data were then analysed with GraphPad Prism to obtain bar graphs whose statistical significances were tested at 95% confidence level relative to the mean positive control LPS.

2.5 LC-MS Conditions

2.5.1 HPLC setup

The system was purged with 100% of each mobile phase for 5 min at a flow rate of 5mL/min. The auto-sampler was flushed using methanol:water (1:1). Appropriate HPLC columns used for the separation of polar and non-polar metabolites. Each column washed for 10 min a flow rate of 0.3 mL/min using mobile phase used during the run.

2.5.2 Chromatographic conditions for columns

A ZIC-pHILIC (150 × 4.6 mm, 5 µm) and ACE C4 (150 × 3.0 mm, 3 µm) HPLC columns supplied by HiChrom (Reading, UK) were used. Samples were run on LC-MS under the conditions shown in **Table 2-1,** where **Table 2-1**the ZIC-pHILIC mobile phase consisted of 20 mM ammonium carbonate in HPLC-grade water (A) and acetonitrile (B). For the ACE C4 column, the mobile phase was 1 mM acetic acid in water (A) and 1 mM acetic acid in acetonitrile (B) (**Table 2-2**).

Table 2-1: ZIC-pHILIC gradient elution program applied in LC-MS

Time (min)	Mobile phase A %	Mobile phase B %	Flow rate (µL/min)
0.00	20.00	80.00	300.0
30.00	80.00	20.00	300.0
31.00	92.00	8.00	300.0
36.00	92.00	8.00	300.0
37.00	20.00	80.00	300.0
46.00	20.00	80.00	300.0

Table 2-2: ACE C4 gradient elution program applied in LC-MS

Time (min)	Mobile phase A %	Mobile phase B %	Flow rate (µL/mim)
0.00	60.00	40.00	400.0
30.00	00.00	100.00	400.0
36.00	00.00	100.00	400.0
37.00	60.00	40.00	400.0
41.00	60.00	40.00	400.0

2.5.3 An ESI-Exactive Orbitrap setup

An Accela HPLC system interfaced to an Exactive Orbitrap mass spectrometer (Thermo Fisher Scientific, Bremen, Germany) was used for the liquid chromatographic separations. The nitrogen sheath and auxiliary gas flow rates were maintained at 50 and 17 arbitrary units. The electrospray ionisation (ESI) interface was employed in a positive/negative dual polarity mode, with a spray voltage of 4.5 kV for positive mode and 4.0 kV for negative mode, while the ion transfer capillary temperature was set at 275 °C. Full scan data were obtained in the mass-to-charge ratio (*m*/*z*) between 75 and 1200 amu for both ionisation modes. Mass calibration was performed for both positive and negative ESI polarities before the analysis using the standard Thermo Calmix solution (Thermo Fisher Scientific, Bremen, Germany) with additional coverage of the lower mass range with signals at *m/z* 83.0604 (2×ACN+H) and *m/z* 195.03765 (caffeine) for the positive and *m/z* 91.0037 (2×HCOO-) for the negative modes respectively. The MS accuracy was tested using standard analytes with intensities between (10^4 -10^7) to check mass accuracy. The calibrant peaks were checked to make sure that the mass deviations were less than 3 ppm; otherwise, the instrument need to be recalibrated to correct the mass errors. The data were collected and processed using Xcalibur 2.1.0 software (Thermo Fisher Scientific, Bremen, Germany). The outcome data quality evaluated using standard mixtures runs with each set of samples to check the peak width, height, retention time and peak resolutions.

2.6 Metabolite Extraction

The PMA-differentiated THP-1 cells were seeded for 48 h in 6-well plates at a density of 4.5×10^5 cells/well (n = 6). The medium was aspirated and replaced with fresh medium for a further 24 h, and then the cells were incubated with LPS (0.5 µg/mL) or a combination of LPS and the investigated samples for an additional 24 h. The medium was then aspirated, and the cells were washed with 3 mL of phosphate-buffered saline (PBS) (Sigma-Aldrich). The cells were extracted (1 mL per 1×10^6 cells) using ice cold extraction solution (methanol:acetonitrile:water, 50:30:20 (*v*/*v*), containing 5 µg/mL of internal standard $^{13}C_2$ glycine (Sigma-Aldrich, Poole, UK)). The cells were scraped, and cell lysates were mixed in a Thermomixer (12 min, 4 °C), and then centrifuged for 15 min at 0 °C (20412 G). The supernatants were collected and stored at −80 °C until required for LC-MS analysis. The stability and reproducibility of the analytical method were ensured by injecting authentic standard metabolite mixtures and quality control (QC) samples throughout the runs. The analytical standards were prepared by adding 10 µg/mL final concentration of each metabolite standard [137] containing $^{13}C_2$ glycine, distributed into seven different standard solutions. The pooled quality control samples were prepared by pipetting 20 µL from each of the samples and mixing them together before transferring them into a high performance liquid chromatography (HPLC) vial.

2.7 Data extraction, processing and statistical analysis

The data were extracted using MZMatch software (SourceForge, La Jolla, USA), http://mzmatch.sourceforge.net/). A macro-enabled Excel Ideom file was used to filter, compare and identify the metabolites

(http://mzmatch.sourceforge.net/ideom.php). The metabolite lists obtained from these searches were then carefully evaluated manually by considering the quality of their peaks and the metabolites were matched with the retention times of authentic standards mixtures run in the same sequences. Library searches were also used for identification and carried out against accurate mass data of the metabolites in the Human Metabolome Data Base, lipid maps and KEGG (Kyoto Encyclopedia of Genes and Genomes). All metabolites were within 3 ppm of their exact masses. Metaboanalyst 3.0 (www.metaboanalyst.ca), a web-based metabolomic data processing tool, was employed also for univariate analysis.

Univariate comparisons were performed using Microsoft Excel and paired t-tests between treated and control cells and differences were considered significant at $p < 0.05$. SIMCA-P software v.14.0 (Umetrics, Umea, Sweden) was used for visualisation and multivariate analysis of the metabolite data by fitting PCA-X and OPLS-DA. Data were log2-transformed and then Pareto scaled, where the responses for each variable were centered by subtracting its mean value and then dividing by the square root of its standard deviation [138]. The RSD of each metabolite was also calculated based on the reading of the pooled sample that run throughout the sequence and metabolites with RSD higher than 30% were excluded. An unsupervised model (PCA) was used for data visualization and to explore how variables clustered based on their metabolic composition regardless of their grouping. In case with the OPLS-DA, the supervised model, the discrimination between groups was applied by neglecting the systemic variations [139].

OPLS-DA models were validated based on multiple correlation coefficient (R2) and cross-validated R2 (Q2) as a diagnostic tools in cross-validation and permutation test. Where, the R2 reflects the percentage of variation explained by the model, while Q2 indicates the percentage of variation in response to cross validation [139]. The model also validated using cross validation ANOVA (CV-ANOVA). A permutations test was also applied to supervised models as a model validation, which were considered valid if they matched the characteristics described previously in (section 0).

2.8 Metabolomics analysis workflow:

The figure 2.1 describes simply the metabolic workflow and the experimental design that followed during each run of samples.

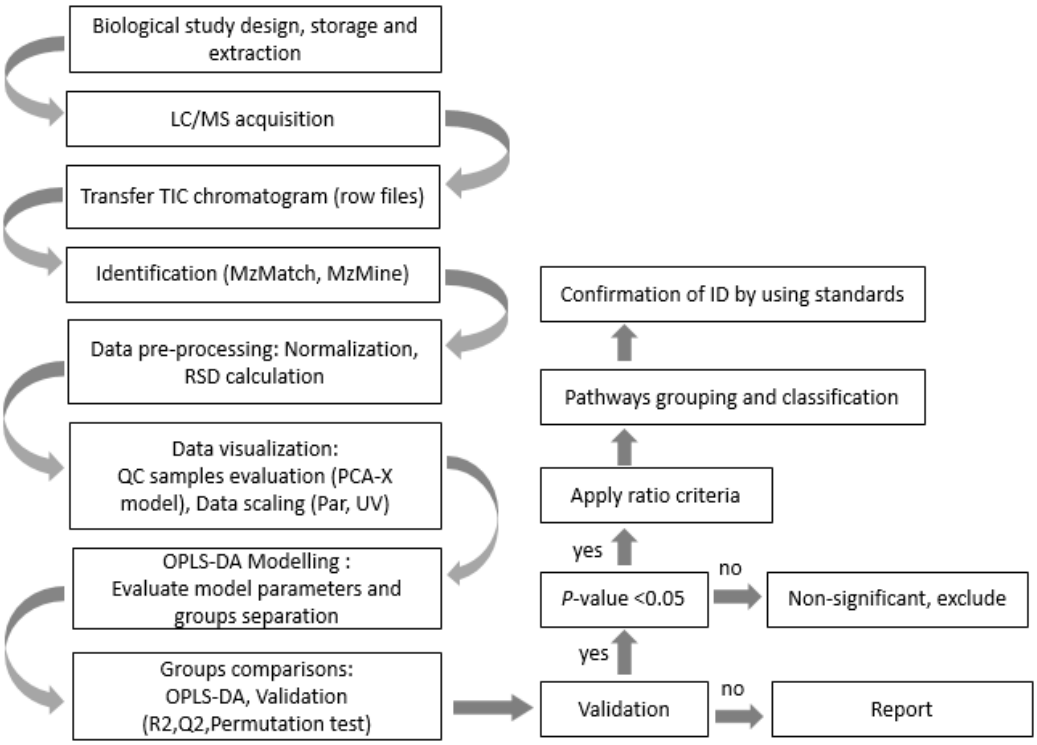

Figure 2-1: Illustration of metabolomics analysis workflow.

Chapter Three

Effect of Melittin on Metabolomic Profile and Cytokine Production in PMA-Differentiated THP-1 Cells

3 Effect of Melittin on Metabolomic Profile and Cytokine Production in PMA-Differentiated THP-1 Cells

3.1 Abstract

Melittin, the major active peptide of honeybee venom (BV), has potential for use in adjuvant immunotherapy. The immune system response to different stimuli depends on the secretion of different metabolites from macrophages. One potent stimulus is lipopolysaccharide (LPS), a component isolated from gram-negative bacteria, which induces the secretion of pro-inflammatory cytokines in macrophage cell cultures. This secretion is amplified when LPS is combined with melittin. In the present study, pure melittin was isolated from whole BV by flash chromatography to obtain pure melittin. The ability of melittin to enhance the release of tumour necrosis factor-α (TNF-α), Interleukin (IL-1β, IL-6, and IL-10) cytokines from a macrophage cell line (THP-1) was then assessed. The response to melittin and LPS, applied alone or in combination, was characterised by metabolic profiling, and the metabolomics results were used to evaluate the potential of melittin as an immune adjuvant therapy. The addition of melittin enhanced the release of inflammatory cytokines induced by LPS. Effective chromatographic separation of metabolites was obtained by liquid chromatography-mass spectrometry (LC-MS) using a ZIC-pHILIC column and an ACE C4 column. The levels of 108 polar and non-polar metabolites were significantly changed ($p < 0.05$) following cell activation by the combination of LPS and melittin when compared to untreated control cells. Overall, the findings of this study suggested that melittin might have a potential application as a vaccine adjuvant.

3.2 Introduction

Correct recognition of inflammatory signals in the body is vital to avoid the risk of autoimmune and chronic inflammatory diseases. Many of these signals arise from macrophages, and thus determination and investigation of the composition of local tissue microenvironments (e.g., metabolites, cytokines, and inflammatory signals) can be performed in order to understand the metabolic behaviour of macrophages following their activation [140]. Inflammation is a primary process that is triggered as a protective response to any stimulus of the innate immune system, such as injuries or infections, which pose a real threat to normal cell biology [141]. Inflammation can be initiated by first-line macrophage cells and dendritic cells to protect the body from external pathogens. Pathogen-associated molecular patterns (PAMPs) present in the invaders are recognised by specific receptors, the pattern recognition receptors (PRRs), present on the surface of these cells. PRRs play a crucial role in the stimulation of the innate immune system and the resulting signalling cascade [142]. The pathogen is targeted by the release of antimicrobial mediators, while further immune cells are recruited to the infection site by chemokine secretion. These chemokines include pro-inflammatory cytokines released by T and B lymphocytes to induce further inflammation and activate the adaptive immune response [143]. Several classes of PRRs have been characterised and investigated, including the toll-like receptors (TLRs) which are expressed on plasma membranes and activated by lipopolysaccharides (LPSs) from gram-negative bacteria [144].

The biosynthesis and/or depletion of cellular metabolites in response to pathogen invasion results in rapid alteration in the cellular metabolome [145]. Upon activation, innate immune cells undergo metabolic changes that can be described as similar to those that occur in cancer cells (Warburg effect) [143]. In the presence of oxygen, the metabolic profile of a tumour shows an increase in glycolysis under normoxic conditions, so that metabolism is shifted to produce lactic acid from pyruvate instead of the acetyl-CoA needed to feed the tricarboxylic acid (TCA) cycle and oxidative phosphorylation (OXPHOS) to generate adenosine triphosphate (ATP) [146]. The consumption of glucose and oxygen has long been known to increase in response to activation of TLR4 in innate immune cells by LPS. However, this oxygen consumption also reflects an increased generation of reactive oxygen species (ROS) [147]. Some enzymes in the glycolysis pathway, such as hexokinase and glucose-6-phosphate dehydrogenase, also show increased expression, leading to a further increase in glycolytic activities [148]. Inflammatory macrophages, when induced with LPS to release pro-inflammatory cytokines, therefore show a decreased utilisation of both the TCA cycle and OXPHOS metabolites as a consequence of this increase in glycolysis (glucose to lactate) to compensate the lack of ATP production via oxidative phosphorylation [149, 150]. Interestingly, the cell metabolite adaptation occurs even in the presence of "aerobic glycolysis" [151]. This metabolic adaptation works as a survival response that serves to maintain mitochondrial membrane potential and cell integrity [152].

Understanding the process of macrophage activation by LPS is important for the identification of suitable immune stimulators, and these metabolic shifts could

therefore be useful in this type of research. Macrophages stimulated by LPS generally show one or more of the following main metabolic shifts [143], which result in the expression of specific sets of genes. The first is a highly increased expression of inducible nitric oxide synthase (iNOS), which leads to the generation of citrulline and nitric oxide (NO) [153]. The latter results in the process of iron–sulphur protein nitrosylation in the electron transport chain which decreases mitochondrial respiration by inhibiting OXPHOS [154]. The second shift occurs due to activation of the glycolysis pathway in macrophages through activation of hypoxia inducible factor-1α (HIF-1α) [143], which then promotes the expression of its target genes, such as GLUT1 [155] and lactate dehydrogenase [156]. The increase in HIF-1α expression can be achieved by the activation of the mammalian target of rapamycin (mTOR), which is promoted by the translation of mRNAs with 5'TOP (5'-terminal oligopyrimidine) [157]. The third shift arises by an increase in the expression of phosphofructokinase-2 (PFK2) isoforms (i.e., u-PFK2), which causes an increase in the level of fructose-2,6-bisphosphate (F-2,6-BP) and activates the 6-phosphofructo-1-kinase glycolytic enzyme [158]. The fourth shift is due to inactivation of adenosine monophosphate-activated protein kinase (AMPK) in macrophages, which causes a decrease in fatty acid β-oxidation and mitochondrial metabolism. These actions boost the biosynthesis of inflammatory mediators and inhibit the catabolic pathways of the AMPK enzyme [159].

One promising immune modulator is melittin, the major lytic peptide of bee venom (BV). Many compounds have been isolated from BV, but melittin is the major component, accounting for as much as 50–60% of dried whole BV. Other

components include peptides and proteins such as apamine, mast cell degranulating (MCD) peptide, secapin, adolapin, phospholipase A2, and hyaluronidase [12]. The enzymes, though present in relatively small amounts, are notable for being powerful allergens, and in some cases (e.g., phospholipase A2) synergise directly with melittin in its lytic action. Melittin is a 26-mer peptide with a characteristic sequence that provides the peptide chain with amphiphilic detergent-like properties and a high positive charge. It can self-assemble into tetramers depending on conditions [29, 34] and has attracted considerable attention for its potential for selective destruction of cancer cells [160, 161].

Melittin shows antiviral, antifungal, antibacterial, and anti-parasitic properties according to several studies and has been proposed to act at cell membrane level [162-164]. However, previous results regarding the effect of melittin on the immune system are inconsistent, indicating a need to perform more investigations. For example, melittin was characterised as an inhibitor of the release of prostaglandin E2 (PGE2) and nitric oxide (NO) from LPS-treated RAW 264.7 cells and synoviocytes, which showed a dose dependent inhibition of LPS-induced Cyclooxygenase enzyme (COX-2) and iNOS when treated with BV and melittin [165]. Similarly, melittin treatment of Propionibacterium acnes (*P. acnes*)-induced THP-1 monocytes significantly inhibited production of the pro-inflammatory cytokines TNF-α and IL-1β and cleavage of caspase-2 and -8 [166]. The mechanism of this inhibition was believed to occur in one of two possible ways: by the inhibition of Nuclear factor-kappa B (NF-κb) activation by melittin through interaction with the p50 subunit or by phosphorylation of IκB subunit [165, 167]. The NF-κB transcription factor is

crucial in inflammation as the expression of most of the pro-inflammatory genes rely on activation by this factor [168]. Anti-inflammatory activity of melittin and its interaction with LPS was referred to its amino acid sequences, particularly hydrophobic leucine zipper sequence [169]. By contrast, Stuhlmeier reported that neither BV nor melittin blocked IL-1β induced activation of NF-κB or had any effect on IκB phosphorylation or degradation using electrophoretic mobility shift (EMSA) assay in several cell types [12]. Moreover, BV and melittin, even at high concentrations, did not compete for NF-κB-p50-DNA binding or show any interactions. However, the mRNA levels of many types of pro-inflammatory genes and COX-2 protein were significantly elevated following exposure to BV and melittin. In addition, oxygen radicals were released in large amounts in a dose-dependent manner in response to BV treatment [12]. Another study, which examined the effects of BV and its isolated compounds on the production of pro-inflammatory cytokines in phorbol 12-myristate 13-acetate (PMA)-differentiated U937 cells, showed that the expressions of TNF-α, IL-1β, and IL-6 cytokines increased in response to melittin and LPS co-stimulation when compared to LPS stimulation alone [136].

Melittin can also be used as an adsorption enhancer in Caco-2 cells [170], indicating its possible usefulness as an adjuvant for nasal administrations [171]. In addition, melittin has been reported to enhance antibody titres when co-administered with tetanus and diphtheria toxoid, which facilitated the longevity of the immune response when compared to antigen administration alone [172]. Based on these observations, melittin shows significant effects on cell inflammatory signalling, which support the

use of melittin as an efficient immunomodulatory agent rather than for pro-inflammatory cytokine neutralisation. More investigations are needed to assess the differences in the mechanism of action of LPS and melittin, and the synergy between melittin and LPS in triggering the immune system. One possible strategy would be to evaluate the metabolic changes that occur in macrophages in response to melittin and LPS when administered singly or in combination.

Metabolomics is one way to provide a quantitative identification of endogenous and exogenous cell metabolites to reveal the relative pathway relationships between metabolites and observed physiological and/or pathological alterations. Metabolomics studies are now providing a number of advantages for determining health status, such as providing predictive powers and diagnosing the disease state, revealing biological markers for drug responses, and defining the links to genetic variants [173]. Most metabolomics studies use untargeted metabolomic profiling for analysis of small molecule metabolites and are typically performed by nuclear magnetic resonance (NMR) spectroscopy and mass spectrometry (MS), highly sensitive and accurate instruments. The coupling of MS to high performance liquid chromatography (HPLC) allows the separation and identification of thousands of metabolites in a single biological sample. Many research studies are now focusing on using metabolomics in diverse areas [160, 174, 175], including the study of inflammatory related metabolites [176, 177]. For instance, Traves et al. characterised the metabolic network flux and changes and its relation to signal transduction in LPS-activated macrophages [178].

Effects on many metabolites have been described in observations of innate immune cell metabolism. Understanding the interface between these immune cells and their metabolism could therefore provide novel tools for manipulating cellular activities. For example, the production of pro-inflammatory cytokines contribute to systemic inflammation [179]. Similarly, the loss of cellular mass promoted by TNF-α has been characterised in cachexia, demonstrating a link between inflammation and metabolism [180]. The quality and the benefit-to-risk ratio of immunisations could be improved by identification of specific metabolites; for example, metabolic profiling of patients pre- and post-smallpox vaccination was able to distinguish patient clinical samples with myocarditis and asymptomatic elevation of troponins, suggesting the potential for identification of biomarkers related to adverse vaccine reactions [181, 182]. Moreover, understanding alterations in metabolomics pathways due to vaccination could help to improve new target vaccine designs (adjuvants, antigens and nanoparticle carrier systems), as reported by Gray et al., who used Ultra high performance liquid chromatography- mass spectrometry (UPLC-MS) metabolomic profiling of plasma in calves following vaccination to determine the immune-correlated metabolite characteristics of immune responses [183]. The current knowledge of immune metabolism has been widely advanced by improvements in metabolomics-based technologies.

Major efforts are now focused on the identification and innovation of new pharmacological compounds to enhance immune responses. The aim of the current study was to use enzyme-linked immunosorbent assay (ELISA) to evaluate the changes in the production of pro- and anti-inflammatory cytokines (TNF-α, IL-1β,

IL-6, and IL-10) following the administration of melittin to PMA-differentiated THP-1 cells. A secondary aim was to examine the changes in the metabolic profile of THP-1 macrophage cells in response to melittin in the presence and absence of LPSs. This was performed using an LC-MS-based metabolomics approach employing ZIC-pHILIC and ACE C4 columns for polar and non-polar metabolites, respectively. The determination of the metabolic changes in response to melittin in stimulated monocyte-derived macrophages cells could be of value for many vaccine applications and the main objective of the present study was to evaluate this potential.

3.3 Materials and Methods

3.3.1 Sample isolation and preparation

Melittin was isolated and purified from BV (supplied lyophilised by Beesen Co. Ltd., Dae Jeon, Korea) using reversed phase medium pressure liquid chromatography (MPLC) on a Reveleris® iES flash chromatography system (Grace Davison Discovery Sciences, Carnforth, UK) with dual UV (λ = 220/280 nm) and evaporative light scattering detection (ELSD). Venom fractions F-1 to F-3 were isolated from 800 mg of crude BV using the same method previously described [135]. The resultant BV fractions were freeze-dried and stored at −20 °C until required for the assays.

3.3.2 Cell culture and differentiation

As detailed in section2.2 2.2.1.

3.3.3 Cell viability assay

The THP-1 cells were seeded at a density of 1×10^5/well in 96-well plates and incubated for 24 h at 37 °C in a humidified atmosphere of 5% CO_2. After 24 h, the cells were treated with different concentrations of melittin (0.39–100 µg/mL) and incubated for a further 24 h. Untreated control cells and medium were added to the plates and dimethyl sulphoxide (DMSO) was used as a positive control. Resazurin salt solution (0.1 mg/mL) was added for Fluorescence readings using GraphPad Prism as described in section 2.2.2.

3.3.4 Cytokine production and ELISA assay

After 48 h of differentiation using PMA (60 ng/mL) in 24-well plates, the media were aspirated, and the cells were incubated for a further 24 h in PMA-free medium. At day 4, the cells were incubated with final concentrations of melittin (0.5 and 1 µg/mL) with and without LPS (Sigma-Aldrich) (0.5 and 1 µg/mL) for an additional 24 h. Conditioned medium was collected and frozen until required for ELISA (n = 3). The ELISA assays were performed according to the manufacturer's instructions to quantify the release of (TNF-α, IL-1β, IL-6, and IL-10) (section2.4).

3.3.5 Metabolite Extraction

The PMA-differentiated THP-1 cells were grown for 48 h in 6-well plates seeded at a density of 4.5×10^5/well (n = 6). The medium was aspirated and replaced with fresh medium for a further 24 h, and then the cells were incubated with LPS, melittin, or a combination of LPS and melittin for an additional 24 h. The final concentrations of LPS and melittin were 0.5 and 1 µg/mL, respectively. After 24 h, the medium was aspirated, and the cells were washed with 3 mL of phosphate-

buffered saline (PBS) (Sigma-Aldrich) at 37 °C. The cells were extracted as detailed in section 2.6. A mixture of fatty acid standards was prepared from a mixture of 37 fatty acid methyl ester standards supplied by Sigma Aldrich (Supelco 37 component FAME Mix) by hydrolysis with 1 M methanolic KOH followed by extraction into hexane.

3.3.6 LC-MS Conditions

An Accela HPLC system interfaced to an Exactive Orbitrap mass spectrometer (Thermo Fisher Scientific, Bremen, Germany) was used for the liquid chromatographic separations. ZIC-pHILIC (150 × 4.6 mm, 5 µm) and ACE C4 (150 × 3.0 mm, 3 µm) HPLC columns supplied were used. Samples were run under the conditions described previously in section 2.5.1, section 2.5.2 and section 2.5.3.

3.3.7 Data Extraction and Statistical Analysis

As detailed in section2.7.

3.4 Results

3.4.1 BV fractionation and isolation of melittin

A crude BV sample was fractionated by MPLC into three major fractions (F-1, F-2 and F-3). As previously described [135], F-1 and F-2 were determined to contain mixed components, while F-3 was determined to contain essentially a single component, melittin with 98% purity (**Figure 3-1**).

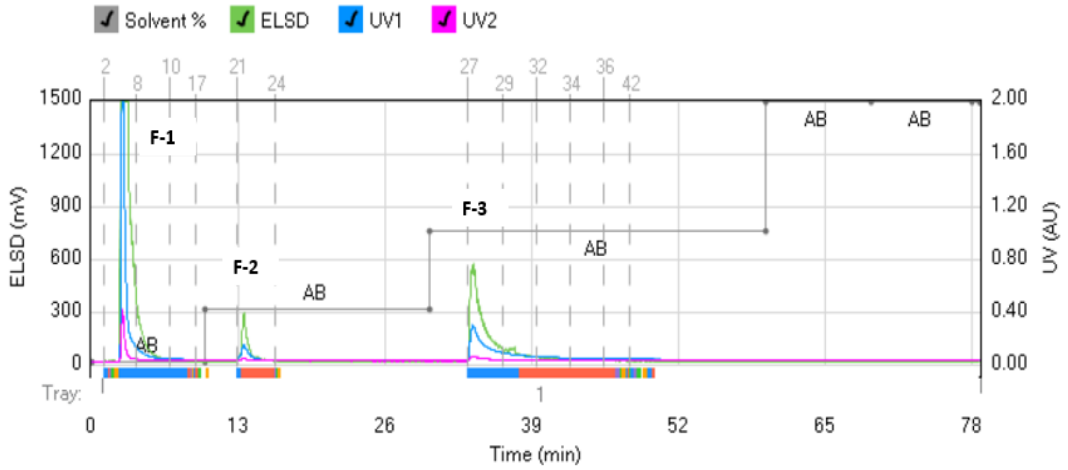

Figure 3-1: Chromatogram obtained from MPLC for the separation of BV components using the Grace® system.
Generic C18, 24g column used; solvents: water (A) and acetonitrile (B) with a gradient of 0-10 min (0% B), 10-20 min (20% B), 20-30 min (50% B), 30-60 min (60% B), 60-70 min (100% B). The colours on the x-axis represent separate collections across with of the peak.

3.4.2 Cytotoxicity of Melittin against Normal and PMA-Differentiated THP-1 Cells

Cytotoxicity assays were used to test the melittin isolated from BV. The studies were performed on THP-1 cell lines before and after differentiation with PMA to evaluate the differences in cell lysis due to melittin (**Figure 3-2**). Normal THP-1 cells were slightly more sensitive to melittin than the differentiated cells, according to their respective IC_{50} values of 3.14 and 3.3 µg/mL. Figure S1 shows a micrograph of the cells before and after PMA differentiation for 48 h. The monocyte-derived macrophages became adherent and showed a much greater increase in their cytoplasmic volume when compared to the untreated control cells [184]. In both cases, dose–response relationships were clearly observed. The cytokine production was analysed by ELISA following melittin administration at 0.5 and 1 µg/mL doses, whereas melittin was added at 1 µg/mL for the metabolomics study. The cells showed >90% viability at these melittin doses.

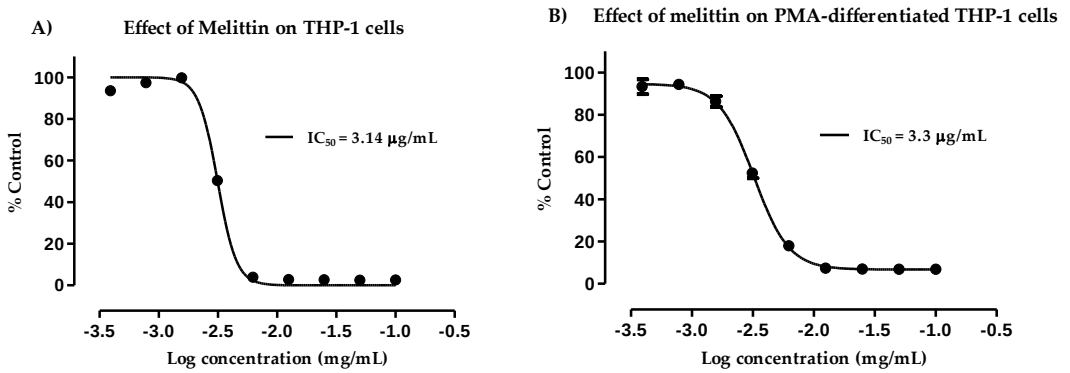

Figure 3-2: Cytotoxic effect of melittin on THP-1 cells (**A**) and phorbol 12-myristate 13-acetate (PMA)-differentiated THP-1 cells (**B**).
The observed effect was determined following administration of varying doses of melittin. Melittin was cytotoxic to normal THP-1 and PMA-treated cells, with IC_{50} values of 3.14 and 3.3 µg/mL, respectively. The data represent the mean ± SD (n = 3).

3.4.3 Effect of melittin on the production of pro-inflammatory TNF-α cytokine

As shown in **Figure 3-3**, the concentrations of pro-inflammatory TNF-α in THP-1 derived macrophages exhibited a slight to negligible effect by the combination treatments (LPS + melittin) when compared to the LPS positive control. The effects in cytokine production in response to LPS + melittin were not statistically significant ($p > 0.05$) from the LPS alone (Table S1); however, they were significant ($p < 0.05$) in comparison to the negative control cells. Two concentrations of melittin were assessed to examine dose dependency. Samples not treated with LPS showed a background level release of cytokine. The lack of effect of melittin on TNF-α production in LPS-stimulated macrophages was previously observed [185].

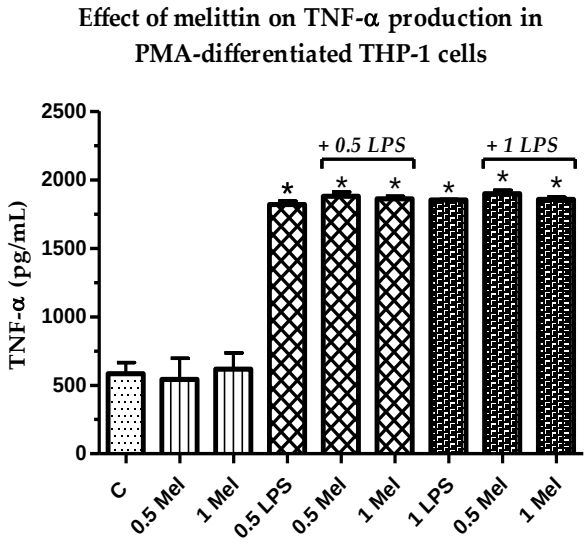

Figure 3-3: Effect of melittin (0.5 & 1 µg/mL) on the production of tumour necrosis factor-α (TNF-α) cytokines in the presence and absence of LPS (0.5 µg/mL) on PMA-differentiated THP-1 cells.
All six treatments were significantly different from the negative control (n = 3). C: control; Mel: melittin; LPS: lipopolysaccharides; *: Significant ($p < 0.05$).

3.4.4 Effect of melittin on the production of pro-inflammatory IL-1β cytokines

A clear increase was noted in the release of the pro-inflammatory IL-1β cytokine (**Figure 3-4**) in response to the combination of melittin and LPS when compared with LPS alone. The effect was statistically significant ($p < 0.05$) for melittin combinations in comparison with cells treated with LPS alone at 0.5 and 1 µg/mL when melittin was used at 1 µg/mL (Table S3.2). In contrast to TNF-α, secretion of LPS-induced IL-1β was induced dose-dependently in the THP-1-derived macrophages in response to melittin treatment. The maximum release of IL-1β was observed after the combined treatment with 1 µg/mL LPS and melittin. The release

of IL-1β was also induced significantly by melittin alone when compared with the negative control cells [185].

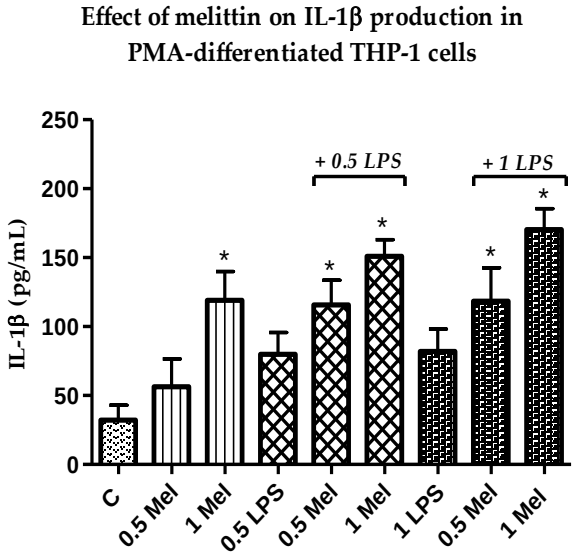

Figure 3-4: Effect of melittin (0.5 & 1 µg/mL) on the production of Interleukin-1β (IL-1β) cytokines by PMA-differentiated THP-1 cells in the presence and absence of LPS (0.5 µg/mL).
Cells treated with all four combination treatments showed significantly higher release when compared with negative control cells (n = 3). C: control; Mel: melittin; LPS: lipopolysaccharides; *: Significant ($p < 0.05$).

3.4.5 Effect of melittin on the production of pro-inflammatory IL-6 cytokines

In agreement with the observed increase in the release of the pro-inflammatory cytokines above, IL-6 also showed an increase in production in response to treatment with a combination of melittin and LPS when compared to LPS alone. The effect was statistically significant ($p < 0.05$) for melittin and LPS combinations when compared with negative control cells and also with 1 µg/mL LPS alone (Table S3). Melittin effects were observed at a final concentration of 0.5 µg/mL, whereas effects were noted for two different doses of LPS (0.5 and 1 µg/mL). Highest detection was

observed at a final concentration of 1 µg/mL and 0.5 µg/mL for LPS and melittin, respectively. Melittin alone had no effect on the level of release of this cytokine or the release was undetectable (**Figure 3-5**).

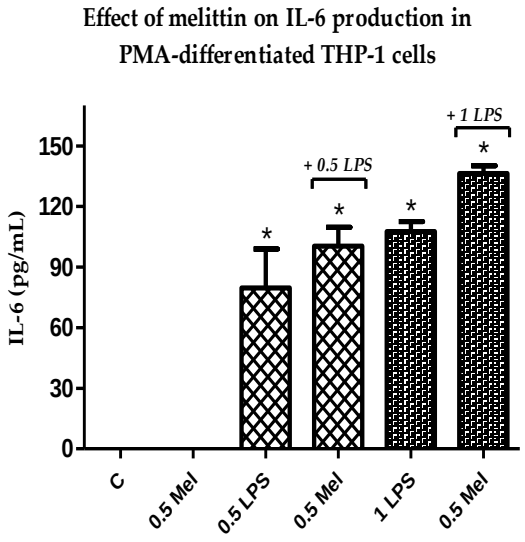

Figure 3-5: Effect of melittin on the production of IL-6 cytokine in the presence and absence of LPS on PMA-differentiated THP-1 cells.
Melittin was tested at a 0.5 µg/mL final concentration in combination with LPS (0.5 and 1 µg/mL) (n = 3). C: control; Mel: melittin; LPS: lipopolysaccharide; *: Significant ($p < 0.05$) compared to negative control cells.

3.4.6 Effect of melittin on the production of anti-inflammatory IL-10 cytokines

The production of anti-inflammatory Il-10 was assessed using 0.5 µg/mL melittin. Interestingly, the release of this anti-inflammatory cytokine was decreased by the combination of melittin and LPS (0.5 and 1 µg/mL) when compared with LPS alone. However, the results of the combination treatments did not reach statistical significance. In addition, no effect was observed for cells treated with melittin alone when compared with the negative control cells (**Figure 3-6**).

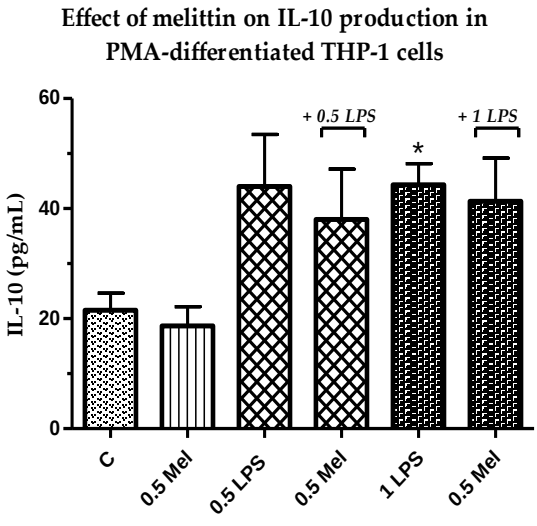

Figure 3-6: Effect of melittin on the production of IL-10 cytokine in the presence and absence of LPS on PMA-differentiated THP-1 cells.
Melittin was tested at a 0.5 µg/mL final concentration in combination with LPS (0.5 and 1 µg/mL) (n = 3). C: control; Mel: melittin; LPS: lipopolysaccharide; *: Significant ($p < 0.05$).

3.4.7 Effect of Melittin on the Cell Metabolome

Understanding how the metabolic response in monocyte-derived macrophages is activated by different stimuli has important clinical ramifications. The aim of the metabolomic profiling of PMA-differentiated THP-1 cells following melittin, LPS, and combination treatments was to identify the mechanism of action of melittin on macrophage cells and to try to understand its synergism with LPS in cytokine production. **Figure 3-7A** shows a clustering of quality control samples (P 1–4) in the middle of the plot, obtained using principal component analysis (PCA) of all the polar metabolites detected by analysis on the ZIC-pHILIC column. This finding validates the analysis and indicates good instrument stability and precision during the run. A clear separation was noted between the treatment and control groups using an

OPLS-DA model (**Figure 3-7B**), which would suggest a different mechanism of action for the combination treatment (melittin + LPS) than for LPS or melittin alone.

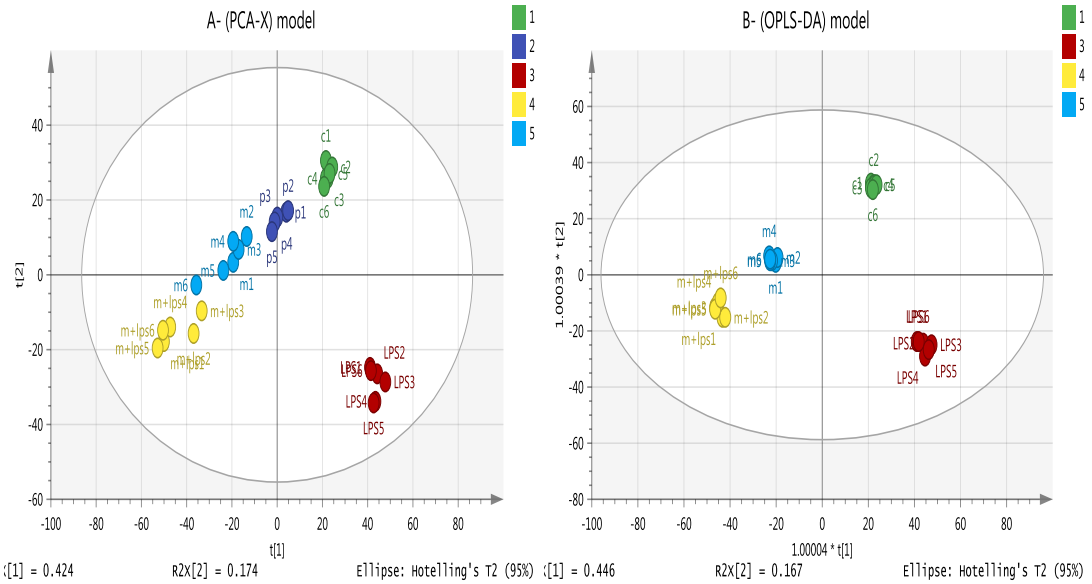

Figure 3-7: (A) PCA-X vs. (B) OPLS-DA score plots of THP-1 cells.
The figures show a clear separation between control, pooled, and treatment groups (LPS, melittin, and LPS + melittin) based on 955 polar metabolites separated on a ZIC-pHILIC column (n = 6). PCA score plot (**A**) has R^2X = 0.668, Q^2 = 0.559. OPLS-DA score plot (**B**) has R^2X = 0.744, R^2Y = 0.99, Q^2 = 0.903. (C: control; M: melittin; LPS: lipopolysaccharide; M + LPS: melittin and LPS combination treatments; *P* = pooled samples). PCA: principal component analysis.

Based on previous observations on the effect of melittin on cell lipids [160], other data sets were obtained using a reversed phase (RP) column (ACE C4 column) to characterise the changes in non-polar metabolites. As shown in **Figure 3-8**, the separation between groups was clearer for lipophilic metabolites than for polar metabolites using an OPLS-DA model. Clustering of pooled (P 1–3) samples in the PCA model showed the validity of the analysis and the stability of the instrument throughout the run.

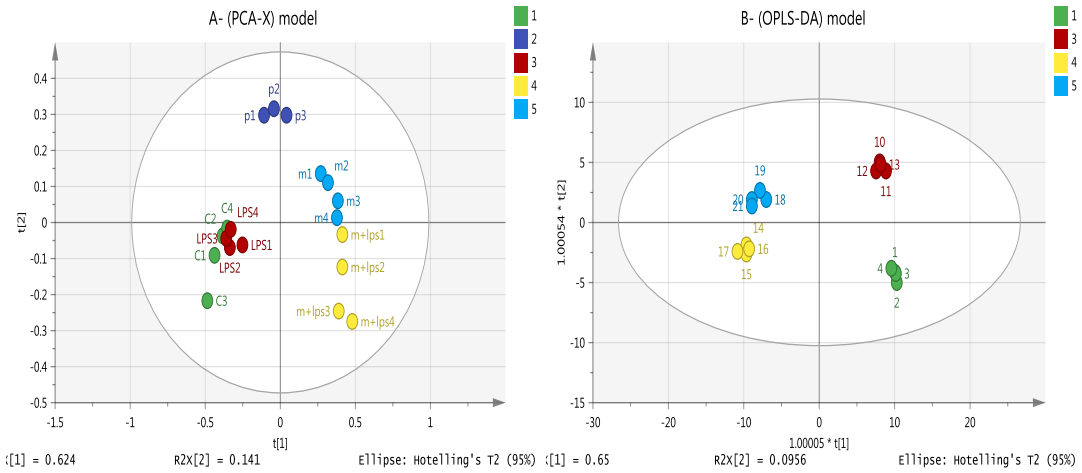

Figure 3-8: (A) PCA-X vs. (B) OPLS-DA score plots of THP-1 cells.
The figures show a clear separation between control, pooled and treatment groups (LPS, melittin and LPS + melittin) based on 128 significant non-polar metabolites separated on an ACE C4 column (*n* = 4). PCA score plot (**A**) has $R^2X = 0.867$, $Q^2 = 0.753$. OPLS-DA score plot (**B**) has $R^2X = 0.896$, $R^2Y = 0.978$, $Q^2 = 0.895$. (C: control; M: melittin; LPS: lipopolysaccharide; M + LPS: melittin and LPS combination treatments; *P* = pooled samples).

Univariate comparisons of the changes in metabolites in each group are shown in Table 1 and demonstrate clear differences in the metabolite levels between cells treated with LPS and melittin alone, thereby confirming distinct metabolic profiles for the combination treatments (melittin + LPS). Several metabolomics pathways were significantly altered (particularly glycolysis, TCA cycle, OXPHOS, arginine and proline metabolism, and nucleotide metabolism). Clearly significant increases were noted in the levels of fatty acids, whereas glycerophospholipid levels were decreased by melittin regardless of the presence or absence of LPS.

Table 3-1: Significantly changed metabolites within THP-1 cells treated with lipopolysaccharide (LPS), melittin, and melittin + LPS in comparison with untreated controls.
The results contain the majority of affected metabolites. (0.5 µg/mL LPS; 1 µg/mL melittin).

Mass	Rt	Putative Metabolite	LPS		Mel		Mel + LPS	
			Ratio	*p* Value	Ratio	*p* Value	Ratio	*p* Value
		Arginine and proline metabolism						
175.096	15.25	L-Citrulline *	1.825	0.048	7.482	0.001	8.657	0.001
174.112	26.50	L-Arginine *	0.255	<0.001	1.111	ns	0.916	ns
240.122	15.55	Homocarnosine	0.640	0.005	1.570	0.002	1.481	0.001
145.085	14.52	4-Guanidinobutanoate	1.122	0.014	0.792	<0.001	1.611	<0.001
246.133	13.55	N2-(D-1-Carboxyethyl)-L-arginine	0.295	<0.001	0.951	ns	1.544	<0.001
113.059	9.30	Creatinine	0.288	<0.001	1.045	ns	1.234	ns
129.043	13.62	Oxoproline	0.135	<0.001	0.192	<0.001	0.182	<0.001
290.123	15.83	N-(L-Arginino) succinate	0.562	<0.001	1.367	0.006	0.832	0.040
132.090	23.04	L-Ornithine *	0.387	<0.001	1.051	ns	1.177	0.004
147.053	13.45	L-Glutamate *	0.661	<0.001	0.917	ns	0.855	0.026
398.137	16.01	S-Adenosyl-L-methionine	0.768	ns	5.717	<0.001	4.267	<0.001
115.063	12.14	L-Proline *	0.439	<0.001	0.909	ns	1.103	ns
		Glycolysis/TCA cycle						
339.996	17.18	D-Fructose 1,6-bisphosphate *	1.397	ns	0.544	<0.001	0.671	0.009
260.030	15.02	D-Fructose 6-phosphate *	1.210	ns	1.620	<0.001	1.590	<0.001
260.020	15.94	D-Glucose 6-sulfate	2.193	0.000	1.359	ns	1.190	0.018
260.030	15.83	D-Glucose 1-phosphate *	1.366	0.004	2.264	<0.001	1.909	<0.001
809.125	12.25	Acetyl-CoA	0.713	0.027	0.946	ns	0.792	0.028
185.993	15.94	3-Phospho-D-glycerate	0.753	0.001	0.610	<0.001	0.501	<0.001
169.998	15.10	Glycerone phosphate	0.381	<0.001	0.315	<0.001	0.249	<0.001
192.027	17.28	Citrate *	0.318	<0.001	1.089	ns	1.297	0.001
192.027	18.47	Isocitrate *	0.489	<0.001	0.580	<0.001	0.466	<0.001
116.011	14.82	Fumarate *	0.751	0.013	0.891	ns	0.677	0.001
665.125	13.23	NADH *	0.324	<0.001	0.492	<0.001	0.584	<0.001

663.109	14.17	NAD+ *	0.482	<0.001	0.923	ns	0.671	<0.001
		OXPHOS/Pentose phosphate pathway						
506.996	15.76	ATP *	0.751	0.006	0.987	ns	0.585	<0.001
427.030	14.31	ADP *	0.534	<0.001	0.812	0.012	0.640	<0.001
258.014	16.69	D-Glucono-1,5-lactone 6-phosphate	1.214	ns	1.207	ns	1.407	0.026
290.041	15.23	D-Sedoheptulose 7-phosphate	1.831	<0.001	1.181	0.002	1.489	<0.001
230.019	14.60	D-Ribulose 5-phosphate	0.932	ns	0.579	0.000	0.713	0.005
370.007	17.42	D-Sedoheptulose 1,7-bisphosphate	1.725	0.002	0.758	ns	1.065	ns
745.091	16.74	NADPH *	1.845	0.049	1.521	ns	0.508	0.048
743.075	16.51	NADP+	0.693	0.030	0.764	0.031	0.820	0.047
		Purine metabolism						
151.049	11.82	Guanine *	1.300	ns	0.632	0.010	1.707	0.001
283.092	12.93	Guanosine	1.310	ns	0.619	0.015	2.185	0.001
348.047	14.40	IMP *	2.093	ns	2.305	0.021	1.727	ns
268.081	10.32	Inosine *	4.079	<0.001	1.852	0.001	6.051	<0.001
168.028	11.38	Urate *	0.168	<0.001	1.372	0.001	1.838	<0.001
136.039	9.74	Hypoxanthine *	7.345	<0.001	4.852	<0.001	33.584	<0.001
152.034	10.46	Xanthine	0.283	<0.001	1.109	0.043	1.264	0.003
284.076	9.72	Xanthosine	0.270	<0.001	1.019	ns	1.259	0.015
135.054	9.22	Adenine	1.246	ns	2.237	0.009	1.649	ns
347.063	12.62	AMP *	0.538	0.002	0.873	ns	0.339	<0.001
		Pyrimidine metabolism						
403.018	16.15	CDP *	0.584	<0.001	0.690	0.001	0.650	0.002
111.043	11.38	Cytosine	0.684	ns	2.434	ns	3.660	0.021
482.985	17.60	CTP *	0.659	0.001	0.719	0.001	0.463	<0.001
243.086	11.36	Cytidine *	0.528	<0.001	2.375	<0.001	3.628	<0.001
483.969	17.02	UTP *	0.617	<0.001	0.685	<0.001	0.437	<0.001
324.036	15.17	UMP *	0.721	0.011	0.630	<0.001	0.589	<0.001
404.003	15.58	UDP *	0.422	<0.001	0.666	0.001	0.534	<0.001
580.035	17.95	UDP-glucuronate	0.604	<0.001	0.560	<0.001	0.495	<0.001

566.055	16.00	UDP-glucose	0.637	0.000	0.555	0.000	0.457	<0.001
605.077	17.17	GDP-mannose	1.812	<0.001	1.996	<0.001	1.532	<0.001
	Fatty acids and metabolites [C4]							
306.256	12.45	Eicosatrienoic acid *	1.650	0.004	1.983	ns	1.977	<0.001
328.240	18.27	Docosahexaenoic acid *	0.346	ns	6.658	0.002	5.846	0.002
318.219	4.10	Leukotriene A4 or isomer	1.115	ns	1.469	ns	2.183	0.002
310.287	17.73	Eicosenoic acid *	1.328	ns	0.477	ns	0.313	0.009
356.256	14.78	Prostaglandin F1alpha or isomer	0.276	0.007	0.479	0.024	0.482	0.048
336.230	4.55	Prostaglandin B1 or isomer	1.004	ns	1.432	ns	2.125	<0.001
402.225	4.00	5S-HETE di-endoperoxide or isomer	1.709	ns	0.850	ns	0.650	0.007
282.256	20.06	Oleic acid *	1.239	0.036	9.007	<0.001	8.089	<0.001
256.240	7.84	Hexadecanoic acid isomer	1.397	0.005	7.235	<0.001	13.602	0.004
338.319	24.61	Docosenoic acid *	1.246	0.005	2.740	<0.001	2.941	<0.001
268.240	11.26	Heptadecenoic acid	1.362	0.013	1.782	<0.001	1.211	ns
366.350	26.59	Tetracosenoic acid *	1.354	0.038	2.665	<0.001	2.800	<0.001
304.240	18.36	Eeicosatetraenoic acid *	1.049	ns	46.370	<0.001	42.444	<0.001
332.272	20.30	Docosatetraenoic acid	0.929	ns	25.404	<0.001	21.474	<0.001
242.225	17.97	Pentadecanoic acid *	0.967	ns	1.787	<0.001	1.758	<0.001
334.287	21.82	Docosatrienoic acid *	0.776	ns	8.679	0.001	7.684	0.001
226.193	15.25	Tetradecenoic acid	0.890	ns	3.570	0.002	3.367	0.003
270.256	12.86	Heptadecanoic acid	0.874	ns	4.801	0.010	1.854	0.009
278.225	17.08	Linolenic acid *	0.789	0.029	3.716	<0.001	2.861	<0.001
280.240	18.38	Linoleate *	1.105	ns	9.760	<0.001	8.943	<0.001
	Glycerophospholipids [C4]							
721.467	12.69	PC 32:6	0.672	ns	0.214	0.016	0.217	0.023
832.654	30.65	PG 41:0 ether	0.665	0.028	0.623	0.019	0.402	0.003
738.448	12.65	PG34:6	0.949	ns	0.357	0.020	0.308	0.015
484.280	13.33	Lyso PG 16:0	1.589	ns	0.449	0.034	0.283	0.013
800.449	12.56	PI 32:5	0.885	ns	0.365	0.009	0.329	0.005
584.333	13.28	Lyso PI 18:0 Ether	0.941	ns	0.558	0.020	0.499	0.004

858.526	13.47	PI 36:4	1.841	ns	0.441	0.025	0.316	0.027
814.501	13.55	PI 34:4 ether	2.088	ns	0.486	0.025	0.317	0.019
785.521	32.15	PS 36:3	0.789	0.008	0.782	0.005	0.779	0.007
517.244	12.56	Lyso PS 18:4	1.184	ns	2.645	<0.001	1.659	0.022
833.520	22.16	PS 40:7	1.118	ns	0.439	0.004	0.470	0.009
777.457	13.50	PS 36:7	0.970	ns	0.432	0.023	0.371	0.010
		Miscellaneous						
131.058	13.88	N-Acetyl-beta-alanine	2.017	0.004	4.879	0.001	5.950	0.001
217.143	15.88	beta-Alanyl-L-lysine	1.543	0.041	3.816	<0.001	1.705	0.021
182.079	13.10	D-Sorbitol *	0.325	<0.001	2.226	<0.001	4.443	<0.001
180.064	12.66	D-Mannose *	0.712	<0.001	1.538	<0.001	1.744	<0.001
180.064	14.19	D-Galactose	1.326	ns	3.785	0.001	4.184	0.001
221.090	11.16	N-Acetyl-D-glucosamine *	0.464	<0.001	0.953	ns	0.806	0.008
146.069	14.34	L-Glutamine *	0.370	<0.001	1.085	ns	1.322	0.002
129.043	10.45	5-Oxoproline *	2.424	0.018	0.897	ns	1.192	ns
220.085	8.96	5-Hydroxy-L-tryptophan *	7.211	<0.001	1.131	0.010	4.305	<0.001
204.090	11.14	L-Tryptophan *	0.190	<0.001	1.189	ns	1.311	0.046
181.074	12.34	L-Tyrosine *	0.309	<0.001	1.050	ns	1.265	0.042
131.095	10.77	L-Leucine *	0.217	0.008	1.038	ns	1.226	0.048
117.079	11.94	L-Valine *	1.615	0.001	6.492	0.000	2.822	0.002
612.152	16.40	Glutathione disulfide	0.652	<0.001	1.186	0.047	1.109	ns
142.074	13.04	Ectoine *	1.164	ns	0.553	<0.001	0.196	<0.001
131.069	13.99	Creatine *	0.547	<0.001	0.615	<0.001	0.439	ns
103.100	20.48	Choline *	0.444	<0.001	3.571	<0.001	2.827	<0.001
105.043	15.44	L-Serine *	1.518	<0.001	1.737	<0.001	1.707	<0.001
121.020	15.41	L-Cysteine *	0.581	<0.001	2.182	<0.001	4.862	<0.001
155.070	15.87	L-Histidine *	1.088	ns	2.089	<0.001	3.122	<0.001
161.105	12.59	L-Carnitine *	0.608	<0.001	0.822	0.008	0.744	0.002
238.230	12.66	2-trans-Hexadecenal [C4]	0.795	ns	16.865	0.000	12.016	0.000

Rt: min; LPS: Lipopolysaccharides; Mel: melittin; C4: Detected by ACE C4 column; *: Matches the standard Rt; ns: Non-significant.

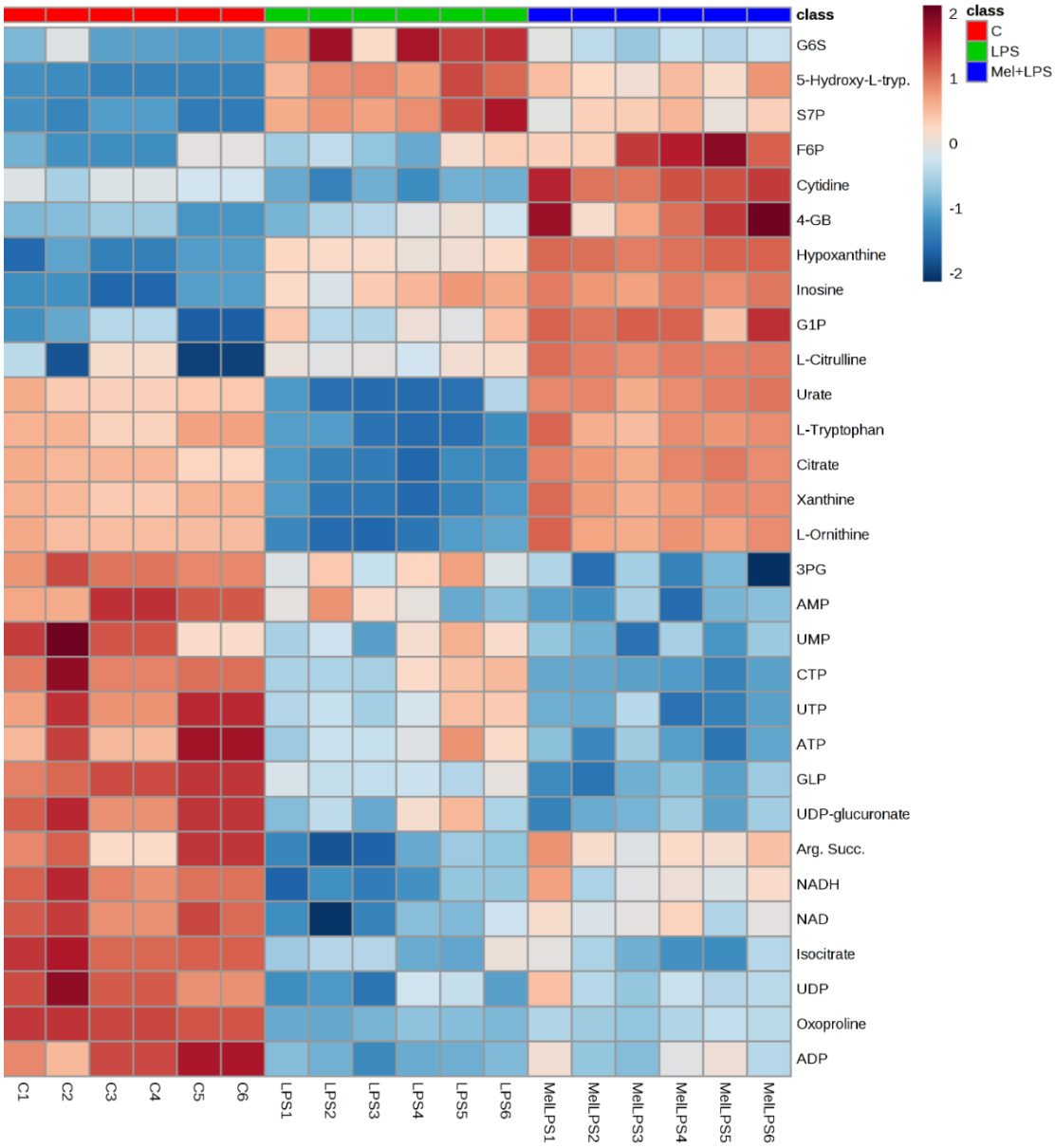

Figure 3-9: Heat map showing the top 30 significant putative metabolites among control (C), LPS, and melittin + LPS (Mel + LPS) using one-way ANOVA.
The data are displayed on a $\log_2$ scale. The differences in colour shades represent intensities of the metabolites vs. sample observations.

The plot shows heat map of the top 30 significant metabolites from **Table 3-1**. The clearest effect in the heat map was that the similarity in the effect between LPS alone and Mel+LPS. Most of the metabolites were decreased with LPS treatment. Some

metabolites are more abundant in combination treatment of Mel + LPS as compared to LPS alone, such as citrulline, hypoxanthine, and inosine (**Figure 3-9**).

3.5 Discussion

The efficacy of vaccines can be improved by the safe use of adjuvant substances, which are substances that modulate and enhance the immunogenicity of a vaccine antigen [186]. The aim of the present study was to investigate the potential usefulness of the BV compound, melittin as a natural vaccine adjuvant to stimulate the innate and adaptive immune systems. The research strategy was to characterise the ability of melittin to modify cytokine production in LPS-stimulated PMA-differentiated THP-1 cells. The effects of melittin, in combination with LPS, on the metabolic profiles of monocyte-derived macrophages were also evaluated to determine if metabolomic profiling of immune-modulating agents can provide a more in-depth understanding of the mechanisms and pathways of cytokine secretion.

The cytotoxicity assays showed that the THP-1 monocytes were no longer viable when exposed to 6.25 µg/mL melittin, while the PMA-differentiated cells retained 18% cell viability. No significant cell lysis was observed below 1.56 µg/mL for the normal THP-1 cells, which confirmed a greater melittin sensitivity of the cells with a lower IC_{50} value, when compared to cells differentiated into macrophages. The pro-inflammatory IL-1β showed the most enhanced release in response to melittin and the response was dose-dependent and also its release was significantly higher than

LPS alone when 1 μg/mL of melittin was used in combination with LPS. A significant enhancement was also observed for IL-6 cytokine comparing with LPS alone with 0.5 μg/mL of melittin, but only a slight enhancement (non-significant) was observed for TNF-α which reflects the findings of an earlier study. Interestingly, the production of the anti-inflammatory IL-10 was not significantly decreased by melittin in the combination treatment with LPS, which might support the use of melittin as a pro-inflammatory enhancer. These results support our previous findings on the effect of melittin on cytokine secretion by the U937 cell line [136], using the same experimental design.

IL-1β, a prototypic pro-inflammatory cytokine, has an essential role in immune responses and possesses adjuvant activity [187, 188]. The production of IL-1β and IL-18 is increased by aluminium hydroxide, a routinely used adjuvant, which is believed to activate caspase-1 [189]. Several studies have reported that melittin has adjuvant activity that may arise by a different mechanism, perhaps by enhancing the absorption properties of vaccines when they are administered nasally [171]. Melittin can serve as a mucosal adjuvant for antigens administered via the nasal route as it enhances antibody titres in a dose-dependent manner when conjugated with tetanus and diphtheria toxoids [172]. Another study has shown that melittin induces the synthesis of TNF-α and IL-1β in a time- and dose-dependent manner through activation of phospholipase A2 (PLA2) [190, 191]. A deeper understanding of the immune-stimulatory mechanism of adjuvants is a prerequisite for the design of more sophisticated vaccines.

The comparisons of control cells versus LPS-, melittin-, and LPS + melittin-treated cells revealed large numbers of metabolite differences. Overall, a synergistic effect was clearly evident in terms of the ratios of some of the inflammatory response metabolites when comparing the combination treatment with LPS alone (**Table 3-1**). The LPS-stimulated macrophages showed upregulation of the arginine metabolism, which resulted in the increased production of citrulline, which is an indicator of increased NO production, a hallmark of inflammation [192]. The levels of citrulline were increased by melittin alone and there was a clear enhancement effect in combination with LPS. The levels of arginine, a precursor of NO and citrulline, and the N-(L-arginino)-succinate level were decreased in response to LPS alone and melittin with LPS treatments, but the N-(L-arginino)-succinate was not depleted when melittin alone was used. This might be due to the increased expression of argininosuccinate synthase (Ass1) and argininosuccinate lyase (Asl) [193]. These two enzymes are used to maintain levels of arginine with arginine succinate being exported from the cells and then retrieved again and converted to arginine when the arginine level is depleted in order to optimize the production of NO [193]. NO nitrosylation inhibits the components of the electron transport chain, thereby leading to OXPHOS inhibition through the suppression of complex II [194].

Several studies have shown an increase in aerobic glycolysis and a decrease in the TCA cycle and electron transport chain in macrophages due to increased release of NO [195, 196]. Decreases in TCA cycle activity will lead to increases in the production of mitochondrial reactive oxygen species (ROS) and subsequent cytokine secretion [152, 194]. The subsequent decrease in ATP production (**Table 3-1**) then

leads to reprogramming of the cell metabolites and switching to glycolysis after the decline in OXPHOS. This serves as a survival response to maintain the level of ATP in the cells [197]. Despite the small effect seen on acetyl-CoA, the LPS and combination treatments caused decreases of ~30% and ~20%, respectively, which confirmed the inhibition of the TCA cycle and diversion of pyruvate to lactate instead of acetyl-CoA [143, 149]. At the same time, shunting glucose through the pentose phosphate pathway (PPP) generates nicotinamide adenine dinucleotide phosphate (NADPH), which showed a significantly increased level in response to LPS treatment alone and is required for oxidative reactions, glutathione recycling, NO production, and ROS production [140]. Melittin was reported to increase the production of ROS and to induce apoptosis in TNF-related apoptosis-inducing ligand (TRAIL)-resistant HepG2 cells and the fall in NADPH with the melittin treatments may indicate increased consumption, this would fit with the higher levels of citrulline in the melittin treatments [198].

An elevation in PPP metabolites can boost the production of purines and pyrimidines for biosynthesis in activated cells [199]. Knockdown of the carbohydrate kinase-like protein (CARKL), a sedoheptulose kinase that catalyses the production of D-sedoheptulose 7-phosphate (S7P), was reported after LPS treatment and could potentiate the production of cytokines and M1 macrophage polarisation [150, 200]. An increased flow of glycolytic intermediate metabolites into the oxidative arm of the PPP generated more NADPH from the conversion of glucose-6-phosphate to ribulose-5-phosphate (Ru5P). When the cellular need for NADPH exceeded that required for biosynthesis of nucleotides, Ru5P passed into the redox arm of PPP to

increase the flux to glycolysis by generating fructose-6-phosphate (F6P) and glucose-6-phosphate (G6P). Thus, F6P was strongly elevated in response to the melittin alone and melittin and LPS combination treatment. S7P, a key control metabolite, was particularly elevated. In the same study, metabolomics analysis to revealed the metabolites linked to CARKL expression demonstrated that ribose-5-phosphate, xyulose-5-phosphate, S7P, glyceraldehyde-3-phosphate (G3P), G6P, and F6P were elevated concomitantly with a marked depletion of some TCA metabolites (such as malate and fumarate) and decreases in NADH levels [150]. These findings are similar to the current metabolomics results of some metabolites including fumarate, Ru5P, S7P and F6P (**Table 3-1**).

In the present study, a strong effect on cellular purine and pyrimidine metabolism was observed for the combination treatment. Guanine, guanosine, inosine, urate, hypoxanthine, xanthine, xanthosine, adenine, AMP, cytosine, cytidine, CTP, UTP, and UMP all showed a clear synergistic effect for the combination treatment when compared with LPS alone (**Table 3-1**). The effect of melittin in lowering UMP, UDP, UTP and UDP–glucose is of interest since UDP–sugar conjugates are involved in protein N-glycosylation and are upregulated in M2 macrophages [192]. It has been proposed that melittin can reduce the number of M2-like macrophages in an increasing cell population, producing a relative increase in M1 macrophages [185]. A reduction in the population of M2 cells has also been linked to a lowering of glutamine catabolism, which was observed in the current case for the melittin LPS combination. These findings resemble those of a previous study that showed elevated levels of xanthine, hypoxanthine, inosine, guanine, and guanosine in gingival

crevicular fluid inflammation sites when compared with a healthy human oral cavity [201]. Higher levels of hypoxanthine were also observed in response to macrophage activation by LPS in the RAW 264.7 cell line [176]. The hyperactivity of purine degradation and the increase in hypoxanthine (33-fold) and inosine (6-fold) in the melittin + LPS-treated cells represent potential biomarkers for inflammation, as these result in greater production of ROS through xanthine oxidase, thereby causing cellular oxidative stress [201]. These results support previous findings in patients with inflammatory arthritis, where the levels of hypoxanthine, xanthine, and urate were higher in synovial fluid than in plasma, and hypoxanthine concentrations were significantly higher in the plasma from patients than from the control group [202]. Metabolic profiling of rheumatoid arthritis patients also indicated a significant increase in hypoxanthine levels when compared to healthy controls [203]. Overall, the results in the present study indicated a significant change in amino acid and nucleotide biosynthesis upon activation by the combination of LPS and melittin. Cell reprogramming was clearly observed by the combination treatment, which supports the use of melittin to stimulate cellular immune responses and its potential use as an immune adjuvant agent.

Metabolic profiling of lipophilic metabolites separated using a reversed phase column revealed significant changes in fatty acids of interest. LPS caused a slight increase in fatty acid synthesis by increasing the expression of the mitochondrial citrate carrier [204]. This would cause an accumulation of citrate in the cell cytoplasm through exchange with malate, and the citrate is then converted to oxaloacetate and acetyl-CoA, using ATP. Acetyl-CoA is then converted to malonyl-

CoA, which is used for fatty acid synthesis [143, 205]. LPS treatment was also found to inhibit the activity of the AMP-kinase in macrophages, causing a decrease in β-oxidation of fatty acids to produce inflammatory mediators [159]. Melittin, alone or in combination with LPS, caused a significant increase in the level of several fatty acids. These increases would explain the ability of melittin to cause disruption of the cell membrane, as confirmed by several previous findings [161, 206]. Arachidonic acid (i.e., eicosatetraenoic acid) release from the cells was significantly increased by 46-fold and 42-fold by treatment with melittin and melittin + LPS, respectively (**Table 3-1** and Figure S3.15). Several studies have shown that melittin activates the arachidonic acid signalling pathway in many cell lines, including PC12 and L1210 [207, 208], and in neurons [209]. The mechanism of arachidonic acid production is argued to occur through multiple pathways to regulate cellular activity. One possibility is that it works through the stimulation of phospholipase A_2; however, this effect was reported to lack selectivity for phospholipase A2 and fatty acid release [207]. The production of linoleic acid and linolenic acid, a precursor of arachidonic acid, was significantly increased in response to melittin, which would support the lytic activity of melittin on the cell membrane and its ability to penetrate phospholipid bilayers [12].

Arachidonic acid has a considerable importance in the immune system and in the promotion of inflammation. It can be metabolised via enzymatic reactions, including cyclooxygenase (COX), lipoxygenase, cytochrome p450 (CYP 450), and the enzymes of the anandamide pathways to create 20-carbon molecules (eicosanoids) such as prostaglandin (PG) and other signalling molecules. Eicosanoids are produced

mainly following stimulation of the inflammatory process and in innate immunity regulation [210, 211]. Melittin was indicated to induce mRNA levels of COX-2 and IL-8 in fibroblast-like synoviocytes [12]. The apparent strong involvement of the arachidonic acid pathway in the production of pro-inflammatory mediators supports the potential use of melittin for immune activation and as an immune-adjuvant vaccine agent. In addition to the enhancement effect of melittin to LPS in most of the amino acids and nucleotides, its effect on cells lipids was very marked, suggesting membrane re-modelling of macrophages cells upon activation by melittin with a particular selectivity for lipids carrying long-chain polyunsaturated fatty acids.

3.6 Conclusions

In conclusion, PMA-differentiated THP-1 cells showed a significant enhancement in the secretion of IL-1β and IL-6 cytokines in response to treatment with a combination of melittin and LPS when compared to LPS alone when a 1 μg/mL concentration was used. Melittin combined with LPS also produced a decrease in the level of the anti-inflammatory IL-10 cytokines. However, there was little not significant effect of melittin on the level of TNF-α, which could mirrors what was observed previously using different cell line. In addition, this study provides an outline of the metabolites associated with cytokine production and immune system activation by LPS, melittin, or LPS + melittin. The clearest effects of the combination of LPS and melittin treatment were on glycolysis, the TCA cycle, OXPHOS, and purine, pyrimidine, and fatty acid metabolism. The most marked effects were on the levels of polyunsaturated fatty acid and associated with this a

reduction in the levels of some long-chain highly unsaturated phospholipids. Exposure to the combination treatment resulted in marked elevation of most fatty acids, and arachidonic acid in particular, suggesting different metabolic responses to LPS, melittin, and the melittin and LPS combination. The effect of melittin in lowering UTP levels and UDP-glucose fits with a previous report that UDP–sugar conjugates may be important for conferring M2-like properties to macrophages. To the author's knowledge, this is the first time that melittin has been shown to work as an immune adjuvant based on results from metabolic profiling of monocyte-derived macrophages. The results emphasise that the use of melittin in combination with LPS could result in improved therapy for vaccine immunisation. Certainly, melittin shows promise as a potential vaccine adjuvant.

Chapter Four

Propolis Exerts an Anti-Inflammatory Effect on PMA-Differentiated THP-1 Cells via Inhibition of Purine Nucleoside Phosphorylase

4 Propolis Exerts an Anti-Inflammatory Effect on PMA-Differentiated THP-1 Cells via Inhibition of Purine Nucleoside Phosphorylase

4.1 Abstract

Previous research has shown that propolis has immunomodulatory activity. Propolis extracts from different geographic origins were assessed for their anti-inflammatory activities by investigating their ability to alter the production of tumour necrosis factor-α (TNF-α) and the cytokines interleukin-1β (IL-1β), IL-6 and IL-10 in THP-1-derived macrophage cells co-stimulated with lipopolysaccharide (LPS). All the propolis extracts suppressed the TNF-α and IL-6 LPS-stimulated levels. Similar suppression effects were detected for IL-1β, but the release of this cytokine was enhanced by propolis samples from Ghana and Indonesia when compared with LPS. Overall, the Cameroonian propolis extract (P-C) was the most active and this was evaluated for its effects on the metabolic profile of unstimulated macrophages or macrophages activated by LPS. The levels of 81 polar metabolites were identified by liquid chromatography (LC) coupled with mass spectrometry (MS) on a ZIC-pHILIC column. LPS altered the energy, amino acid and nucleotide metabolism in THP-1 cells, and interpretation of the metabolic pathways showed that P-C reversed some of the effects of LPS. Overall, the results showed that propolis extracts exert an anti-inflammatory effect by inhibition of pro-inflammatory cytokines and by metabolic reprogramming of LPS activity in macrophage cells, suggesting an immunomodulatory effect.

4.2 Introduction

In recent years, the discovery and development of new and existing anti-inflammatory therapies have been an intense research focus, particularly for the control of chronic inflammatory conditions. Inflammatory cells, such as leukocytes, mast cells, endothelial cells, monocytes, macrophages and lymphocytes, are now recognised to produce chemical inflammatory mediators that have the purpose of repairing tissue injury [212]. These mediators include amines (histamine and serotonin), arachidonic acid, eicosanoids, leukotrienes, prostaglandins, cytokines (tumour necrosis factor alpha, TNF-α and interleukins, IL) and free oxygen radicals [213, 214]. The inflammatory process can be categorised into acute and chronic stages, according to the duration and frequency of the injurious agent. The acute-stage response includes supportive or exudative, as well as cellular and microvascular, actions. By contrast, chronic inflammation is proliferative and the resulting histological alterations differ from those in the acute stage to include cell migration and mitotic activity [215, 216].

In certain instances, inflammation needs to be regulated by specific drugs to avoid further consequences to the organism. Current anti-inflammatory treatments, which include nuclear factor kappa B (NF-κB) inhibitors, anti-cytokine antibodies, anti-inflammatory cytokines, enzyme inhibitors and kinase inhibitors, can be classified according to their mechanisms of action. Modulation of different signal transduction pathways having similar endpoints (e.g., TNF-α inhibition) might induce different cellular reactions, thereby giving rise to the observed complexity of the inflammatory

process [217]. Therefore, high throughput screening methods need to be applied in the drug discovery process.

Currently, several drug discovery studies have been targeted to investigate the direct health benefits and pharmacological properties of honey bee products. One of the most common is propolis, also known as bee glue, which is a resinous substance collected by bees from their surrounding environment (namely from plants) [218]. The wide range of biological activities of propolis is due to the presence of a complex mixture of bioactive compounds, which impart antioxidant, antimicrobial, anticancer and anti-inflammatory actions [219-221]. The effective medical applications of propolis have led to an increased interest in its chemical composition, which is highly variable depending on the climate and environmental conditions of the site, the collecting season and the geographic region [222]. Over 300 compounds have been identified in propolis, with the most abundant being phenolics (e.g., flavonoids, flavanones and flavonolols), aromatic aldehydes, steroids, alcohols, fatty acids, terpenes, amino acids and sugars [221, 223, 224]. The chemical compounds also differ between propolis samples originating from tropical and temperate zones. For example, the phenolic constituents in temperate zone propolis include the flavonoids pinocembrin, chrysin, ferulic acid, cinnamic acid and caffeic acid [225, 226], whereas propolis from tropical areas contains only traces of these phenolic components, but is rich in prenylated derivatives of benzophenones, p-coumaric acid, lignans and diterpenes [227-229].

Many of these propolis components have anti-inflammatory action and can act on common and/or distinct anti-inflammatory pathways that function in basic immune

cell responses. One example is the pathway that involves special receptors, the Toll-like receptors (TLRs), which recognise various microbial structures called pathogen-associated molecular patterns (PAMPs). Consequently, several transcriptional factors (e.g., NF-κB) are activated and lead to gene expression and the release of inflammatory cytokines to promote host defence [230]. This response is mediated by B and T cells and results in pathogen-specific adaptive immunity [231].

Previous studies have shown that propolis components have direct regulatory action on these basic immune cell functions. For instance, neovestitol, an isoflavonoid from propolis, had an immune modulatory effect in lipopolysaccharide (LPS)-stimulated RAW264.7 macrophages, where it clearly inhibited nitric oxide (NO) production and reduced pro-inflammatory cytokine levels [232]. In Th1- and Th2-type T cells, propolis extracts and propolis compounds (e.g., caffeic acid, phenethyl ester, quercetin and hesperidin) strongly depress DNA synthesis and the production of inflammatory cytokines (i.e., IL-1β, IL-12, IL-2 and IL-4) and enhance the production of transforming growth factor-β1 (TGF-β1) [233]. Large amounts of apigenin, galangin and pinocembrin were quantified by flavonoid profiling of propolis from southern Brazil [234]. Zhang et al. reported the ability of apigenin to decrease the mRNA levels of IL-1β, IL-6 and TNF-α in human THP-1-derived macrophages [235]. The levels of these pro-inflammatory cytokines were also significantly decreased by pinocembrin in RAW 264.7 macrophage cells, whereas IL-10 was significantly increased [236]. In the same RAW 264.7 line, the level of IL-6 and TNF-α cytokines was clearly reduced by galangin [237]. In vivo, propolis administration to C57BL/6 mice for 14 days led to inhibition in the production of IL-

1β, IL-6, IL-2, IL-10 and IFN-γ by spleen cells [238]. In addition, ethanolic extract of Brazilian propolis reduced the expression of IL-17 in collagen-induced arthritis in mice [239]. Thus, bee propolis and its constituents can be considered as potential natural anti-inflammatory agents that act by modulating immune responses.

New compounds have recently been reported from propolis samples from Africa, including two new stilbene compounds isolated from Ghanaian samples and a new phloroglucinonone compound isolated from Cameroon samples [240]. Cameroonian propolis has been used in traditional medicine as an antibacterial and antiradical agent [241, 242]. Chemical investigations by Kardar et al. of the triterpenes and phenolic compounds in Cameroonian propolis led to the isolation of 13 alk(en)ylphenols, nine triterpenes and nine alk(en)ylresorcinols [243, 244]. This propolis also contained diprenyl flavonoids, two monoterpenic alcohols and one fatty acid ester, as reported previously [245]. Only a few reports have used Cameroonian propolis to study the anti-inflammatory effects of propolis; however, the assessment of its antagonist effects on LPS activation of macrophage cells could be improved by the use of a metabolomics approach.

Metabolomics is a recently introduced tool that has now joined genomics, transcriptomics and proteomics for the analysis of biological systems [246]. The use of metabolomics analysis for metabolic profiling has attracted increasing interest, as it allows for simultaneous and reproducible recognition of both endogenous and exogenous metabolites that could directly reflect the biological alterations in a test sample. Conventionally, a biomarker from a metabolomics study is achieved by comparing the metabolic profile between two states (e.g., control versus treatment or

health versus disease) [247]. For research on inflammatory diseases, metabolomics has been highlighted as a promising analytical technique for identifying particular metabolites or metabolic pathways associated with a disease. For example, possible clinically useful metabolic biomarkers for patients with Crohn's disease were identified as tyrosine and phenylalanine metabolism and bile acid and fatty acid biosynthesis, based on non-targeted metabolic profiling of faecal samples [248]. Similarly, comprehensive metabolic analysis of LPS-stimulated and unstimulated macrophage cells by LPS [176] following targeted metabolic profiling of individual pathways, such as amino acids [249], carbohydrates [158] and lipids [250], provided a broad determination of the pathogenic mechanism involved in inflammatory macrophage biology and/or disease.

Macrophages, upon stimulation with LPS, perform a multitude of functions for tissue remodelling and immune responses, and they secrete a wide range of factors associated with inflammatory pathways, including pro-inflammatory cytokines, growth factors and prostaglandins [251]. The effects on the characteristic metabolic changes that LPS-activated macrophages undergo could help to assess the activities of anti-inflammatory compounds. In the present study, we assessed propolis samples from different regions (UK, Ghana, Cameroon and Indonesia) for their effects on cytokine production (TNF-α, IL-1β, IL-6 and IL-10), using phorbol 12-myristate 13-acetate (PMA)-differentiated THP-1 cells stimulated with LPS. We then used enzyme-linked immunosorbent assays (ELISAs) for cytokine level assessments. The most effective propolis for modulating cytokine levels was then assessed by liquid chromatography-mass spectrometry (LC-MS)-based metabolomics to confirm

whether or not metabolomics was an effective tool for elucidating the mechanism of action of the propolis.

4.3 Materials and Methods

4.3.1 Extract preparation

Nine propolis samples from the UK (P-UK1-5), Ghana (P-G), Cameroon (P-C) and Indonesia (P-Ind1-2) were extracted. Ethanol extracts of approximately 10 g propolis were prepared by vigorous mixing and sonication for 60 min using a sonicating bath (Fisher Scientific, Loughborough, UK). The extracts were filtered and the propolis was re-extracted twice with 100 mL ethanol (Fisher Scientific, Loughborough, UK). The extracts were combined and evaporated, and the residue was stored at room temperature until required for the assays.

4.3.2 Cell culture and differentiation

As detailed in section2.2 2.2.1.

4.3.3 Cell viability assay

The THP-1 cells were seeded at a density of 1×10^5/well in 96-well plates and incubated for 24 h at 37 °C in a humidified atmosphere of 5% CO_2. After 24 h, the cells were treated with different concentrations of propolis (2.0-250 µg/mL) and incubated for a further 24 h. Untreated control cells and medium were added to the plates and dimethyl sulphoxide (DMSO) was used as a positive control. Resazurin salt solution (0.1 mg/mL) was added for Fluorescence readings using GraphPad Prism as described in section 2.2.2.

4.3.4 Cytokine production and ELISA assay

After 48 h of differentiation using PMA (60 ng/mL) in 24-well plates, the media were aspirated, and the cells were incubated for a further 24 h in PMA-free medium. At day 4, the cells were incubated with final concentrations of propolis samples (**Table 4-1**) with and without LPS (Sigma-Aldrich) (0.5 µg/mL) for an additional 24 h. Conditioned medium was collected and frozen until required for ELISA (n = 3). The ELISA assays were performed according to the manufacturer's instructions to quantify the release of (TNF-α, IL-1β, IL-6, and IL-10) (section2.4).

4.3.5 Metabolite Extraction

The PMA-differentiated THP-1 cells were grown for 48 h in 6-well plates seeded at a density of 4.5×10^5/well (n = 6). The medium was aspirated and replaced with fresh medium for a further 24 h, and then the cells were incubated with LPS, P-C, or a combination of LPS and P-C for an additional 24 h. The final concentrations of LPS and P-C were 0.5 and 70 µg/mL, respectively. After 24 h, the medium was aspirated, and the cells were washed with 3 mL of phosphate-buffered saline (PBS) (Sigma-Aldrich) at 37 °C. The cells were extracted as detailed in section 2.6.

4.3.6 LC-MS Conditions

An Accela HPLC system interfaced to an Exactive Orbitrap mass spectrometer (Thermo Fisher Scientific, Bremen, Germany) was used for the liquid chromatographic separations. ZIC-pHILIC (150 × 4.6 mm, 5 µm) HPLC columns supplied were used. Samples were run under the conditions described previously in section 2.5.1, section 2.5.2 and section 2.5.3.

4.3.7 Data Extraction and Statistical Analysis

As detailed in section2.7.

4.4 Results

4.4.1 Cytotoxicity of propolis extracts against PMA-differentiated THP-1 cells

Crude propolis extracts from samples collected from the UK (P-UK), Ghana (P-G), Cameroon (P-C) and Indonesia (P-Ind) were tested for cytotoxicity using assays performed on PMA-differentiated THP-1 cells (**Figure 4-1** and S4.1). Dose-response relationships were clearly observed, except with the P-G and P-Ind2 extracts. The P-UK1-5 extracts showed a slight dose effect on THP-1 cells, with a range of IC50 values between 46 and 58 µg/mL. The P-Ind1 extract was the most toxic and gave an IC50 value of 25.73 µg/mL. By contrast, P-Ind2 and P-C gave the lowest toxicity at >250 and 106 µg/mL, respectively (**Table 4-1**).

The level of secretion of four cytokines was analysed by ELISA following treatment of the cells with propolis extract. **Table 4-1** shows the final selected propolis concentrations used for cytokine production assessments. The cells remained > 90% viable at these concentrations, which were below their respective IC50 Values. P-C extract was chosen as the best model extract to study the metabolic responses of propolis as an anti-inflammatory agent and was used at a final concentration of 70 µg/mL.

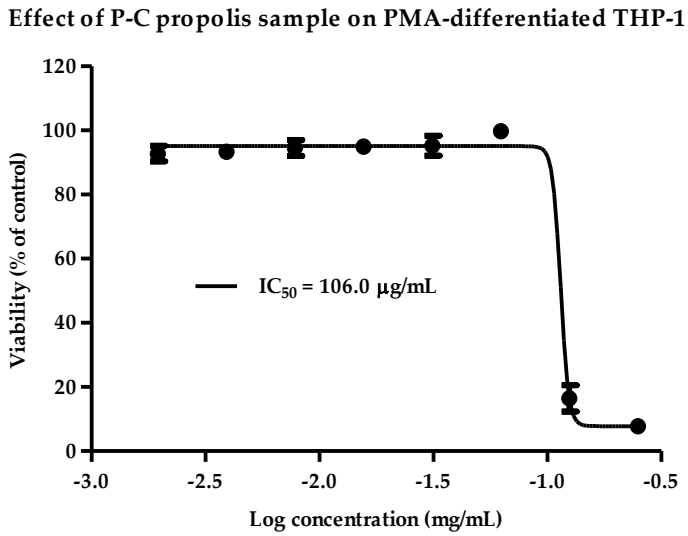

Figure 4-1: Cytotoxic effects of the Cameroon (P-C) propolis extract at varying doses on phorbol 12-myristate 13-acetate (PMA)-differentiated THP-1 cells.
The P-C extract was cytotoxic to PMA-treated cells, with an IC50 of 106.0 µg/mL. Each data point represents the mean ± SD (*n* = 3).

Table 4-1: Regions where propolis was collected and the concentrations of different propolis samples used on phorbol 12-myristate 13-acetate (PMA)-differentiated THP-1 cells.

Propolis Samples		IC50 (µg/mL)	Selected Final Concentration (µg/mL)
Region	**Extract Code**		
United Kingdom	P-UK1	57.95	30
	P-UK2	48.99	15
	P-UK3	53.55	20
	P-UK4	48.08	15
	P-UK5	46.28	15
Ghana	P-G	86.95	15
Cameroon	P-C	106	70
Indonesia	P-Ind1	25.73	15
	P-Ind2	>250	250

4.4.2 Effect of propolis extracts on pro-inflammatory TNF-α cytokine production

The sample extracts on their own showed no effect on the production of pro-inflammatory TNF-α in THP-1 cells when compared to a negative untreated control. However, when the cells were stimulated with LPS, the extracts inhibited the secretion of TNF-α, compared with LPS alone (ratio <1.0). Treatment with P-Ind2 extract greatly decreased the cytokine levels by approximately 80% and reached statistical significance when compared to LPS alone. Clear inhibitions of 15% and 20% were also observed with the P-UK1 and P-C extracts, respectively. As shown in **Figure 4-2**, the inhibitions were statistically significant when compared to negative control cells in all combination treatments with LPS, except for the P-Ind2 extract.

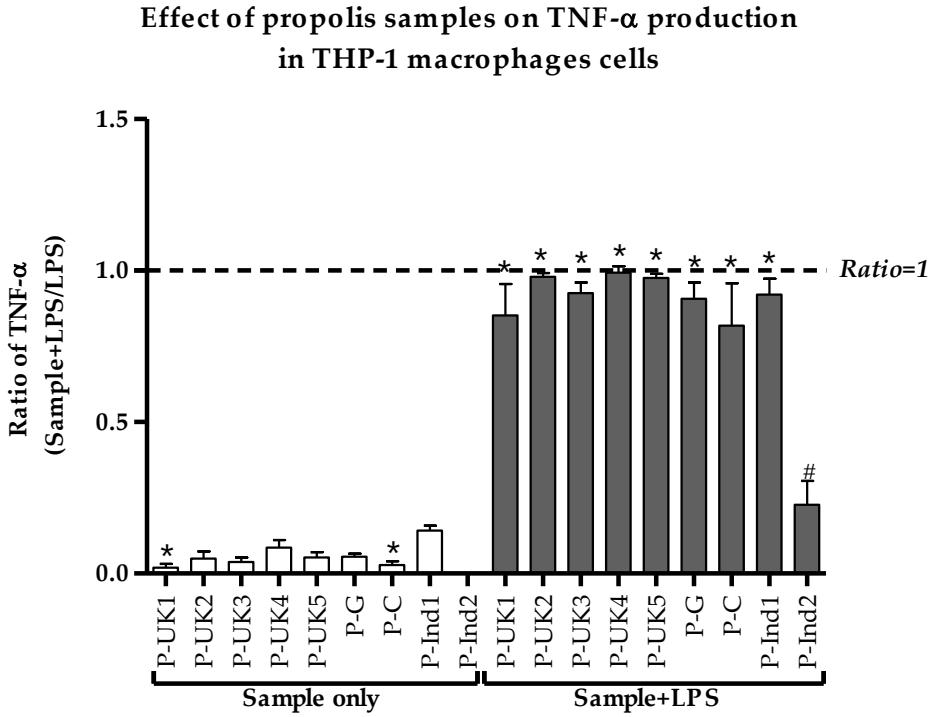

Figure 4-2: Effect of propolis extracts on the production of TNF-α by phorbol 12-myristate 13-acetate (PMA)-differentiated THP-1 cells in the absence and presence of lipopolysaccharide (LPS) (0.5 µg/mL).
The TNF-α levels were significantly different from the negative control levels in all eight combination treatments, except for the P-Ind2 extract (n = 3). *: Significant ($p < 0.05$) when compared with untreated control; #: Significant ($p < 0.05$) when compared with LPS alone; P-UK (1–5): Five propolis extracts from the UK; P-G: Propolis from Ghana; P-C: Propolis from Cameroon; P-Ind (1 and 2): Two Propolis extracts from Indonesia.

4.4.3 Effect of propolis extracts on pro-inflammatory Il-1β cytokine production

An inhibition of secretion of the pro-inflammatory IL-1β was clearly observed for five of the propolis extracts (**Figure 4-3**). The P-UK4 and P-C extracts, in combination with LPS, gave the highest inhibitory effect on cytokine secretion, at about 40%, when compared with LPS alone (ratio <1.0). In contrast to the TNF-α

level, the levels of IL-1β were surprisingly enhanced by treatment with P-UK1, P-G, P-Ind1 and P-Ind2, at ~11%, ~70%, ~50% and ~70%, respectively, when the cells were co-stimulated by LPS. The ratios of secreted cytokines differed significantly in response to the combination treatments of LPS and propolis extracts when compared to those of the negative control cells. Cells treated with propolis extracts only showed a slight increase in the background level release of cytokine, and this was only significant ($p < 0.05$) with the P-G extract (**Figure 4-3**).

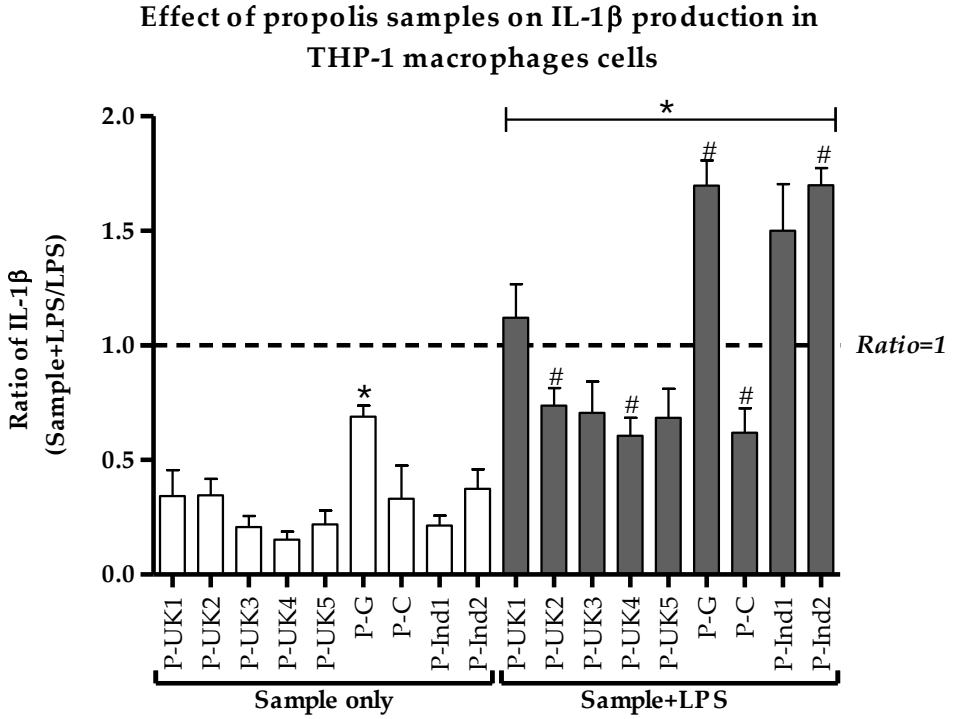

Figure 4-3: Effect of propolis extracts on the production of IL-1β by phorbol 12-myristate 13-acetate (PMA)-differentiated THP-1 cells in the absence and presence of LPS (0.5 µg/mL).
All nine combined treatments were significantly different from the negative control cells (n = 3). LPS: Lipopolysaccharides; *: Significant ($p < 0.05$) when compared with untreated control; #: Significant ($p < 0.05$) when compared with LPS alone; P-UK (1–5): Five propolis extracts from the UK; P-G: Propolis from Ghana; P-C: Propolis from Cameroon; P-Ind (1 and 2): Two Propolis extracts from Indonesia.

4.4.4 Effect of propolis extracts on pro-inflammatory Il-6 cytokine production

The secretion of IL-6 produced by LPS-stimulated THP-1 cells in response to all propolis extracts was lower when compared to cells stimulated with LPS alone (**Figure 4-4**). The P-UK1 extract showed the greatest effect on the cytokine level; however, the P-Ind2 extract had no effect on the level of this cytokine from the background level. The concentrations of secreted IL-6 were significantly lower when compared to the concentrations secreted by the positive control LPS. Propolis extract alone either had no effect on the release of this cytokine or the release was undetectable (Table S4.3).

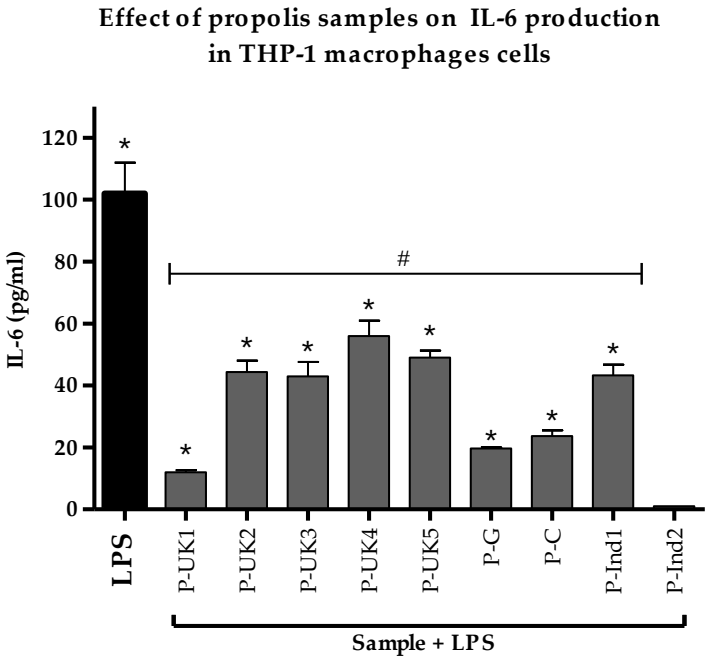

Figure 4-4: Effect of propolis extracts on the production of IL-6 by phorbol 12-myristate 13-acetate (PMA)-differentiated THP-1 cells in the absence and presence of LPS (0.5 µg/mL). All eight combined treatments apart from the P-Ind2 extract were significantly different from the negative and positive control ($n = 3$). LPS: Lipopolysaccharides; *: Significant ($p < 0.05$) when compared with untreated control; #: Significant ($p < 0.05$) when compared with LPS; P-UK (1–5): Five propolis extracts from the UK; P-G: Propolis from Ghana; P-C: Propolis from Cameroon; P-Ind (1 and 2): Two Propolis extracts from Indonesia.

4.4.5 Effect of propolis extracts on anti-inflammatory IL-10 cytokine production

The effect of propolis extracts on the secretion of the anti-inflammatory IL-10 cytokines by THP-1 cells was measured by adding the extracts on their own and in combination with 0.5 µg/mL LPS. Surprisingly, the levels of these cytokines were only slightly or negligibly affected following combined treatment with LPS when compared with LPS alone (**Figure 4-5**). The secretions were slightly altered from their negative control cells. The differences were not statistically significant from negative control cells; however, these negative effects could explain a more subtle mechanism of the anti-inflammatory action of propolis.

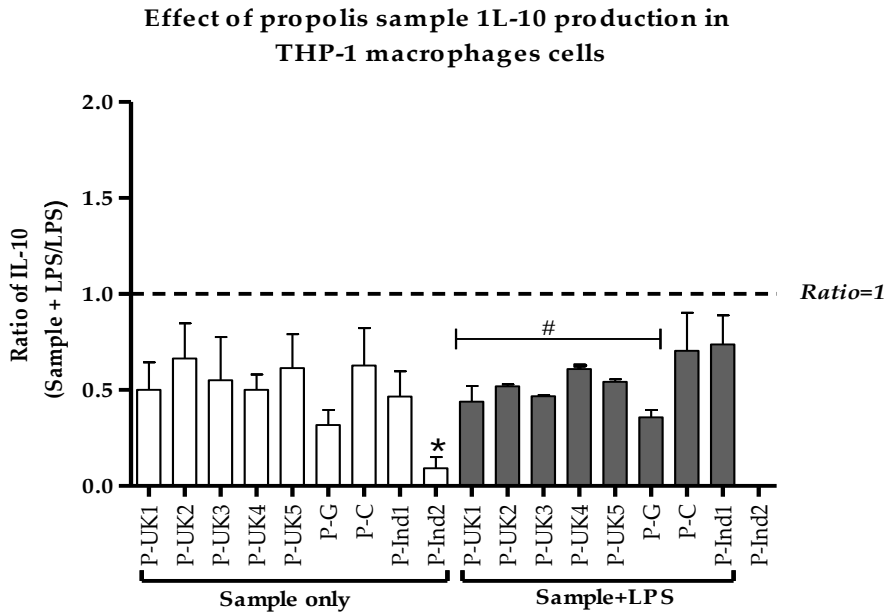

Figure 4-5: Effect of propolis extracts on the production of IL-10 cytokines by phorbol 12-myristate 13-acetate (PMA)-differentiated THP-1 cells in the absence and presence of LPS (0.5 µg/mL).
P-UK1-5 and P-G combined treatments of propolis and LPS were statistically different from LPS alone (n = 3). LPS: Lipopolysaccharides; *: Significant ($p < 0.05$) when compared with untreated control; #: Significant ($p < 0.05$) when compared with LPS; P-UK (1–5): Five propolis extracts from the UK; P-G: Propolis from Ghana; P-C: Propolis from Cameroon; P-Ind (1 and 2): Two Propolis extracts from Indonesia.

4.4.6 Effect of Cameroonian propolis (P-C) on the cell metabolome

Understanding the mechanism underlying the anti-inflammatory response to each propolis extract would be worthwhile; however, since the P-C extract showed the highest activity on TNF-α, IL-1β and IL-6 cytokines levels, it was selected for further metabolomic evaluation of its anti-inflammatory action. Metabolomics profiling of the PMA-differentiated THP-1 cells following LPS, P-C and P-C+LPS treatments were examined to assess the antagonistic effect of the P-C extract to LPS. Principle component analysis (PCA) gave a perfect clustering of quality control samples in the middle of the **Figure 4-6A** (P 1-6). This indicates the precision and

stability of the instruments during the sample runs on the ZIC-pHILIC column for all the polar metabolites. Comparison of the control, LPS, P-C alone and P-C+LPS groups showed clear group separations using an OPLS-DA model (**Figure 4-6B**). The separation between treatment and control groups would suggest different biochemical interactions of P-C+LPS compared with LPS alone.

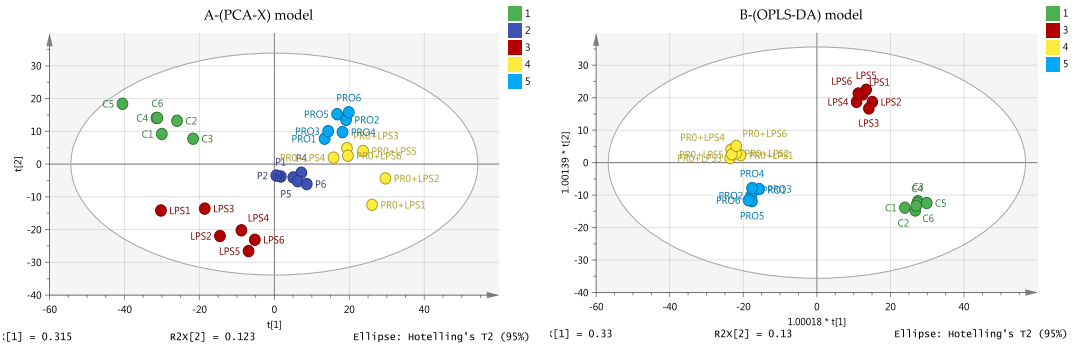

Figure 4-6: (A) PCA-X versus (B) OPLS-DA score plots of THP-1 cells.
The figures show a clear separation between control, pooled and treatment groups (LPS, Propolis and Propolis+LPS) based on 403 polar metabolites separated on a ZIC-pHILIC column (*n* = 6). The PCA score plot **(A)** gives R2X = 0.583, Q2 = 0.409. The OPLS-DA score plot **(B)** gives R2X = 0.640, R2Y = 0.984, Q2 = 0.753. (C: Control; Pro: Cameroonian propolis (P-C) propolis extract; LPS: Lipopolysaccharides; Pro+LPS: Propolis and LPS (= P-C + LPS) combination treatments; P = pooled samples). PCA: Principle component analysis.

The data set for all polar metabolites was filtered by excluding metabolites with relative standard deviation (RSD) values >20% within the pooled samples. The most significantly altered metabolites are summarised in **Table 4-2**. The LPS and propolis extract groups were compared to normal control cells (LPS/C and P-C/C, respectively), whereas the LPS-treated cells were compared to the combination treatments to give a clearer depiction of the effect of propolis alone and to explain the difference due to LPS effects (P-C+LPS/LPS). The aim was to confirm the distinct metabolic profile for the treatment with propolis in the presence and absence

of LPS. The univariate analysis in **Table 4-2** shows that different pathways were significantly changed, including glycolysis, the tricarboxylic acid (TCA) cycle, oxidative phosphorylation (OXPHOS), arginine and proline metabolism and purine and pyrimidine metabolism.

Table 4-2: Significantly changed metabolites in THP-1 cells.
The cells were treated with either lipopolysaccharide (LPS) or Cameroonian propolis (P-C) extract alone in comparison with untreated controls and in cells treated with a combination of P-C and LPS compared with LPS treated cells. The results show the majority of affected metabolites. (0.5 µg/mL LPS; 70 µg/mL P-C).

Mass	Rt	Putative Metabolite	LPS/C		P-C/C		(P-C+LPS)/LPS	
			Ratio	*p*-Value	Ratio	*p*-Value	Ratio	*p*-Value
		Arginine and Proline Metabolism	-	-	-	-	-	-
145.08	15.39	4-Guanidinobutanoate	1.991	<0.001	1.549	0.002	1.419	0.002
115.06	13.01	L-Proline *	1.137	0.046	1.467	<0.001	1.303	0.001
113.06	11.14	Creatinine	0.884	ns	1.112	ns	1.454	0.030
175.10	16.04	L-Citrulline *	1.790	<0.001	2.148	<0.001	1.090	ns
129.09	16.02	4-Guanidinobutanal	1.494	0.032	1.723	<0.001	1.062	ns
290.12	16.78	N-(L-Arginino)succinate	0.556	0.001	0.919	ns	1.278	0.020
189.06	13.95	N-Acetyl-L-glutamate *	0.662	<0.001	3.983	<0.001	4.955	<0.001
145.16	26.37	Spermidine *	1.198	ns	0.169	<0.001	0.078	<0.001
		Glycolysis/TCA cycle						
260.03	16.83	D-Glucose 1-phosphate *	0.996	ns	0.531	<0.001	0.476	<0.001
260.03	15.95	D-Fructose 6-phosphate *	1.424	0.001	1.486	0.001	1.229	0.046
340.00	18.05	D-Fructose 1,6-bisphosphate *	2.242	<0.001	1.163	0.006	0.754	0.003
170.00	16.00	D-Glyceraldehyde 3-phosphate *	0.717	0.001	1.899	<0.001	1.622	<0.001
260.02	17.72	D-Glucose 6-sulfate	1.339	0.004	1.461	<0.001	1.118	ns
167.98	17.45	Phosphoenolpyruvate	1.254	ns	2.503	0.001	2.062	0.004
88.02	7.67	Pyruvate *	1.609	0.007	0.916	ns	0.483	<0.001
809.13	12.28	Acetyl-CoA	0.681	0.002	1.678	<0.001	1.912	0.001
190.01	15.80	Oxalosuccinate	0.588	0.044	5.385	ns	1.691	ns
132.01	15.74	Oxaloacetate *	0.700	0.041	1.064	ns	1.566	0.016

192.03	18.08	Citrate *	1.453	0.002	1.636	<0.001	1.214	0.040
118.03	14.94	Succinate *	1.323	0.005	1.534	<0.001	1.182	ns
116.01	14.92	Fumarate	0.894	ns	0.752	0.001	0.842	ns
131.07	14.89	Creatine *	0.647	<0.001	1.179	0.011	1.544	<0.001
427.03	15.19	ADP *	0.814	0.041	3.140	<0.001	2.425	<0.001
443.02	18.08	GDP *	0.727	0.003	1.917	<0.001	2.158	<0.001
507.00	16.55	ATP *	0.776	0.019	1.341	0.022	1.303	0.004
522.99	19.50	GTP *	0.923	ns	1.309	0.002	1.237	0.016
665.12	13.29	NADH *	0.757	0.004	1.623	<0.001	1.620	0.001
663.11	14.24	NAD+ *	0.363	<0.001	0.877	ns	1.893	<0.001
		Oxidative Stress/ Pentose Phosphate Pathway						
276.02	17.61	6-Phospho-D-gluconate *	1.355	0.001	0.521	<0.001	0.273	<0.001
196.06	13.15	D-Gluconic acid *	0.889	0.006	1.539	<0.001	1.310	<0.001
177.94	15.81	Pyrophosphate	1.271	0.009	1.406	<0.001	1.189	0.024
290.04	16.09	D-Sedoheptulose 7-phosphate	1.367	<0.001	1.970	<0.001	1.570	<0.001
370.01	18.21	D-Sedoheptulose 1,7-bisphosphate	1.900	<0.001	1.757	<0.001	0.893	ns
210.07	14.03	Sedoheptulose	1.741	0.002	1.202	ns	0.931	ns
230.02	15.68	D-Ribose 5-phosphate *	1.572	0.036	1.018	ns	0.736	ns
307.08	14.22	Glutathione	0.579	<0.001	1.508	<0.001	1.856	<0.001
612.15	17.27	Glutathione disulphide *	0.838	0.017	3.157	<0.001	3.791	<0.001
745.09	16.87	NADPH	0.494	<0.001	00.00	<0.001	00.00	<0.001
743.08	16.68	NADP+ *	0.896	ns	2.267	<0.001	2.063	<0.001
		Purine Metabolism						
347.06	15.61	dGMP	0.461	<0.001	1.575	0.001	1.937	<0.001
267.10	9.35	Adenosine *	1.276	ns	3.435	<0.001	2.445	<0.001
283.09	12.80	Guanosine *	1.677	ns	4.070	<0.001	3.202	0.004
268.08	11.06	Inosine *	2.967	<0.001	10.511	<0.001	13.160	<0.001

284.08	10.51	Xanthosine*	2.064	ns	2.378	0.005	1.002	ns
251.10	7.93	Deoxyadenosine	2.912	<0.001	0.399	<0.001	0.292	<0.001
152.04	11.30	Xanthine *	1.766	0.002	1.772	<0.001	1.013	ns
168.03	12.34	Urate *	1.752	0.008	1.897	0.000	1.135	ns
136.04	10.41	Hypoxanthine *	14.695	<0.001	2.277	0.009	0.714	0.013
398.14	16.78	S-Adenosyl-L-methionine *	1.237	ns	2.578	<0.001	1.695	<0.001
297.09	16.78	5'-Methylthioadenosine *	0.700	0.001	2.727	<0.001	1.570	<0.001
348.05	15.39	IMP *	2.815	<0.001	3.341	<0.001	1.168	ns
347.06	13.75	AMP *	0.558	<0.001	2.164	<0.001	2.080	<0.001
		Pyrimidine Metabolism/Glycan Chain Formation						
125.06	10.94	5-Methylcytosine	1.486	0.004	2.124	<0.001	1.396	0.003
482.98	18.68	CTP *	0.603	<0.001	0.894	ns	1.403	<0.001
244.07	12.14	Pseudouridine	1.199	0.038	1.914	<0.001	1.668	<0.001
323.05	15.42	CMP *	0.742	0.002	1.915	<0.001	1.760	<0.001
111.04	11.13	Cytosine*	0.250	<0.001	0.359	0.003	1.142	ns
114.04	14.89	5,6-Dihydrouracil	0.631	<0.001	1.150	ns	1.604	<0.001
259.05	11.93	Glucosamine 1-phosphate	1.202	ns	1.711	0.001	1.360	0.020
324.04	15.06	UMP *	0.630	<0.001	2.223	<0.001	1.878	<0.001
404.00	16.48	UDP *	0.433	<0.001	2.482	<0.001	2.412	<0.001
483.97	17.79	UTP *	0.591	0.000	0.669	0.002	0.954	ns
566.05	16.04	UDP-glucose *	0.503	<0.001	0.955	ns	1.711	<0.001
536.04	16.07	UDP-D-xylose	0.666	0.002	2.042	<0.001	2.321	<0.001
580.03	18.83	UDP-glucuronate	0.583	<0.001	1.426	0.001	1.706	<0.001
607.08	14.91	UDP-N-acetyl-D-glucosamine *	0.579	<0.001	0.984	ns	1.539	0.001
		Tryptophan Metabolism						
220.09	9.74	5-Hydroxy-L-tryptophan isomer	8.133	<0.001	1.285	0.014	0.228	<0.001
191.06	10.29	5-Hydroxyindoleacetate *	1.527	<0.001	0.869	0.035	0.503	<0.001

219.05	10.31	5-Hydroxyindolepyruvate	1.515	<0.001	0.872	0.015	0.523	<0.001
117.06	11.07	Indole *	1.723	0.011	1.565	0.002	0.987	ns
204.09	11.85	L-Tryptophan *	1.182	ns	1.849	<0.001	1.531	0.013
208.09	11.09	L-Kynurenine *	1.835	0.001	1.591	0.001	0.810	ns
		Miscellaneous						
131.06	14.61	N-Acetyl-beta-alanine	1.306	<0.001	1.521	<0.001	1.263	0.011
210.04	17.19	D-Glucarate	0.611	0.005	1.385	0.020	2.367	<0.001
161.11	13.50	L-Carnitine *	0.899	ns	1.267	<0.001	1.504	0.002
149.05	11.72	L-Methionine *	1.380	0.011	1.527	<0.001	1.230	0.037
175.05	14.17	N-Acetyl-L-aspartate *	0.625	<0.001	1.117	ns	1.721	<0.001
203.12	11.26	O-Acetylcarnitine *	0.945	ns	3.291	<0.001	3.114	<0.001
226.11	15.85	Carnosine *	1.166	ns	1.558	<0.001	1.279	0.025
119.06	14.52	L-Threonine	1.432	<0.001	1.558	<0.001	1.140	ns
105.04	15.85	L-Serine *	1.432	0.008	1.625	<0.001	1.194	ns

Rt: Retention time (min); LPS: Lipopolysaccharide; P-C: Cameroonian propolis; P-C + LPS: combination treatment; *: Matches the analytical standard retention time; ns: non-significant.

Ratio plot analysis (**Figure 4-7**) of the metabolomics data from THP-1 derived macrophages cells characterise the highest and lowest abundance and accumulated metabolites. Statistically significant differences between P-C+LPS and LPS were observed in 62 polar metabolites. It visualises the error associated with the ratio calculation for each metabolite (n = 6). Upregulation of most of the metabolites was observed clearly upon treatment with propolis extract. It was characterized that inflammatory-related metabolites, such as hypoxanthine, putative acetyl-CoA and citrate, were altered by the combination treatments.

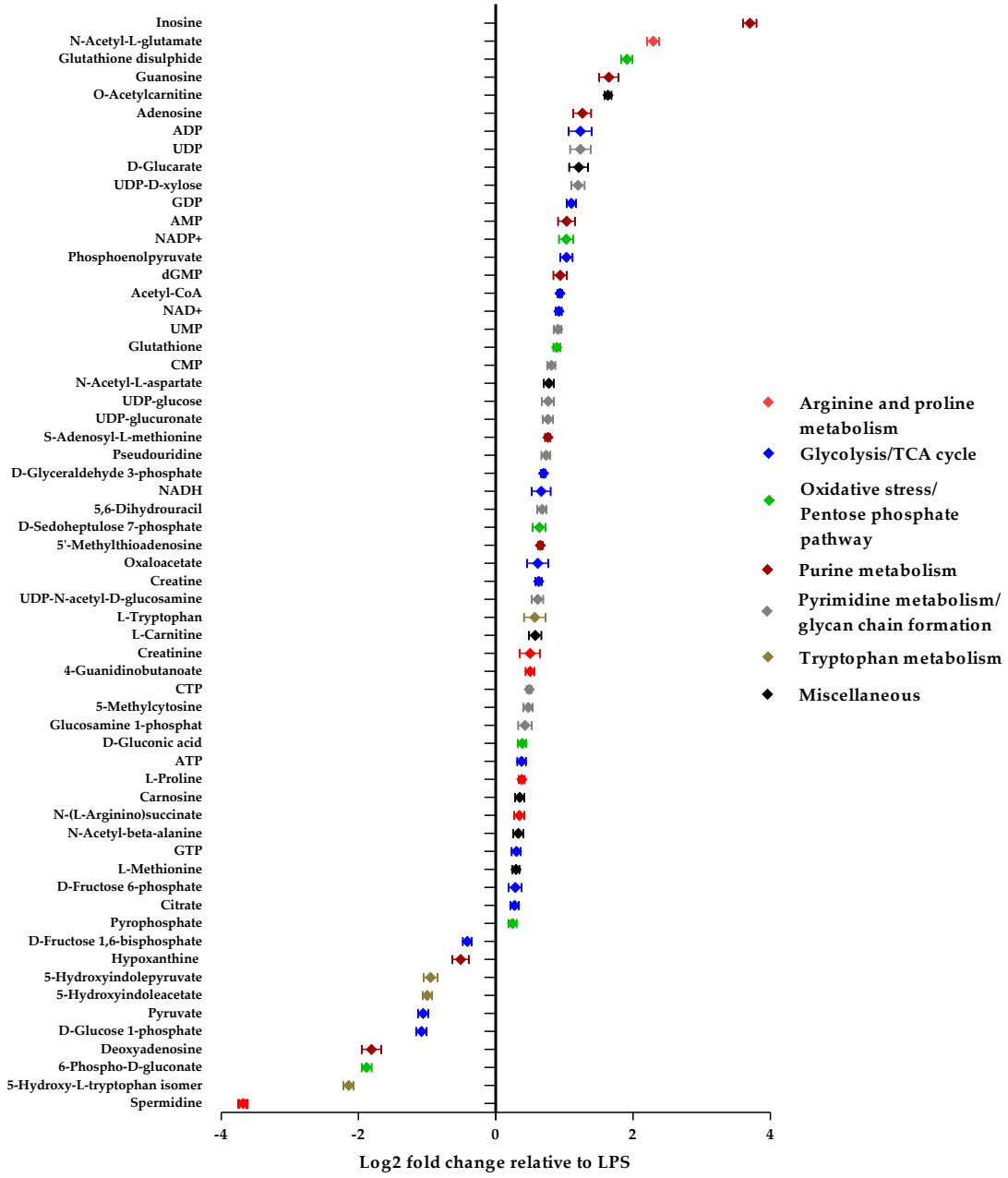

Figure 4-7: The log2- fold change between P-C+LPS and LPS alone in PMA-differentiated THP-1 cells.
The y-axis plots individual metabolites. The x-axis plots log2 transformed relative ratio of abundance of each metabolite in the P-C and LPS combination treatment normalized to the levels of the metabolite in the positive control LPS.

4.5 Discussion

Macrophages, upon stimulation by various microbial and environmental signals, polarise into different subpopulations with distinct purposes. These cell subpopulations are crucial for the inflammatory process and for defence against infections, and they conduct these processes through the secretion of such molecules nitric oxide (NO) and inflammatory cytokines, such as TNF-α, IL-1β and IL-6 [237]. Over-secretion of these mediators has been observed in several inflammatory diseases and cancer [252]. The aim of the present study was to assess the use of propolis samples from different regions as anti-inflammatory agents.

Cytotoxicity assays were performed on THP-1 cells using nine different propolis extracts. The ethanolic extracts of the propolis showed different cytotoxicities towards the cells, which might be explained by their different chemical compositions. The sensitivity of the cells to propolis extracts from the UK (P-UK1-5) were very close to each other (Figure S4.1), with respect to their differences in cytokine responses. P-Ind1 showed the highest toxicity to THP-1 cells; however, the cells were still >90% viable at the dose chosen for cytokine assessments (15 µg/mL). Based on the cytokine production and anti-inflammatory performance of the propolis extracts, P-C was chosen for further metabolic investigations at 70 µg/mL. Among the assessed cytokines, pro-inflammatory IL-6 showed the strongest reduction in secretion in response to all propolis extracts at their respective selected concentrations (**Table 4-1**). The secretion of TNF-α was significantly decreased with P-UK1, P-C and P-Ind2 and only slightly decreased with the other extracts. P-UK4 and P-C showed the most pronounced anti-IL-1β effects. Interestingly, the secretion

of this cytokine in LPS-stimulated THP-1 cells was enhanced by P-UK1, P-G, P-Ind1 and P-Ind2, suggesting the possibility that different mechanisms might exist for the secretion of each cytokine in LPS-stimulated macrophages [237].

Since P-C showed the most consistent effects in lowering the cytokine response, it was selected for further study. The metabolite responses were observed in THP-1 cells following administration of LPS, P-C and P-C+LPS with the goal of determining whether the metabolite alterations induced by propolis in the presence or absence of LPS could provide a better understanding of the mechanisms and pathways involved in the anti-inflammatory characteristics of propolis.

Cameroonian propolis has been chemically investigated and contains triterpenes [243] that have shown dose-dependent anti-inflammatory actions [253]. In addition, its biological activity might reflect the presence of many caffeic acid derivatives [254, 255]. Propolis and its isolated compounds were also reported to decrease the release of inflammatory cytokines through suppression of NF-κB activation [256, 257]. The NF-κB pathway can be activated by LPS through TLR recognition [177, 204]. Blockade of cytokines, and particularly of IL-1 and TNF-α, in immune inflammatory diseases has provided the greatest advances in medicine and in the development of novel treatments for inflammation [258]. TNF-α plays a crucial role in initiating the cascade of pro-inflammatory cytokines and their subsequent inflammatory processes. IL-6 is also produced rapidly in acute inflammatory responses [237, 258].

Several studies have shown that propolis has immunological activity [259]. Another study has shown that the antioxidant and anti-inflammatory activity of Brazilian green propolis in stimulated J774A.1 macrophages occurs by the inhibition of reactive oxygen species (ROS), NO and pro-inflammatory cytokines, including TNF-α, IL-1β and IL-6 [260]. In the present study, production of these cytokines was clearly inhibited by propolis extracts apart from P-UK1, P-G and P-Ind1 and 2 in IL-1β. We therefore sought to gain further insight into their immunosuppressive mechanism of action by conducting non-targeted metabolic profiling of the effect of Cameroonian propolis on THP-1 cells. Using the same method of metabolic identification, no trace of any metabolites was found in the P-C sample.

Activation of TLRs, particularly with LPS, leads to a switch from oxidative phosphorylation (OXPHOS) towards glycolysis in immune cells [261], similar to the response observed in tumour cells. Stimulation with LPS revealed significant changes in amino acid, carbohydrate and nucleotide metabolism [262]. In addition, clear differences were previously reported for the fat metabolome [143, 262]. The results of the present study confirm the effect of LPS on macrophage cells and further examine anti-LPS activity by propolis extracts using a metabolomics approach.

While there appear to be effects of LPS on glycolysis, these are not that prominent and there is no marked effect of P-C in countering these. Taking the data as a whole, the very large effects on metabolite levels can be seen in purine metabolism. LPS produces a 14-fold increase in the level of hypoxanthine and treatment with P-C completely abolishes this and promotes a 13-fold increase in the precursor of

hypoxanthine, inosine. P-C treatment on its own also produces a 10-fold increase in inosine. Thus, it would seem that P-C is acting as an inhibitor of purine nucleoside phosphorylase (PNP). This is an enzyme that can hydrolyse a range of nucleosides and the proposed mode of action is supported by accumulation of adenosine, guanosine and xanthosine, which are also substrates of the enzyme [263-265]. In addition, methylthioadenosine [266] and possibly S-adenosylmethionine are hydrolysed by a similar mechanism and these metabolites also accumulate. PNP deficiency causes severe immunosuppression in people who are deficient in the enzyme [267]. PNP-deficient mice were found to accumulate guanosine and inosine [268]. It is currently not completely known why PNP deficiency causes immunosuppression. Deficiency in purine nucleotide deaminase that converts adenosine monophosphate to inosine monophosphate (AMP to IMP) also causes immunosuppression. Our previous study examined the effect of LPS and a combination of LPS and melittin on THP-1 cells and identified an increase in the level of hypoxanthine [262]. Interestingly, in the current case, this increased level was suppressed by ~30% following treatment with P-C and LPS together, compared to LPS alone. One possible explanation for the effect on the immune response is that hypoxanthine is a major substrate for the production of superoxide via the action of xanthine oxidase [269, 270] and impairment of superoxide production might impair the immune response. Coupled to the production of superoxide from hypoxanthine oxidation is indole dioxygenase (IDO), and this enzyme is responsible for degrading tryptophan via the kynurenine pathway [271, 272]. This degradative pathway lowers the immune response through producing various molecules in the kynurenine

pathway, including kynurenine, which can bind to the aryl hydrocarbon receptor (AHR) receptor causing immune suppression [273, 274]. Regan et al. reported depletion in tryptophan with an accumulation of kynurenine following stimulation by LPS and IFN-α [275, 276]. The anti-inflammatory drug indomethacin caused a significant attenuation of the effects of LPS on tryptophan and a reduction in the level of kynurenine was observed following IFN-α stimulation, but no effect on kynurenine was observed after LPS treatment [276].

In the current case, kynurenine levels are increased by both the LPS and P-C treatments and may contribute to immune-modulation. Thus, the production of hypoxanthine in the purine nucleotide cycle (PNC) could both simulate the immune response through acting as a substrate for xanthine oxidase, resulting in the production of superoxide, and also reduce it through promoting production of kynurenine.

IMP is formed as a result of an excessive demand for ATP, such as in skeletal muscle during intense exercise [277, 278]. The high demand results in some of the ATP pool in the muscle being used up, and the AMP formed as a result is converted to IMP and enters the purine nucleotide cycle (PNC) with subsequent conversion into inosine and hypoxanthine that are lost from the muscle and enter the blood. It may be that the high demand for ATP in activated macrophages is analogous to the situation in skeletal muscle. IMP is recycled back to AMP via an enzymatic reaction involving aspartate and guanosine 5’-triphosphate (GTP), thus conserving purines and ultimately supporting the production of ATP; this process with regard to skeletal muscle and exercise is more efficient in trained individuals. In the THP

macrophages, there is a marked increase in GTP resulting from the P-C treatment both with and without LPS and there is a corresponding rise in AMP in the presence of P-C. Associated with this, there are elevations in both ATP and ADP in the P-C-treated cells. The source of the elevated GTP cannot be exactly pinpointed from the metabolic profile. GTP can be formed in the tricarboxylic acid (TCA) cycle in the conversion of succinyl coenzyme A (succinyl CoA) to succinate; succinate levels are slightly higher in the P-C-treated samples. However, it is difficult to infer from the levels of metabolites in a cycle whether or not higher levels of a particular metabolite are due to increased flux through the cycle or accumulation due to slowing down. The recent literature indicates that the TCA cycle is disrupted by treatment of macrophages with LPS, resulting in an accumulation of succinate and the dicarboxylic acid itaconate [143]. In the current case, there was no evidence of itaconate accumulation. Significant increases in pyruvate with acetyl-CoA reduction by LPS are supported by several previous studies [143, 262], which also support the shift towards lactate rather than acetyl-CoA production. The combination of LPS with P-C antagonised this effect and reversed the effects of LPS pyruvate and acetyl-CoA so that they were significantly decreased and increased, respectively. An increase in putative acetyl-CoA would favour an increased flux towards the TCA cycle, as detected here, which would, in turn, enhance the formation of citrate and oxaloacetate. The citrate is converted to acetyl-CoA and oxaloacetate via the ATP-citrate lyase enzyme in the presence of ATP. Acetyl-CoA helps activated macrophages to meet their lipid biosynthesis and biosynthetic demands [143]. At the same time, citrate enhances the production of NO and ROS through the conversion

of oxaloacetate to pyruvate and nicotinamide adenine dinucleotide phosphate (NADPH). The latter generates ROS by NADPH oxidase and is used for NO and citrulline production from L-arginine [140]. This also would explain the increased production of the putative acetyl-CoA and oxaloacetate reported in this study in response to LPS alone (**Table 4-2**). However, these two metabolites were increased significantly in LPS and P-C combination treatment, which suppressed LPS activity.

An increase in the levels of NADH in the P-C-treated samples also supports the proposal that the treatment is promoting the TCA cycle. Increased flux through the TCA cycle could support the increase in levels of ATP and GTP resulting from the propolis treatments. Increases in ATP would support the immunological response; thus, the propolis as a complex mixture seems to have more than one mode of action and overall the effect is immunomodulatory, both supporting the immune response and decreasing it as evidenced by the decreased release of cytokines. Overall, the P-C treatment increases the high-energy phosphates, which are derived from ATP, in the cells with cytidine triphosphate (CTP), uridine mono- and di-phosphate (UMP and UDP) levels also increasing in the presence of P-C. UTP levels are decreased by the P-C treatment, but this might be due to the UTP being consumed in producing increased levels of the UDP conjugates with glucose, xylose and N-acetyl glucosamine. These conjugates are employed for the biosynthesis of glycan chains attached to cell-surface proteins. It has been proposed that increases in these conjugates occur when the macrophages polarise towards their M2 phenotype, where glycation of receptors may be responsible for a decrease in response to LPS [279, 280].

Both L-citrulline and NO are by-products of arginine metabolism by the inducible nitric oxide synthase (iNOS) [281], and citrulline levels were significantly increased in response to LPS (**Table 4-2**). The production of citrulline was also elevated by propolis alone; however, citrulline production was not significantly different in cells treated with a combination of P-C and LPS when compared to LPS alone and was accompanied by a significant increase in its putative product metabolite N-(L-arginino) succinate, which is required to recycle citrulline back into arginine. Ethanolic extracts of propolis significantly and dose-dependently inhibited the production of NO in macrophage cells [260]. The ability to sustain NO generation plays a crucial role in macrophage adaptation that allows for killing of intracellular mycobacteria [282, 283]. Moreover, IL-1β cytokines also have an important role in infected macrophages [284]. Conversely, continuous production of NO from iNOS activation inhibits IL-1β through the inflammasome [285]. Thus, an environment-dependent adjustment of macrophage function might be activated through the activity of the arginine, including pathways such as the citrulline-arginine cycle and argininosuccinate pathway [152].

The antagonism of LPS by the LPS+P-C combination treatment was also observed in this study through the increase in NADP+ and a decrease in pyruvate level, which would prevent further ROS and NO production. Furthermore, the TCA cycle is interrupted by LPS through the inhibition of succinate dehydrogenase (SDH), causing an elevation in the succinate level [192, 286]. The elevation in succinate in response to LPS alone promotes inflammation by inhibiting prolyl hydroxylase (PHD) activity and subsequent accumulation of the hypoxia induced factor-1α (HIF-

1α) protein [286]. SDH is an integral component of the respiratory chain complex II; its inhibition by the LPS leads to a reduction in mitochondrial respiration [140]. The activity of complex I in the mitochondria can also be suppressed by the accumulated succinate, which causes further ROS production [152, 287].

Several previous studies have described the reprogramming of macrophage cells upon stimulation, particularly with respect to glucose-PPP (pentose phosphate pathway) metabolism [200]. In M1 macrophages, LPS downregulates carbohydrate kinase-like protein (CARKL), leading to a high cellular redox state [150]. This would lead to a build-up of several metabolites [150, 281], including putative sedoheptulose-7-phosphate (S7P), ribose-5-phosphate and fructose-6-phosphate, which increased significantly in response to LPS (**Table 4-2**). Cell reprogramming occurs to refocus the macrophage in order to increase PPP and glycolysis to support M1 polarisation [200]. However, a general increase was observed in the present study in the level of glycolysis, TCA cycle, OXPHOS and PPP by the effect of the P-C and LPS combination treatment. Consequently, the levels of ADP, ATP, NADP+ and nicotinamide adenine dinucleotide (NADH and NAD+) were enhanced by the combination of P-C and LPS compared to LPS alone (**Figure 4-7**).

4.6 Conclusion

The present study addressed the main features involved in LPS activation of THP-1-derived macrophage cells and the possible use of propolis extracts as an anti-inflammatory treatment. The study results suggested that key pathways are perturbed by propolis in macrophage cells. Suppression of the LPS effects on cytokine production in these cells was confirmed for propolis samples from different regions.

The antagonistic effects were detected in the levels of TNF-α, IL-1β and IL-6 pro-inflammatory cytokines. Although P-UK1, P-G and P-Ind1-2 extracts inhibited TNF-α and IL-6, they produced a stimulatory effect on IL-1β release. However, the P-C samples suppressed the release of all four cytokines. Further study using a metabolic approach identified metabolic alterations that may contribute to the subsequent anti-inflammatory events. Both LPS and propolis changed the levels of metabolites in several different pathways, but the really major shifts in levels were in purine metabolism. The accumulation of several substrates of PNP in the presence of the P-C both with and without LPS being present suggested that it was acting as an inhibitor of PNP. Deficiency in PNP is associated particularly with a deficiency in T-cell immunity [288]. In addition, metabolic reprogramming by LPS caused an enhanced production of glycolysis and PPP products to replenish the disrupted TCA cycle and maintain ATP generation. Upregulation of some intermediate metabolites within glycolysis, the TCA cycle, oxidative phosphorylation and PPP in response to the combination of P-C and LPS were observed to counteract LPS activity. This metabolic investigation revealed the complexity of the macrophage responses to different treatments. Taken together, these data support several previous studies that suggest that propolis has clinical potential as a natural anti-inflammatory agent. Although a complex mixture varying in composition, propolis has a remarkably consistent biological effect that is possibly due to the selection pressure on bees causing collection of a material that provides similar biological properties regardless of its composition.

Chapter Five

Metabolomic Profiling of the Immune Stimulatory Effect of Eicosenoids on PMA-Differentiated THP-1 Cells

5 Metabolomic Profiling of the Immune Stimulatory Effect of Eicosenoids on PMA-Differentiated THP-1 Cells

5.1 Abstract

Honey bee venom has been established to have significant effect in immunotherapy. In the present study, (Z)-11-eicosenol-a major constituent of bee venom, along with its derivations methyl cis-11-eicosenoate and cis-11-eicosenoic acid, were synthesised to investigate their immune stimulatory effect and possible use as vaccine adjuvants. Stimuli that prime and activate the immune system have exerted profound effects on immune cells, particularly macrophages; however, the effectiveness of bee venom constituents as immune stimulants has not yet been established. Here, the abilities of these compounds to act as pro-inflammatory stimuli were assessed, either alone or in combination with lipopolysaccharide (LPS), by examining the secretion of tumour necrosis factor-α (TNF-α) and the cytokines interleukin-1β (IL-1β), IL-6 and IL-10 by THP-1 macrophages. The compounds clearly increased the levels of IL-1β and decreased IL-10, whereas a decrease in IL-6 levels suggested a complex mechanism of action. A more in-depth profile of macrophage behaviour was therefore obtained by comprehensive untargeted metabolic profiling of the cells using liquid chromatography mass spectrometry (LC-MS) to confirm the ability of the eicosenoids to trigger the immune system. The level of 358 polar and 315 non-polar metabolites were changed significantly ($p < 0.05$) by all treatments. The LPS-stimulated production of most of the inflammatory metabolite biomarkers in glycolysis, the tricarboxylic acid (TCA) cycle, the pentose phosphate pathway, purine, pyrimidine and fatty acids metabolism were significantly

enhanced by all three compounds, and particularly by methyl cis-11-eicosenoate and cis-11-eicosenoic acid. These findings support the proposed actions of (Z)-11-eicosenol, methyl cis-11-eicosenoate and cis-11-eicosenoic acid as immune system stimulators.

5.2 Introduction

The immune stimulating effects of adjuvants was first established with the addition of aluminium potassium sulphate or aluminium salts to human vaccines [289, 290]. Today, a better understanding of immune responses has increased the availability and variety of vaccine adjuvants to include virosomes, MF59 and AS04 [290]. Adjuvants, in the context of vaccines, are described as substances capable of enhancing and modulating antigen-specific immune responses to improve vaccine efficacy [291]. Adjuvants are now in widespread use, but their development has been empirical, without a clear understanding of their molecular and cellular mechanisms of action. However, several studies have suggested that adjuvants act by enhancing T and B cell responses, by stimulating innate immunity and by increasing the magnitude of the adaptive responses to the vaccine [292-294]. Adjuvants also stimulate a strong and comprehensive immune response to antigen by mimicking natural defensive trigger molecules, such as endogenous immune-active substances (e.g. chemokines and cytokines) or other natural compounds (e.g. vitamin E and saponins) [290].

A crucial need exists for the development and investigation of new vaccine adjuvant compounds that have the ability to induce immune responses. However, the molecular and cellular mechanisms that regulate the activity of the majority of

human-licensed adjuvants are still only partially characterised. The adjuvant derivatives of bacterial components, such as lipopolysaccharide (LPS), cytidine–phosphate–guanosine (CpG) oligonucleotides and monophosphoryl lipid A (MPL), are probably the most characterised at present [295]. MPL works as an agonist of Toll-like receptor (TLR4), which is expressed on antigen presenting cells (APCs), such as dendritic cells (DCs) and macrophages, and promotes cytokine expression, antigen presentation and migration of the APCs to the T cell area [296, 297]. These compounds act as microbial sensors called pathogen-associated molecular patterns (PAMPs), and they activate pattern recognition receptors (PRR) and subsequently TLR [298].

LPS is the most widely studied of the TLR4 ligands, and its adjuvant derivatives (which are less toxic) have been the basis of virtually all clinical trials of adjuvant TLR4 agonists [299]. The interactions of LPS derivatives with TLR4 are restricted mainly to their lipid A portion, which are composed of polyacylated diglucosamine lipids [300]. A combination of specific adjuvants with TLR agonists has been proposed to optimise vaccines [86]. Therefore, evaluation of the LPS enhancement of cytokine productions and a metabolic interpretation of LPS immune-modulatory effects would be a promising strategy for investigating proposed new adjuvants.

Honey bee (*Apis mellifera*) venoms is a very complex mixture of substances, including organics, peptides and enzymes. These ingredients contribute a variety of biological activities towards the overall toxic shock [301], and have attracted attention as possible leads for drug discovery. Some components have been applied to the treatment of inflammation and cancer, for example, [174, 302, 303], but their

use as vaccine adjuvants is still under investigation. Melittin, a major lytic peptide found in bee venom, has been proposed as a vaccine adjuvant due to its confirmed ability to enhance TNF-α, IL-1β and IL-6 cytokine production within the THP-1 monocyte-derived macrophage cell line [136, 262].

An organic compound of interest in honey bee venom is (Z)-11-eicosen-1-ol. This is a major component of the alarm pheromone mixture co-secreted with the venom [304]. Insect pheromones are typically volatile organics that are released to warn of danger [305]. (Z)-11-eicosen-1-ol prolongs the effectiveness of isopentyl acetate, another key component of the alarm pheromone secretion, thereby increasing the speed of the aggressive response [301, 304]. A similar compound, (Z)-9-eicosen-1-ol, was detected in *A. mellifera* venom, resembling the compound described by Pickett *et al.* and differing only with respect to the double bond position [136]. It was found to enhance the release of pro-inflammatory cytokines, other than IL-6 [136].

Immune metabolism is a rapidly growing area of research. Recently, several studies have shown the importance of metabolites, such as succinate and itaconate, in the modulation of the innate immune response of macrophages [82, 306]. The exposure of macrophages to various immune stimuli, including pathogenic antigens and cytokines, initiates a number of signalling cascades by interactions with receptors (*i.e.* cytokine receptors or PRR) [281]. This intracellular and extracellular signalling is expected to elicit major changes in metabolites to promote the required alteration of the cell phenotype and changes in anabolic and catabolic pathways [281]. Immune cells use different metabolic pathways to provide adequate energy generation and cell survival during cell growth and proliferation. These metabolic pathways, which

include fatty acid synthesis, rely on products from other pathways, such as glycolysis and the tricarboxylic acid (TCA) cycle, to provide key synthetic precursors [72]. For this reason, metabolomics analysis of immune cells can provide a more complete understanding of the physiological state of an organism and of the alterations occurring in the metabolome, as metabolites are often considered the end stage of biological processes.

A growing number of findings highlight the crucial role of metabolic reprogramming in macrophage activation. Immune cells utilise five metabolic pathways: glycolysis, the TCA cycle, the pentose phosphate pathway (PPP), fatty acid synthesis and amino acid metabolism [72]. The present study investigated the metabolic responses of phorbol 12-myristate 13-acetate (PMA)-differentiated THP-1 cells treated with three different forms of synthetic honey bee venom eicosenoid compounds: (Z)-11-eicosenol, methyl cis-11-eicosenoate and cis-11-eicosenoic acid. The overall goal was to determine how these compounds might trigger an immune response and further used as vaccine adjuvants. Comprehensive metabolic profiling and assessments of pro- and anti-inflammatory cytokines (TNF-α, IL-1β, IL-6 and IL-10) were also conducted following exposure of LPS-stimulated THP-1 macrophage cells with these compounds. The observation of a synergistic effect of the investigated compounds with LPS in enhancement of immune stimulatory activation and cytokine production suggested the potential use of honey bee venom components as immune-modulatory agents and as vaccine adjuvants, which support their use as pro- rather than anti-inflammatory agents.

5.3 Materials and Methods

5.3.1 Sample preparation

Methyl-*cis*-11-eicosenoate (CAS 2390-09-2) and *cis*-11-eicosenoic acid (CAS 5561-99-9) were purchased from Sigma-Aldrich and used directly.

The following synthetic work was carried out by a fourth year project student in the Department of Pure and Applied Chemistry at Strathclyde. *Cis* (Z)-11-eicosenol (CAS 62442-62-0) was obtained by selective reduction of methyl-*cis*-11-eicosenoate with lithium aluminium hydride. Briefly, dry diethyl ether was added to the hydride and stirred in an ice bath for 30 min. The ester was added dropwise, stirred for 30 min, then refluxed gently for 60min. The reaction mixture was worked up by quenching with wet ether and washing with potassium sodium tartrate solution and water. The extracted organic layer was dried over sodium sulfate, filtered and excess solvent evaporated with an air stream to obtain the product. Confirmation of the reduction was obtained via IR and the full structure of the intended product was confirmed by NMR, including by 1D ^{1}H and ^{13}C-^{1}H NMR spectra and 2D [^{1}H, ^{13}C]-HSQC and 2D [^{1}H, ^{1}H] DQFCOSY and TOCSY NMR spectra Data and their assignments were confirmed directly with that of the natural product as previously assigned [136].

^{1}H NMR (1D, 600 MHz, DMSO-d_6): δ_H 0.84 – 0.86 (t, J = 13Hz, 3H, C1), 1.24 – 1.30 (m, 26H, C2/C3/C4/C5/C6/C7/C12/C13/C14/C15/C16/C17/C18), 1.35 -1.40 (m, 2H, C19) 1.96-1.99 (q, J = 19 Hz, 4H, C8/C11), 3.35 – 3.38 (m, 2H, C20), 4.30 – 4.31 (m, 1H, OH), 5.29 -5.34 (sept, 2H, C9/10).

^{13}C-^{1}H NMR (1D, 150 MHz, DMSO- d_6): δ 13.90 (C1), 22.07 (C2), 25.50 (C18), 26.53 (C8/C11), 28.56 (C5), 28.67 (C6), 28.81 (C7), 28.85 (C12), 28.95 (C14), 29.00 (C15), 29.07 (C16), 29.08 (C17), 31.28 (C3), 32.54 (C19), 60.70 (C20), 129.61 (C9/C10).

5.3.2 Cell culture and differentiation

As detailed in section2.2 2.2.1.

5.3.3 Cell viability assay

The THP-1 cells were seeded at a density of 1×10^5/well in 96-well plates and incubated for 24 h at 37 °C in a humidified atmosphere of 5% CO_2. After 24 h, the cells were treated with eicosenoid compounds at various concentrations (1.2 to 150 µg/mL) and incubated for a further 24 h. Untreated control cells and medium were added to the plates and dimethyl sulphoxide (DMSO) was used as a positive control. Resazurin salt solution (0.1 mg/mL) was added for Fluorescence readings using GraphPad Prism as described in section 2.2.2.

5.3.4 Cytokine production and ELISA assay

After 48 h of differentiation using PMA (60 ng/mL) in 24-well plates, the media were aspirated, and the cells were incubated for a further 24 h in PMA-free medium. At day 4, the cells were incubated with eicosenoid concentrations presented in **Table 5-1**. with and without LPS (Sigma-Aldrich) (0.5 µg/mL) for an additional 24 h. Conditioned medium was collected and frozen until required for ELISA (n = 3). The ELISA assays were performed according to the manufacturer's instructions to quantify the release of (TNF-α, IL-1β, IL-6, and IL-10) (section2.4).

5.3.5 Metabolite Extraction

The PMA-differentiated THP-1 cells were grown for 48 h in 6-well plates seeded at a density of 4.5×10^5/well (n = 6). The medium was aspirated and replaced with fresh medium for a further 24 h, and then the cells were incubated with LPS (0.5 µg/mL) either alone or together with (Z)-11-eicosenol (9 µg/mL), eicosenoate (150 µg/mL) and eicosenoic acid (40 µg/mL) for an additional 24 h. After 24 h, the medium was aspirated, and the cells were washed with 3 mL of phosphate-buffered saline (PBS) (Sigma-Aldrich) at 37 °C. The cells were extracted as detailed in section 2.6.

5.3.6 LC-MS Conditions

An Accela HPLC system interfaced to an Exactive Orbitrap mass spectrometer (Thermo Fisher Scientific, Bremen, Germany) was used for the liquid chromatographic separations. ZIC-pHILIC (150 × 4.6 mm, 5 µm) and ACE C4 (150 × 3.0 mm, 3 µm) HPLC columns supplied were used. Samples were run under the conditions described previously in section 2.5.1, section 2.5.2 and section 2.5.3.

5.3.7 Data Extraction and Statistical Analysis

As detailed in section2.7.

5.4 Results

5.4.1 Cytotoxicity of eicosenoids against PMA-differentiated THP-1 Cells

The potential cytotoxicity of (Z)-11-eicosenol (11E-OH), eicosenoate (11E-ester) and eicosenoic acid (11E-acid) (**Figure 5-1**) on PMA-differentiated THP-1 cells was evaluated to select an appropriate final concentration for further tests. Clear dose-dependent toxicity to THP-1 cells was observed for 11E-OH and its 11E-acid form. The lowest IC50 value at 19.88 µg/mL was observed for 11E-OH, whereas this value was 90.98 µg/mL for 11E-acid (**Figure 5-2 A & C**). By contrast, the 11E-ester form was nontoxic to THP-1 cells, with an IC_{50} value greater than 150 µg/mL. ELISAs were also conducted to assess the cytokine levels in THP-1 derived-macrophage cells upon treatment with these three compounds. As shown in **Table 5-1**, the final concentrations for cytokine assessments were chosen as those that were below the IC_{50} values and resulted in >90% of the cells remaining viable.

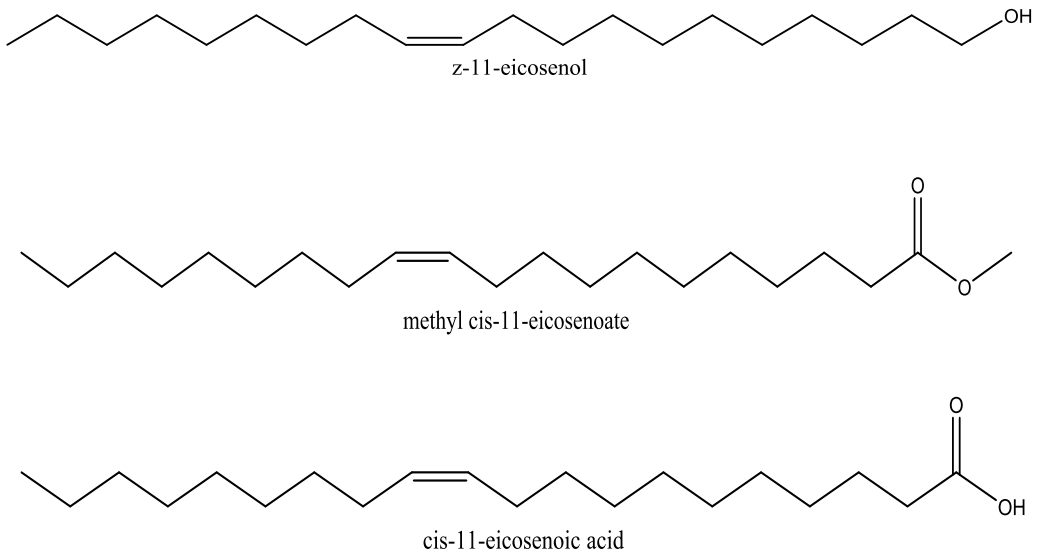

Figure 5-1: Chemical structures of (Z)-11-eicosenol, methyl cis-11-eicosenoate and cis-11-eicosenoic acid.

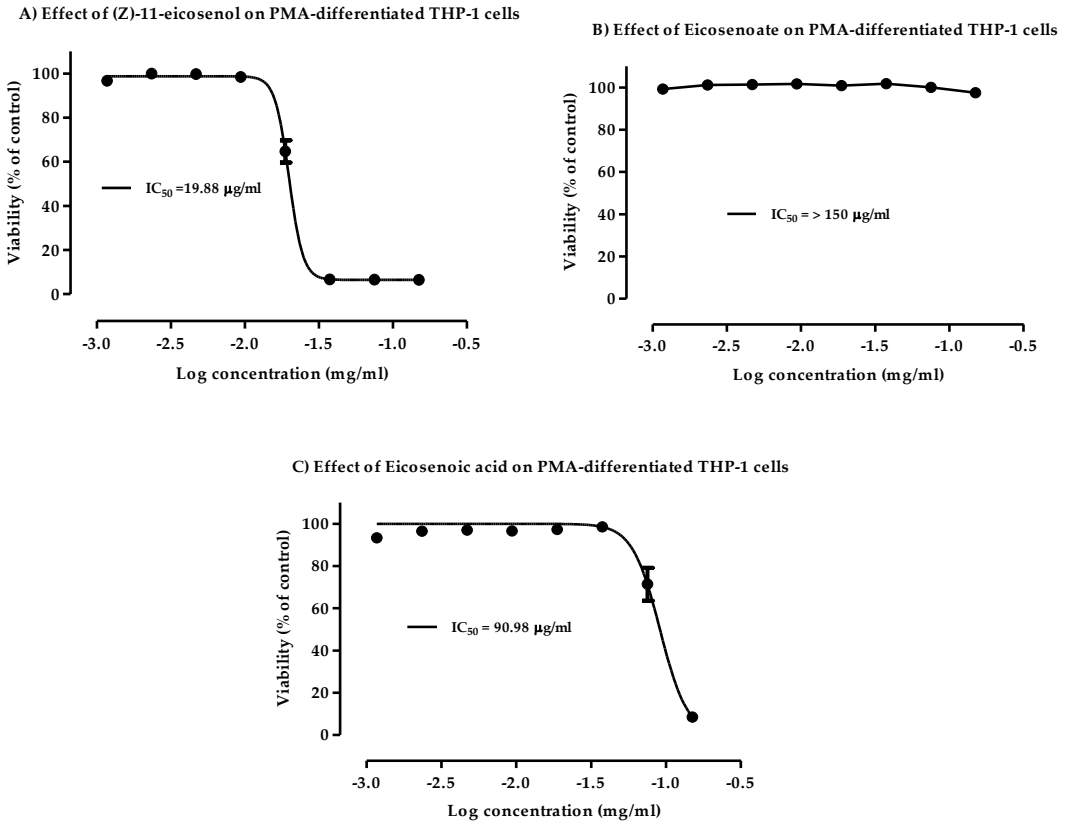

Figure 5-2: Cytotoxic effects of eicosenoid compounds at varying doses on phorbol 12-myristate 13-acetate (PMA)-differentiated THP-1 cells.
A) (Z)-11-eicosenol (11E-OH) compound was cytotoxic to PMA-treated cells. **B)** Eicosenoate (11E-ester) compound was non-cytotoxic to PMA-treated cells. **C)** Eicosenoic acid (11E-acid) compound was cytotoxic to PMA-treated cells. Each data point represents the mean ± SD (*n*=3).

Table 5-1: Sample groups, IC_{50} concentrations and final chosen concentrations of synthetic bee venom compounds tested in phorbol 12-myristate 13-acetate (PMA)-differentiated THP-1 cells.

Synthetic compounds		IC50	Selected final
Group ID	**Chemical name**	**(µg/mL)**	**concentration (µg/mL)**
11E-OH	(Z)-11-eicosenol	19.88	9.0
11E-ester	methyl cis-11-eicosenoate	>150	150
11E-acid	cis-11-eicosenoic acid	90.98	40.0

5.4.2 Effect of eicosenoid compounds on pro-inflammatory TNF-α cytokine production

Using ELISA, the effects of the eicosenoid compounds on the production of TNF-α cytokine are shown in **Figure 5-3**. The levels of secreted TNF-α by PMA-differentiated THP-1 cells were slightly or negligibly affected by all three forms of eicosanoid when combined with LPS. The increase was only statistically significant ($p < 0.05$) with 11E-acid when compared with LPS alone. (Z)-11-eicosenol compounds on their own significantly enhanced the production of TNF-α when compared with untreated cells.

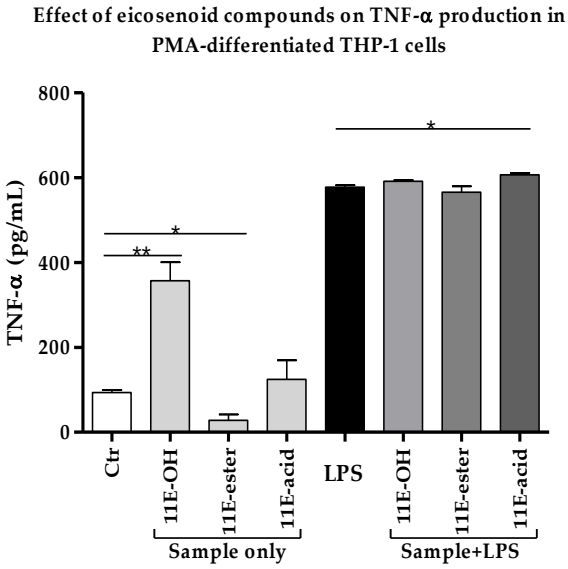

Figure 5-3: Effect of eicosenoid compounds on the production of TNF-α by PMA-differentiated THP-1 cells in the absence and presence of LPS (0.5 µg/mL).
The TNF-α levels were significantly increased by 11E-acid when compared with LPS alone (*n*=3). Ctr: Untreated control; LPS: Lipopolysaccharide; (11E-OH): (Z)-11-eicosenol; (11E-ester): Eicosenoate; (11E-acid): Eicosenoic acid; *: Significant ($p<0.05$); **: Significant ($p<0.01$).

5.4.3 Effect of eicosenoid compounds on pro-inflammatory IL-1β cytokine production

Compared to TNF-α, the enhancement in the production of IL-1β by (Z)-11-eicosenol, eicosenoate and eicosenoic acid in LPS co-stimulated THP-1 cells was much more pronounced. The release of IL-1β was greatly enhanced (ratio > 1.0) by approximately 84% and was statistically significant when compared with LPS alone. (Z)-11-eicosenol (~50%) enhanced the production of this cytokine upon stimulation with LPS, although the increase was not significant when compared with LPS alone (**Figure 5-4**). The level of IL-1β was enhanced by (Z)-11-eicosenol and eicosenoic acid alone, in the absence of LPS, when compared with the untreated control; however, the effects were not statistically significant.

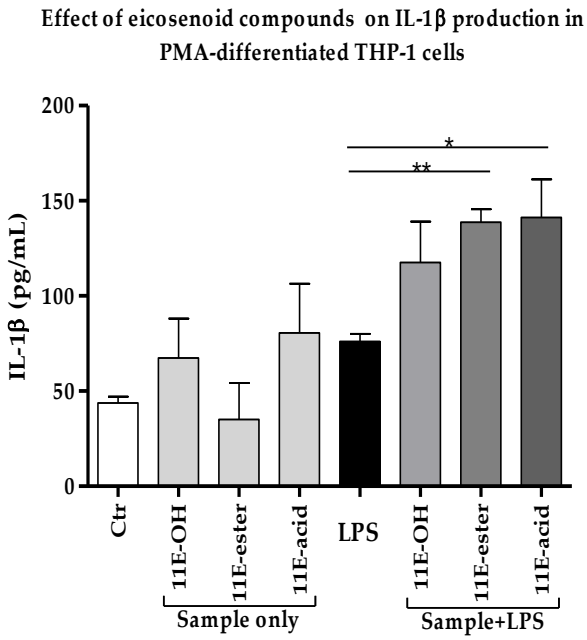

Figure 5-4: Effect of eicosenoid compounds on the production of IL-1β by phorbol 12-myristate 13-acetate (PMA)-differentiated THP-1 cells in the absence and presence of LPS (0.5 µg/mL).
The IL-1β levels were significantly enhanced in 11E-ester and 11E-acid combination treatments when compared with LPS alone (*n*=3). Ctr: Untreated control; LPS: Lipopolysaccharide; (11E-OH): (Z)-11-eicosenol; (11E-ester): Eicosenoate; (11E-acid): Eicosenoic acid; *: Significant ($p<0.05$); **: Significant ($p<0.01$).

5.4.4 Effect of eicosenoid compounds on pro-inflammatory IL-6 cytokine production

The levels of IL-6 cytokine were evaluated to confirm the previously reported decrease in response to eicosenoid compounds [136]. A decrease in IL-6 levels in THP-1 derived macrophage cells was also observed in the present study in response to all three forms of synthetically prepared eicosenoids. The levels of this cytokine were significantly decreased ($p < 0.05$) when compared with LPS alone. Surprisingly, no detectable amount of IL-6 was produced by the cells treated with

eicosenoate (11E-ester) in the presence of LPS (**Figure 5-5**). Unstimulated macrophage-like THP-1 cells did not produce any IL-6. The same was true for cells stimulated with eicosenoids alone (Table S5.3).

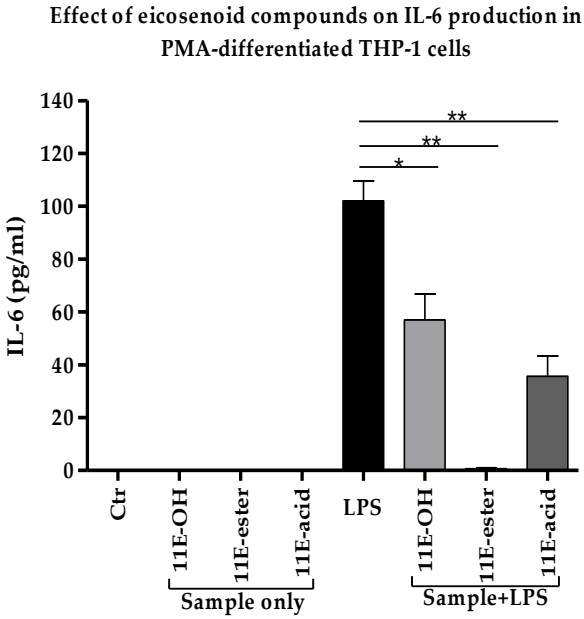

Figure 5-5: Effect of eicosenoid compounds on the production of IL-6 by phorbol 12-myristate 13-acetate (PMA)-differentiated THP-1 cells in the absence and presence of LPS (0.5 µg/mL).
The IL-6 levels were significantly decreased in all three combination treatments when compared with positive control LPS (*n*=3). Ctr: Untreated control; LPS: Lipopolysaccharide; (11E-OH): (Z)-11-eicosenol; (11E-ester): Eicosenoate; (11E-acid): Eicosenoic acid; *: Significant ($p<0.05$); **: Significant ($p<0.01$).

5.4.5 Effect of eicosenoid compounds on anti-inflammatory IL-10 cytokine production

A decrease in the levels of the anti-inflammatory IL-10 cytokine would support the use of the eicosenoid compounds as immune response stimulators. Combination treatments with LPS significantly decreased the level of this cytokine in PMA-

differentiated THP-1 cells when compared with LPS alone. The extent of the reductions in the release of IL-10 were about 30%, 80% and 50% in response to (Z)-11-eicosenol, eicosenoate and eicosenoic acid treatments, respectively, when compared to treatment with LPS alone (**Figure 5-6**).

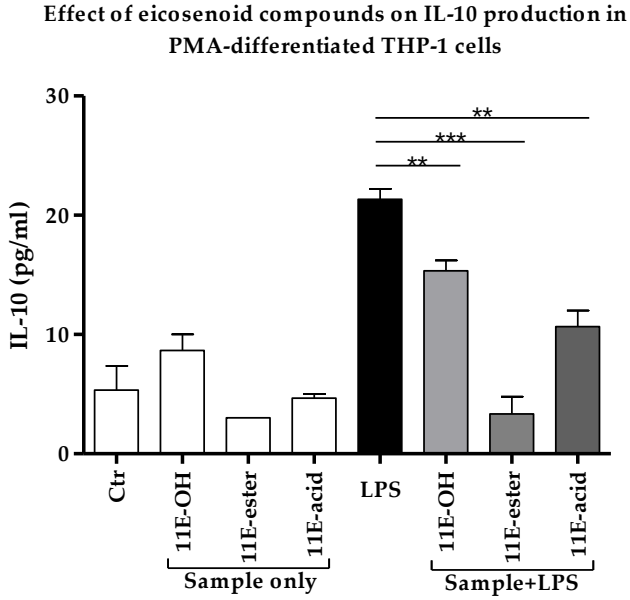

Figure 5-6: Effect of eicosenoid compounds on the production of IL-10 by phorbol 12-myristate 13-acetate (PMA)-differentiated THP-1 cells in the absence and presence of LPS (0.5 µg/mL).
The IL-10 levels were significantly decreased in all three combination treatments when compared with positive control LPS (*n*=3). Ctr: Untreated control; LPS: Lipopolysaccharide; (11E-OH): (Z)-11-eicosenol; (11E-ester): Eicosenoate; (11E-acid): Eicosenoic acid; *: Significant ($p<0.05$); **: Significant ($p<0.01$); ***: Significant ($p<0.001$).

5.4.6 Effect of eicosenoid compounds on polar THP-1 cell metabolites

Untargeted metabolic profiling of PMA-differentiated THP-1 cells was performed using LC-MS analysis. Samples were prepared by incubation of the macrophage cells with LPS and one of the three forms of the eicosenoids and compared to control untreated cells (C). Multivariate and univariate statistical analysis were used to

visualise and examine the metabolite effects on the following treatment combinations: T1 (9 µg/mL (Z)-11-eicosenol + 0.5 µg/mL LPS), T2 (150 µg/mL eicosenoate + 0.5 µg/mL LPS) and T3 (40 µg/mL eicosenoic acid + 0.5 µg/mL LPS). The effect of LPS alone was also evaluated to confirm the previous findings [262] and to investigate new pathways that might be involved in immune stimulation by eicosenoids. LPS synergism was clearly evident from the cytokine assessment, particularly with IL-1β and IL-10. Further metabolic profiling of these combination treatments would aid in determining how they inhibit or stimulate the immune response.

As shown in **Figure 5-7A**, principle component analysis (PCA) showed an absence of outliers. In addition, pooled quality control samples (QC, P1-6) produced a single tight cluster in the centre of the dataset, confirming the stability, precision and validity of the instrumental analytical method. Orthogonal partial least squares discriminant analysis (OPLS-DA), a supervised model for sample classification, showed a clear separation of each combination treatment, indicating unique metabolite profiling (**Figure 5-7B**). The OPLS-DA model parameters and validation of the plot suggest a strong model, with the *p* value associated with the cross-validation (CV)-ANOVA = 1.96×10^{-21}, indicating that the model was valid.

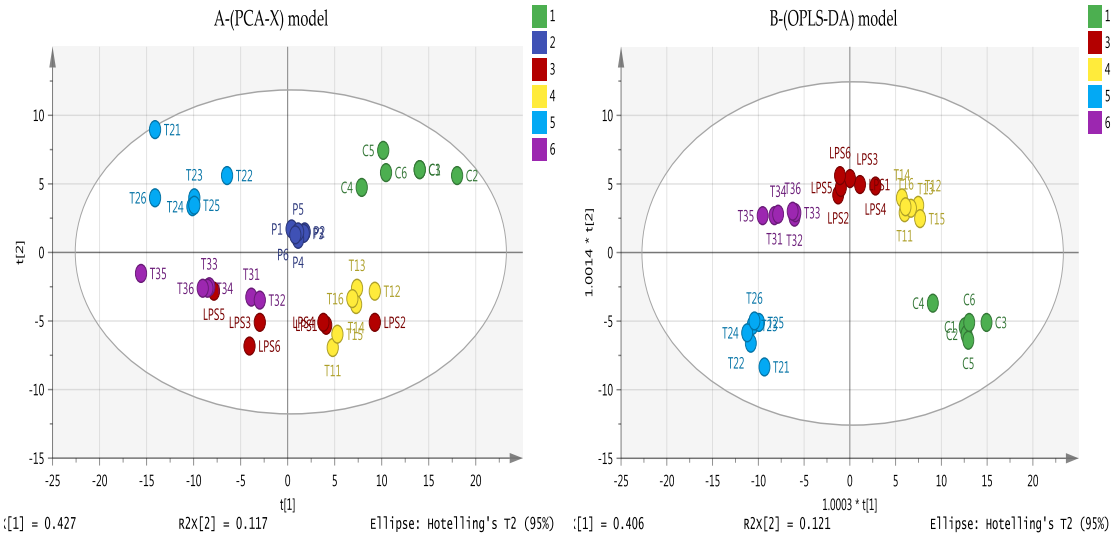

Figure 5-7: (A) Principle component analysis (PCA-X) vs. **(B)** Orthogonal Partial Least Squares Discriminant Analysis (OPLS-DA) score plots of THP-1 cells.
The figures show a clear separation between control, pooled and treatment groups based on 358 polar metabolites separated on a ZIC-pHILIC column (*n* = 6). PCA score plot (A) gives the goodness of fit (R^2X) = 0.807, and the goodness of prediction (Q^2) = 0.641. OPLS-DA score plot (B) gives R^2X= 0.829, R^2Y= 0.962, Q^2= 0.874. (C: Control; LPS: Lipopolysaccharides; T1(1-6): (11E-OH) (Z)-11-eicosenol + LPS; T2(1-6): (11E-ester) Eicosenoate + LPS; T3(1-6): (11E-acid) Eicosenoic acid + LPS*; P*=pooled samples).

Pooled quality control samples were injected at intervals (*n*=6) during the course of the run and used for further filtration of the dataset based on relative standard deviations (RSD). Metabolites with RSD values >30% within the pooled samples were excluded. The univariate analysis shown in **Table 5-2** reveals a large number of metabolic changes resulting from application of eicosenoid treatments. Greater effects were observed with the 11E-ester and 11E-acid forms when combined with LPS and compared to untreated control cells. Increases in abundance were detected for a large number of metabolites, including arginine and proline, Krebs cycle (TCA cycle) compounds and purine metabolites, which are all critically involved in inflammatory processes and immune responses of the cells.

Table 5-2: Significantly changed polar metabolites in THP-1 cells.
The cells were treated with lipopolysaccharide (LPS), alone or in combination with one of three synthetic forms of honey bee eicosenoids (0.5µg/mL LPS; 9 µg/mL 11E-OH; 150 µg/mL 11E-ester; 40 µg/mL 11E-acid). Data are compared with those from untreated control cells.

Mass	Rt	Putative Metabolite	LPS/C		11E-OH + LPS/C		11E-ester + LPS/C		11E-acid + LPS/C	
			Ratio	p.value	Ratio	p.value	Ratio	p.value	Ratio	p.value
		Arginine and proline metabolism								
129.090	15.79	4-Guanidinobutanal	1.523	0.030	1.580	0.008	0.880	ns	1.539	0.010
111.032	20.00	Pyrrole-2-carboxylate	1.200	0.012	1.384	<0.001	1.068	ns	1.260	0.003
189.064	14.09	N-Acetyl-L-glutamate*	0.547	0.007	0.599	0.001	1.139	ns	0.757	0.031
132.054	14.39	N-Carbamoylsarcosine	1.100	ns	1.051	ns	1.395	0.003	1.367	0.011
240.122	16.51	Homocarnosine	1.382	0.049	0.900	ns	1.593	<0.001	1.866	<0.001
211.036	15.28	Phosphocreatine*	0.944	ns	0.970	ns	1.723	0.001	1.285	0.024
113.059	9.94	Creatinine	1.625	ns	0.939	ns	2.104	<0.001	2.199	<0.001
130.122	26.73	Agmatine	1.509	0.021	1.041	ns	2.149	<0.001	1.884	<0.001
129.043	10.08	Oxoproline*	1.732	0.013	0.850	ns	2.331	<0.001	2.525	<0.001
175.096	16.21	L-Citrulline*	1.554	0.011	0.923	ns	2.379	<0.001	2.180	<0.001
246.133	18.71	N2-(D-1-Carboxyethyl)-L-arginine	2.225	0.008	1.233	ns	3.317	<0.001	3.245	<0.001
290.122	16.97	N-(L-Arginino)succinate	0.794	ns	1.022	ns	1.153	ns	1.596	0.015
115.063	13.07	L-Proline*	1.102	ns	0.897	ns	0.995	ns	1.208	0.036
174.112	26.73	L-Arginine*	1.593	0.022	1.089	ns	2.172	<0.001	2.160	<0.001
132.090	26.73	L-Ornithine*	1.834	0.003	1.223	ns	2.665	<0.001	2.501	<0.001
		Glycolysis/TCA cycle								
260.030	16.93	D-Glucose 1-phosphate*	1.231	ns	1.450	<0.001	0.833	ns	1.508	0.001
180.063	15.08	D-Glucose*	3.076	<0.001	1.901	<0.001	3.638	<0.001	3.309	<0.001
339.996	18.13	D-Fructose 1,6-bisphosphate*	1.789	<0.001	1.930	<0.001	2.217	<0.001	1.734	<0.001

260.030	16.10	D-Fructose 6-phosphate*	1.580	<0.001	1.716	<0.001	1.515	<0.001	1.653	<0.001
169.998	16.16	D-Glyceraldehyde 3-phosphate*	0.600	<0.001	0.441	<0.001	0.519	<0.001	0.404	<0.001
185.993	16.75	3-Phospho-D-glycerate	0.775	ns	1.849	ns	0.886	ns	0.934	ns
169.998	15.33	Glycerone phosphate	1.244	ns	2.368	0.014	1.804	<0.001	1.293	0.023
177.943	15.96	Pyrophosphate	0.832	0.002	0.946	ns	1.040	ns	1.015	ns
97.977	15.96	Orthophosphate	0.768	0.003	0.912	ns	1.031	ns	1.036	ns
192.027	18.13	Citrate*	1.594	<0.001	1.187	0.021	1.939	<0.001	1.904	<0.001
134.022	15.88	(S)-Malate*	1.116	ns	0.943	ns	0.869	0.002	1.124	ns
174.016	18.13	cis-Aconitate*	1.265	ns	0.984	ns	1.662	0.001	1.633	0.001
192.027	19.36	Isocitrate*	1.388	ns	1.493	ns	2.417	0.002	1.788	0.014
116.011	15.02	Fumarate*	1.186	ns	0.831	ns	1.445	0.002	1.826	<0.001
118.027	14.98	Succinate*	1.557	0.002	1.170	ns	1.346	0.005	1.819	0.001
131.070	14.97	Creatine*	1.437	0.001	1.061	ns	3.014	<0.001	1.365	0.002
809.126	12.49	Acetyl-CoA	0.730	0.006	0.907	ns	1.001	ns	0.995	ns
665.125	13.44	NADH*	0.553	<0.001	0.642	<0.001	1.330	ns	0.752	0.008
663.109	14.39	NAD+*	0.490	<0.001	0.499	<0.001	0.683	<0.001	0.548	<0.001
506.995	16.67	ATP*	0.689	0.002	0.769	0.001	0.584	<0.001	0.724	0.001
427.030	15.30	ADP*	0.598	<0.001	0.671	<0.001	0.638	<0.001	0.762	<0.001
443.024	18.01	GDP*	0.772	0.011	0.978	ns	1.004	ns	0.931	ns
522.990	19.36	GTP*	0.975	ns	1.385	0.003	1.297	0.002	1.051	ns
		Oxidative stress/ Pentose phosphate pathway								
370.007	18.36	D-Sedoheptulose 1,7-bisphosphate	1.475	0.002	1.817	<0.001	1.565	<0.001	1.513	<0.001
232.035	15.75	D-Ribitol 5-phosphate*	0.683	0.007	0.744	ns	0.563	0.002	0.862	0.027
276.025	17.73	6-Phospho-D-gluconate*	1.606	0.006	1.480	0.004	0.568	0.001	0.921	ns
196.058	13.26	D-Gluconic acid*	0.886	ns	0.800	<0.001	0.795	0.002	0.925	ns
150.053	13.64	D-Ribose	1.307	0.017	0.899	ns	1.286	0.018	1.289	0.011

290.040	16.33	D-Sedoheptulose 7-phosphate	1.481	0.001	2.016	<0.001	1.654	<0.001	1.884	<0.001
230.019	15.35	D-Ribulose 5-phosphate	1.566	ns	4.634	0.030	1.410	0.010	1.438	0.007
230.019	15.75	D-Ribose 5-phosphate*	1.525	<0.001	1.516	<0.001	1.796	<0.001	1.230	<0.001
745.091	17.14	NADPH*	0.733	0.002	0.331	<0.001	00.00	n/a	0.347	0.004
743.076	16.87	NADP+*	0.722	0.024	1.983	<0.001	1.879	<0.001	2.419	0.001
152.068	13.11	Xylitol*	1.423	0.001	1.063	ns	0.907	ns	1.189	0.049
196.058	13.89	D-Mannonate	2.006	ns	0.860	ns	2.406	<0.001	2.454	<0.001
166.048	13.43	D-Xylonate	1.673	0.019	0.929	ns	3.156	<0.001	2.964	<0.001
150.053	13.64	D-Ribose	1.307	0.017	0.899	ns	1.286	0.018	1.289	0.011
307.084	14.37	Glutathione	0.691	<0.001	0.774	<0.001	0.683	<0.001	0.738	<0.001
612.152	17.52	Glutathione disulfide*	1.113	ns	1.679	0.003	3.605	<0.001	3.221	<0.001
		Purine metabolism								
363.058	19.36	Guanosine 3'-phosphate	0.909	ns	1.551	0.005	1.406	0.001	1.043	ns
168.028	12.41	Urate*	1.487	ns	0.738	ns	1.778	0.003	2.285	0.001
268.081	11.11	Inosine*	1.804	0.004	5.853	<0.001	12.553	<0.001	9.126	<0.001
283.092	12.83	Guanosine*	1.454	ns	4.991	<0.001	16.908	<0.001	4.976	<0.001
136.038	10.39	Hypoxanthine*	33.258	<0.001	31.216	<0.001	56.447	<0.001	67.586	<0.001
284.075	12.01	Xanthosine*	1.564	0.004	1.306	0.020	1.651	0.003	1.825	0.001
152.033	11.31	Xanthine*	1.907	0.005	1.171	ns	2.376	<0.001	2.492	<0.001
363.058	16.78	GMP*	1.016	ns	1.100	ns	0.809	ns	1.201	0.006
363.058	19.36	Guanosine 3'-phosphate	0.909	ns	1.551	0.005	1.406	0.001	1.043	ns
283.092	12.83	Guanosine*	1.454	ns	4.991	<0.001	16.908	<0.001	4.976	<0.001
347.063	13.89	AMP*	0.656	<0.001	0.660	0.001	0.326	<0.001	0.680	<0.001
		Pyrimidine metabolism								
483.968	17.92	UTP*	0.355	<0.001	0.440	<0.001	0.393	<0.001	0.417	<0.001
308.041	13.81	dUMP	0.357	<0.001	0.394	<0.001	0.548	<0.001	0.394	<0.001

482.984	18.48	CTP*	0.473	<0.001	0.596	<0.001	0.688	<0.001	0.492	<0.001
403.018	17.14	CDP*	0.363	<0.001	0.440	<0.001	0.822	ns	0.541	<0.001
323.052	15.35	CMP*	0.763	0.001	0.882	0.040	1.148	ns	0.999	ns
128.058	10.57	5,6-Dihydrothymine	1.664	ns	0.698	0.006	1.395	0.007	2.075	0.033
126.043	15.31	Thymine	1.439	0.031	1.125	ns	1.995	<0.001	1.893	0.001
125.059	10.93	5-Methylcytosine	1.826	ns	1.021	ns	2.013	<0.001	2.139	0.002
244.069	12.15	Pseudouridine	1.780	0.007	1.058	ns	2.266	<0.001	2.134	<0.001
243.085	12.15	Cytidine*	3.051	0.009	1.812	ns	4.662	<0.001	4.849	<0.001
176.043	16.65	N-Carbamoyl-L-aspartate	0.576	<0.001	0.446	<0.001	0.295	<0.001	0.351	<0.001
324.036	15.18	UMP*	0.417	<0.001	0.412	<0.001	0.475	<0.001	0.482	<0.001
404.002	16.59	UDP*	0.218	<0.001	0.347	<0.001	0.413	<0.001	0.350	<0.001
536.044	16.19	UDP-D-xylose	0.593	<0.001	0.699	0.001	1.017	ns	0.745	0.002
580.034	18.96	UDP-glucuronate	0.615	<0.001	0.736	<0.001	0.701	<0.001	0.664	<0.001
566.055	16.31	UDP-glucose*	0.539	<0.001	0.662	<0.001	0.628	<0.001	0.620	<0.001
		Tryptophan metabolism								
175.063	10.37	Indole-3-acetate	1.537	<0.001	1.545	<0.001	0.417	<0.001	1.527	<0.001
236.079	10.37	L-Formylkynurenine	1.507	0.002	1.431	<0.001	0.418	<0.001	1.453	<0.001
191.058	10.37	5-Hydroxyindoleacetate*	1.512	<0.001	1.506	<0.001	0.523	<0.001	1.547	<0.001
208.085	11.15	L-Kynurenine*	1.483	ns	1.114	ns	1.565	0.003	2.087	<0.001
220.085	9.99	5-Hydroxy-L-tryptophan isomer	8.354	<0.001	7.721	<0.001	1.655	0.007	8.798	<0.001
205.074	7.56	Indolelactate	2.315	0.009	1.399	ns	2.267	<0.001	3.333	<0.001
117.058	11.92	Indole*	1.413	0.011	1.216	ns	3.554	<0.001	2.257	<0.001
204.090	11.91	L-Tryptophan*	1.311	ns	1.050	ns	3.194	<0.001	2.019	0.003
		Miscellaneous								
146.069	15.31	L-Glutamine*	1.445	0.001	1.105	ns	1.965	<0.001	1.889	<0.001
147.053	14.71	D-Glutamate*	1.035	ns	0.777	0.002	1.259	0.002	1.355	0.003

301.056	14.93	N-Acetyl-D-glucosamine 6-phosphate*	0.785	0.006	0.755	<0.001	0.642	<0.001	0.878	ns
103.100	20.65	Choline*	1.277	ns	1.336	0.002	1.268	0.005	1.944	<0.001
141.019	15.91	Ethanolamine phosphate*	0.869	ns	0.987	ns	0.555	<0.001	0.797	0.016
105.043	16.02	L-Serine*	1.646	0.004	1.228	0.030	1.835	<0.001	1.927	<0.001
119.058	14.68	L-Threonine	2.719	<0.001	1.618	0.001	3.190	<0.001	2.821	<0.001
155.070	15.16	L-Histidine*	2.450	<0.001	1.285	0.018	3.175	<0.001	2.737	<0.001
146.106	25.28	L-Lysine*	1.520	0.001	1.254	0.017	1.862	<0.001	1.734	<0.001
384.122	13.99	S-Adenosyl-L-homocysteine*	1.163	ns	1.047	ns	1.580	0.001	1.545	0.002
203.116	11.29	O-Acetylcarnitine*	0.702	0.001	0.688	<0.001	0.644	<0.001	0.689	0.001
175.048	14.53	N-Acetyl-L-aspartate*	0.758	0.003	0.628	<0.001	0.797	0.003	0.970	ns
133.038	15.04	L-Aspartate*	1.136	ns	0.888	ns	1.306	0.003	1.618	<0.001
89.048	14.97	L-Alanine*	0.671	0.001	0.731	0.004	1.041	ns	0.720	0.001
226.106	16.03	Carnosine*	1.088	ns	1.080	ns	1.203	0.016	1.201	0.012
132.054	15.48	L-Asparagine*	1.211	ns	0.798	ns	1.310	0.001	1.416	0.001
149.051	11.79	L-Methionine*	1.358	ns	0.910	ns	1.822	<0.001	1.869	<0.001
222.067	17.33	Cystathionine*	0.714	ns	0.833	ns	0.508	<0.001	0.811	ns
181.074	13.24	L-Tyrosine*	1.360	ns	0.989	ns	1.930	<0.001	1.840	0.001
131.095	11.11	L-Leucine*	1.383	0.007	0.962	ns	1.836	<0.001	1.949	<0.001
131.094	11.51	L-Isoleucine*	1.424	ns	0.915	ns	1.838	<0.001	1.852	<0.001
117.079	12.77	L-Valine*	1.739	0.006	1.045	ns	1.901	<0.001	1.876	<0.001

Rt: Retention time (min); LPS: Lipopolysaccharides; *: Matches the analytical standard retention time; ns: Non-significant; n/a: Not applicable.

5.4.7 Effect of eicosenoid compounds on lipophilic metabolites

In order to gain a comprehensive overview, further analysis was also carried out on the non-polar lipophilic metabolites in the cells using a reversed phase (RP) column. As shown in **Figure 5-8A**, PCA was employed for the 314 lipophilic compounds and shows the absence of the outliers. In addition, pooled quality control samples (QC, P1-6) clustered together which indicates the stability, precision and validity of the instrumental analytical method. OPLS-DA shows a clear separation of the each combination treatments and represents unique metabolite profiling (**Figure 5-8B**). The OPLS-DA model parameters and validation of the plot suggest a strong model with the *p* CV-ANOVA = 0.0094, indicating that the model was valid ($p < 0.5$). From the data visualisation below (**Figure 5-8B**), strong effects can be predicted on the level of lipophilic metabolites when ester (T2) and acid (T3) treatments are applied to the THP-1 cells.

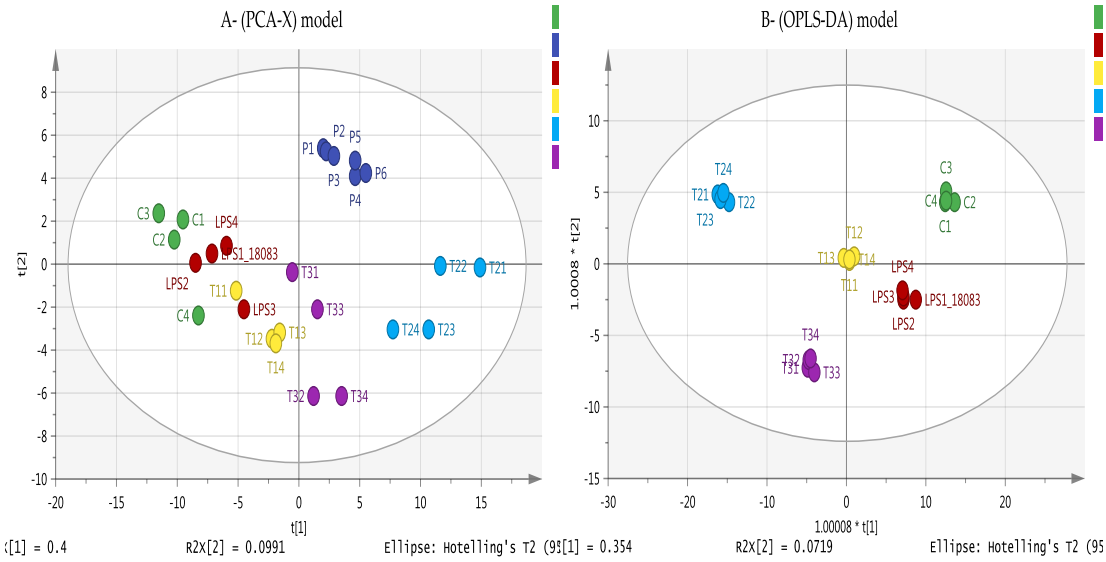

Figure 5-8: (A) Principle component analysis (PCA-X) vs. **(B)** Orthogonal Partial Least Squares Discriminant Analysis (OPLS-DA) score plots of THP-1 cells.
The figures show a clear separation between control, pooled and treatment groups based on 314 non-polar metabolites separated on an ACE C4 column (*n* = 4). PCA score plot (A) gives the goodness of fit (R^2X) = 0.571, and the goodness of prediction (Q^2) = 0.403. OPLS-DA score plot (B) gives R^2X= 0.697, R^2Y = 0.982, Q^2= 0.628. (C: Control; LPS: Lipopolysaccharide; T1(1-4): (11E-OH) eicosenol + LPS; T2(1-4): (11E-ester) eicosenoate + LPS; T3(1-4): (11E-acid) eicosenoic acid + LPS*; P*=pooled samples).

Table 5-3 summarises the list of metabolites separated on the ACE C4 column in cells treated with eicosenoids in combination with LPS. The metabolites were identified by matching the retention times to those of a standard mixture of known fatty acids.

Table 5-3: Significantly changed non-polar metabolites in THP-1 cells.
The cells were treated with lipopolysaccharide (LPS), alone or in combination with one of three synthetic forms of honey bee eicosenoids (0.5µg/mL LPS; 9 µg/mL 11E-OH; 150 µg/mL 11E-ester; 40 µg/mL 11E-acid). Data are compared with those from untreated control cells.

Mass	Rt	Putative Metabolite	LPS/C		11E-OH + LPS/C		11E-ester + LPS/C		11E-acid + LPS/C	
			Ratio	p.value	Ratio	p.value	Ratio	p.value	Ratio	p.value
Fatty acid and related metabolites										
306.256	19.23	Icosatrienoic acid*	1.963	<0.001	2.976	0.001	7.296	<0.001	2.941	<0.001
328.240	18.11	Docosahexaenoic acid*	1.637	0.007	2.005	0.003	4.187	<0.001	2.336	<0.001
336.303	22.99	Docosadienoic acid*	1.058	ns	1.021	ns	2.301	<0.001	1.027	ns
282.256	19.94	Oleic acid*	1.126	ns	1.189	0.034	2.938	<0.001	1.391	0.003
216.136	4.28	Undecanedioic acid	1.181	0.041	1.463	0.001	9.890	<0.001	1.487	0.003
214.193	14.92	Tridecanoic acid*	1.138	ns	1.102	ns	1.731	0.018	1.323	0.004
334.287	21.67	Docosatrienoic acid*	1.288	0.050	1.346	0.018	3.345	<0.001	1.523	0.006
398.339	24.40	Axillarenic acid*	1.167	ns	1.118	0.023	1.331	0.039	1.190	0.007
366.350	26.47	Tetracosenoic acid*	1.322	0.001	1.632	<0.001	6.416	<0.001	4.085	0.018
230.152	7.29	Dodecanedioic acid	1.071	ns	1.313	ns	23.842	<0.001	1.352	0.023
258.183	12.16	Tetradecanedioic acid	1.342	ns	1.231	ns	23.897	0.009	1.573	0.030
242.225	17.85	Pentadecanoic acid*	1.021	ns	1.084	ns	1.711	0.017	1.233	0.039
248.178	12.32	Hexadecatetraenoic acid	1.205	ns	1.837	ns	2.553	0.017	2.041	0.044
298.287	23.03	Nonadecanoic acid*	1.133	0.001	1.133	ns	1.310	0.001	1.219	<0.001
332.272	20.18	Docosatetraenoic acid*	1.664	0.004	2.549	<0.001	4.261	<0.001	2.348	<0.001
304.240	18.24	Eicosatetraenoic acid*	1.578	0.006	2.874	<0.001	6.998	<0.001	2.985	<0.001
338.319	24.50	Docosenoic acid*	1.155	0.050	1.871	<0.001	22.311	<0.001	8.335	<0.001
394.381	28.24	Hexacosenoic acid*	1.433	<0.001	1.047	ns	1.903	<0.001	1.685	<0.001
364.334	25.02	Tetracosadienoic acid*	0.888	ns	1.409	ns	3.193	<0.001	2.568	<0.001
202.120	4.64	Decanedioic acid	1.134	ns	1.441	0.008	1.944	0.007	1.204	ns

226.193	15.21	Tetradecenoic acid*	0.820	ns	0.941	ns	1.660	0.009	0.963	ns
186.162	11.81	Undecanoic acid*	1.065	ns	0.898	ns	1.864	0.015	1.238	ns
158.131	8.54	Nonanoic acid*	1.084	ns	0.946	ns	1.714	0.019	1.370	ns
280.240	18.26	Linoleate*	1.169	ns	1.052	ns	1.617	<0.001	1.202	ns
172.110	4.54	9-Oxononanoic acid	1.213	ns	1.231	ns	1.497	ns	1.388	0.031
368.220	11.57	Prostaglandin G2	1.358	ns	1.841	0.026	3.300	0.003	2.432	0.008
356.257	14.60	Prostaglandin F1alpha	1.203	ns	1.446	0.021	1.927	<0.001	1.544	0.001
		Glycerophospholipids								
638.396	13.80	PA(32:5)	1.549	ns	1.510	ns	2.748	0.021	2.678	ns
847.645	29.88	PC(42:6)	0.963	ns	3.742	<0.001	4.541	<0.001	2.501	0.019
825.530	18.21	PC(40:10)	0.897	0.042	0.753	0.031	0.551	0.002	0.563	<0.001
851.546	18.59	PC(42:11)	0.821	0.016	0.574	<0.001	0.269	<0.001	0.406	<0.001
881.593	21.81	PC(44:10)	1.016	ns	1.743	0.002	2.051	<0.001	1.090	ns
722.545	24.76	PG(33:0)	0.884	ns	0.933	ns	0.857	ns	0.515	0.001
484.280	22.13	Lyso PG(16:0)	1.056	ns	0.876	ns	0.817	0.002	0.942	ns
482.264	7.32	Lyso PG(16:1)	0.833	ns	1.097	ns	0.820	0.050	0.942	ns
572.296	7.29	Lyso PI(16:0)	1.028	ns	1.137	0.027	1.268	0.001	1.200	0.001
598.312	7.95	Lyso PI(18:1)	1.031	ns	1.241	0.007	1.563	<0.001	1.303	0.004
622.312	7.71	Lyso PI(20:3)	1.119	ns	1.302	0.020	1.154	ns	1.255	0.031
620.296	7.04	lyso PI (20:4)	1.152	ns	1.187	0.045	1.891	<0.001	1.770	<0.001
495.260	6.38	lyso PS(16:1)	1.015	ns	0.885	ns	0.730	0.004	0.818	0.036
771.505	24.05	PS(35:3)	0.647	0.001	0.434	<0.001	0.315	<0.001	0.272	<0.001
497.275	7.72	Lyso PS(16:0)	1.033	ns	1.139	ns	0.801	0.011	1.036	ns
517.244	12.63	Lyso PS 18:4	1.689	0.040	1.922	<0.001	2.208	0.020	1.390	ns
691.441	12.63	PS(29:1)	1.380	ns	2.276	0.038	2.380	ns	2.448	ns

Rt: Retention time (min); LPS: Lipopolysaccharides; *: Matches the analytical standard retention time; ns: Non-significant; n/a: Not applicable.

5.5 Discussion

A recognition of the crucial role of the regulation of the adaptive response and induction of the innate immune response has led to a reassessment of the role of adjuvants in vaccinology. Recent studies on the innate immunity activation of macrophages and DCs are now providing better glimpses into the mechanisms underlying adjuvant actions. These new insights now support the development of novel adjuvants and combinations of adjuvants to enhance the recognition of antigens by the immune system and to induce more potent cellular immune responses that exploit the advantages of each individual component. To the best of our knowledge, no study has yet investigated the eicosenoid effect on immune macrophage cells. Therefore, the aim of this study was to assess the ability of three eicosenoid derivatives to induce specific immunological functions of THP-1 macrophage cells by examining cytokine production and eicosenoid-induced alterations in the cell metabolome.

THP-1 cell viability in the presence of (Z)-11-eicosenol, methyl cis-11-eicosenoate and cis-11-eicosenoic acid revealed different IC_{50} values, indicating an effect of functional group substitution on cellular respiration. The lowest IC_{50} value was obtained with (Z)-11-eicosenol, which contains a hydroxyl group (**Figure 5-1**), in comparison with the ester and carboxylic acid forms. Several studies have assessed the effect of functional groups on different cell lines. For example, Sakagami *et al.* reported the structure–activity relationships of eleven piperic acid ester derivatives based on their cytotoxic effects against oral squamous cell carcinoma cell lines and found that addition of two hydroxyl groups had the highest cytotoxic effect [307].

Similarly, polyhydroxylated analogues of resveratrol, a natural polyphenol compound, showed higher cytotoxic effects [308].

Previously, (Z)-9-eicosenol was purified from honey bee venom and its stimulatory effect on TNF-α and IL-1β secretion was reported in the U937 cell line stimulated with LPS, where a surprising observation was significant inhibition of the level of IL-6 in response to this compound [136]. For this reason, in the present study, other eicosenoid derivatives were examined for their effects on the cellular immune response and in particular for their effects on the production of pro and anti-inflammatory cytokines by THP-1 macrophage cells. All three derivatives showed similar bioactivity with respect to the induction of cytokine levels, as described previously [136]. A small effect was observed for the secretion of TNF-α, whereas IL-1β production was enhanced significantly by the 11E-ester and 11E-acid forms, when combined with LPS. By contrast, the level of IL-6 decreased, suggesting the presence of a more subtle mechanism of action for eicosenoids. In addition, release of the anti-inflammatory IL-10 cytokine was largely inhibited, supporting their immune stimulatory effect.

The complexity of the IL-6 cytokine responses has been reported extensively [309]. This cytokine has dual properties pro- and anti-inflammatory, which are referred to as its classic and trans-signaling pathways [309]. IL-6 promotes a protective effect in some inflammatory diseases, such as inflammatory bone destruction and dextran sodium sulphate-induced colitis [310, 311]. Several studies have also demonstrated an association between IL-6 and IL-10 and a requirement for IL-6 in IL-10 production by T cells to suppress inflammation [312, 313]. Interestingly, in the

current case, both IL-6 and IL-10 were decreased in the same manner (*i.e*. the 11E-ester form strongly decreased their secretion, with weaker decreases by the 11E-acid and still weaker effects by the 11E-OH form). Thus, the important consequences on the therapeutic blockade of IL-6 as a treatment of chronic inflammatory diseases should be carefully considered.

The ability of synthetic eicosenoid derivatives to induce immune responses and to alter cytokine production was investigated further by a comprehensive untargeted metabolomics assessment of PMA-stimulated THP-1 cells. Induction of the characteristic morphology of activated macrophages as a result of Toll-like receptor (TLR4) activation by LPS has been previously described [314]. Several biomarkers, including nitric oxide (NO), are used to monitor the inflammatory status of these cells. Inducible nitric oxide synthase (iNOS) is the main enzyme responsible for the release of large amounts of NO through the conversion of L-arginine to NO and citrulline [315]. Arginine metabolism is also involved in the regulation of inflammation through its breakdown into ornithine and urea by arginase [316]. Upregulation of arginine and proline metabolism was significantly identified by metabolomic analysis in response to treatment with the ester and acid forms, as indicated by the alterations in the levels of NO-related metabolites, including L-arginine, L-citrulline, N-(L-arginino)succinate, L-proline and L-ornithine (**Table 5-2**). L-proline and L-ornithine work as precursors for the formation of pro-proliferative polyamines and production of extracellular matrix, as a repair phase response [316]. The enhancement of cytokine production by the 11E-acid form is evident mainly by the alteration of several pathways, including arginine and proline

metabolism, where a significantly higher number of metabolites was altered by this treatment (Figure S5.14).

Several studies have shown that metabolic reprogramming of the cell regulates macrophage activation. In the present study, the findings for LPS activation of THP-1 macrophages regarding specific pathway and biomarker metabolites are consistent with those of previous reports [262, 317]. In general, pro-inflammatory stimuli cause the macrophages to undergo a metabolic switch from oxidative phosphorylation (OXPHOS) to glycolysis [143]. The lactate flux from pyruvate increases in response to a reduction in acetyl-coenzyme A (acetyl-CoA) levels [143, 199] leading to dysfunctional activity of the TCA cycle, which is, in turn, compensated for by an increase in the PPP to ensure a rapid regeneration of adenosine triphosphate (ATP) [150].

LPS enhanced activities clearly shown by the combination treatments with eicosenoid derivatives in this study. The levels of ATP were reduced in the treatments with LPS alone and in combination with eicosenoids, when compared with untreated control cells suggesting an increased requirement in the treated cells, leading to upregulation of most of the glycolysis metabolites, including fructose 1,6-bisphosphate and fructose 6-phosphate. In order to maintain a high cellular redox state, PPP activity was increased. LPS is reported to suppress the expression of carbohydrate kinase-like protein (CARKL), which is associated with a greater flux into glycolysis and away from the non-oxidative PPP [150]. This would lead to a significant decrease of sedoheptulose-7-phosphate (S7P) [200], however, the

opposite was observed for all three treatments with LPS when compared with the untreated control. The reason for this is not clear.

The TCA cycle intermediates, such as succinate and citrate, are critical in M1 macrophage activation and are positively associated with inflammation. High levels of succinate were observed in the present study in response to LPS alone and with the 11E-acid and LPS combination. This increase has been attributed to glutamine metabolism following dysfunction of the TCA cycle, which normally would provide the source for succinate generation [158]. Succinate drives inflammation through the inhibition of prolyl hydroxylase (PHD) and further stabilisation of hypoxia-inducible factor-1α (HIF-1α) [143]. LPS triggers T-cell activation and the adaptive immune system through an increased expression of the citrate transport carrier, which could lead to cytosolic citrate accumulation. This citrate is then converted to acetyl-CoA and oxaloacetate for fatty acid synthesis and generation of NO and reactive oxygen species (ROS), respectively [83]. Interestingly, in the current study, the citrate levels were approximately 20% higher in the 11E-ester and 11E-acid combinations with LPS when compared with LPS alone. Clearly, citrate and succinate are important signaling molecules in innate and adaptive immunity. Furthermore, the levels of itaconate, a metabolite synthesised via decarboxylation of cis-aconitate, were elevated in the LPS-activated macrophages. This metabolite has been suggested to work as an anti-microbial, to limit inflammation and to have a crucial role in macrophage-based immune responses [318-320]. Interestingly, cis-aconitate was significantly elevated following the ester and acid form treatments, while itaconate was not detected (**Table 5-2**).

An imbalance between cellular oxidants and antioxidants can potentially lead to oxidative stress and cell damage. Thus, antioxidant defence is required for cellular adaptation to stress conditions [321]. Glutathione (GSH), an important protective antioxidant tripeptide, has been implicated in inflammatory responses and immune modulation [322]. GSH is oxidised to glutathione disulphide (GSSG) when it reacts with peroxide (H_2O_2) in the presence of glutathione peroxidase, an enzyme that facilitates the inactivation of peroxide [323]. GSSG can be reduced again using nicotinamide adenine dinucleotide phosphate (NADPH). Thus, regulation of both the NADPH/$NADP^+$ and GSH/GSSG ratios is tightly coupled to the control of oxidative stress (**Figure 5-9**) [324, 325]. A decrease in the level of GSH and an increase in its product GSSG was observed in this study; this response has been reported as a hallmark of oxidative stress [326, 327]. A large depletion in the level of NADPH and an increase in $NADP^+$ were observed in the current study after the combination treatment of eicosenoids and LPS (**Table 5-2**). NADPH generates ROS through NADPH oxidase, and it also serves as a substrate for the conversion of arginine to citrulline and NO [140, 152]; arginine and citrulline were also strongly elevated in response to the treatments with LPS in combination with 11E-ester or 11E-acid (**Figure 5-9**).

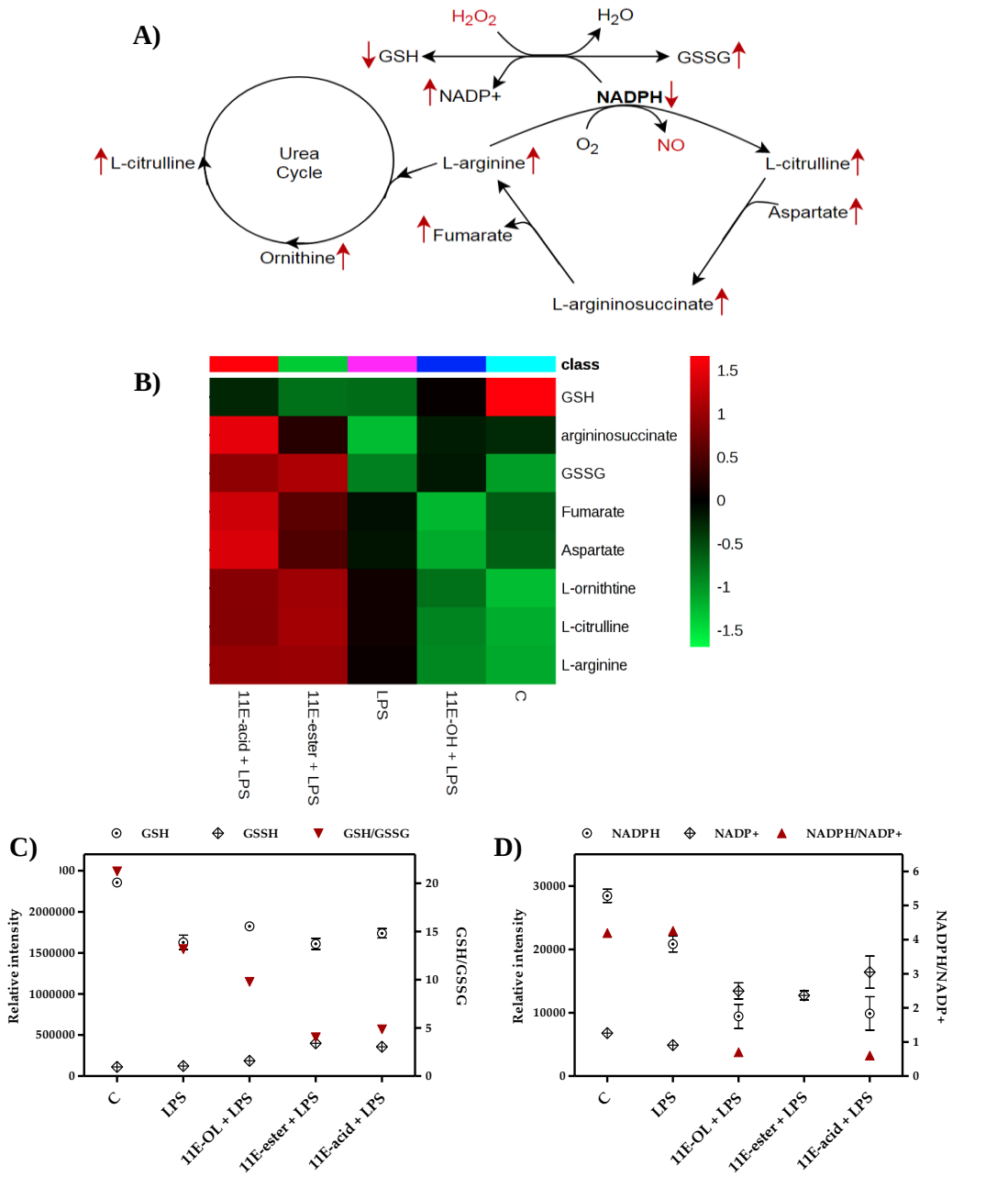

Figure 5-9: Role of nicotinamide adenine dinucleotide phosphate (NADPH) in generating hydrogen peroxide (H_2O_2) and nitric oxide (NO) through glutathione metabolism and arginine biosynthesis in THP-1 macrophages.
The figure show **(A)** Enhanced activity of oxidative stress related metabolites after treatment with 11E-ester+LPS and 11E-acid+LPS when compared with LPS alone. **(B)** Overexpression (dark red) of most of the significant metabolites can be observed in a heat map visualizing by 11E-ester+LPS and 11E-acid+LPS treatments. **(C)** GSH, GSSG and GSH/GSSG responses after each group treatments. **(D)** NADPH, NADP+ and NADPH/NADP+ responses after each group treatments. C: Untreated control; LPS: Lipopolysaccharide; (11E-OH): (Z)-11-eicosenol; (11E-ester): Eicosenoate; (11E-acid): Eicosenoic acid; (Red rows): Response of 11E-ester+LPS and 11E-acid+LPS combination treatments.

Enhanced activity of the PPP boosts the production of purine and pyrimidine nucleotides for further biosynthesis in activated cells [143]. An increase in inosine, guanosine, hypoxanthine, xanthine and urate levels was detected in the present study. In purine metabolism, xanthine oxidase enzymes catalyse the oxidation of hypoxanthine to xanthine and H_2O_2 and then to uric acid [281]. Xanthine oxidase inhibitors, such as allopurinol, can limit the inflammation in a mouse model of arthritis [328]. This is suppression of inflammation is associated with an elevation of a number of metabolites, including inosine, guanosine and xanthosine, which are substrates of purine nucleoside phosphorylase (PNP). A loss of PNP activity or accumulation of one or more enzyme substrates has been linked extensively to immune deficiency [267]. However, the observation of upregulation in the level of substrates and products of xanthine oxidase and PNP enzymes in the present study (**Figure 5-10**) suggests an ability of eicosenoid derivatives (particularly 11E-ester and 11E-acid form) to modulate the activity of these enzymes and to perturb the purine nucleotide pathway in order to boost the immune system through the provision of ROS.

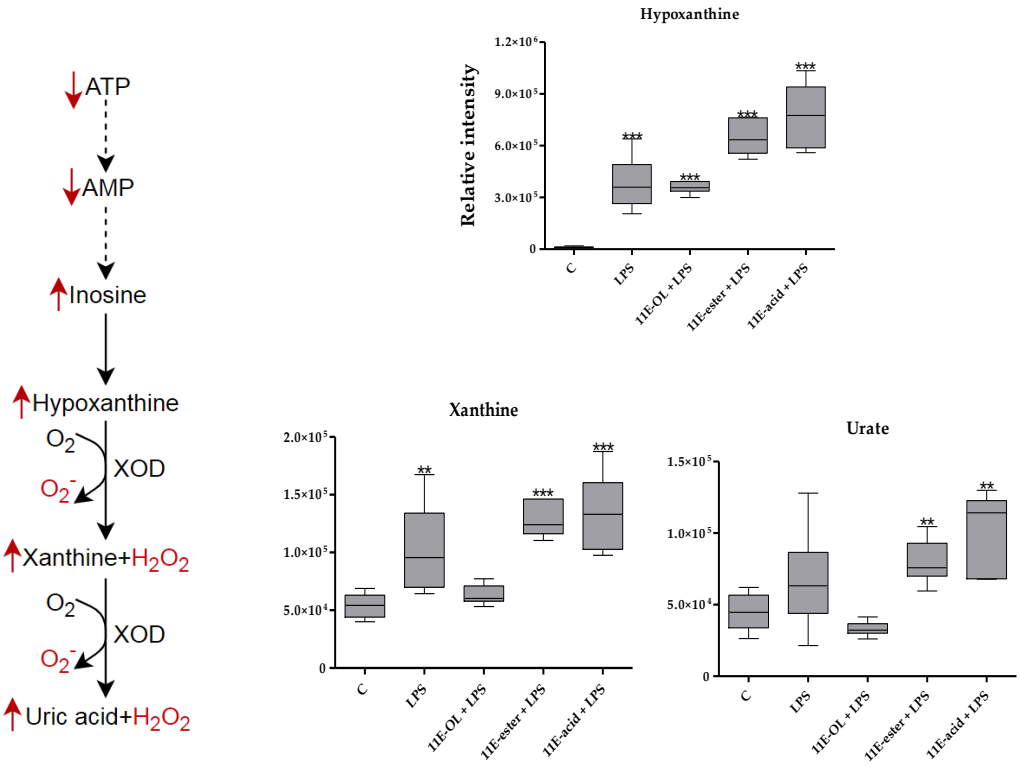

Figure 5-10: Schematic representation of the purine metabolism.
This reflects how 11E-ester+LPS and 11E-acid+LPS synergise the effect of LPS alone focusing on hypoxanthine, xanthine and uric acid, which accumulated with H_2O_2 and superoxide (O_2^-) during purine degradations. C: Untreated control; LPS: Lipopolysaccharide; (11E-OH): (Z)-11-eicosenol; (11E-ester): Eicosenoate; (11E-acid): Eicosenoic acid; (Red rows): Response of 11E-ester+LPS and 11E-acid+LPS combination treatments; ATP: Adenosine triphosphate; AMP: Adenosine monophosphate; *: Significant ($p<0.05$); **: Significant ($p<0.01$); **: Significant ($p<0.001$).

Recent research has reflected a significantly increased interest in fatty acid metabolism and its effects on inflammation and immune cells. In activated macrophages, the importance of mitochondrial fatty acid metabolism or fatty acid oxidation (FAO) has been considered to reflect the regeneration of ATP and a compensation for the reduction in ATP levels [329]. Several studies have highlighted the possibility of attenuating inflammation by promoting macrophage FAO, which also reduces lipid-induced triglyceride accumulation [330]. Inhibition of FAO in

THP-1 cells macrophages exacerbates palmitate-induced endoplasmic reticulum stress and inflammation responses [331]. In addition, LPS-induced inflammation results in elevated levels of kidney triglyceride, fatty acid and cholesteryl ester through a decrease in fatty acid beta oxidation [332]. Intriguingly, the levels of fatty acids were highly elevated in response to the treatments with LPS in combination with eicosenoids when compared with cells treated with LPS alone or untreated controls. In the present study, treatment with 11E-ester and 11E-acid in particular led to increases in a large number of fatty acids, such as arachidonic acid (*i.e.* eicosatetraenoic acid), docosenoic acid, tetracosenoic acid, eicosanoic acid and icosatrienoic acid (**Table 5-3**), which all are strongly correlated with inflammation and immune activation. The presence of elevated levels of several dioic acids (decandioic, dodecandioic and tetradecandoic acids) suggests that the eicosenoic acid and its ester are functioning as peroxisome proliferator ligands since dioic acids are products of peroxisome activity [333].

Lipid profiles (lipidomics) and full assessment of their levels, including eicosanoid, are effective ways to diagnose the severity and progression of a number of diseases [334, 335]. Arachidonic acid (AA), a precursor of eicosanoids, is considered to represent a potent signal of cellular responses. AA metabolites are involved in the inflammatory and immune responses [336], and the activation of phospholipase A2 (PLA_2) is critical for increasing the AA level and subsequent eicosanoid biosynthesis. TLR4-mediated priming has been observed to activate cytosolic calcium-dependent PLA_2 ($cPLA_2$) and to enhance cyclooxygenase (COX2) production via Nuclear factor-kappa B (NF-κB), which results in release of AA and

pro-inflammatory eicosanoids [337]. In the present study, the level of AA was strongly elevated by all the combination treatments when compared to LPS alone; however, this elevation was more pronounced with 11E-ester form, which resulted in a 7-fold increase in the AA level.

Comprehensive assessment of lipid-correlated inflammatory signalling could provide a better understanding of cytokine integration with fatty acid metabolism and particular the production of eicosanoids. In general, the suppression of β-oxidation of fatty acids could result in the apparent boost in fatty acid synthesis and the reductions in ATP levels and citrate accumulation observed in the present study. A more targeted investigation is therefore required to confirm the proposed use of these eicosenoid derivatives as immune system stimulators and as vaccine adjuvants.

5.6 Conclusion

A deeper understanding of the modes of action that regulate the immune stimulatory properties of new or existing adjuvants is prerequisite for the rational design of more sophisticated vaccines. The present study identifies the main effects of synthetic compounds related to 11-eicosanol, which is found in bee venom, in modulating macrophage behaviour. In agreement with previous findings [262, 317], a stimulatory effect of LPS was confirmed in PMA-differentiated THP-1 cells. Furthermore, the possible use of (Z)-11-eicosenol, methyl cis-11-eicosenoate and cis-11-eicosenoic acid to alter macrophage cytokine production was studied. Although these eicosenoid compounds enhanced the production of IL-1β and suppressed the

production of IL-10, which mirrored their immune stimulatory effects, IL-6 release was inhibited, suggesting the presence of a more subtle mechanism of immune modulation. Further metabolic investigations were therefore performed to obtain a better understanding of changes in the macrophage metabolome. Alterations in metabolite levels in response to LPS treatment in the presence or absence of eicosenoids reflected the strength of the actions of each component and confirmed the potential of these compounds, particularly the ester and acid forms, to synergise LPS action. Overall, the findings supported their actions as pro- rather than anti-inflammatory agents.

Significant alterations were observed in the metabolite levels associated with different pathways, including redox cell signalling pathways, which have been extensively associated with transcriptional immune factors and immune functions [323, 338]. These alterations occurred concomitantly with upregulation of the levels of several metabolites within the arginine and proline pathways, glycolysis, the TCA cycle and purine metabolism. Moreover, marked increases occurred in the levels of several fatty acids and inflammatory biomarker metabolites, including arachidonic acid. Cellular activation and enhanced immune response were confirmed by the effects of (Z)-11-eicosenol, methyl cis-11-eicosenoate and cis-11-eicosenoic acid, the findings suggested their possible use as immune-modulating agents and vaccine adjuvants. Taken together, these findings provide a better understanding of the mechanism of immune stimulation, and they support the potential use of new adjuvants in shaping a desired immune response. Comparison with existing adjuvants would need to be carried out in order to confirm any advantages of the eicosenoids.

Chapter Six

Metabolomic Profiling of the Anti-inflammatory Effects of Gypenoside on PMA-Differentiated THP-1 Cells

6 Metabolomic Profiling of the Anti-inflammatory Effects of Gypenoside on PMA-Differentiated THP-1 Cells

6.1 Abstract

Gypenoside (Gyp), used here as a collective term for the major triterpene saponins in *Gynostemma pentaphyllum*, has been proposed as a potential therapeutic agent for the treatment of several diseases. The anti-inflammatory effects of Gyp were examined by determining its ability to suppress lipopolysaccharide (LPS) induction of inflammatory macrophages. THP-1 derived macrophages were stimulated with LPS and treated with Gyp (25, 50 and 75 µg/mL) for 24 h. Gyp treatments suppressed the production of pro-inflammatory cytokines, including tumour necrosis factor (TNF-α), interleukin-1β (IL-1β), and IL-6. Interestingly, anti-inflammatory IL-10 levels were also decreased by Gyp, indicating a complex mechanism. Untargeted liquid chromatography-mass spectrometry (LC-MS) was used to determine in-depth metabolome changes in LPS-stimulated macrophages treated with Gyp. A large number of amino acids and nucleotides were significantly ($p < 0.05$) altered in LPS-stimulated macrophages treated with Gyp when compared with untreated control. Gyp attenuated the LPS stimulation responses and activated the tricarboxylic acid cycle, as well as glycolysis and the pentose phosphate pathway. Gyp also counteracted the LPS effects on tryptophan-related metabolites, suggesting that a therapeutic targeting of indoleamine 2,3-dioxygenase might be useful in treating inflammatory diseases. Analysis of urate metabolites revealed downregulation of purine metabolism, suggesting a possible role for Gyp in treating hyperuricemia. These findings highlight the potential use of Gyp in the treatment of several inflammation-related diseases.

6.2 Introduction

Inflammation is an immunological defence against tissue injury or other external stimuli, including pathogens, irritants and allergens [339]. Immune system cells play a crucial role by recognising substances like lipopolysaccharides (LPS) and other foreign pathogens. LPS binds to toll-like receptors (TLRs) and activates mitogen-activated protein kinase (MAPK) and nuclear factor κB (NF-κB)[340], triggering the high expression of pro-inflammatory cytokines, such as tumour necrosis factor (TNF-α) and interleukins (such as IL-1β and IL-6) [341]. As a protective response, controlling inflammation is very important. Inflammatory responses are usually treated with steroidal or non-steroidal anti-inflammatory drugs (NSAID). However, the adverse side effects of these drugs have prompted a search for naturally originating agents with fewer unfavourable effects.

Natural products have been extensively used for different clinical purposes due to their therapeutic efficacy and low cytotoxicity [342]. For example, Chinese folk medicine makes wide use of extracts from *Gynostemma pentaphyllum* (Thunb.), a member of the Cucurbitaceae [343]. These extracts show several biological activities, including antioxidant, hypoglycaemic, immune-stimulatory, anti-allergic and anticancer activities [344-348]. The major active components include flavonoids, vitamins, amino acids, and gypenosides (Gyp), the major saponin components of *G. pentaphyllum* [349].

Gyp bioactivities have been reported in several previous studies and are due to the presence of hydroxyl functional groups attached to the core structure of a dammarane-type ring [350]. Gyp has shown antitumor [351] and neuroprotective effects [352], and has been reported to show potential anti-inflammatory activity

[353, 354]. For example, Gyp treatment attenuated airway inflammation and Th2 cell activation in ovalbumin-sensitised mice [355]. It also inhibited H_2O_2-induced oxidative stress and cytokine production to show a protective effect on retinal pigment epithelium cells [348]. Gyp treatment was reported to downregulate LPS-induced optic neuritis through the inhibition of different inflammatory factors, including mRNA expression of the pro-inflammatory TNF-α and IL-6 cytokines and cyclooxygenase 2 (COX2) and inducible nitric oxide synthase (iNOS) [356]. Gyp also attenuated the cerebral β-amyloid-induced inflammation in microglial cells, a typical pathogenesis of Alzheimer disease [353]. The antioxidant ability of Gyp was reported to involve an enhancement of superoxide dismutase (SOD) and a decrease in the levels of oxidised low-density lipoprotein [357]. Gyp also suppressed the LPS-induced upregulation of the iNOS and the NF-κB-mediated iNOS protein expression in murine RAW 264.7 macrophages [358]. These findings imply that Gyp could represent a promising therapeutic option for the treatment of inflammatory diseases.

The effectiveness of anti-inflammatory agents has been studied by many researchers using metabolomics approaches to determine treatment-associated alterations in metabolic networks and pathways and patient medical status. However, metabolomics approaches have rarely been used to determine the metabolic function of Gyp as an anti-inflammatory agent. For example, Song *et al*. evaluated the anti-fibrosis effects of Gyp by examining alterations in different metabolic pathways [359]. Metabolic profiling has also been used to detect metabolites in rat urine after oral and intravenous administration of Gyp [360]. Another study showed the ability of Gyp to improve bile acid regulation and restore the normal lipid profile in mice treated with a high-fat diet [361].

Evaluating the changes in the cellular metabolome would confirm the previous findings of bees natural compounds in this thesis and assess the ability of using THP-1 cell line as a good model with regards to immune inflammatory related diseases. The aim of the present study was to examine the anti-inflammatory effects of Gyp in LPS-induced PMA-differentiated THP-1 cells, focusing on LPS-stimulated cytokine production (TNF-α, IL-1β, IL-6 and IL-10). The association of these cytokine changes with changes in the THP-1 cell metabolome was also assessed using mass spectrometry-based metabolomic profiling.

6.3 Materials and Methods

6.3.1 Sample preparation

Gypenoside (Gyp) was supplied Dr. Xinhua Shua (Glasgow Caledonian university, Glasgow, UK) which was purchased from Xi'an Jiatian Biotech Co. Ltd. (China, purity 98%).

6.3.2 Cell culture and differentiation

As detailed in section2.2 2.2.1.

6.3.3 Cell viability assay

The THP-1 cells were seeded at a density of 1×10^5/well in 96-well plates and incubated for 24 h at 37 °C in a humidified atmosphere of 5% CO_2. After 24 h, the cells were treated with Gyp at various concentrations (1.2 to 150 µg/mL) and incubated for a further 24 h. Untreated control cells and medium were added to the plates and dimethyl sulphoxide (DMSO) was used as a positive control. Resazurin

salt solution (0.1 mg/mL) was added for Fluorescence readings using GraphPad Prism as described in section 2.2.2.

6.3.4 Cytokine production and ELISA assay

After 48 h of differentiation using PMA (60 ng/mL) in 24-well plates, the media were aspirated, and the cells were incubated for a further 24 h in PMA-free medium. At day 4, the cells were incubated with Gyp at different concentrations (5, 25, 50 and 75 µg/mL). with and without LPS (Sigma-Aldrich) (0.5 µg/mL) for an additional 24 h. Conditioned medium was collected and frozen until required for ELISA (n = 3). The ELISA assays were performed according to the manufacturer's instructions to quantify the release of (TNF-α, IL-1β, IL-6, and IL-10) (section2.4).

6.3.5 Metabolite Extraction

The PMA-differentiated THP-1 cells were grown for 48 h in 6-well plates seeded at a density of 4.5×10^5/well (n = 6). The medium was aspirated and replaced with fresh medium for a further 24 h, and then the cells were incubated with LPS (0.5 µg/mL) either alone or together with Gyp (25, 50 and 75 µg/mL) for an additional 24 h. After 24 h, the medium was aspirated, and the cells were washed with 3 mL of phosphate-buffered saline (PBS) (Sigma-Aldrich) at 37 °C. The cells were extracted as detailed in section 2.6.

6.3.6 LC-MS Conditions

An Accela HPLC system interfaced to an Exactive Orbitrap mass spectrometer (Thermo Fisher Scientific, Bremen, Germany) was used for the liquid chromatographic separations. ZIC-pHILIC (150 × 4.6 mm, 5 µm) HPLC column

supplied was used. Samples were run under the conditions described previously in section 2.5.1, section 2.5.2 and section 2.5.3.

6.3.7 Data Extraction and Statistical Analysis

As detailed in section2.7.

6.4 Results

6.4.1 Cytotoxicity of Gyp compound against PMA-differentiated THP-1 Cells

The concentration required to maintain 90% cell viability was determined by cytotoxicity assays of Gyp in THP-1 macrophages. As shown in **Figure 6-1**, no cytotoxic effect was observed at Gyp concentrations below 75 µg/mL. An IC_{50} of > 150 µg/mL was obtained; at that concentration, a significant decrease in cell viability of about 40% was observed. Concentrations of 5, 25, 50 and 75 µg/mL were used in all subsequent cytokine and metabolomic assessments.

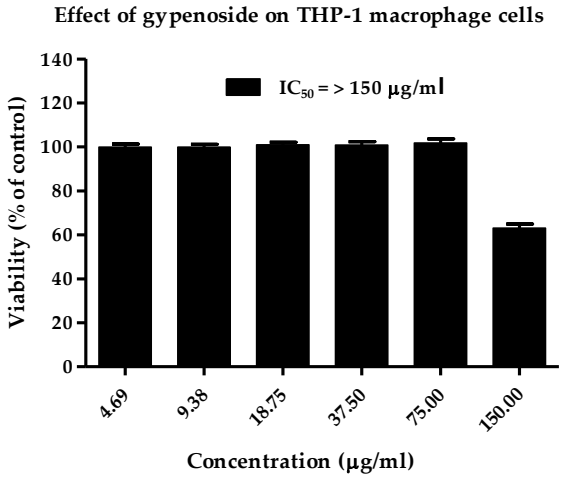

Figure 6-1: Gypenoside (Gyp) cytotoxicity effects at different doses in phorbol 12-myristate 13-acetate (PMA)-differentiated THP-1 cells.
Gyp was non-cytotoxic to PMA-treated cells, with an IC_{50} of >150 µg/mL. Each data point represents the mean ± SD (*n*=3).

6.4.2 Effect of Gyp compound on pro-inflammatory TNF-α cytokine production

Small, but statistically significant ($p < 0.05$), decreases were observed in the level of the pro-inflammatory TNF-α cytokine in LPS-stimulated THP-1 macrophages in response to treatment with Gyp at 25, 50 and 75 µg/mL cells when compared to LPS alone. Decreases in this cytokine were also observed in unstimulated cells in response to Gyp (**Figure 6-2**).

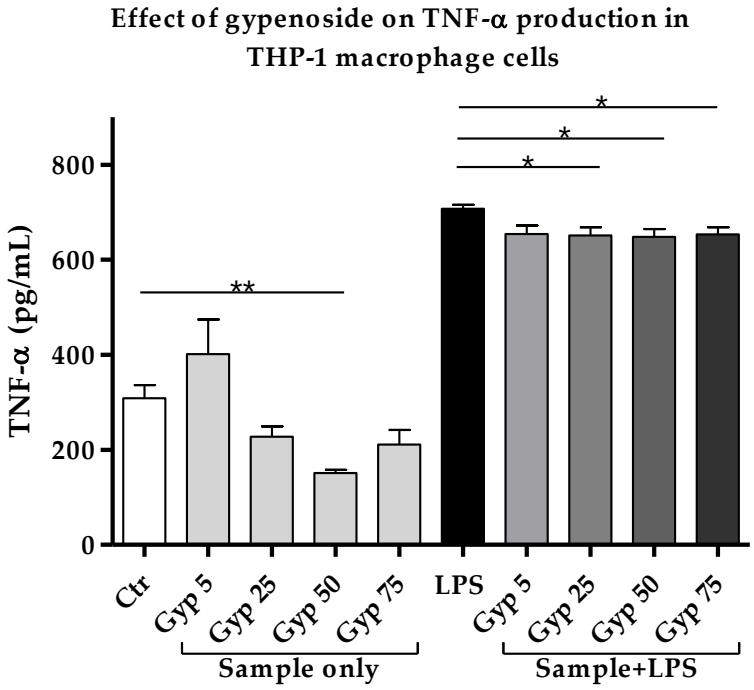

Figure 6-2: Gypenoside (Gyp) effects on the production of TNF-α by PMA-differentiated THP-1 cells in the absence and presence of LPS (0.5 µg/mL).
The TNF-α levels in the LPS-stimulated cells were significantly decreased by Gyp at 25, 50 and 75 µg/mL (n=3). Ctr: Untreated control; LPS: Lipopolysaccharide; Gyp: Gypenoside; *: Significant ($p<0.05$); **: Significant ($p<0.01$).

6.4.3 Effect of Gyp compound on pro-inflammatory IL-1β cytokine production

Gyp had a much more pronounced effect on the level of the IL-1β cytokine than on TNF-α, with statistically significant decreases observed in LPS-stimulated cells exposed to Gyp at 25, 50 and 75 µg/mL. Gyp treatment at 75 µg/mL also increased the level of this cytokine compared to unstimulated control cells (**Figure 6-3**).

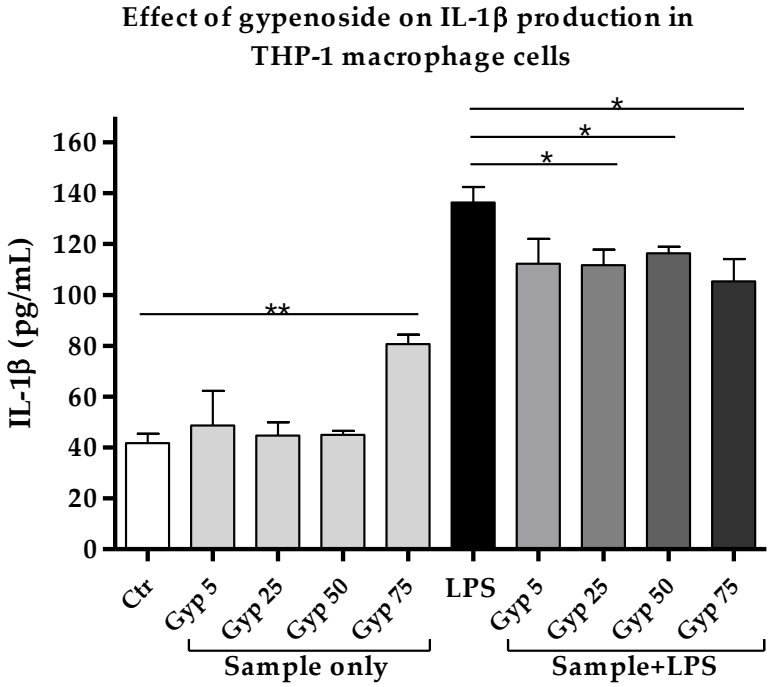

Figure 6-3: Gypenoside effect on the production of IL-1β by PMA-differentiated THP-1 cells in the absence and presence of LPS (0.5 µg/mL).
The IL-1β levels in the LPS-stimulated cells were significantly decreased by Gyp at 25, 50 and 75 µg/mL (*n*=3). Ctr: Untreated control; LPS: Lipopolysaccharide; Gyp: Gypenoside; *: Significant ($p<0.05$); **: Significant ($p<0.01$).

6.4.4 Effect of Gyp compound on pro-inflammatory IL-6 cytokine production

Gyp showed dose-dependent inhibition of the levels of IL-6 in the LPS-stimulated THP-1 macrophages, with decreases of about 45%, 71% and 89% observed for Gyp doses of 25, 50 and 75 µg/mL, respectively (**Figure 6-4**). These decreases were statistically significant when compared with LPS-stimulated control cells, although the decrease obtained with Gyp at 5 µg/mL was not significant. In the unstimulated cells, the cytokine levels did not differ from the background level at any Gyp doses.

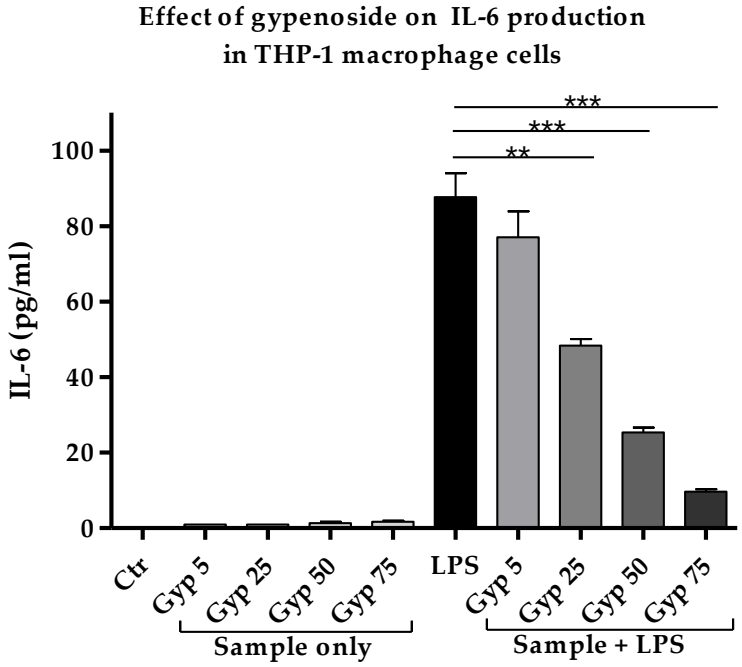

Figure 6-4: Gypenoside effect on the production of IL-6 by PMA-differentiated THP-1 cells in the absence and presence of LPS (0.5 µg/mL).
The IL-6 levels in the LPS-stimulated cells were significantly decreased by Gyp at 25, 50 and 75 µg/mL (*n*=3). Ctr: Untreated control; LPS: Lipopolysaccharide; Gyp: Gypenoside; *: Significant ($p<0.05$); **: Significant ($p<0.01$); ***: Significant ($p<0.001$).

6.4.5 Effect of Gyp compound on anti-inflammatory IL-10 cytokine production

The levels of the anti-inflammatory IL-10 cytokines were also significantly decreased by Gyp treatment. No significant differences were observed in the levels of this cytokine in unstimulated cells treated with Gyp or in LPS-stimulated cells treated with 5 µg/mL Gyp. As shown in **Figure 6-5**, the Gyp-mediated decreases in IL-10 levels occurred in a dose-dependent manner.

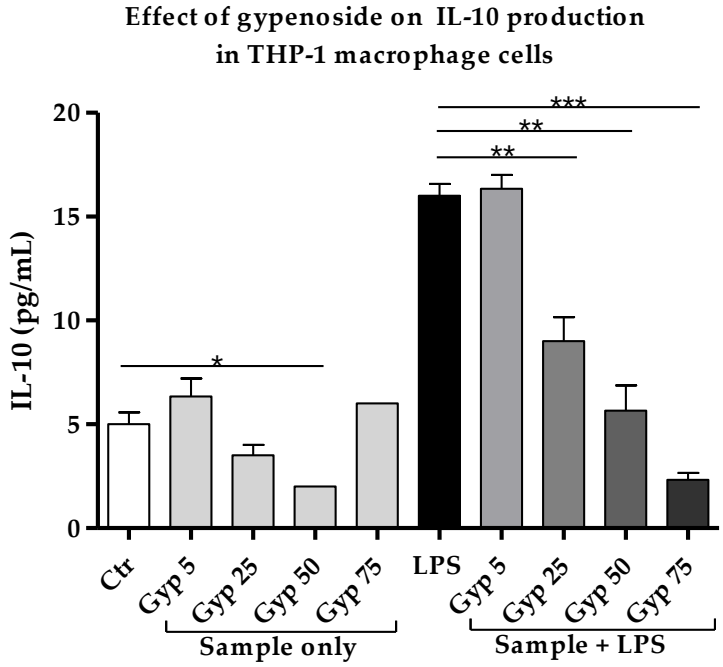

Figure 6-5: Gypenoside effect on the production of IL-10 by PMA-differentiated THP-1 cells in the absence and presence of LPS (0.5 µg/mL).
The IL-10 levels in the LPS-stimulated cells were significantly decreased by Gyp at 25, 50 and 75 µg/mL (*n*=3).
Ctr: Untreated control; LPS: Lipopolysaccharide; Gyp: Gypenoside; *: Significant ($p<0.05$); **: Significant ($p<0.01$); ***: Significant ($p<0.001$).

6.4.6 Effect of Gyp compound on the THP-1 cell metabolome

The inhibitory effects of Gyp on cytokine production were further investigated by untargeted metabolic profiling. PMA-differentiated THP-1 cells were stimulated with LPS (0.5 µg/mL) and treated with Gyp (25, 50 and 75 µg/mL) and their intracellular metabolites were then assessed to elucidate the pathways leading to the Gyp anti-inflammatory effects.

The metabolome was assessed using LC-MS, and principal component analysis (PCA), used for data visualisation, reflected the absence of outliers (**Figure 6-6A**). The instrumental analytical method was validated by clustering the quality control samples (P1-7), thereby confirming the precision and stability of the instrument. Relative standard deviation (RSD) was calculated for the pooled quality control samples, and metabolites with >30% RSD were excluded. Orthogonal partial least squares discriminant analysis (OPLS-DA) provided a unique discrimination between groups (**Figure 6-6B**), but discrimination was difficult between the Gyp 50 and Gyp75 groups, indicating a high similarity between them. The cross-validated (CV)-ANOVA of the model ($p = 3.58^{-18}$) indicated that the model was both valid and strong.

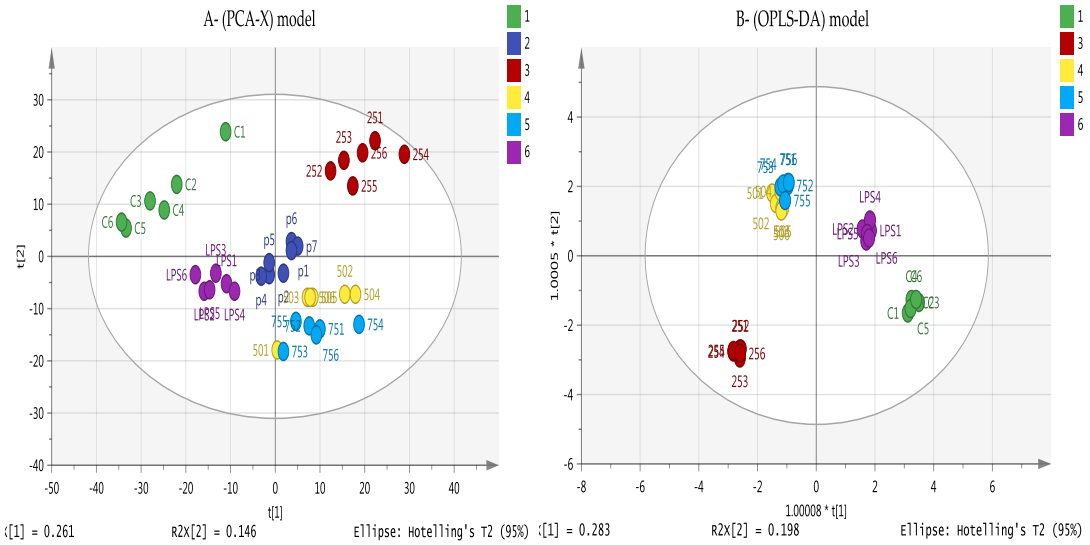

Figure 6-6: (A) Principle component analysis (PCA-X) vs. **(B)** Orthogonal Partial Least Squares Discriminant Analysis (OPLS-DA) score plots of THP-1 cells.
The figures show a clear separation between control, pooled and treatment groups based on 254 metabolites separated on a ZIC-pHILIC column (*n* = 6). PCA score plot (A) gives the goodness of fit (R^2X) = 0.608, and the goodness of prediction (Q^2) = 0.446. OPLS-DA score plot (B) gives R^2X= 0.692, R^2Y= 0.966, Q^2= 0.860. (C: Control; LPS: Lipopolysaccharides; 25, 50 and 75: Three different concentration of treatments (Gyp) + LPS*; P*=pooled samples).

Table 6-1: Metabolites showing significant changes in LPS-stimulated THP-1 cells and LPS-stimulated cells treated with 50 µg/mL Gypenoside.
Data are compared versus untreated control cells.

Mass	Rt	Putative Metabolite	LPS/C		Gyp 50+LPS/C	
			Ratio	p.value	Ratio	p.value
		Arginine and proline metabolism				
246.133	18.78	N2-(D-1-Carboxyethyl)-L-arginine	1.316	0.003	2.246	0.000
145.085	15.48	4-Guanidinobutanoate	1.162	0.015	1.380	0.001
129.042	10.06	4-Oxoproline*	1.246	0.002	1.565	0.002
113.059	9.95	Creatinine	1.237	0.000	1.530	0.004
211.036	15.19	Phosphocreatine*	0.825	ns	0.663	0.000
175.096	16.21	L-Citrulline*	1.333	0.000	1.351	ns
189.064	13.87	N-Acetyl-L-glutamate*	0.666	0.001	0.853	ns
115.063	13.05	L-Proline*	1.058	ns	1.304	0.014
174.112	26.93	D-Arginine	1.230	0.000	1.635	0.001
132.090	23.85	D-Ornithine	1.245	0.000	1.595	0.001
		Glycolysis/TCA cycle				
260.030	16.84	D-Glucose 6-phosphate*	0.887	0.024	1.637	0.006
180.063	14.46	D-Glucose*	1.811	0.003	3.605	0.000
339.996	18.05	D-Fructose 1,6-bisphosphate*	1.273	0.024	1.953	0.006
260.030	16.31	D-Fructose 6-phosphate*	1.526	0.013	1.953	0.006
169.998	16.10	D-Glyceraldehyde 3-phosphate*	0.313	0.000	0.239	0.000
185.993	16.79	3-Phospho-D-glycerate	0.415	0.000	0.312	0.001
809.125	12.40	Acetyl-CoA	0.639	0.016	3.476	0.000
767.115	13.66	CoA*	0.740	0.000	1.133	ns
174.016	18.07	cis-Aconitate*	1.025	ns	1.278	0.009
192.027	18.08	Citrate*	1.012	ns	1.328	0.003
131.069	14.96	Creatine*	0.743	0.001	0.732	0.005
665.125	13.37	NADH*	0.518	0.000	0.640	0.000
663.109	14.36	NAD+*	0.510	0.000	0.675	0.000
506.996	16.75	ATP*	0.503	0.000	0.438	0.000
427.029	15.33	ADP*	0.702	0.000	1.085	ns
443.024	18.04	GDP*	0.813	0.010	0.904	ns
522.991	19.44	GTP*	0.868	0.021	0.720	0.002
		Oxidative stress/ Pentose phosphate pathway				
196.058	13.26	D-Gluconic acid	0.889	ns	1.622	0.000
290.040	16.22	D-Sedoheptulose 7-phosphate	1.573	0.000	2.475	0.000
230.019	15.73	D-Ribose 5-phosphate*	1.253	0.105	0.676	0.012
745.091	17.03	NADPH*	0.459	0.027	n.d.	n/a
743.075	16.81	NADP+*	0.951	ns	1.992	0.000
166.047	13.36	Xylonate	1.256	ns	2.373	0.000

196.058	13.75	Mannonate	0.772	ns	1.432	ns
307.084	14.36	Glutathione	0.306	0.022	0.209	0.029
		Purine metabolism				
168.028	12.43	Urate*	1.700	0.010	9.151	0.000
136.038	10.38	Hypoxanthine*	3.065	0.000	4.445	0.000
363.058	16.73	GMP*	0.539	0.005	0.413	0.002
		Pyrimidine metabolism				
243.085	12.15	Cytidine*	2.283	0.000	4.184	0.000
244.069	12.12	Pseudouridine	1.370	0.009	3.941	0.000
482.984	18.57	CTP*	0.657	0.000	0.624	0.000
483.968	18.00	UTP*	0.711	0.000	0.740	0.000
324.036	16.24	Pseudouridine 5'-phosphate	0.674	0.000	0.714	0.000
111.043	11.52	Cytosine*	1.283	ns	1.693	0.008
323.052	15.19	CMP*	0.660	0.004	0.895	ns
404.002	16.50	UDP*	0.543	0.000	0.693	0.019
536.044	16.14	UDP-D-xylose	0.677	0.000	0.726	0.001
580.034	18.87	UDP-glucuronate	0.592	0.000	0.549	0.000
566.055	16.23	UDP-glucose*	0.724	0.000	0.745	0.004
607.082	15.04	UDP-N-acetyl-D-glucosamine*	0.657	0.000	0.638	0.000
589.082	17.48	GDP-L-fucose	0.796	0.001	0.819	0.026
605.077	18.16	GDP-mannose	1.159	0.011	1.519	0.000
		Tryptophan metabolism				
236.079	10.39	L-Formylkynurenine	0.950	ns	0.525	0.000
191.058	11.18	5-Hydroxyindoleacetate*	1.268	0.008	1.259	ns
220.085	9.98	5-Hydroxy-L-tryptophan isomer	5.497	0.000	4.638	0.000
208.085	11.18	L-Kynurenine*	1.347	0.000	1.197	ns
204.090	11.94	L-Tryptophan*	1.250	0.002	2.255	0.000
		Miscellaneous				
146.069	15.32	L-Glutamine*	1.264	0.000	1.677	0.002
147.053	14.68	D-Glutamate*	0.772	0.000	0.715	0.000
301.056	14.98	N-Acetyl-D-glucosamine 6-phosphate	0.706	0.003	0.791	0.011
103.100	20.80	Choline*	1.366	0.000	2.001	0.000
131.058	14.70	N-Acetyl-beta-alanine	1.167	0.003	1.490	0.003
105.043	16.02	L-Serine*	1.193	0.001	1.512	0.000
155.069	15.13	L-Histidine*	1.136	0.020	1.559	0.001
146.105	25.45	L-Lysine*	1.403	0.000	1.847	0.001
203.116	11.28	O-Acetylcarnitine*	0.653	0.000	0.611	0.000
175.048	14.53	N-Acetyl-L-aspartate*	0.517	0.000	0.722	0.038
149.051	11.83	L-Methionine*	1.291	0.000	1.678	0.002
181.074	13.25	L-Tyrosine*	1.235	0.000	1.583	0.005
131.094	11.13	L-Leucine*	1.237	0.000	1.577	0.005
131.094	11.59	L-Isoleucine*	1.261	0.000	1.637	0.005

117.079	12.78	L-Valine*	1.269	0.000	1.589	0.002
240.024	16.36	L-Cystine*	2.353	0.001	7.406	0.000

Rt: Retention time (min); LPS: Lipopolysaccharides; *: Matches the analytical standard retention time; ns: Non-significant; n.d.: Not detected; n/a: Not applicable.

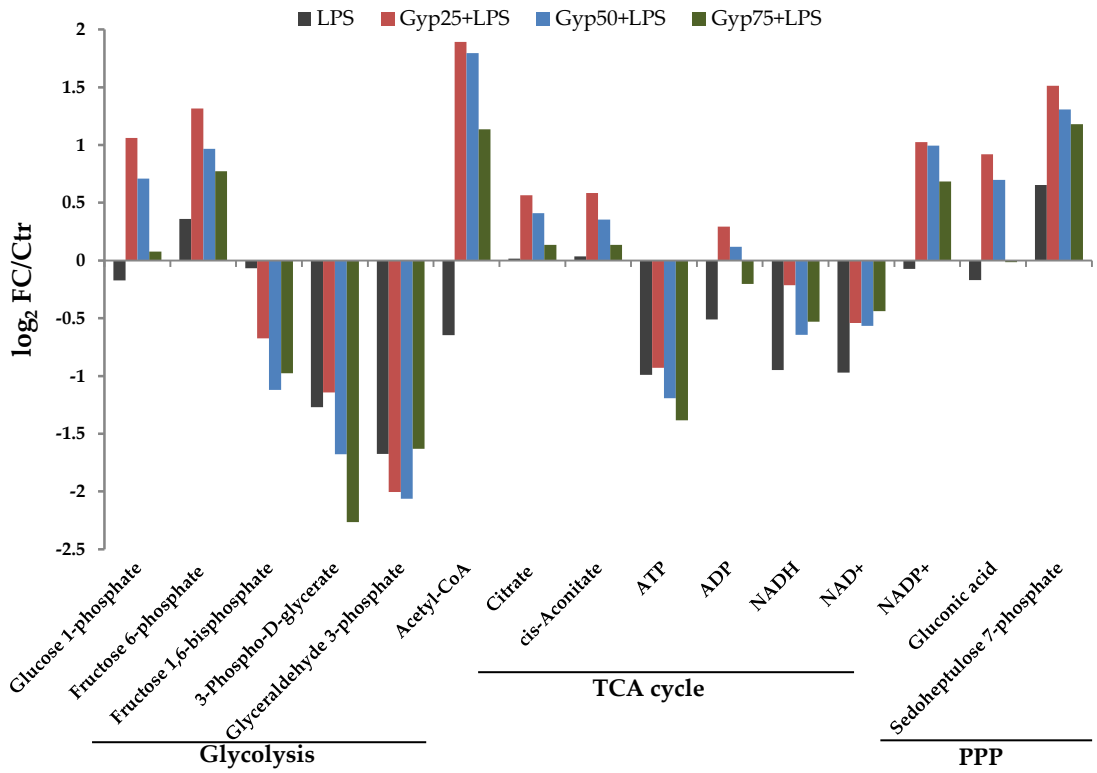

Figure 6-7: Log2 fold change (FC) in 15 amino acid metabolites associated with the glycolysis, the tricarboxylic acid (TCA) cycle and the pentose phosphate pathway (PPP). The ratios relative to the unstimulated control (Ctr) clearly correlated with the Gyp doses applied (Gyp 25, 50 and 75 µg/mL) in the LPS-stimulated cells.

Gyp treatment clearly affected different pathways when compared with LPS-stimulated THP-1 cells and unstimulated control (**Table 6-1**). **Figure 6-7** shows that

Gyp significantly affected pathways associated with macrophage immune responses, including glycolysis, the tricarboxylic acid (TCA) cycle and the pentose phosphate pathway (PPP). The levels of most metabolites were higher in LPS-stimulated cells treated with 25 μg/mL Gyp. Several metabolites were suppressed by LPS stimulation included glucose-1-phosphate, acetyl-CoA, gluconic acid and nicotinamide adenine dinucleotide phosphate (NADP+), while they were increased by adding Gyp treatment. **Figure 6-8** shows the association between the increase in Gyp treatment concentration and the relative abundance of various metabolites. The increase in Gyp treatment was strongly correlated with the levels of several biomarker metabolites, including L-citrulline, L-kynurenine and urate, within arginine/proline, tryptophan and purine metabolic pathways, respectively. This would suggest the involvement of these metabolites in macrophage reprogramming and in the Gyp-mediated anti-inflammatory mechanism.

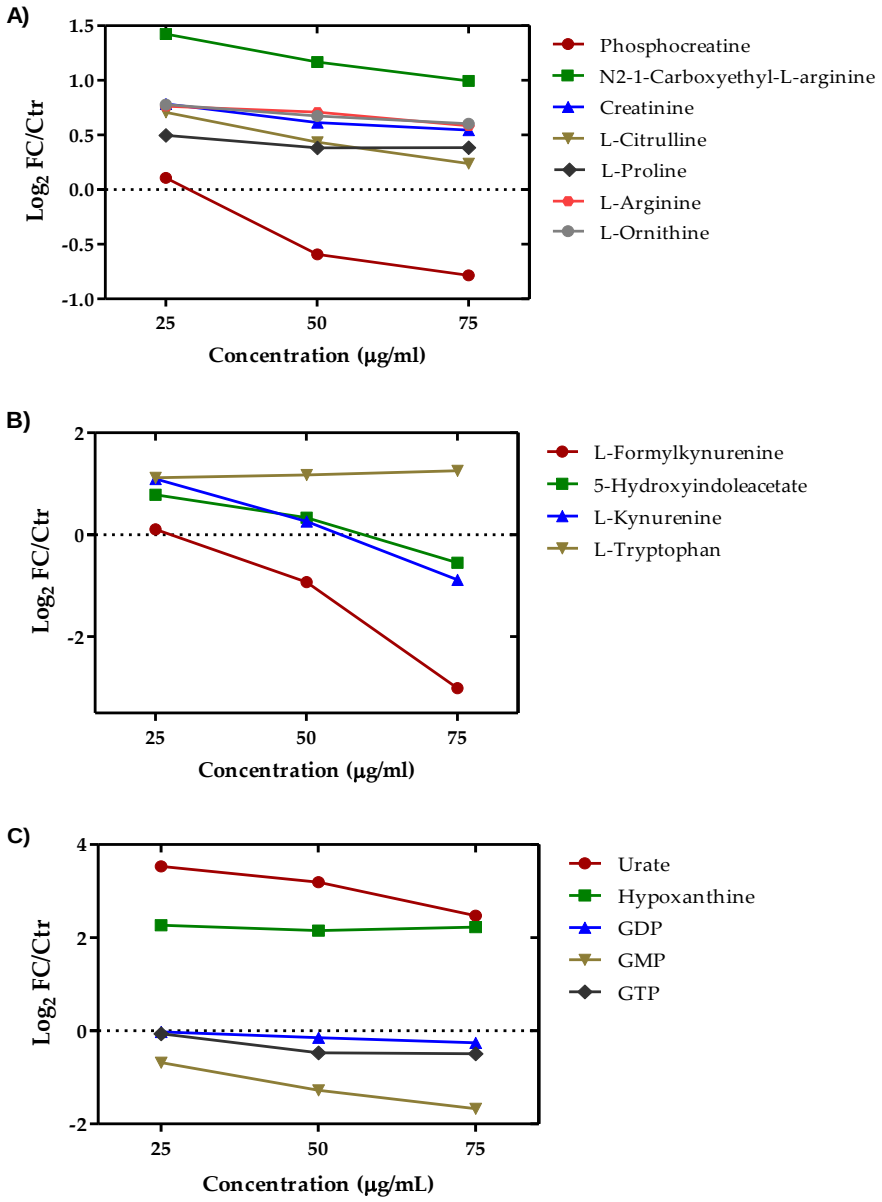

Figure 6-8: Metabolites in LPS-stimulated THP-1 cells were affected by Gyp treatment (25, 50 and 75 µg/mL) in a dose-dependent manner.
The data represent the Log2 fold change (FC) relative to unstimulated control cells (Ctr) **(A)** Arginine and proline metabolism. **(B)** Tryptophan metabolism. **(C)** Purine metabolism.

6.5 Discussion

Gypenosides are well-known anti-inflammatory plant components. The anti-inflammatory property of Gyp was further examined in the present study using LPS-stimulated PMA-differentiated THP-1 cells as an inflammation model. Specifically, the protective effect of Gyp on THP-1 macrophages and the possible mechanism of Gyp in attenuating LPS-induced inflammatory signalling were evaluated.

The LPS stimulation of THP-1 cells resulted in clear increases in the production of pro-inflammatory cytokines (TNF-α, IL-1β and IL-6). Gyp treatment inhibited the production of these cytokines and counteracted the LPS stimulation of THP-1 macrophages. Dose-dependent decreases were determined for both IL-6 and anti-inflammatory IL-10 in response to Gyp, in agreement with previous studies [356] that showed attenuation of LPS-induced optic neuritis and cytokine production by Gyp through the inhibition of the NF-κB and the signal transducer and activator of transcription (STAT) pathways. Gyp treatment has also been reported to improve cognitive function and reduce neuroinflammation in rats via NF-κB/iNOS/TLR4 modulation [362]. Gyp was also reported to inhibit NF-κB and suppress IL-1β-induced nitric oxide (NO) and prostaglandin E2 (PGE2) secretion in human osteoarthritis chondrocytes [363]. However, contrary to the dose-dependent decrease in the level of IL-10 in THP-1 cells observed in the present study, this cytokine was increased by the effect of Gyp treatment on β amyloid (Aβ)-induced microglial activation by inducing a decrease in the M1 marker and enhancing the level of M2 markers [353], suggesting a complex mechanism for Gyp responses. For this reason, a comprehensive metabolic profile was prepared for LPS-stimulated THP-1

macrophages treated with Gyp. The aim here was to determine which pathways might be altered by Gyp and the possible mechanism of action by which Gyp counteracts LPS stimulation.

Metabolic reprogramming in response to a stimulus is one determinant that regulates the transition between M1 and M2 macrophages; therefore, this might represent a novel approach to target for the regulation of inflammatory diseases [280]. As shown in **Table 6-1**, Gyp treatment alters the metabolites associated with glycolysis, the TCA cycle and the PPP. After LPS stimulation, Gyp treatment increases upper part of glycolysis pathway significantly, and particularly glucose levels, leading to a high flow through both glycolysis and the PPP. The resulting imbalance between the oxidative and non-oxidative arms of the PPP would increase levels of D-sedoheptulose 7-phosphate (S7P), which could then re-enter glycolysis. Carbohydrate kinase-like protein (CARKL), a sedoheptulose kinase that catalyses the production of S7P and is primarily responsible for proper macrophage reprogramming and changes in glucose metabolism, is downregulated by LPS [79]. The data presented in the current study indicate an upregulation of glycolytic components, including glucose 6-phosphate, fructose 1,6-bisphosphate and fructose 6-phosphate, which would aid in minimising oxidative damage and suppressing apoptosis [364]. The metabolic mechanism of Gyp treatments has been reported to involve an increase in glycolysis [359], in agreement with the present findings.

The importance of acetyl-CoA in macrophage stimulation has been extensively reported [78, 83]. LPS limits the production of acetyl-CoA and diverts pyruvate to lactate [80, 365], as observed in the current study (**Figure 6-7**). Gyp antagonises LPS

action, resulting in a significant increase in the level of acetyl-CoA. However, acetyl-CoA is also generated from citrate in the cytoplasm for fatty acid biosynthesis and the production of reactive oxygen species (ROS) [280]. The accumulation of acetyl-CoA in response to Gyp could support Gyp use as an antioxidant, as described previously [348]. Enhancement of the TCA cycle to compensate for ATP reduction was observed as an increase in citrate, cis-aconitate and nicotinamide adenine dinucleotide (NAD+ and NADH) in response to Gyp in LPS-stimulated cells (**Figure 6-7**). Fatty acids can break down into acetyl-CoA through the mitochondrial β-oxidation processes [366] and the findings presented here might reflect this. Interestingly, Gyp dose dependently decreased fat accumulation and improved the mRNA expression of mitochondrial activity and lipid β-oxidation, suggesting that it may be useful in treating diet-induced obesity and insulin intolerance [367]. By contrast, LPS stimulation alters lipid metabolism and decreases fatty acid oxidation [262, 332]. An examination of the anti-inflammatory properties of propolis using a metabolic approach has also revealed a high production of acetyl-CoA [317].

The antioxidant activity of Gyp was further confirmed by the biomarker-related oxidative stress metabolites detected in this study. Despite the increased production of arginine and proline metabolites in response to Gyp in LPS-stimulated cells when compared to LPS alone (**Table 6-1**), a dose-dependent decrease was observed in the level of the majority of these metabolites in response to Gyp higher concentration, as shown in **Figure 6-8A**. Overall, this would reflect the importance of the Gyp dose chosen for use as an anti-inflammatory and anti-oxidant treatment. L-citrulline, produced together with NO from L-arginine, was decreased to the lowest level in

response to 75 µg/ml Gyp. The levels of urea cycle metabolites, including L-arginine and L-ornithine, were dose-dependently decreased by increases in Gyp. These findings support previous studies that addressed the inhibitory effect of Gyp on NO production. For example, Gyp dose-dependently suppressed NO synthesis in murine macrophages through the inhibition of iNOS, an enzyme that converts arginine to citrulline [358]. The iNOS enzyme is predominantly responsible for NO overproduction in injury and inflammatory processes [368]; consequently, inhibition of this enzyme is important in the regulation of inflammation and immune responses [316, 369]. Nicotinamide adenine dinucleotide phosphate (NADPH) is required as a substrate to convert L-arginine to L-citrulline, and it is also generated from NADP+ to be used by NADPH oxidases to produce ROS [365, 370]. Interestingly, while NADPH was not detected in the present study, the production of NADP+ was elevated (2-fold) by Gyp treatment of LPS-stimulated cells when compared with unstimulated cells and LPS alone. This might reveal the involvement of these mechanisms within Gyp anti-inflammatory action.

Another pathway apparently affected by Gyp was purine metabolism. Xanthine oxidoreductase is considered the rate-limiting enzyme in the uric acid catalytic pathway [371]. It catalyses the last two steps of purine breakdown, namely the conversion of hypoxanthine to xanthine and the oxidation of xanthine to uric acid [372]. Increases in purine metabolism will lead to the abnormally elevated levels of uric acid associated with the disorder known as hyperuricemia [373]. The mechanism leading to the high levels of uric acid is associated with the production of ROS, particularly superoxide (O_2^-) and hydrogen peroxide (H_2O_2). Interestingly, saponin

extracts from *Dioscorea collettii* rhizomes have shown a potential anti-hyperuricemic effect through the reduction in serum uric acid [374]. Similarly, Pang et al. [375] have reported an effective role of Gyp for the treatment of hyperuricemia and determined that its anti-hyperuricemic effect arose due to the enhancement of urate excretion and lowering of serum uric acid. In the same study, Gyp treatment was also shown to decrease the levels of xanthine oxidase (XOD), adenosine deaminase (ADA) and xanthine dehydrogenase (XDH). Consistent with this finding, our results show that Gyp dose-dependently decreases purine metabolism, specifically urate production, with maximal effects observed at 75 μg/mL Gyp (**Figure 6-8C**). However, the level of the urate by Gyp combination treatment with LPS remain higher than that with LPS alone, which suggests the presence of more complex mechanism. The stable levels of hypoxanthine may reflect the effects of Gyp treatment on both the ADA and XOD/XDH systems, which are enzymes that work before and after the hypoxanthine step, respectively. In general, the Gyp anti-hyperuricemic effect might be exerted through the modulation of purine metabolites.

Another enzyme associated with inflammation is indoleamine 2,3-dioxygenase 1 (IDO1), the rate limiting enzyme in the oxidation of tryptophan to kynurenine [376]. IDO1 is expressed in dendritic cells, monocytes and macrophages [377], and its regulation is very important in the modulation of systemic and local immune responses [378]. Pro-inflammatory cytokines have been shown to induce the expression of IDO1 in chronic inflammation disorders, such as inflammatory bowel diseases (IBD) [378, 379]. Tryptophan synthesis is reduced in IBD, concomitantly with an increased expression of IDO1 mRNA, indicating a strong degradation of

tryptophan and increased production of its by-products, such as quinolinic acid [376]. IDO expression is induced by LPS treatment [380], and IDO is activated by the LPS-induced production of TNF-α [381]. Tryptophan concentrations were reduced in conjunction with an increase in the level of kynurenine after stimulation of IDO expression by LPS in a porcine model [382]. Interestingly, in the present study, Gyp administration enhanced the tryptophan levels by about 2-fold in LPS-stimulated THP-1 cells, when compared to LPS alone (**Table 6-1**), and the levels were slightly increased at higher Gyp concentrations (**Figure 6-8B**). In the same pathway, kynurenine levels were decreased in a dose-dependent manner in response to Gyp treatments. Taken together, the results suggest another possible mode of action of Gyp, namely as an anti-inflammatory agent that counteracts the LPS-induced IDO activity.

To the author's knowledge, this is the first study to assess the metabolic profile of macrophages in response to Gyp treatment. The observed effects of Gyp treatment on the cell metabolome suggest a possible mechanism for Gyp responses.

6.6 Conclusion

In conclusion, Gyp treatment of LPS-stimulated THP-1 cells significantly inhibited the expression of pro-inflammatory mediators, such as TNF-α, IL-1β and IL-6. Exposure to Gyp disrupted the metabolism of PMA-differentiated THP-1 cells. Gyp attenuated the reprogramming and inflammatory responses of LPS-stimulated macrophages. It exerted an anti-inflammatory-like effect that might be mediated, at least in part, by enhancing cellular responses through the modulation of several biomarker metabolites. Gyp improved the activity of glycolysis, the PPP and the

TCA cycle, in agreement with its proposed action. Untargeted metabolic profiling clearly showed other possible mechanisms that might be associated with the use of Gyp for anti-inflammatory therapy, including antioxidant and anti-hyperuricemic action. The antioxidant effect of Gyp was associated, in part, with the inhibition of synthesis of ornithine, arginine, citrulline and uric acid metabolites. The catabolism of purine nucleotides and reduction in uric acid was observed. In addition, the activation of tryptophan metabolism in inflammatory conditions identified IDO overexpression as an important area of investigation. Collectively, our results indicate that metabolic profiling can map the effects of immune stimuli on the immune system and that Gyp may have useful therapeutic activity. In future work, further prospective targeted analyses and validation studies of the affected pathways and metabolites will enable the evaluation of the distinctive role of each biomarker metabolite in regulating macrophage stimulation. In short, this study provides evidence for the mechanism underlying the therapeutic effects of Gyp treatments.

Chapter Seven

General Discussion and Conclusion

7 General discussion and conclusion

This thesis describes comprehensive investigations of the metabolic responses to different natural products which might have direct or related effects on cellular immune responses. Metabolomic profiling helps in understanding and elucidating the mechanisms underlying the metabolic changes in activated macrophages following a pro-inflammatory stimulus and the impact of those changes on immune functions [143]. A comparative study of the effects of natural products on these stimulus responses could help to identify new drugs with unique characteristics and different therapeutic actions.

The main objectives of the present study were to investigate the immunomodulatory potentials of melittin and eicosenoids (and two related derivatives) in stimulating the production of pro- and anti- inflammatory cytokines in PMA- differentiated THP-1 cells and to assess the possible synergistic actions of these potential immunomodulators with LPS. In addition, this work involved the study of some natural anti-inflammatory components that can counter LPS action by inhibition of cytokine production. This work was expanded by including an extensive assessment of the metabolic responses as a way to achieve a deeper understanding of the mechanism of action and to identify potential new biomarker metabolites.

The melittin and eicosenoid fractions from bee venom were assessed in terms of their ability to modulate the production of pro-inflammatory (TNF-α, IL-1β and IL-6) and anti-inflammatory (IL-10) cytokines in PMA-differentiated U937 cells [136]. Cytokine production and metabolic profiling in response to melittin and synthetic

eicosenoids, with and without LPS, were examined in this study to assess the extent of any immune stimulation. The ELISA assays confirmed that LPS treatment triggered the production of a significant amount of cytokines. In comparison, melittin treatment enhanced the LPS stimulation of IL-1β and IL-6 and inhibited the production of anti-inflammatory IL-10 [262]. Treatment with eicosenoid compounds caused a slight induction of TNF-α and a greater induction of IL-1β, while inhibiting the production of IL-10. By contrast, the inhibitory effects on IL-6 levels reflected the operation of subtler mechanisms.

The cytokine release assessments were combined with metabolomic profiling of the THP-1-derived macrophage cells to obtain a better understanding of the possible mechanisms of immune stimulation. THP-1 cells were treated with LPS alone, melittin alone and a combination of melittin and LPS. Macrophage metabolic profiling has typically revealed the utilisation of glucose, mainly through the TCA cycle, and oxygen, through oxidative phosphorylation (OXPHOS). By contrast, macrophages activated by LPS or IFNγ (i.e. inflammatory macrophages) undergo a metabolic switch from OXPHOS to glycolysis and a further flux to the pentose phosphate pathway (PPP) to generate energy, concomitant with a general inhibition of the TCA cycle [152]. The findings of the present study support these observations, as LPS treatment triggered macrophage activation and an increased shift towards glycolysis and PPP and an inhibition of OXPHOS and TCA cycle activity. In addition, the levels of several inflammatory biomarker metabolites, such as L-citrulline and hypoxanthine, were increased.

Treatment with melittin in combination with LPS enhanced the overall effect of LPS and significantly increased the levels of these metabolites. Furthermore, the melittin response indicated a strong involvement of arachidonic acid and several fatty acids, supporting its potential use in immune stimulation and its proposed actions as a vaccine adjuvant.

The metabolic responses of (Z)-11-eicosenol and its two derivatives (eicosenoate and eicosenoic acid) were comprehensively investigated in THP-1 monocyte-derived macrophage cells. Several pathways were altered, in agreement with previously published observations [152]; however, more inflammatory biomarker metabolites were detected, confirming the ability of eicosenoid compounds to synergise LPS action. The altered metabolites included L-arginine, l-ornithine, L-argininosuccinate and L-citrulline, which are associated with the urea cycle and arginine biosynthesis. The levels of NADPH and glutathione disulphide (GSSG) were also increased. The NADPH/NADP+ and GSH/GSSG ratios were decreased by the combination of eicosenoate or eicosenoic acid and LPS when compared with untreated control cells and cells treated with LPS alone. The findings confirmed the crucial role of these treatments in generating reactive oxygen species (ROS), including hydrogen peroxide (H_2O_2) and nitric oxide (NO). The levels of substrates and products of xanthine oxidase and purine nucleoside phosphorylase (PNP) enzymes also increased; these included inosine, guanosine, hypoxanthine, xanthine and urate metabolites. Xanthine oxidase and PNP enzymes are extensively involved in inflammatory conditions and immune deficiency [267, 328]. Substantial increases were also observed in the levels of arachidonic acid, a metabolite that is involved

mainly in inflammatory and immune responses. Taken together, the findings confirm that the eicosenoid compounds act primarily as pro-inflammatory rather than as anti-inflammatory agents.

In certain instances, acute and chronic inflammations need to be regulated differently using specific agents. Thus, understanding the exact mechanisms by which anti-inflammatory agents act would advance the treatment of specific inflammatory diseases. One compound of interest in this respect is propolis, as it has anti-inflammatory activity; however, information is lacking regarding the effects of propolis on metabolic profiles and the relationship of these profiles to the anti-inflammatory properties. In chapter 2, PMA-differentiated THP-1 cells were used to evaluate the propolis effects on pro- and anti-inflammatory cytokines and on cellular metabolite levels.

Crude propolis extracts from samples collected from the UK (P-UK), Ghana (P-G), Cameroon (P-C) and Indonesia (P-Ind) were tested for cytotoxicity, and all showed a significant inhibitory effect on cell viability at high concentrations. When exposed to nontoxic concentrations of propolis, THP-1 macrophages showed reduced cytokine release. Most of the propolis extracts, regardless of propolis source, inhibited the production of TNF-α, IL-1β and IL-6, but had only negligible effects on IL-10 levels.

The propolis extract from Cameroon (P-C) caused the greatest decrease in TNF-α, IL-1β and IL-6 levels, so it was selected for further metabolomic evaluations of the anti-inflammatory action of propolis. Significantly altered metabolite levels were detected in response to treatment with P-C in combination with LPS and to treatment

with LPS alone [317], and the metabolite changes were biologically relevant to immune responses. Interestingly, the combination treatment suppressed LPS action by countering the release of several LPS-related metabolites. For example, the inclusion of P-C decreased the levels of L-citrulline, which is a by-product with nitric oxide (NO) of arginine metabolism. By contrast, the levels of acetyl-CoA were significantly increased by the combined treatment, reflecting an increased metabolite supply to the TCA cycle. In addition, the combined treatment resulted in suppression of NADPH, pyruvate, citrate and succinate levels, coupled with an increase in oxaloacetate levels; these changes could explain the inhibition of the release of IL-1β [143] and could support the use of propolis as an anti-inflammatory agent. Major accumulations of several substrates of the PNP enzyme and purine metabolism were observed in response to P-C, both with and without LPS, suggesting that P-C was acting as an inhibitor of PNP. These finding support several previous reports that propose the use of propolis as a potential anti-inflammatory agent.

The final objective of the present study was to evaluate the anti-inflammatory effects of gypenoside (Gyp) on LPS-stimulated THP-1 monocyte-derived macrophages. After determination of the Gyp IC50, suitable non-toxic concentrations were used in further analyses. A slight, but statistically significant, decrease in the level of TNF-α was observed in response to Gyp at 25, 50 and 75 μg/mL, whereas the decrease in the level of IL-1β was more pronounced. Interestingly, dose-dependent decreases were detected in the levels of IL-6 and IL-10 in response to the combination of Gyp and LPS, suggesting that further metabolomic analysis of these inhibitory effects

would confirm the previous effects observed with inflammatory biomarker metabolites in this thesis.

The Gyp action on the cellular metabolome mirrored the anti-inflammatory activities, as evident by the increase in several metabolites, including acetyl-CoA, tryptophan, NADP+ and D-glucose. Moreover, dose-dependent effects were detected for the levels of several metabolites related to arginine and proline metabolism, tryptophan metabolism and purine metabolism. Gyp was therefore proposed to exert an anti-inflammatory activity through its action on indoleamine 2,3-dioxygenase 1 (IDO1).

In conclusion, these results have filled many gaps identified at the beginning of the study and have improved the general understanding of macrophage reprogramming and the modulation of related biomarker metabolites. The use of LC-MS-based metabolomics in this study allowed the characterisation of natural drug effects and represents a remarkable tool for obtaining a general understanding of the possible mechanisms of action of natural compounds. The biological effects show the possibility of using melittin and eicosenoids as valuable additions to immune therapy and confirm their possible function as vaccine adjuvants. However, these compounds would need to be compared with existing adjuvants to verify whether they have any clear advantages.

The effects of propolis and Gyp on the metabolomic profiles and cytokine levels suggest that these natural products have anti-inflammatory potential. However, despite the not-insignificant amounts of information in some of the evidence generated in this study, there remains a need for further research and work in the

future. Examination of the effects of these natural products on the metabolomes of different cell lines and *in vivo* models should also be performed to obtain a broader assessment of the affected metabolites. Further study of the impact of LPS on specific enzymes and their related metabolites could also provide significant advances in the understanding of how the immune system responds to different stimuli. Future work would benefit from the use of different instruments, including LC-MS/MS or NMR, for more targeted analysis, as this would give further insights into the therapeutic potential of natural compounds.

- **Proposed future work**

The following follow up studies would be of immediate interest:

1. Examine the effect of melittin and LPS on primary macrophages and carry out metabolomics profiling of the treatments.
2. Examine the effect of melittin as an adjuvant for an antigenic component vaccine such as the hepatitis B vaccine.
3. Examine the metabolomics effects of the additional propolis extracts in combination with LPS in order to see if their anti-inflammatory effects work by different mechanisms.
4. Study the methyleicosanoate as a vaccine adjuvant for an antigenic component vaccine.
5. Further investigate extracts of the Cucurbitaceae for their anti-inflammatory. Some preliminary work, not included in the thesis, was carried out on an anti-inflammatory compound isolated from cucumber.

8 References:

1. Parsaeimehr, A., H.M. Iqbal, and R. Parra-Saldívar, *Natural Products as Immune System Modulators, and Against Infections of the Central Nervous System*, in *The Microbiology of Central Nervous System Infections*2018, Elsevier. p. 99-119.
2. Kaas, Q. and D.J. Craik, *Bioinformatics- Aided Venomics.* Toxins, 2015. **7**(6): p. 2159.
3. Isbell, L.A., *Snakes as agents of evolutionary change in primate brains.* Journal of Human Evolution, 2006. **51**(1): p. 1-35.
4. Fry, B.G., et al., *The toxicogenomic multiverse: convergent recruitment of proteins into animal venoms.* Annual review of genomics and human genetics, 2009. **10**: p. 483-511.
5. Vetter, I., et al., *Venomics: a new paradigm for natural products-based drug discovery.* Amino Acids, 2011. **40**(1): p. 15-28.
6. Sforcin, J., *Propolis and the immune system: a review.* Journal of ethnopharmacology, 2007. **113**(1): p. 1-14.
7. Matysiak, J., et al., *Immune and clinical response to honeybee venom in beekeepers.* Annals of Agricultural and Environmental Medicine, 2016. **23**(1): p. 120-124..
8. Chase, T.N. and J.D. OH-LEE, *Composition for treating parkinson's disease*, 2013, Google Patents.
9. Habermann, E., *Bee and Wasp Venoms.* Science, 1972. **177**(4046): p. 314-322.
10. Chen, C., F.J. Gonzalez, and J.R. Idle, *LC-MS-based metabolomics in drug metabolism.* Drug metabolism reviews, 2007. **39**(2-3): p. 581-597.
11. de Abreu, R.M.M., R.L.M. Silva de Moraes, and M.I. Camargo-Mathias, *Biochemical and cytochemical studies of the enzymatic activity of the venom glands of workers of honey bee Apis mellifera L. (Hymenoptera, Apidae).* Micron, 2010. **41**(2): p. 172-175.
12. Stuhlmeier, K.M., *Apis mellifera venom and melittin block neither NF- kappa B- p50-DNA interactions nor the activation of NF- kappa B, instead they activate the transcription of proinflammatory genes and the release of reactive oxygen intermediates.* Journal of immunology (Baltimore, Md. : 1950), 2007. **179**(1): p. 655.
13. Gajski, G. and V. Garaj-Vrhovac, *Melittin: A lytic peptide with anticancer properties.* Environmental Toxicology and Pharmacology, 2013. **36**(2): p. 697-705.
14. Cherniack, E.P., *Bugs as drugs, Part 1: Insects: the" new" alternative medicine for the 21st century.* Altern Med Rev, 2010. **15**(2): p. 124-135.
15. Son, D.J., et al., *Therapeutic application of anti- arthritis, pain- releasing, and anti-cancer effects of bee venom and its constituent compounds.* Pharmacology and Therapeutics, 2007. **115**(2): p. 246-270.
16. Lee, M.S., et al., *Bee venom acupuncture for musculoskeletal pain: A review*, in *J. Pain*2008. p. 289-297.
17. Ghabili, K., M.M. Shoja, and M. Parvizi, *Bee venom therapy: A probable etiology of aneurysm formation in aorta*. *Medical hypotheses,* 2009. 3(73), p. 459-460.
18. Kokot, Z. and J. Matysiak, *Simultaneous Determination of Major Constituents of Honeybee Venom by LC- DAD.* Chroma, 2009. **69**(11): p. 1401-1405.

19. Pacáková, V., et al., *Comparison of high- performance liquid chromatography and capillary electrophoresis for the determination of some bee venom components.* Journal of Chromatography A, 1995. **700**(1): p. 187-193.
20. Haghi, G., A. Hatami, and M. Mehran, *Qualitative and quantitative evaluation of melittin in honeybee venom and drug products containing honeybee venom.* Journal of Apicultural Science, 2013. **57**(2) p. 37-44.
21. Francese, S., et al., *Detection of honeybee venom in envenomed tissues by direct MALDI MSI.* J Am Soc Mass Spectrom, 2009. **20**(1): p. 112-123.
22. Yang, L., et al., *Barrel- stave model or toroidal model? A case study on melittin pores.* Biophysical Journal, 2001. **81**(3): p. 1475-1485.
23. Zhou, J., et al., *Quantification of melittin and apamin in bee venom lyophilized powder from Apis mellifera by liquid chromatography–diode array detector–tandem mass spectrometry.* Analytical biochemistry, 2010. **404**(2): p. 171-178.
24. Dotimas, E., et al., *Isolation and structure analysis of bee venom mast cell degranulating peptide.* Biochimica et Biophysica Acta (BBA)-Protein Structure and Molecular Enzymology, 1987. **911**(3): p. 285-293.
25. Meng, Y., et al., *A novel peptide from Apis mellifera and solid-phase synthesis of its analogue.* Chinese Chemical Letters, 2012. **23**(10): p. 1161-1164.
26. Chen, J. and W.R. Lariviere, *The nociceptive and anti-nociceptive effects of bee venom injection and therapy: a double-edged sword.* Progress in neurobiology, 2010. **92**(2): p. 151-183.
27. Balsinde, J., et al., *Regulation and inhibition of phospholipase A 2.* Annu. Rev. Pharmacol. Toxicol., 1999. **39**(1): p. 175-189.
28. Marković-Housley, Z., et al., *Crystal Structure of Hyaluronidase, a Major Allergen of Bee Venom.* Structure, 2000. **8**(10): p. 1025-1035.
29. Terwilliger, T.C. and D. Eisenberg, *The structure of melittin. I. Structure determination and partial refinement.* Journal of Biological Chemistry, 1982. **257**(11): p. 6010-6015.
30. Popplewell, J., et al., *Quantifying the effects of melittin on liposomes.* Biochimica Et Biophysica Acta-Biomembranes, 2007. **1768**(1): p. 13-20.
31. Yan, H., et al., *Individual substitution analogs of Mel(12– 26), melittin's C-terminal 15- residue peptide: their antimicrobial and hemolytic actions.* FEBS Letters, 2003. **554**(1-2): p. 100-104.
32. Irudayam, S.J. and M.L. Berkowitz, *Influence of the arrangement and secondary structure of melittin peptides on the formation and stability of toroidal pores.* Biochimica Et Biophysica Acta- Biomembranes, 2011. **1808**(9): p. 2258-2266.
33. Raghuraman, H. and A. Chattopadhyay, *Melittin: a membrane- active peptide with diverse functions.* Biosci Rep, 2007. **27**(4): p. 189-223.
34. Terwilliger, T.C. and D. Eisenberg, *The structure of melittin. II. Interpretation of the structure.* The Journal of Biological Chemistry, 1982. **257**(11): p. 6016.
35. Miura, Y., *NMR studies on the monomer–tetramer transition of melittin in an aqueous solution at high and low temperatures.* Eur Biophys J, 2012. **41**(7): p. 629-636.
36. Dempsey, C.E., *Quantitation of the effects of an internal proline residue on individual hydrogen bond stabilities in an α- helix: pH- Dependent amide exchange in melittin and [Ala- 14] melittin.* Biochemistry, 1992. **31**(19): p. 4705-4712.

37. Raghuraman, H. and A. Chattopadhyay, *Interaction of melittin with membrane cholesterol: A fluorescence approach.* Biophysical Journal, 2004. **87**(4): p. 2419-2432.
38. Lee, M.-T., et al., *Mechanism and kinetics of pore formation in membranes by water- soluble amphipathic peptides.* Proceedings of the National Academy of Sciences of the United States, 2008. **105**(13): p. 5087.
39. van Den Bogaart, G., et al., *On the mechanism of pore formation by melittin.* The Journal of Biological Chemistry, 2008. **283**(49): p. 33854.
40. Wang, J., K.-W. Liu, and S.L. Biswal, *Characterizing α- helical peptide aggregation on supported lipid membranes using microcantilevers.* Analytical chemistry, 2014. **86**(20): p. 10084.
41. Steinem, C., H.-j. Galla, and A. Janshoff, *Interaction of melittin with solid supported membranes.* Physical Chemistry Chemical Physics, 2000. **2**(20): p. 4580-4585.
42. Kemeny, D.M., et al., *The purification and characterisation of hyaluronidase from the venom of the honey bee, Apis mellifera.* European Journal of Biochemistry, 1984. **139**(2): p. 217-223.
43. Spoerri, E., J. Jentsch, and P. Glees, *Apamin from bee venom. Effects of the neurotoxin on subcellular particles of neural cultures.* FEBS Letters, 1975. **53**(2): p. 143-147.
44. Moreno, M. and E. Giralt, *Three valuable peptides from bee and wasp venoms for therapeutic and biotechnological use: melittin, apamin and mastoparan.* Toxins, 2015. **7**(4): p. 1126.
45. Habermann, E. and K. Fischer, *Bee Venom Neurotoxin (Apamin): Iodine Labeling and Characterization of Binding Sites.* European Journal of Biochemistry, 1979. **94**(2): p. 355-364.
46. Mourre, C., C. Fournier, and B. Soumireu-Mourat, *Apamin, a blocker of the calcium-activated potassium channel, induces neurodegeneration of Purkinje cells exclusively.* Brain Research, 1997. **778**(2): p. 405-408.
47. Ziai, M.R., et al., *Mast cell degranulating peptide: a multi- functional neurotoxin*, 1990: Oxford, UK. p. 457-461.
48. Shkenderov, S. and K. Koburova, *Adolapin - A newly isolated analgetic and anti-inflammatory polypeptide from bee venom.* Toxicon, 1982. **20**(1): p. 317-321.
49. Kitamura, H., Y. Kurachi, and M. Yamada, *Tertiapin potently and selectively blocks muscarinic K+ channels in rabbit cardiac myocytes.* Biophysical Journal, 2000. **78**(1): p. 173A-173A.
50. Greenaway, W., T. Scaysbrook, and F. Whatley, *The composition and plant origins of propolis: a report of work at Oxford.* Bee world, 1990. **71**(3): p. 107-118.
51. Sung, S.-H., et al., *External use of propolis for oral, skin, and genital diseases: a systematic review and meta-analysis.* Evidence-Based Complementary and Alternative Medicine, 2017. **2017**.
52. Toreti, V.C., et al., *Recent progress of propolis for its biological and chemical compositions and its botanical origin.* Evidence-Based Complementary and Alternative Medicine, 2013. **2013**.
53. Kuropatnicki, A.K., E. Szliszka, and W. Krol, *Historical aspects of propolis research in modern times.* Evidence-Based Complementary and Alternative Medicine, 2013. **2013**.

54. Chan, G.C.-F., K.-W. Cheung, and D.M.-Y. Sze, *The immunomodulatory and anticancer properties of propolis.* Clinical reviews in allergy & immunology, 2013. **44**(3): p. 262-273.
55. Martinotti, S. and E. Ranzato, *Propolis: a new frontier for wound healing?* Burns & Trauma, 2015. **3**(1): p. 9.
56. Sforcin, J.M., V. Bankova, and A.K. Kuropatnicki, *Medical benefits of honeybee products.* Evidence-Based Complementary and Alternative Medicine, 2017. **2017**.
57. Sforcin, J.M., *Biological properties and therapeutic applications of propolis.* Phytotherapy research, 2016. **30**(6): p. 894-905.
58. Thomson, W.M., *Propolis.* Medical Journal of Australia, 1990. **153**(11/12).
59. Kumazawa, S., T. Hamasaka, and T. Nakayama, *Antioxidant activity of propolis of various geographic origins.* Food chemistry, 2004. **84**(3): p. 329-339.
60. Silici, S. and S. Kutluca, *Chemical composition and antibacterial activity of propolis collected by three different races of honeybees in the same region.* Journal of ethnopharmacology, 2005. **99**(1): p. 69-73.
61. Xu, Y., et al., *Recent development of chemical components in propolis.* Frontiers of Biology in China, 2009. **4**(4): p. 385.
62. Razmovski-Naumovski, V., et al., *Chemistry and pharmacology of Gynostemma pentaphyllum.* Phytochemistry Reviews, 2005. **4**(2-3): p. 197-219.
63. Shen, N., et al., *Effect of five leaf gynostemma herb saponin on lipid metabolism in hyperlipidemia rats.* Zhongguo Zhongxiyi Jiehe Zazhi, 2011. **9**: p. 1081-1083.
64. Chen, J.-C., et al., *Gypenosides induced apoptosis in human colon cancer cells through the mitochondria-dependent pathways and activation of caspase-3.* Anticancer research, 2006. **26**(6B): p. 4313-4326.
65. Sun, H. and Q. Zheng, *Haemolytic activities and adjuvant effect of Gynostemma pentaphyllum saponins on the immune responses to ovalbumin in mice.* Phytotherapy Research: An international journal devoted to pharmacological and toxicological evaluation of natural product derivatives, 2005. **19**(10): p. 895-900.
66. Murry, R.K., et al., *Harper's illustrated biochemistry*, 2003, Mc Graw Hill: New York.
67. Pelicano, H., et al., *Glycolysis inhibition for anticancer treatment*, *Oncogene,* 2006. 25(34): p. 4633-4646.
68. Zheng, J., *Energy metabolism of cancer: Glycolysis versus oxidative phosphorylation.* Oncology letters, 2012. **4**(6): p. 1151-1157.
69. Korla, K. and C.K. Mitra, *Modelling the Krebs cycle and oxidative phosphorylation.* Journal of Biomolecular Structure and Dynamics, 2014. **32**(2): p. 242-256.
70. Akram, M., *Citric acid cycle and role of its intermediates in metabolism.* Cell Biochem Biophys, 2014. **68**(3): p. 475-478.
71. Apte, S. and R. Sarangarajan, *Cellular respiration and carcinogenesis*2008: Springer Science & Business Media.
72. O'Neill, L.A., R.J. Kishton, and J. Rathmell, *A guide to immunometabolism for immunologists.* Nature Reviews Immunology, 2016. **16**(9): p. 553.
73. Rodríguez-Prados, J.-C., et al., *Substrate fate in activated macrophages: a comparison between innate, classic, and alternative activation.* The Journal of Immunology, 2010. **185**(1): p. 605-614.
74. Krawczyk, C.M., et al., *Toll-like receptor–induced changes in glycolytic metabolism regulate dendritic cell activation.* Blood, 2010. **115**(23): p. 4742-4749.

75. Michalek, R.D., et al., *Cutting edge: distinct glycolytic and lipid oxidative metabolic programs are essential for effector and regulatory CD4+ T cell subsets.* The Journal of Immunology, 2011. **186**(6): p. 3299-3303.
76. Doughty, C.A., et al., *Antigen receptor–mediated changes in glucose metabolism in B lymphocytes: role of phosphatidylinositol 3-kinase signaling in the glycolytic control of growth.* Blood, 2006. **107**(11): p. 4458-4465.
77. Donnelly, R.P., et al., *mTORC1-dependent metabolic reprogramming is a prerequisite for NK cell effector function.* The Journal of Immunology, 2014. **193**(9): p. 4477-4484.
78. Everts, B., et al., *TLR-driven early glycolytic reprogramming via the kinases TBK1-IKKε supports the anabolic demands of dendritic cell activation.* Nature immunology, 2014. **15**(4): p. 323.
79. Haschemi, A., et al., *The sedoheptulose kinase CARKL directs macrophage polarization through control of glucose metabolism.* Cell metabolism, 2012. **15**(6): p. 813-826.
80. Kasmi, K.C.E. and K.R. Stenmark. *Contribution of metabolic reprogramming to macrophage plasticity and function*. in *Seminars in immunology*. 2015. Elsevier.
81. Infantino, V., et al., *The mitochondrial citrate carrier: a new player in inflammation.* Biochemical Journal, 2011. **438**(3): p. 433-436.
82. Tannahill, G., et al., *Succinate is an inflammatory signal that induces IL-1β through HIF-1α.* Nature, 2013. **496**(7444): p. 238.
83. Infantino, V., et al., *ATP-citrate lyase is essential for macrophage inflammatory response.* Biochemical and biophysical research communications, 2013. **440**(1): p. 105-111.
84. Huang, S.C.-C., et al., *Metabolic reprogramming mediated by the mTORC2-IRF4 signaling axis is essential for macrophage alternative activation.* Immunity, 2016. **45**(4): p. 817-830.
85. Moon, J.-S., et al., *NOX4-dependent fatty acid oxidation promotes NLRP3 inflammasome activation in macrophages.* Nature medicine, 2016. **22**(9): p. 1002.
86. Guy, B., *The perfect mix: recent progress in adjuvant research.* Nature Reviews Microbiology, 2007. **5**(7): p. 505.
87. Awate, S., L.A.B. Babiuk, and G. Mutwiri, *Mechanisms of action of adjuvants.* Frontiers in immunology, 2013. **4**: p. 114.
88. Beutler, B. and E.T. Rietschel, *Innate immune sensing and its roots: the story of endotoxin.* Nature reviews immunology, 2003. **3**(2): p. 169.
89. Raetz, C.R. and C. Whitfield, *Lipopolysaccharide endotoxins.* Annual review of biochemistry, 2002. **71**(1): p. 635-700.
90. Miller, S.I., R.K. Ernst, and M.W. Bader, *LPS, TLR4 and infectious disease diversity.* Nature Reviews Microbiology, 2005. **3**(1): p. 36.
91. Warshakoon, H.J., et al., *Potential adjuvantic properties of innate immune stimuli.* Human vaccines, 2009. **5**(6): p. 381-394.
92. McNair, H.M. and J.M. Miller, *Basic gas chromatography*2011: John Wiley & Sons.
93. Snyder, L.R., J.J. Kirkland, and J.W. Dolan, *Introduction to Modern Liquid Chromatography*2009: Wiley.
94. David, G.W., E.-E. With ContributiRuangelie, and P. Bha, *Pharmaceutical Analysis E-Book: A Textbook for Pharmacy Students and Pharmaceutical Chemists*. Fourth edition. ed2015: United Kingdom: Elsevier.

95. Mader, W.J., *Principles of adsorption chromatography: The separation of nonionic organic compounds . By Lloyd R. Snyder. Marcel Dekker, Inc., 95 Madison Avenue, New York, Journal of Pharmaceutical Sciences, 1*968. 57(10): p. 1824-1824.
96. Marchand, D.H., L.R. Snyder, and J.W. Dolan, *Characterization and applications of reversed- phase column selectivity based on the hydrophobic- subtraction model.* Journal of Chromatography A, 2008. **1191**(1): p. 2-20.
97. Carr, P., et al., *Contributions to reversed- phase column selectivity. I. Steric interaction.* Journal Of Chromatography A, 2011. **1218**(13): p. 1724-1742.
98. Gama, M.R., et al., *Hydrophilic interaction chromatography.* Trends in Analytical Chemistry, 2012. **37**: p. 48-60.
99. McCalley, D.V. and U.D. Neue, *Estimation of the extent of the water-rich layer associated with the silica surface in hydrophilic interaction chromatography.* Journal of Chromatography A, 2008. **1192**(2): p. 225-229.
100. Harris, D.C., *Quantitative chemical analysis* 2010: New York, W. H., Macmillan.
101. Sepsey, A., I. Bacskay, and A. Felinger, *Molecular theory of size exclusion chromatography for wide pore size distributions.* Journal of Chromatography A, 2014. **1331**: p. 52-60.
102. Striegel, A.M., *Modern Size-Exclusion Liquid Chromatography Practice of Gel Permeation and Gel Filtration Chromatography*. 2nd ed. ed2009: United States: John Wiley & Sons Inc.
103. Nawrocki, J., *Silica surface controversies, strong adsorption sites, their blockage and removal. Part I.* Chromatographia, 1991. **31**(3-4): p. 177-192.
104. Jandera, P. and J. Churacek, *Gradient elution in column liquid chromatography: theory and practice*. Vol. 31. 1985: Elsevier.
105. Moldoveanu, S. and V. David, *Selection of the HPLC Method in Chemical Analysis*2016: Elsevier.
106. Horváth, C., *High-performance liquid chromatography: advances and perspectives*2013: Elsevier.
107. Swartz, M.E., *UPLC™: an introduction and review.* Journal of Liquid Chromatography & Related Technologies, 2005. **28**(7-8): p. 1253-1263.
108. Nováková, L., L. Matysová, and P. Solich, *Advantages of application of UPLC in pharmaceutical analysis.* Talanta, 2006. **68**(3): p. 908-918.
109. Hostettmann, K. and C. Terreaux, *Medium-pressure liquid chromatography*, 2000.
110. Pavia, D.L., et al., *Introduction to spectroscopy*2008: Cengage Learning.
111. Arndt, J.H., T. Macko, and R. Brüll, *Application of the evaporative light scattering detector to analytical problems in polymer science.* Journal of Chromatography A, 2013. **1310**: p. 1-14.
112. Watson, J.T. and O.D. Sparkman, *Introduction to mass spectrometry: instrumentation, applications, and strategies for data interpretation*2007: John Wiley & Sons.
113. Cech, N.B. and C.G. Enke, *Practical implications of some recent studies in electrospray ionization fundamentals*, 2001: New York. p. 362-387.
114. El-Aneed, A., A. Cohen, and J. Banoub, *Mass Spectrometry, Review of the Basics: Electrospray, MALDI, and Commonly Used Mass Analyzers.* Applied Spectroscopy Reviews, 2009. **44**(3): p. 210-230.
115. Awad, H., M.M. Khamis, and A. El-Aneed, *Mass Spectrometry, Review of the Basics: Ionization.* Applied Spectroscopy Reviews, 2014. **50**(2): p. 00-00.

116. Binkley, J. and M. Libarondi, *Comparing the capabilities of time-of-flight and quadrupole mass spectrometers.* Current Trends in Mass Spectrometry, 2010: p. 1-5.
117. Chernushevich, I.V., A.V. Loboda, and B.A. Thomson, *An introduction to quadrupole–time-of- flight mass spectrometry.* Journal of Mass Spectrometry, 2001. **36**(8): p. 849-865.
118. Snyder, D.T., W.-P. Peng, and R.G. Cooks, *Resonance methods in quadrupole ion traps.* Chemical Physics Letters, 2017. **668**: p. 69-89.
119. Scigelova, M. and A. Makarov, *Orbitrap mass analyzer – overview and applications in proteomics.* PROTEOMICS, 2006. **6**(S2): p. 16-21.
120. Hu, Q., et al., *The Orbitrap: a new mass spectrometer.* Journal of Mass Spectrometry, 2005. **40**(4): p. 430-443.
121. Johnson, C., et al., *Xenobiotic Metabolomics: Major Impact on the Metabolome*, in *Annu. Rev. Pharmacol. Toxicol.*2012. p. 37-56.
122. Guengerich, F., *Common and uncommon cytochrome P450 reactions related to metabolism and chemical toxicity*, in *Chem. Res. Toxicol.*2001. p. 611-650.
123. Li, F., F.J. Gonzalez, and X. Ma, *LC–MS- based metabolomics in profiling of drug metabolism and bioactivation.* Acta Pharmaceutica Sinica B, 2012. **2**(2): p. 116-123.
124. Patti, G.J., O. Yanes, and G. Siuzdak, *Metabolomics: the apogee of the omic triology.* Nature reviews. Molecular cell biology, 2012. **13**(4): p. 263.
125. Ellis, D.I., et al., *Metabolic fingerprinting as a diagnostic tool.* Pharmacogenomics, 2007. **8**(9): p. 1243-1266.
126. Dettmer, K., P.A. Aronov, and B.D. Hammock, *Mass spectrometry- based metabolomics*, in *Mass Spectrom. Rev.*2007. p. 51-78.
127. Hendriks, M.M.W.B., et al., *Data- processing strategies for metabolomics studies.* Trends in Analytical Chemistry, 2011. **30**(10): p. 1685-1698.
128. Sussulini, A., *Metabolomics: From Fundamentals to Clinical Applications*2017, Cham: Cham: Springer International Publishing.
129. Lazar, A.G., et al., *Bioinformatics Tools for Metabolomic Data Processing and Analysis Using Untargeted Liquid Chromatography Coupled With Mass Spectrometry. Bulletin of University of Agricultural Sciences and Veterinary Medicine Cluj-Napoca. Animal Science and Biotechnologies*, 2015. **72**(2): p. 115.
130. Alonso, A., S. Marsal, and A. Julià, *Analytical Methods in Untargeted Metabolomics: State of the Art in 2015.* Frontiers in Bioengineering and Biotechnology, 2015. **3**.
131. Yi, L., et al., *Chemometric methods in data processing of mass spectrometry- based metabolomics: A review.* Analytica chimica acta, 2016. **914**: p. 17.
132. Eriksson, L., J. Trygg, and S. Wold, *CV-ANOVA for significance testing of PLS and OPLS® models.* Journal of Chemometrics: A Journal of the Chemometrics Society, 2008. **22**(11-12): p. 594-600.
133. Liland, K.H., *Multivariate methods in metabolomics–from pre-processing to dimension reduction and statistical analysis.* TrAC Trends in Analytical Chemistry, 2011. **30**(6): p. 827-841.
134. Eriksson, L., et al., *Multi-and megavariate data analysis basic principles and applications*. Vol. 1. 2013: Umetrics Academy.
135. Tusiimire, J., et al., *An LCMS method for the assay of melittin in cosmetic formulations containing bee venom.* Anal Bioanal Chem, 2015. **407**(13): p. 3627-3635.

136. Tusiimire, J., et al., *Effect of Bee Venom and Its Fractions on the Release of Pro-Inflammatory Cytokines in PMA-Differentiated U937 Cells Co-Stimulated with LPS.* Vaccines, 2016. **4**(2).
137. Zhang, R., et al., *Evaluation of mobile phase characteristics on three zwitterionic columns in hydrophilic interaction liquid chromatography mode for liquid chromatography-high resolution mass spectrometry based untargeted metabolite profiling of Leishmania parasites.* Journal of Chromatography A, 2014. **1362**: p. 168-179.
138. van den Berg, R.A., et al., *Centering, scaling, and transformations: improving the biological information content of metabolomics data.* BMC genomics, 2006. **7**(1): p. 142.
139. Kirwan, G.M., et al., *Building multivariate systems biology models.* Analytical chemistry, 2012. **84**(16): p. 7064-7071.
140. Neill, L.A.J., *A critical role for citrate metabolism in LPS signalling.* Biochemical Journal, 2011. **438**(3): p. e5.
141. Nathan, C., *Points of control in inflammation*, C. Nathan, Editor 2002. p. 846-852.
142. Janeway Jr, C.A. and R. Medzhitov, *Innate immune recognition.* Annual Review of Immunology, 2002. **20**(1): p. 197-216.
143. Kelly, B. and L.A.J. Neill, *Metabolic reprogramming in macrophages and dendritic cells in innate immunity.* Cell Research, 2015. **25**(7).
144. Iwasaki, A. and R. Medzhitov, *Control of adaptive immunity by the innate immune system.(Report).* Nature Immunology, 2015. **16**(4): p. 343.
145. Pesce, J., et al., *Arginase-1αExpressing Macrophages Suppress Th2 CytokineaDriven Inflammation and Fibrosis.* PLoS Pathogens, 2009. **5**(4): p. e1000371-e1000371.
146. Weinberg, Samuel e., Laura a. Sena, and Navdeep s. Chandel, *Mitochondria in the Regulation of Innate and Adaptive Immunity.* Immunity, 2015. **42**(3): p. 406-417.
147. Guthrie, L.A., et al., *Priming of neutrophils for enhanced release of oxygen metabolites by bacterial lipopolysaccharide: Evidence for increased activity of the superoxide- producing enzyme.* Journal of Experimental Medicine, 1984. **160**(6): p. 1656-1671.
148. Newsholme, P., et al., *Metabolism of glucose, glutamine, long- chain fatty acids and ketone bodies by murine macrophages.* Biochemical Journal, 1986. **239**(1): p. 121-125.
149. Palsson-Mcdermott, Eva m., et al., *Pyruvate Kinase M2 Regulates Hif-1α Activity and IL-1β Induction and Is a Critical Determinant of the Warburg Effect in LPS-Activated Macrophages*, in *Cell Metabolism*2015. p. 347-347.
150. Haschemi, A., et al., *The Sedoheptulose Kinase CARKL Directs Macrophage Polarization through Control of Glucose Metabolism.* Cell Metabolism, 2012. **15**(6): p. 813-826.
151. Tannahill, G.M., et al., *Succinate is an inflammatory signal that induces IL-1[beta] through HIF-1[alpha].(Report).* Nature, 2013. **496**(7444): p. 238.
152. El Kasmi, K.C. and K.R. Stenmark, *Contribution of metabolic reprogramming to macrophage plasticity and function.* Seminars in Immunology, 2015. **27**(4): p. 267-275.
153. Meera, E., et al., *Metabolism via arginase or nitric oxide synthase: two competing arginine pathways in macrophages.* Frontiers in Immunology, 2014. **5**.

154. Clementi, E., et al., *Persistent inhibition of cell respiration by nitric oxide: Crucial role of S- nitrosylation of mitochondrial complex I and protective action of glutathione.* Proceedings of the National Academy of Sciences of the United States of America, 1998. **95**(13): p. 7631-7636.
155. Kihira, Y., et al., *Basic fibroblast growth factor regulates glucose metabolism through glucose transporter 1 induced by hypoxia- inducible factor-1α in adipocytes.* International Journal of Biochemistry and Cell Biology, 2011. **43**(11): p. 1602-1611.
156. Semenza, G., et al., *Hypoxia response elements in the aldolase A, enolase 1, and lactate dehydrogenase A gene promoters contain essential binding sites for hypoxia-inducible factor 1.* Journal of Biological Chemistry, 1996. **271**(51): p. 32529-32537.
157. Huo, Y., et al., *Stable isotope- labelling analysis of the impact of inhibition of the mammalian target of rapamycin on protein synthesis.* Biochemical Journal, 2012. **444**(1): p. 141-151.
158. Rodríguez-Prados, J.C., et al., *Substrate fate in activated macrophages: A comparison between innate, classic, and alternative activation.* Journal of Immunology, 2010. **185**(1): p. 605-614.
159. Sag, D., et al., *Adenosine 5'- monophosphate- activated protein kinase promotes macrophage polarization to an anti- inflammatory functional phenotype.* Journal of Immunology, 2008. **181**(12): p. 8633-8641.
160. Alonezi, S., et al., *Metabolomic Profiling of the Effects of Melittin on Cisplatin Resistant and Cisplatin Sensitive Ovarian Cancer Cells Using Mass Spectrometry and Biolog Microarray Technology.* Metabolites, 2016. **6**(4): p. 35.
161. Rady, I., et al., *Melittin, a major peptide component of bee venom, and its conjugates in cancer therapy.* Cancer Letters, 2017. **402**: p. 16-31.
162. Skalickova, S., et al., *Perspective of Use of Antiviral Peptides against Influenza Virus*, 2015, MDPI AG: Basel. p. 5428-5442.
163. Adade, C.M., et al., *Melittin peptide kills Trypanosoma cruzi parasites by inducing different cell death pathways.* Toxicon, 2013. **69**: p. 227-239.
164. Shi, W., et al., *Antimicrobial peptide melittin against Xanthomonas oryzae pv. oryzae, the bacterial leaf blight pathogen in rice.* Applied Microbiology and Biotechnology, 2016. **100**(11): p. 5059.
165. Park, H.J., et al., *Antiarthritic effect of bee venom: Inhibition of inflammation mediator generation by suppression of NF-κB through interaction with the p50 subunit.* Arthritis & Rheumatism, 2004. **50**(11): p. 3504-3515.
166. Lee, W.-R., et al., *Protective effect of melittin against inflammation and apoptosis on Propionibacterium acnes-induced human THP-1 monocytic cell.* European Journal of Pharmacology, 2014. **740**: p. 218-226.
167. Phelps, C.B., et al., *Mechanism of κB DNA binding by Rel/ NF-κb dimers.* Journal of Biological Chemistry, 2000. **275**(32): p. 24392-24399.
168. Baeuerle, P.A., *Pro- inflammatory signaling: Last pieces in the NF-κB puzzle?* Current Biology, 1998. **8**(1): p. R19-R22.
169. Srivastava, R.M., et al., *Consequences of alteration in leucine zipper sequence of melittin in its neutralization of lipopolysaccharide-induced proinflammatory response in macrophage cells and interaction with lipopolysaccharide.* Journal of Biological Chemistry, 2012. **287**(3): p. 1980-1995.

170. Liu, P., et al., *Evaluation of cytotoxicity and absorption enhancing effects of melittin – a novel absorption enhancer.* European Journal of Pharmaceutics and Biopharmaceutics, 1999. **48**(1): p. 85-87.
171. Alpar, H.O., et al., *Intranasal vaccination against plague, tetanus and diphtheria.* Advanced Drug Delivery Reviews, 2001. **51**(1): p. 173-201.
172. Bramwell, V., et al., *Adjuvant action of melittin following intranasal immunisation with tetanus and diphtheria toxoids.* Journal of drug targeting, 2003. **11**(8-10): p. 525-530.
173. Beger, R.D., et al., *Metabolomics enables precision medicine: "A White Paper, Community Perspective".(Report).* Metabolomics, 2016. **12**(9): p. 1.
174. Alonezi, S., et al., *Metabolomic profiling of the synergistic effects of melittin in combination with cisplatin on ovarian cancer cells.* 2017.
175. Howe, C.C.F., et al., *Untargeted metabolomics profiling of an 80.5 km simulated treadmill ultramarathon.* 2018.
176. Sugimoto, M., et al., *Non- targeted metabolite profiling in activated macrophage secretion.* Metabolomics, 2012. **8**(4): p. 624-633.
177. Liu, K., et al., *Metabolomics Analysis to Evaluate the Anti- Inflammatory Effects of Polyphenols: Glabridin Reversed Metabolism Change Caused by LPS in RAW 264.7 Cells.* Journal of Agricultural and Food Chemistry, 2017. **65**(29): p. 6070-6079.
178. Traves, P., et al., *Relevance of the MEK/ ERK Signaling Pathway in the Metabolism of Activated Macrophages: A Metabolomic Approach.* Journal of Immunology, 2012. **188**(3): p. 1402-1410.
179. Berg, H.A. and E.P. Scherer, *Adipose Tissue, Inflammation, and Cardiovascular Disease.* Circulation Research, 2005. **96**(9): p. 939-949.
180. Fitzpatrick, M. and S.P. Young, *Metabolomics–a novel window into inflammatory disease.* Swiss medical weekly, 2013. **143**: p. w13743.
181. McClenathan, B.M., et al., *Metabolites as biomarkers of adverse reactions following vaccination: A pilot study using nuclear magnetic resonance metabolomics.* Vaccine, 2017. **35**(9): p. 1238-1245.
182. Engler, R.J.M., et al., *A Prospective Study of the Incidence of Myocarditis/ Pericarditis and New Onset Cardiac Symptoms following Smallpox and Influenza Vaccination.(Clinical report).* 2015. **10**(3).
183. Gray, D.W., et al., *Identification of systemic immune response markers through metabolomic profiling of plasma from calves given an intra- nasally delivered respiratory vaccine.* Veterinary Research, 2015. **46**(1): p. <xocs:firstpage xmlns:xocs=""/>.
184. Daigneault, M., et al., *The Identification of Markers of Macrophage Differentiation in PMA- Stimulated THP- 1 Cells and Monocyte-Derived Macrophages.* PLoS One, 2010. **5**(1): p. e8668.
185. Lee, C., et al., *Melittin suppresses tumor progression by regulating tumor-associated macrophages in a Lewis lung carcinoma mouse model.* Oncotarget, 2017. **8**(33): p. 54951.
186. Alberta Di, P., et al., *Vaccine Adjuvants: from 1920 to 2015 and Beyond.* Vaccines, 2015. **3**(2): p. 320-343.
187. Reed, S.G., et al., *IL- 1 as adjuvant. Role of T cells in augmentation of specific antibody production by recombinant human IL-1α.* Journal of Immunology, 1989. **142**(9): p. 3129-3133.

188. Pape, K., et al., *Inflammatory cytokines enhance the in vivo clonal expansion and differentiation of antigen-activated CD4 super(+) T cells.* Journal of Immunology, 1997. **159**(2): p. 591-598.
189. Li, H., S. Nookala, and F. Re, *Aluminum Hydroxide Adjuvants Activate Caspase- 1 and Induce IL- 1 beta and IL- 18 Release.* Journal of Immunology, 2007. **178**(8): p. 5271-5276.
190. Bomalaski, J., et al., *Phospholipase A sub(2)- activating protein induces the synthesis of IL- 1 and TNF in human monocytes.* Journal of Immunology, 1995. **154**(8): p. 4027-4031.
191. Bomalaski, J.S., et al., *A phospholipase A 2 - activating protein (PLAP) stimulates human neutrophil aggregation and release of lysosomal enzymes, superoxide, and eicosanoids.* Journal of Immunology, 1989. **142**(11): p. 3957-3962.
192. Jha, Abhishek k., et al., *Network Integration of Parallel Metabolic and Transcriptional Data Reveals Metabolic Modules that Regulate Macrophage Polarization.* Immunity, 2015. **42**(3): p. 419-430.
193. Qualls, Joseph e., et al., *Sustained Generation of Nitric Oxide and Control of Mycobacterial Infection Requires Argininosuccinate Synthase 1.* Cell Host & Microbe, 2012. **12**(3): p. 313-323.
194. Brown, G.C., *Nitric oxide and mitochondrial respiration.* BBA - Bioenergetics, 1999. **1411**(2): p. 351-369.
195. Mateo, R.B., et al., *Impact of nitric oxide on macrophage glucose metabolism and glyceraldehyde- 3- phosphate dehydrogenase activity.* American Journal of Physiology - Cell Physiology, 1995. **268**(3): p. C669-C675.
196. Albina, J. and B. Mastrofrancesco, *Modulation of glucose metabolism in macrophages by products of nitric oxide synthase.* American Journal of Physiology, 1993. **33**(6): p. C1594.
197. Everts, B., et al., *Commitment to glycolysis sustains survival of nitric oxide-producing inflammatory dendritic cells.* Blood, 2012: p. blood-2012-03-419747.
198. Wang, C., et al., *Melittin, a major component of bee venom, sensitizes human hepatocellular carcinoma cells to tumor necrosis factor-related apoptosis-inducing ligand (TRAIL)-induced apoptosis by activating CaMKII-TAK1-JNK/p38 and inhibiting IkappaBalpha kinase-NFkappaB.* The Journal of biological chemistry, 2009. **284**(6): p. 3804.
199. Freemerman, A.J., et al., *Metabolic reprogramming of macrophages: Glucose transporter 1 (GLUT1)-mediated glucose metabolism drives a proinflammatory phenotype.* Journal of Biological Chemistry, 2014. **289**(11): p. 7884-7896.
200. Blagih, J. and Russell g. Jones, *Polarizing Macrophages through Reprogramming of Glucose Metabolism.* Cell Metabolism, 2012. **15**(6): p. 793-795.
201. Barnes, V.M., et al., *Acceleration of Purine Degradation by Periodontal Diseases.* Journal of Dental Research, 2009. **88**(9): p. 851-855.
202. Gudbjornsson, B., et al., *Hypoxanthine, xanthine, and urate in synovial fluid from patients with inflammatory arthritides.* Annals of the Rheumatic Diseases, 1991. **50**(10): p. 669-672.
203. Madsen, R.K., et al., *Diagnostic properties of metabolic perturbations in rheumatoid arthritis.* Arthritis Research and Therapy, 2011. **13**(1): p.R19.
204. Infantino, V., et al., *The mitochondrial citrate carrier: A new player in inflammation.* Biochemical Journal, 2011. **438**(3): p. 433-436.

205. Wellen, K.E., et al., *ATP- citrate lyase links cellular metabolism to histone acetylation.* Science, 2009. **324**(5930): p. 1076.
206. Do, N., et al., *Cationic membrane-active peptides–anticancer and antifungal activity as well as penetration into human skin.* Experimental dermatology, 2014. **23**(5): p. 326-331.
207. Lee, S.Y., et al., *Melittin Exerts Multiple Effects on the Release of Free Fatty Acids from L1210 Cells: Lack of Selective Activation of Phospholipase A2by Melittin.* Archives of Biochemistry and Biophysics, 2001. **389**(1): p. 57-67.
208. Palomba, L., et al., *Downregulation of nitric oxide formation by cytosolic phospholipase A 2- released arachidonic acid.* Free Radical Biology and Medicine, 2004. **36**(3): p. 319-329.
209. Geddis, M.S., et al., *PLA 2 and secondary metabolites of arachidonic acid control filopodial behavior in neuronal growth cones.* Cell Motility and the Cytoskeleton, 2004. **57**(1): p. 53-67.
210. Norris, P.C., et al., *Specificity of eicosanoid production depends on the TLR-4-stimulated macrophage phenotype.* Journal of leukocyte biology, 2011. **90**(3): p. 563-574.
211. Hanna, V.S. and E.A.A. Hafez, *Synopsis of arachidonic acid metabolism: A review.* Journal of Advanced Research, 2018. **11**: p. 23-32.
212. Fiala, M., et al., *Cyclooxygenase- 2- positive macrophages infiltrate the Alzheimer's disease brain and damage the blood– brain barrier.* European Journal of Clinical Investigation, 2002. **32**(5): p. 360-371.
213. Ohishi, S., *Evaluation of time course and inter-relationship of inflammatory mediators in experimental inflammatory reaction.* Yakugaku zasshi: Journal of the Pharmaceutical Society of Japan, 2000. **120**(5): p. 455-462.
214. Marcio, A.R.A., et al., *Mechanisms of action underlying the anti-inflammatory and immunomodulatory effects of propolis: a brief review.* Revista Brasileira de Farmacognosia, 2011. **22**(1): p. 208-219.
215. Ramos, A. and J. Miranda, *Propolis: a review of its anti- inflammatory and healing actions.* Journal of Venomous Animals and Toxins including Tropical Diseases, 2007. **13**(4): p. 697-710.
216. Majno, G., *Chronic Inflammation.* The American Journal of Pathology, 1998. **153**(4): p. 1035-1039.
217. Verhoeckx, K.C., et al., *Characterization of anti-inflammatory compounds using transcriptomics, proteomics, and metabolomics in combination with multivariate data analysis.* International Immunopharmacology, 2004. **4**(12): p. 1499-1514.
218. Silva, B.B., et al., *Chemical composition and botanical origin of red propolis, a new type of Brazilian propolis.* Evidence-based complementary and alternative medicine, 2008. **5**(3): p. 313-316.
219. Tiveron, A.P., et al., *Chemical Characterization and Antioxidant, Antimicrobial, and Anti- Inflammatory Activities of South Brazilian Organic Propolis.* PLoS ONE, 2016. **11**(11): p. e0165588.
220. Zancanela, D., et al., *Physical, chemical and antimicrobial implications of the association of propolis with a natural rubber latex membrane.* Materials Letters, 2017. **209**: p. 39.

221. Andrade, J.K.S., et al., *Evaluation of bioactive compounds potential and antioxidant activity of brown, green and red propolis from Brazilian northeast region.* Food Research International, 2017. **101**: p. 129-138.
222. López, B.G.-C., et al., *Phytochemical markers of different types of red propolis.* Food Chemistry, 2014. **146**: p. 174-180.
223. Akyol, S., et al., *In vivo and in vitro antıneoplastic actions of caffeic acid phenethyl ester (CAPE): therapeutic perspectives.* Nutrition and cancer, 2013. **65**(4): p. 515-526.
224. Sahinler, N. and O. Kaftanoglu, *Natural product propolis: chemical composition.* Natural Product Research, 2005. **19**(2): p. 183-188.
225. Marcucci, M.C., *Propolis: chemical composition, biological properties and therapeutic activity.* Apidologie, 1995. **26**(2): p. 83-99.
226. Falcão, S.I., et al., *Phenolic characterization of Northeast Portuguese propolis: usual and unusual compounds.* Analytical and bioanalytical chemistry, 2010. **396**(2): p. 887-897.
227. Raghukumar, R., et al., *Antimethicillin-resistant Staphylococcus aureus (MRSA) activity of 'pacific propolis' and isolated prenylflavanones.* Phytotherapy research, 2010. **24**(8): p. 1181-1187.
228. Cuesta-Rubio, O., et al., *Polyisoprenylated Benzophenones In Cuban Propolis; Biological Activity Of Nemorosone §.* Zeitschrift für Naturforschung C, 2002. **57**(3-4): p. 372-378.
229. Marcucci, M., *Chemical composition, plant origin and biological activity of Brazilian propolis.* Current Topics Phytochem., 1999. **2**: p. 115-123.
230. Kumar, H., T. Kawai, and S. Akira, *Toll- like receptors and innate immunity.* Biochemical and Biophysical Research Communications, 2009. **388**(4): p. 621-625.
231. Pasare, C. and R. Medzhitov, *Toll- like receptors and acquired immunity.* Seminars in Immunology, 2004. **16**(1): p. 23-26.
232. Bueno-Silva, B., et al., *Anti- inflammatory mechanisms of neovestitol from Brazilian red propolis in LPS-activated macrophages.* Journal of Functional Foods, 2017. **36**: p. 440-447.
233. Ansorge, S., D. Reinhold, and U. Lendeckel, *Propolis and some of its constituents down-regulate DNA synthesis and inflammatory cytokine production but induce TGF-ß1 production of human immune cells.* Zeitschrift für Naturforschung C, 2003. **58**(7-8): p. 580-589.
234. Park, Y.K., S.M. Alencar, and C.L. Aguiar, *Botanical origin and chemical composition of Brazilian propolis.* Journal of Agricultural and Food Chemistry, 2002. **50**(9): p. 2502-2506.
235. Zhang, X., et al., *Flavonoid Apigenin Inhibits Lipopolysaccharide- Induced Inflammatory Response through Multiple Mechanisms in Macrophages.* PLoS One, 2014. **9**(9): p. e107072.
236. Soromou, L.W., et al., *In vitro and in vivo protection provided by pinocembrin against lipopolysaccharide- induced inflammatory responses.* International Immunopharmacology, 2012. **14**(1): p. 66-74.
237. Lee, H.N., et al., *Anti- inflammatory effect of quercetin and galangin in LPS-stimulated RAW264.7 macrophages and DNCB- induced atopic dermatitis animal models.(lipopolysaccharides)(Report).* International Journal of Molecular Medicine, 2018. **41**(2): p. 888.

238. Missima, F., et al., *The Effect of propolis on Th1/Th2 cytokine expression and production by melanoma-bearing mice submitted to stress.* Phytotherapy Research, 2010. **24**(10): p. 1501-1507.
239. Tanaka, M., et al., *Suppression of interleukin 17 production by Brazilian propolis in mice with collagen-induced arthritis.* Inflammopharmacology, 2012. **20**(1): p. 19-26.
240. Almutairi, S., et al., *New anti- trypanosomal active prenylated compounds from African propolis.* Phytochemistry Letters, 2014. **10**: p. 35-39.
241. Mbawala, A., et al., *Spectra of antibacterial activity of propolis (Promax-C) samples from two localities of Adamaoua Province (Cameroon).* Research Journal of Microbiology, 2009. **4**(4): p. 150-157.
242. Njintang, Y., et al., *Antiradical activity and polyphenol content of ethanolic extracts of Propolis.* International Journal of Biosciences (IJB), 2012. **2**(4): p. 56-63.
243. Kardar, M.N., et al., *Characterisation of triterpenes and new phenolic lipids in Cameroonian propolis.* Phytochemistry, 2014. 106: pp.156-163.
244. Ngenge, T.A., et al., *Chemical constituents and anti-ulcer activity of propolis from the North-West region of Cameroon.* Research Journal of Phytochemistry, 2016. **10**(2): p. 45-57.
245. Papachroni, D., et al., *Phytochemical analysis and biological evaluation of selected African propolis samples from Cameroon and Congo.* Natural product communications, 2015. **10**(1): p. 67-70.
246. Rochfort, S., *Metabolomics Reviewed: A New " Omics" Platform Technology for Systems Biology and Implications for Natural Products Research*, S. Rochfort, Editor 2005. p. 1813-1820.
247. Krivov, S.V., et al., *Optimal reaction coordinate as a biomarker for the dynamics of recovery from kidney transplant.(Report).* PLoS Computational Biology, 2014. **10**(7).
248. Jansson, J., et al., *Metabolomics Reveals Metabolic Biomarkers of Crohn's Disease.* PLoS One, 2009. **4**(7): p. e6386.
249. Li, P., et al., *Amino acids and immune function.* British Journal of Nutrition, 2007. **98**(2): p. 237-252.
250. Young, S.P., et al., *The Impact of Inflammation on Metabolomic Profiles in Patients With Arthritis.* Arthritis & Rheumatism, 2013. **65**(8): p. 2015-2023.
251. Bingle, L., N.J. Brown, and C.E. Lewis, *The role of tumour-associated macrophages in tumour progression: implications for new anticancer therapies*, 2002: Chichester, UK. p. 254-265.
252. Lin, W.-W. and M. Karin, *A cytokine-mediated link between innate immunity, inflammation, and cancer.* The Journal of clinical investigation, 2007. **117**(5): p. 1175-1183.
253. Ngenge, T.A., et al., *A New Spinastane-type Triterpenoid from a Cameroonian Propolis sample and Evaluation of Antibacterial and Anti-inflammatory Potential of Extracts J. Chem. Chem. Sci, 2017. 7: pp.763-770..*
254. Zingue, S., et al., *Ethanol-extracted Cameroonian propolis exerts estrogenic effects and alleviates hot flushes in ovariectomized Wistar rats.* BMC complementary and alternative medicine, 2017. **17**(1): p. 65.
255. Natarajan, K., et al., *Caffeic acid phenethyl ester is a potent and specific inhibitor of activation of nuclear transcription factor NF-kappa B.* Proceedings of the National Academy of Sciences, 1996. **93**(17): p. 9090-9095.

256. Franchin, M., et al., *The use of Brazilian propolis for discovery and development of novel anti- inflammatory drugs.* European Journal of Medicinal Chemistry, 2018. **153**: p. 49-55.
257. Wen-Chien, H., et al., *The effects of propolis to anti-inflammatory in tumor necrosis factor-o-stimulated human periodontal.* Research Journal of Biotechnology Vol, 2016. **11**: p. 9.
258. Möller, B. and P.M. Villiger. *Inhibition of IL-1, IL-6, and TNF-α in immune-mediated inflammatory diseases*. in *Springer seminars in immunopathology*. 2006. Springer.
259. Chan, G.C.-F., K.-W. Cheung, and D.M.-Y. Sze, *The Immunomodulatory and Anticancer Properties of Propolis.* Clinical Reviews in Allergy and Immunology, 2012. **44**(3): p. 1-12.
260. Ewelina, S., et al., *Chemical Composition and Anti- Inflammatory Effect of Ethanolic Extract of Brazilian Green Propolis on Activated J774A. 1 Macrophages.* Evidence-Based Complementary and Alternative Medicine, 2013. **2013**.
261. Krawczyk, C.M., et al., *Toll-like receptor induced changes in glycolytic metabolism regulate dendritic cell activation.* Blood, 2010: p. blood-2009-10-249540.
262. Alqarni, A., et al., *Effect of Melittin on Metabolomic Profile and Cytokine Production in PMA-Differentiated THP-1 Cells.* Vaccines, 2018. **6**(4): p. 72.
263. Peña-Altamira, L.E., et al., *Release of soluble and vesicular purine nucleoside phosphorylase from rat astrocytes and microglia induced by pro-inflammatory stimulation with extracellular ATP via P2X7 receptors.* Neurochemistry international, 2018. **115**: p. 37-49.
264. Kazmers, I.S., et al., *Inhibition of purine nucleoside phosphorylase by 8-aminoguanosine: selective toxicity for T lymphoblasts.* Science, 1981. **214**(4525): p. 1137-1139.
265. Markert, M.L., *Purine nucleoside phosphorylase deficiency.* Immunodeficiency reviews, 1991. **3**(1): p. 45-81.
266. Savarese, T.M., G.W. Crabtree, and R.E. Parks Jr, *5'-methylthioadenosine phosphorylase—I: Substrate activity of 5'-deoxyadenosine with the enzyme from Sarcoma 180 cells.* Biochemical pharmacology, 1981. **30**(3): p. 189-199.
267. Arpaia, E., et al., *Mitochondrial Basis for Immune Deficiency: Evidence from Purine Nucleoside Phosphorylase–deficient Mice.* Journal of Experimental Medicine, 2000. **191**(12): p. 2197-2208.
268. Herken, H., et al., *Adenosine deaminase, nitric oxide, superoxide dismutase, and xanthine oxidase in patients with major depression: impact of antidepressant treatment.* Archives of medical research, 2007. **38**(2): p. 247-252.
269. Tritsch, G. and P. Niswander, *Positive correlation between superoxide release and intracellular adenosine deaminase activity during macrophage membrane perturbation regardless of nature or magnitude of stimulus.* Molecular and cellular biochemistry, 1982. **49**(1): p. 49-51.
270. Sono, M., *The roles of superoxide anion and methylene blue in the reductive activation of indoleamine 2, 3-dioxygenase by ascorbic acid or by xanthine oxidase-hypoxanthine.* Journal of Biological Chemistry, 1989. **264**(3): p. 1616-1622.
271. Munn, D.H. and A.L. Mellor, *Indoleamine 2, 3 dioxygenase and metabolic control of immune responses.* Trends in immunology, 2013. **34**(3): p. 137-143.

272. Tomek, P., et al., *Discovery and evaluation of inhibitors to the immunosuppressive enzyme indoleamine 2, 3-dioxygenase 1 (IDO1): Probing the active site-inhibitor interactions.* European journal of medicinal chemistry, 2017. **126**: p. 983-996.
273. Esser, C., A. Rannug, and B. Stockinger, *The aryl hydrocarbon receptor in immunity.* Trends in immunology, 2009. **30**(9): p. 447-454.
274. Gutierrez-Vazquez, C. and F.J. Quintana, *Regulation of the immune response by the aryl hydrocarbon receptor.* Immunity, 2018. **48**(1): p. 19-33.
275. Fukuda, K., *Etiological classification of depression based on the enzymes of tryptophan metabolism.* BMC psychiatry, 2014. **14**(1): p. 372.
276. Regan, T., et al., *Effects of anti-inflammatory drugs on the expression of tryptophan-metabolism genes by human macrophages.* Journal of leukocyte biology, 2018. **103**(4): p. 681-692.
277. Hellsten-Westing, Y., et al., *Decreased resting levels of adenine nucleotides in human skeletal muscle after high-intensity training.* Journal of Applied Physiology, 1993. **74**(5): p. 2523-2528.
278. Ipata, P.L. and R. Pesi, *Metabolic interaction between purine nucleotide cycle and oxypurine cycle during skeletal muscle contraction of different intensities: a biochemical reappraisal.* Metabolomics, 2018. **14**(4): p. 42.
279. Puchalska, P., et al., *Isotope Tracing Untargeted Metabolomics Reveals Macrophage Polarization-State-Specific Metabolic Coordination across Intracellular Compartments.* iScience, 2018. **9**: p. 298-313.
280. Mills, E.L. and L.A. O'Neill, *Reprogramming mitochondrial metabolism in macrophages as an anti-inflammatory signal.* European journal of immunology, 2016. **46**(1): p. 13-21.
281. Rattigan, K.M., et al., *Metabolomic profiling of macrophages determines the discrete metabolomic signature and metabolomic interactome triggered by polarising immune stimuli.* PLoS ONE, 2018. **13**(3): p. e0194126.
282. Qualls, J.E., et al., *Sustained generation of nitric oxide and control of mycobacterial infection requires argininosuccinate synthase 1.* Cell host & microbe, 2012. **12**(3): p. 313-323.
283. El Kasmi, K.C., et al., *Toll-like receptor–induced arginase 1 in macrophages thwarts effective immunity against intracellular pathogens.* Nature immunology, 2008. **9**(12): p. 1399.
284. Mayer-Barber, K.D., et al., *Cutting edge: caspase-1 independent IL-1β production is critical for host resistance to Mycobacterium tuberculosis and does not require TLR signaling in vivo.* The Journal of Immunology, 2010: p. ji_0904189.
285. Mishra, B.B., et al., *Nitric oxide controls the immunopathology of tuberculosis by inhibiting NLRP3 inflammasome–dependent processing of IL-1β.* Nature immunology, 2013. **14**(1): p. 52.
286. Tannahill, G.M., et al., *Succinate is an inflammatory signal that induces IL-1β through HIF-1α.* Nature, 2013. **496**(7444): p. 238-242.
287. Dröse, S., *Differential effects of complex II on mitochondrial ROS production and their relation to cardioprotective pre- and postconditioning.* BBA - Bioenergetics, 2012. **1827**(5).
288. Stoop, J., et al., *Purine nucleoside phosphorylase deficiency associated with selective cellular immunodeficiency.* New England Journal of Medicine, 1977. **296**(12): p. 651-655.

289. McKee, A.S. and P. Marrack, *Old and new adjuvants.* Current Opinion in Immunology, 2017. **47**: p. 44-51.
290. Garçon, N., G. Leroux-Roels, and W.-F. Cheng, *Vaccine adjuvants.* Perspectives in Vaccinology, 2011. **1**(1): p. 89-113.
291. Reed, S.G., M.T. Orr, and C.B. Fox, *Key roles of adjuvants in modern vaccines.* Nature medicine, 2013. **19**(12): p. 1597-1608.
292. Coffman, R.L., A. Sher, and R.A. Seder, *Vaccine adjuvants: putting innate immunity to work.* Immunity, 2010. **33**(4): p. 492-503.
293. McKee, A.S., M.W. Munks, and P. Marrack, *How do adjuvants work? Important considerations for new generation adjuvants.* Immunity, 2007. **27**(5): p. 687-690.
294. McCartney, S., et al., *Distinct and complementary functions of MDA5 and TLR3 in poly (I: C)-mediated activation of mouse NK cells.* Journal of Experimental Medicine, 2009. **206**(13): p. 2967-2976.
295. Tritto, E., F. Mosca, and E. De Gregorio, *Mechanism of action of licensed vaccine adjuvants.* Vaccine, 2009. **27**(25-26): p. 3331-3334.
296. De Gregorio, E., U. D'Oro, and A. Wack, *Immunology of TLR-independent vaccine adjuvants.* Current opinion in immunology, 2009. **21**(3): p. 339-345.
297. Fraser, C.K., et al., *Improving vaccines by incorporating immunological coadjuvants.* Expert review of vaccines, 2007. **6**(4): p. 559-578.
298. Akira, S., S. Uematsu, and O. Takeuchi, *Pathogen recognition and innate immunity.* Cell, 2006. **124**(4): p. 783-801.
299. Steinhagen, F., et al., *TLR-based immune adjuvants.* Vaccine, 2011. **29**(17): p. 3341-3355.
300. GALANOS, C., et al., *Synthetic and natural Escherichia coli free lipid A express identical endotoxic activities.* European journal of biochemistry, 1985. **148**(1): p. 1-5.
301. El-Wahed, A.A.A., et al., *Bee Venom Composition: From Chemistry to Biological Activity*, in *Studies in Natural Products Chemistry*2018, Elsevier. p. 459-484.
302. Hider, R.C., *Honeybee venom: a rich source of pharmacologically active peptides.* Endeavour, 1988. **12**(2): p. 60-65.
303. Rady, I., et al., *Melittin, a major peptide component of bee venom, and its conjugates in cancer therapy.* Cancer letters, 2017. **402**: p. 16-31.
304. Pickett, J.A., I.H. Williams, and A.P. Martin, *(Z)-11-eicosen-1-ol, an important new pheromonal component from the sting of the honey bee,Apis mellifera L. (Hymenoptera, Apidae.).* Journal of chemical ecology, 1982. **8**(1): p. 163-175.
305. Free, J., *The stimuli releasing the stinging response of honeybees.* Animal Behaviour, 1961. **9**(3-4): p. 193-196.
306. Lampropoulou, V., et al., *Itaconate links inhibition of succinate dehydrogenase with macrophage metabolic remodeling and regulation of inflammation.* Cell metabolism, 2016. **24**(1): p. 158-166.
307. Sakagami, H., et al., *Quantitative structure–cytotoxicity relationship of newly synthesized piperic acid esters.* Anticancer research, 2017. **37**(11): p. 6161-6168.
308. Murias, M., et al., *Antioxidant, prooxidant and cytotoxic activity of hydroxylated resveratrol analogues: structure–activity relationship.* Biochemical pharmacology, 2005. **69**(6): p. 903-912.

309. Scheller, J., et al., *The pro-and anti-inflammatory properties of the cytokine interleukin-6.* Biochimica et Biophysica Acta (BBA)-Molecular Cell Research, 2011. **1813**(5): p. 878-888.
310. Balto, K., H. Sasaki, and P. Stashenko, *Interleukin-6 deficiency increases inflammatory bone destruction.* Infection and immunity, 2001. **69**(2): p. 744-750.
311. Grivennikov, S., et al., *IL-6 and Stat3 are required for survival of intestinal epithelial cells and development of colitis-associated cancer.* Cancer cell, 2009. **15**(2): p. 103-113.
312. Stumhofer, J.S., et al., *Interleukins 27 and 6 induce STAT3-mediated T cell production of interleukin 10.* Nature immunology, 2007. **8**(12): p. 1363.
313. Jin, J.-O., X. Han, and Q. Yu, *Interleukin-6 induces the generation of IL-10-producing Tr1 cells and suppresses autoimmune tissue inflammation.* Journal of autoimmunity, 2013. **40**: p. 28-44.
314. Mukhopadhyay, S., L. Peiser, and S. Gordon, *Activation of murine macrophages by Neisseria meningitidis and IFN-γ in vitro: distinct roles of class A scavenger and Toll-like pattern recognition receptors in selective modulation of surface phenotype.* Journal of leukocyte biology, 2004. **76**(3): p. 577-584.
315. Li, H. and T.L. Poulos, *Structure–function studies on nitric oxide synthases.* Journal of inorganic biochemistry, 2005. **99**(1): p. 293-305.
316. Satriano, J., *Arginine pathways and the inflammatory response: interregulation of nitric oxide and polyamines.* Amino acids, 2004. **26**(4): p. 321-329.
317. Alqarni, A.M., et al., *Propolis Exerts an Anti-Inflammatory Effect on PMA-Differentiated THP-1 Cells via Inhibition of Purine Nucleoside Phosphorylase.* Metabolites, 2019. **9**(4): p. 75.
318. Strelko, C.L., et al., *Itaconic acid is a mammalian metabolite induced during macrophage activation.* Journal of the American Chemical Society, 2011. **133**(41): p. 16386-16389.
319. Mills, E.L., et al., *Itaconate is an anti-inflammatory metabolite that activates Nrf2 via alkylation of KEAP1.* Nature, 2018. **556**(7699): p. 113.
320. Michelucci, A., et al., *Immune-responsive gene 1 protein links metabolism to immunity by catalyzing itaconic acid production.* Proceedings of the National Academy of Sciences, 2013. **110**(19): p. 7820-7825.
321. Sies, H., *Oxidative stress: oxidants and antioxidants.* Experimental physiology, 1997. **82**(2): p. 291-295.
322. Rahman, I. and W. MacNee, *Oxidative stress and regulation of glutathione in lung inflammation.* European Respiratory Journal, 2000. **16**(3): p. 534-554.
323. Ghezzi, P., *Role of glutathione in immunity and inflammation in the lung.* International journal of general medicine, 2011. **4**: p. 105.
324. Fan, J., et al., *Quantitative flux analysis reveals folate-dependent NADPH production.* Nature, 2014. **510**(7504): p. 298.
325. Moreno-Sánchez, R., et al., *Control of the NADPH supply and GSH recycling for oxidative stress management in hepatoma and liver mitochondria.* Biochimica et Biophysica Acta (BBA)-Bioenergetics, 2018. **1859**(10): p. 1138-1150.
326. Kalkan, I.H. and M. Suher, *The relationship between the level of glutathione, impairment of glucose metabolism and complications of diabetes mellitus.* Pakistan journal of medical sciences, 2013. **29**(4): p. 938.

327. Margonis, K., et al., *Oxidative stress biomarkers responses to physical overtraining: implications for diagnosis.* Free Radical Biology and Medicine, 2007. **43**(6): p. 901-910.
328. Alorainy, M., *Effect of allopurinol and vitamin E on rat model of rheumatoid arthritis.* International journal of health sciences, 2008. **2**(1): p. 59.
329. Newsholme, P., S. Gordon, and E.A. Newsholme, *Rates of utilization and fates of glucose, glutamine, pyruvate, fatty acids and ketone bodies by mouse macrophages.* Biochemical Journal, 1987. **242**(3): p. 631-636.
330. Malandrino, M.I., et al., *Enhanced fatty acid oxidation in adipocytes and macrophages reduces lipid-induced triglyceride accumulation and inflammation.* American Journal of Physiology-Endocrinology and Metabolism, 2015. **308**(9): p. E756-E769.
331. Namgaladze, D., et al., *Inhibition of macrophage fatty acid β-oxidation exacerbates palmitate-induced inflammatory and endoplasmic reticulum stress responses.* Diabetologia, 2014. **57**(5): p. 1067-1077.
332. Feingold, K.R., et al., *LPS decreases fatty acid oxidation and nuclear hormone receptors in the kidney.* Journal of lipid research, 2008. **49**(10): p. 2179-2187.
333. Wanders, R.J. and H.R. Waterham, *Biochemistry of mammalian peroxisomes revisited.* Annu. Rev. Biochem., 2006. **75**: p. 295-332.
334. Li, P., et al., *NCoR Repression of LXRs Restricts Macrophage Biosynthesis of Insulin-Sensitizing Omega 3 Fatty Acids.* Cell, 2013. **155**(1): p. 200-214.
335. Dennis, E.A. and P.C. Norris, *Eicosanoid storm in infection and inflammation.* Nature reviews. Immunology, 2015. **15**(8): p. 511-523.
336. Lewis, J.G. and D.O. Adams, *Enhanced Release of Hydrogen Peroxide and Metabolites of Arachidonic Acid by Macrophages from SENCAR Mice following Stimulation with Phorbol Esters.* Cancer Research, 1986. **46**(11): p. 5696-5700.
337. Dennis, E.A. and P.C. Norris, *Eicosanoid storm in infection and inflammation.* Nature Reviews Immunology, 2015. **15**(8): p. 511.
338. Dröge, W., et al., *Functions of glutathione and glutathione disulfide in immunology and immunopathology.* The FASEB Journal, 1994. **8**(14): p. 1131-1138.
339. Mehta, J.P., et al., *In-vitro antioxidant and in-vivo anti-inflammatory activities of aerial parts of Cassia species.* Arabian Journal of Chemistry, 2017. **10**: p. S1654-S1662.
340. Coussens, L.M. and Z. Werb, *Inflammation and cancer.* Nature, 2002. **420**(6917): p. 860.
341. Dantzer, R., et al., *From inflammation to sickness and depression: when the immune system subjugates the brain.* Nature reviews neuroscience, 2008. **9**(1): p. 46.
342. Pezzuto, J.M., *Plant-derived anticancer agents.* Biochemical pharmacology, 1997. **53**(2): p. 121-133.
343. Piao, X.-L., et al., *Novel dammarane saponins from Gynostemma pentaphyllum and their cytotoxic activities against HepG2 cells.* Bioorganic & medicinal chemistry letters, 2014. **24**(20): p. 4831-4833.
344. Huang, W.-C., et al., *Gynostemma pentaphyllum decreases allergic reactions in a murine asthmatic model.* The American journal of Chinese medicine, 2008. **36**(03): p. 579-592.
345. Schild, L., et al., *Selective induction of apoptosis in glioma tumour cells by a Gynostemma pentaphyllum extract.* Phytomedicine, 2010. **17**(8-9): p. 589-597.

346. Megalli, S., N.M. Davies, and B.D. Roufogalis, *Anti-hyperlipidemic and hypoglycemic effects of Gynostemma pentaphyllum in the Zucker fatty rat.* J Pharm Pharm Sci, 2006. **9**(3): p. 281-91.
347. Yang, X., et al., *Isolation and characterization of immunostimulatory polysaccharide from an herb tea, Gynostemma pentaphyllum Makino.* Journal of agricultural and food chemistry, 2008. **56**(16): p. 6905-6909.
348. Alhasani, R.H., et al., *Gypenosides protect retinal pigment epithelium cells from oxidative stress.* Food and chemical toxicology, 2018. **112**: p. 76-85.
349. Xing, S.-F., et al., *A new dammarane-type saponin from Gynostemma pentaphyllum induces apoptosis in A549 human lung carcinoma cells.* Bioorganic & medicinal chemistry letters, 2016. **26**(7): p. 1754-1759.
350. Shang, L., et al., *Gypenosides protect primary cultures of rat cortical cells against oxidative neurotoxicity.* Brain research, 2006. **1102**(1): p. 163-174.
351. Zhang, H.-K., et al., *Neuroprotective effects of gypenosides in experimental autoimmune optic neuritis.* International journal of ophthalmology, 2017. **10**(4): p. 541.
352. Ahmad, B., et al., *Natural gypenosides: targeting cancer through different molecular pathways.* Cancer management and research, 2019. **11**: p. 2287.
353. Cai, H., Q. Liang, and G. Ge, *Gypenoside attenuates β amyloid-induced inflammation in N9 microglial cells via SOCS1 signaling.* Neural plasticity, 2016. **2016**.
354. Xie, Z., et al., *Chemical composition and anti-proliferative and anti-inflammatory effects of the leaf and whole-plant samples of diploid and tetraploid Gynostemma pentaphyllum (Thunb.) Makino.* Food chemistry, 2012. **132**(1): p. 125-133.
355. Liou, C.-J., et al., *Long-term oral administration of Gynostemma pentaphyllum extract attenuates airway inflammation and Th2 cell activities in ovalbumin-sensitized mice.* Food and Chemical Toxicology, 2010. **48**(10): p. 2592-2598.
356. Wang, F., et al., *Gypenosides attenuate lipopolysaccharide-induced optic neuritis in rats.* Acta histochemica, 2018. **120**(4): p. 340-346.
357. Li, H., et al., *Therapeutic effect of Gypenosides on nonalcoholic steatohepatitis via regulating hepatic lipogenesis and fatty acid oxidation.* Biological and Pharmaceutical Bulletin, 2017. **40**(5): p. 650-657.
358. Aktan, F., et al., *Gypenosides derived from Gynostemma pentaphyllum suppress NO synthesis in murine macrophages by inhibiting iNOS enzymatic activity and attenuating NF-κB-mediated iNOS protein expression.* Nitric oxide, 2003. **8**(4): p. 235-242.
359. Song, Y.-N., et al., *Metabolomic mechanisms of gypenoside against liver fibrosis in rats: An integrative analysis of proteomics and metabolomics data.* PLoS ONE, 2017. **12**(3): p. e0173598.
360. Chen, D.-J., et al., *Metabolite profiling of gypenoside LVI in rat after oral and intravenous administration.* Archives of pharmacal research, 2015. **38**(6): p. 1157-1167.
361. Lu, Y., et al., *Gypenosides altered hepatic bile acids homeostasis in mice treated with high fat diet.* Evidence-Based Complementary and Alternative Medicine, 2018. **2018**.
362. Lee, B., I. Shim, and H. Lee, *Gypenosides attenuate lipopolysaccharide-induced neuroinflammation and memory impairment in rats.* Evidence-Based Complementary and Alternative Medicine, 2018. **2018**.

363. Wan, Z.H. and Q. Zhao, *Gypenoside inhibits interleukin-1β-induced inflammatory response in human osteoarthritis chondrocytes.* Journal of biochemical and molecular toxicology, 2017. **31**(9): p. e21926.
364. Gohil, V.M., et al., *Nutrient-sensitized screening for drugs that shift energy metabolism from mitochondrial respiration to glycolysis.* Nature biotechnology, 2010. **28**(3): p. 249.
365. Kelly, B. and L.A. O'neill, *Metabolic reprogramming in macrophages and dendritic cells in innate immunity.* Cell research, 2015. **25**(7): p. 771.
366. Tang, Y., et al., *Fatty acid activation in carcinogenesis and cancer development: Essential roles of long‐chain acyl‐CoA synthetases.* Oncology letters, 2018. **16**(2): p. 1390-1396.
367. Liu, J., et al., *Gypenosides reduced the risk of overweight and insulin resistance in C57BL/6J mice through modulating adipose thermogenesis and gut microbiota.* Journal of agricultural and food chemistry, 2017. **65**(42): p. 9237-9246.
368. Wilson, K.T., et al., *Helicobacter pylori stimulates inducible nitric oxide synthase expression and activity in a murine macrophage cell line.* Gastroenterology, 1996. **111**(6): p. 1524-1533.
369. Bogdan, C., *Nitric oxide and the immune response.* Nature immunology, 2001. **2**(10): p. 907.
370. Calvani, M., et al., *Time-dependent stabilization of hypoxia inducible factor-1α by different intracellular sources of reactive oxygen species.* PLoS ONE, 2012. **7**(10): p. e38388.
371. Harrison, R., *Physiological roles of xanthine oxidoreductase.* Drug metabolism reviews, 2004. **36**(2): p. 363-375.
372. Harrison, R., *Structure and function of xanthine oxidoreductase: where are we now?* Free Radical Biology and Medicine, 2002. **33**(6): p. 774-797.
373. Remedios, C., et al., *Hyperuricemia: a Reality in the Indian Obese.(Report).* Obesity Surgery, 2012. **22**(6): p. 945.
374. Zhu, L., et al., *Saponins extracted from Dioscorea collettii rhizomes regulate the expression of urate transporters in chronic hyperuricemia rats.* Biomedicine & Pharmacotherapy, 2017. **93**: p. 88-94.
375. Pang, M., et al., *Gypenosides Inhibits Xanthine Oxidoreductase and Ameliorates Urate Excretion in Hyperuricemic Rats Induced by High Cholesterol and High Fat Food (Lipid Emulsion).* Medical science monitor: international medical journal of experimental and clinical research, 2017. **23**: p. 1129.
376. Nikolaus, S., et al., *Increased tryptophan metabolism is associated with activity of inflammatory bowel diseases.* Gastroenterology, 2017. **153**(6): p. 1504-1516. e2.
377. Richard, D.M., et al., *L-tryptophan: basic metabolic functions, behavioral research and therapeutic indications.* International Journal of Tryptophan Research, 2009. **2**: p. IJTR. S2129.
378. Ciorba, M.A., *Indoleamine 2, 3 dioxygenase (IDO) in intestinal disease.* Current opinion in gastroenterology, 2013. **29**(2): p. 146.
379. Kim, C.J., et al., *l-Tryptophan exhibits therapeutic function in a porcine model of dextran sodium sulfate (DSS)-induced colitis.* The Journal of nutritional biochemistry, 2010. **21**(6): p. 468-475.
380. King, N.J. and S.R. Thomas, *Molecules in focus: indoleamine 2, 3-dioxygenase.* The international journal of biochemistry & cell biology, 2007. **39**(12): p. 2167-2172.

381. Fujigaki, H., et al., *The signal transducer and activator of transcription 1α and interferon regulatory factor 1 are not essential for the induction of indoleamine 2, 3-dioxygenase by lipopolysaccharide: involvement of p38 mitogen-activated protein kinase and nuclear factor-κB pathways, and synergistic effect of several proinflammatory cytokines.* Journal of biochemistry, 2006. **139**(4): p. 655-662.
382. Wirthgen, E., et al., *Activation of indoleamine 2, 3-dioxygenase by LPS in a porcine model.* Innate immunity, 2014. **20**(1): p. 30-39.

Appendices

Chapter 3:

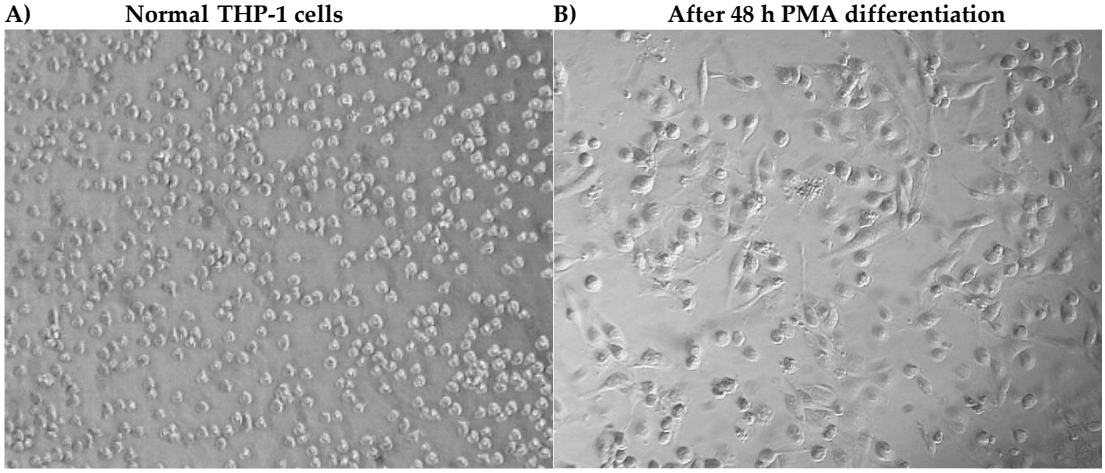

Figure S3.1 : Negative control THP-1 cells **(A)** and it is derived macrophages by the effect of PMA treatment **(B)** at final concentration of 60ng/mL.

TNF-α production

Table S3.1: Effect of melittin (Mel) on the production of TNF-α cytokines in the presence and absence of LPS on PMA-differentiated THP-1 cells (*n*=3).

	TNF-α *concentration (pg/ml)*								
Dose (µg/ml)	**Media**	**LPS**		**Sample**		**Sample + 0.5 LPS**		**Sample + 1 LPS**	
		0.5 LPS	**1 LPS**	**0.5 Mel**	**1 Mel**	**0.5 Mel**	**1Mel**	**0.5 Mel**	**1 Mel**
n=1	458	1856	1862	315	381	1942	1879	1947	1885
n=2	736	1830	1848	833	752	1839	1881	1869	1825
n=3	561	1776	1847	482	722	1859	1826	1881	1862
Mean	585	1820.67	1852.3	543.33	618.33	1880	1862	1899	1857.33
RSD	24.02	2.24	0.45	48.66	33.33	2.91	1.68	2.21	1.63
***p*.value**	n/a	<0.001	<0.001	ns	ns	ns	ns	ns	ns

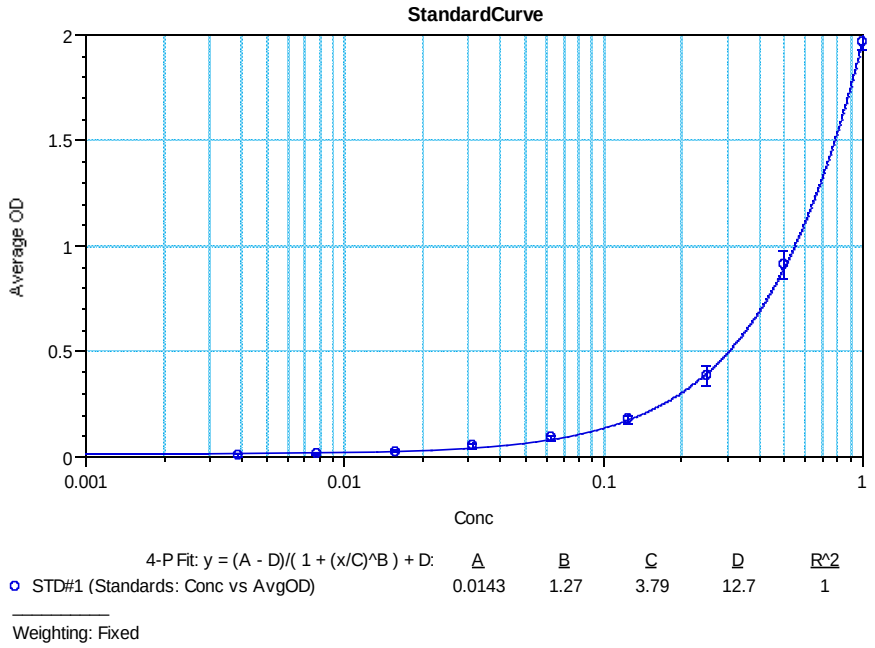

Figure S3.2: A representative 4-parameter logistic plot of TNF-α standard samples of 9 points showing the values of a, b, c, and d constants and the calibration equation with a best fit (R^2=1.0). The data represents the mean ± SD of optical density (OD) values for duplicate standard concentrations (*n*=2).

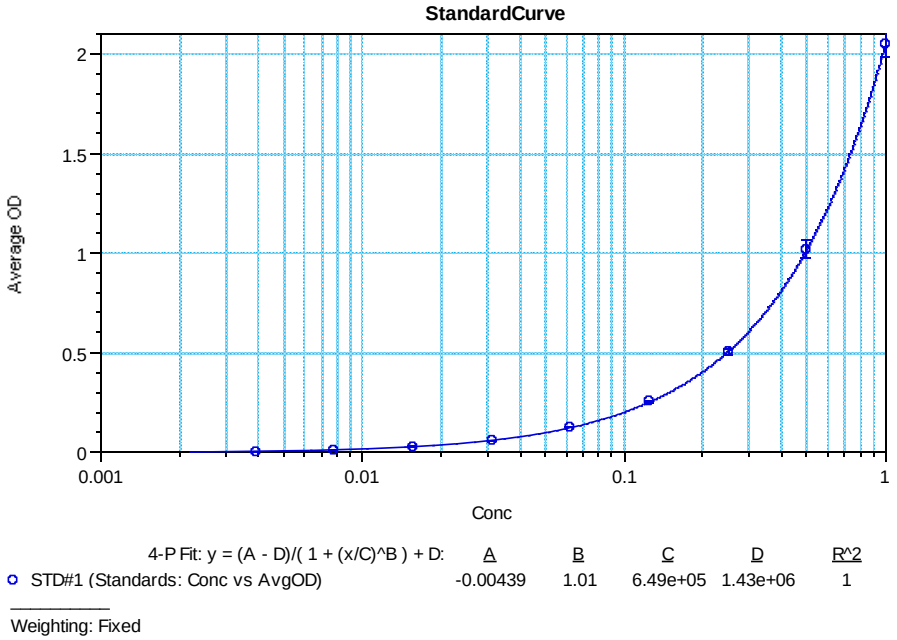

Figure S3.3: A representative 4-parameter logistic plot of TNF-α standard samples of 9 points showing the values of a, b, c, and d constants and the calibration equation with a best fit (R2=1.0). The data represents the mean ± SD of optical density (OD) values for duplicate standard concentrations (n=2).

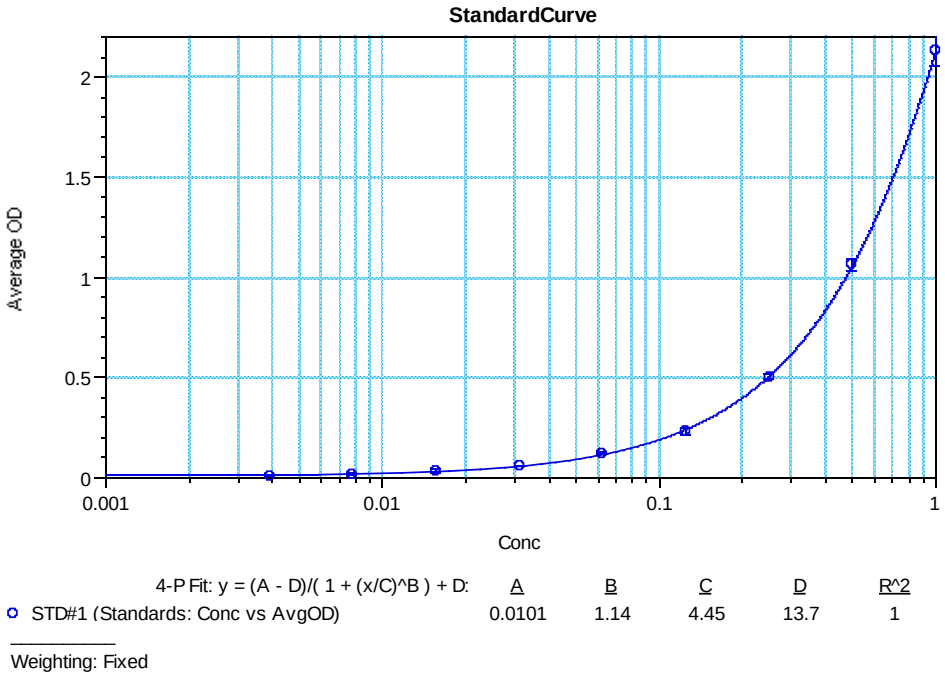

Figure S3.4: A representative 4-parameter logistic plot of TNF-α standard samples of 9 points showing the values of a, b, c, and d constants and the calibration equation with a best fit (R^2=1.0). The data represents the mean ± SD of optical density (OD) values for duplicate standard concentrations (*n*=2).

IL-1β production

Table S3.2: Effect of melittin (Mel) on the production of IL-1β cytokines in the presence and absence of LPS on PMA-differentiated THP-1 cells (*n*=3).

	IL-1β *concentration (pg/ml)*								
Dose (µg/ml)	**Media**	**LPS**		**Sample**		**Sample+ 0.5 LPS**		**Sample + 1 LPS**	
		0.5 LPS	**1 LPS**	**0.5 Mel**	**1 Mel**	**0.5 Mel**	**1Mel**	**0.5 Mel**	**1Mel**
n=1	10.5	48.5	52	16	85	80	175	70	200
n=2	45	92	86	73	115	130	137	147	161
n=3	41	99	108	80	157	137	141	138	150
Mean	32.17	79.83	82.00	56.33	119.00	115.67	151	118.33	170.33
RSD	58.66	34.27	34.41	62.32	30.39	26.88	13.83	35.58	15.43
***p*.value**	n/a	ns	ns	ns	0.021	ns	0.026	ns	0.017

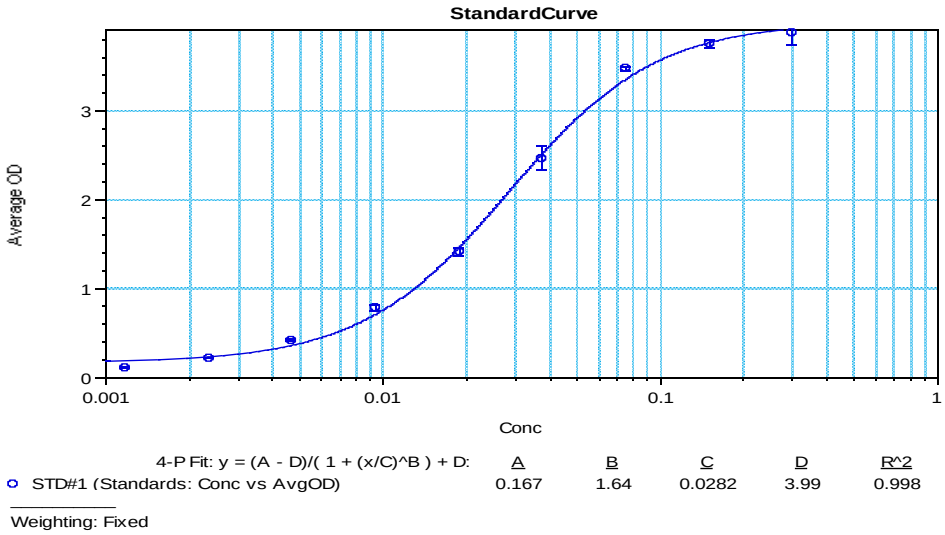

Figure S3.5: A representative 4-parameter logistic plot of IL-1β standard samples of 9 points showing the values of a, b, c, and d constants and the calibration equation with a best fit (R^2=0.998). The data represents the mean ± SD of optical density (OD) values for duplicate standard concentrations (*n*=2).

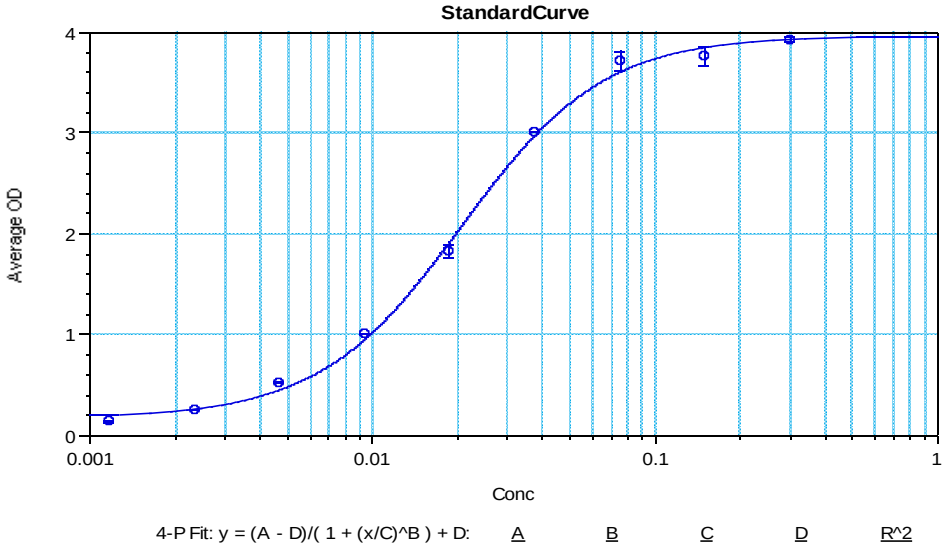

Figure S3.6: A representative 4-parameter logistic plot of IL-1β standard samples of 9 points showing the values of a, b, c, and d constants and the calibration equation with a best fit (R^2=0.998). The data represents the mean ± SD of optical density (OD) values for duplicate standard concentrations (*n*=2).

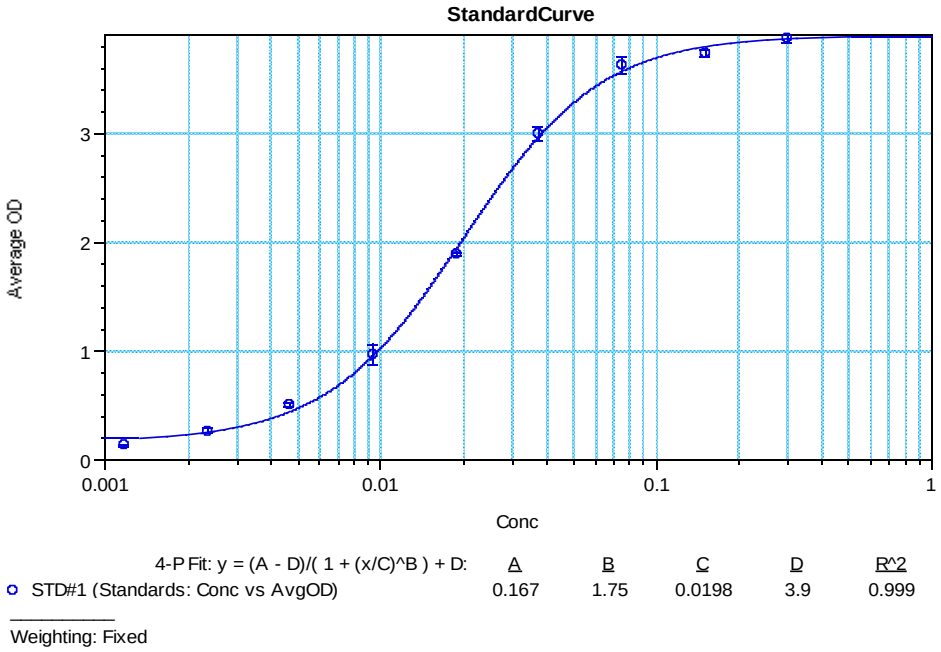

Figure S3.7: A representative 4-parameter logistic plot of IL-1β standard samples of 9 points showing the values of a, b, c, and d constants and the calibration equation with a best fit (R^2=0.999). The data represents the mean ± SD of optical density (OD) values for duplicate standard concentrations (*n*=2).

IL-6 production

Table S3.3: Effect of melittin (Mel) on the production of IL-6 cytokines in the presence and absence of LPS on PMA-differentiated THP-1 cells (*n*=3).

	IL-6 *concentration (pg/ml)*					
Dose (µg/ml)	**Media**	**LPS**		**Sample**	**Sample + 0.5 LPS**	**Sample + 1 LPS**
		0.5 LPS	**1 LPS**	**0.5 Mel**	**0.5 Mel**	**0.5 Mel**
n=1	< 2.0	41	99	< 2.0	82	132
n=2	< 2.0	100	108	< 2.0	106	133
n=3	< 2.0	98	116	< 2.0	113	144
Mean	n/a	79.66	107.66	n/a	100.33	136.33
RSD	n/a	42.05	7.89	n/a	16.20	4.88
P value	n/a	n/a	n/a	n/a	ns	0.010

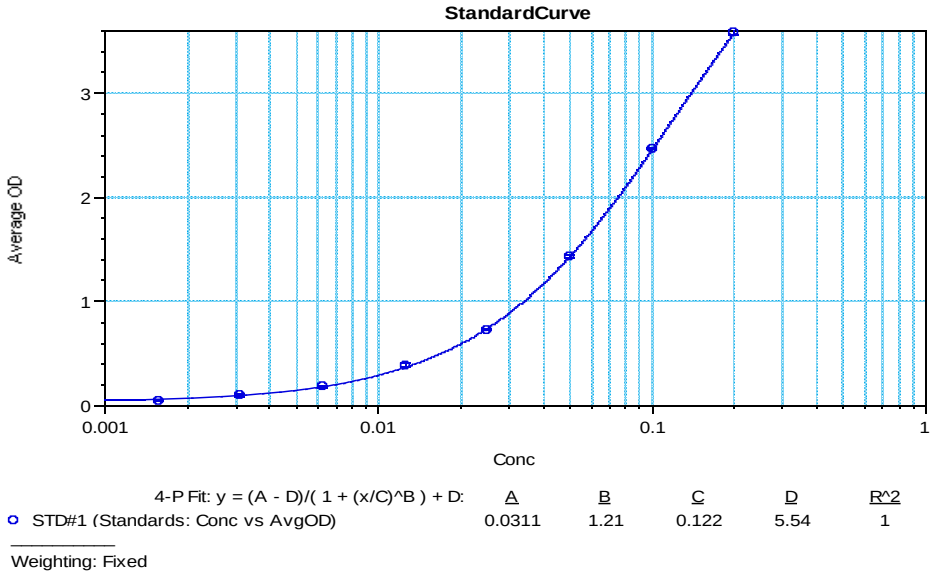

Figure S3.8: A representative 4-parameter logistic plot of IL-6 standard samples of 8 points showing the values of a, b, c, and d constants and the calibration equation with a best fit (R^2=1). The data represents the mean ± SD of optical density (OD) values for duplicate standard concentrations (*n*=2).

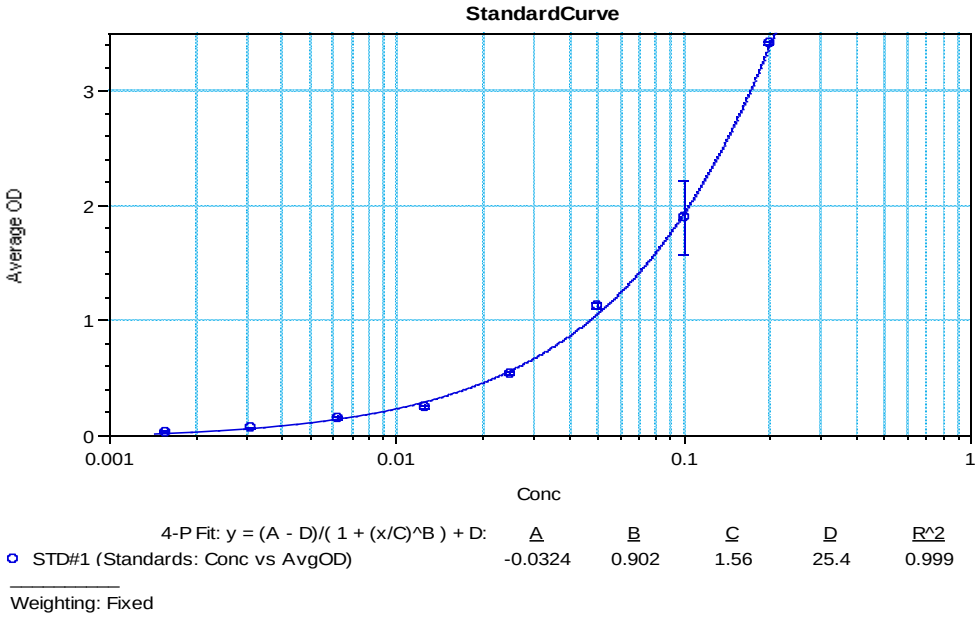

Figure S3.9: A representative 4-parameter logistic plot of IL-6 standard samples of 8 points showing the values of a, b, c, and d constants and the calibration equation with a best fit (R^2=0.999). The data represents the mean ± SD of optical density (OD) values for duplicate standard concentrations (*n*=2).

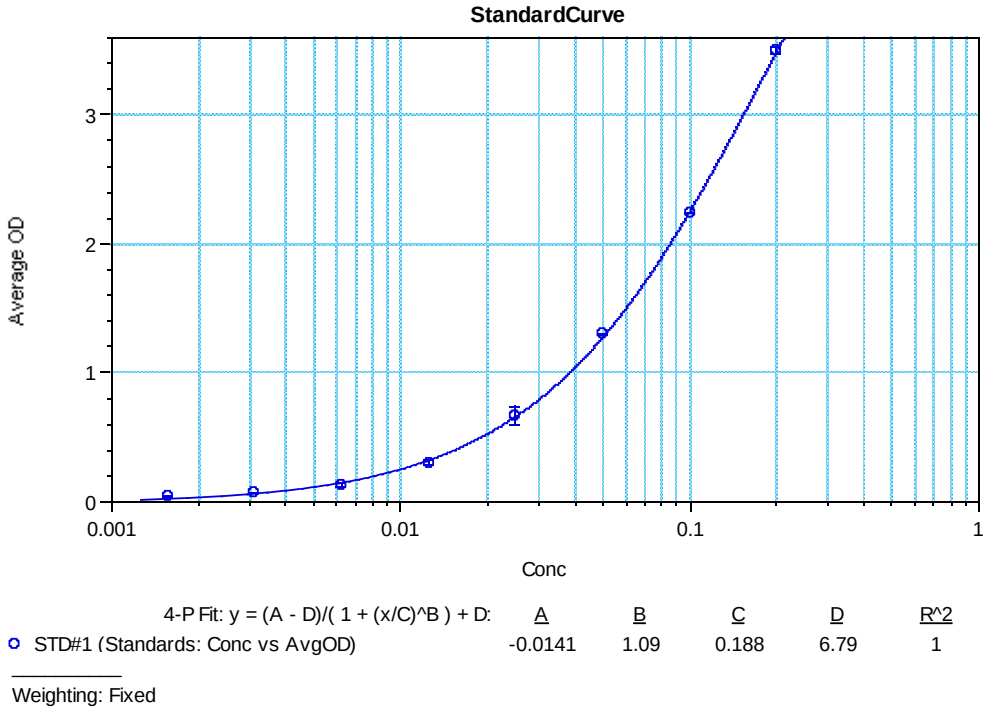

Figure S3.10: A representative 4-parameter logistic plot of IL-6 standard samples of 8 points showing the values of a, b, c, and d constants and the calibration equation with a best fit (R^2=1). The data represents the mean ± SD of optical density (OD) values for duplicate standard concentrations (*n*=2).

IL-10 production

Table S3.4: Effect of melittin (Mel) on the production of IL-10 cytokines in the presence and absence of LPS on PMA-differentiated THP-1 cells (*n*=3).

	IL-10 *concentration (pg/ml)*					
Dose (µg/ml)	**Media**	**LPS**		**Sample**	**Sample + 0.5 LPS**	**Sample + 1 LPS**
		0.5 LPS	**1 LPS**	**0.5 Mel**	**0.5 Mel**	**0.5 Mel**
n=1	27.5	62	52	24	56	57
n=2	17	30	41	12	32	33
n=3	20	40	40	20	26	34
Mean	21.50	44.00	44.33	18.67	38.00	41.33
RSD	25.16	37.21	15.02	32.73	41.78	32.85
P value	n/a	ns	0.010	ns	ns	ns

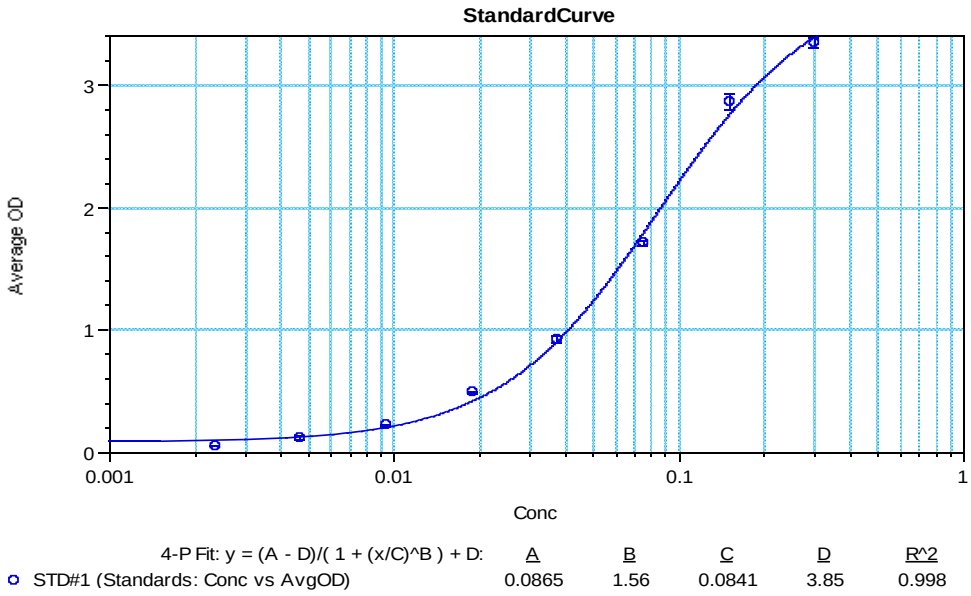

Figure S3.11: A representative 4-parameter logistic plot of IL-10 standard samples of 8 points showing the values of a, b, c, and d constants and the calibration equation with a best fit (R^2=0.998). The data represents the mean ± SD of optical density (OD) values for duplicate standard concentrations (*n*=2).

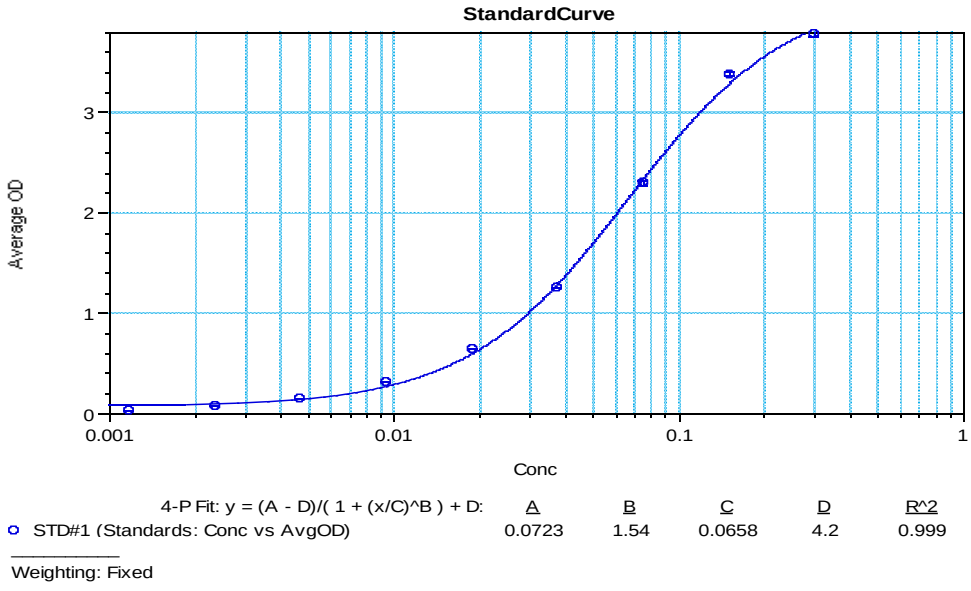

Figure S3.12: A representative 4-parameter logistic plot of IL-10 standard samples of 8 points showing the values of a, b, c, and d constants and the calibration equation with a best fit (R^2=0.999). The data represents the mean ± SD of optical density (OD) values for duplicate standard concentrations (*n*=2).

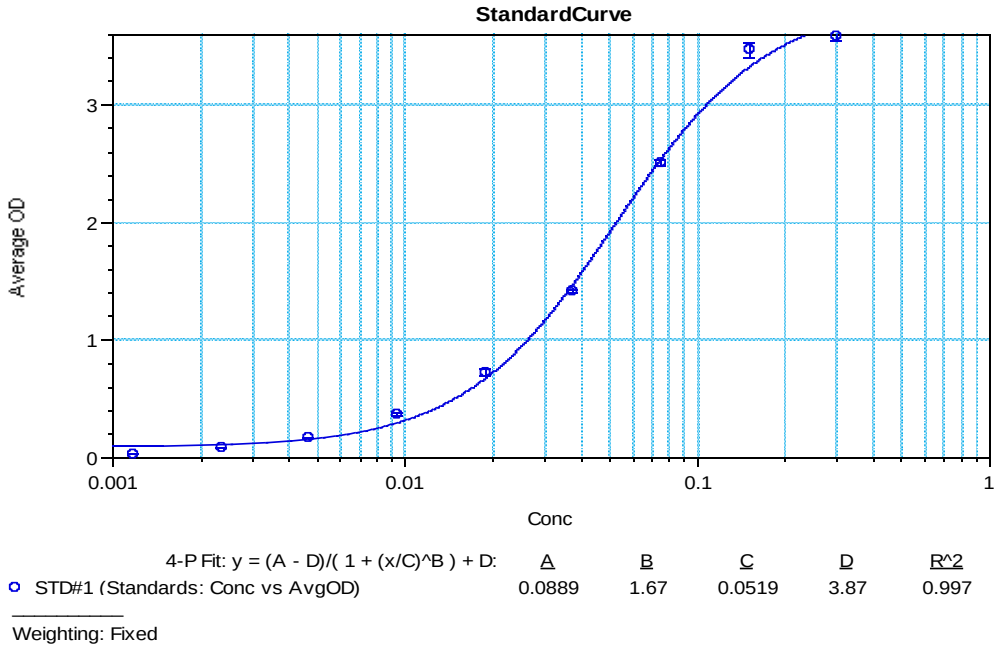

Figure S3.13: A representative 4-parameter logistic plot of IL-10 standard samples of 8 points showing the values of a, b, c, and d constants and the calibration equation with a best fit (R^2=0.997). The data represents the mean ± SD of optical density (OD) values for duplicate standard concentrations (*n*=2).

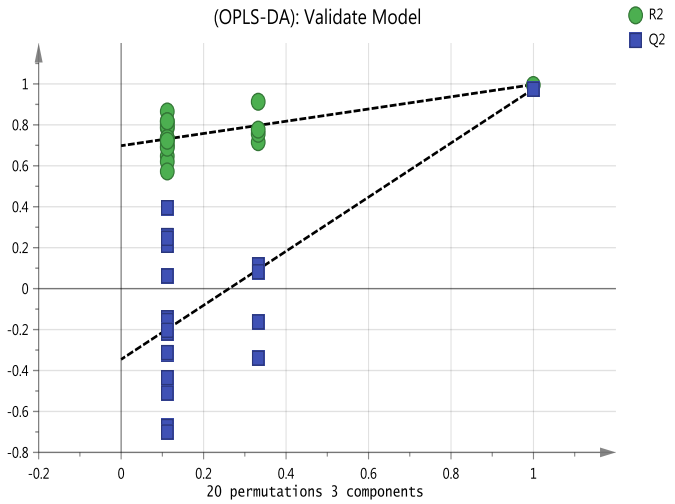

Figure S3.14: Validation of OPLS-DA by permutation test of THP-1 cells treated with LPS, Melittin and Melittin +LPS. The plot shows, the vertical axis gives the R2Y and Q2Y values of each model. The horizontal axis represents the correlation coefficient between the original Y (= 1.0), and the permuted Y.

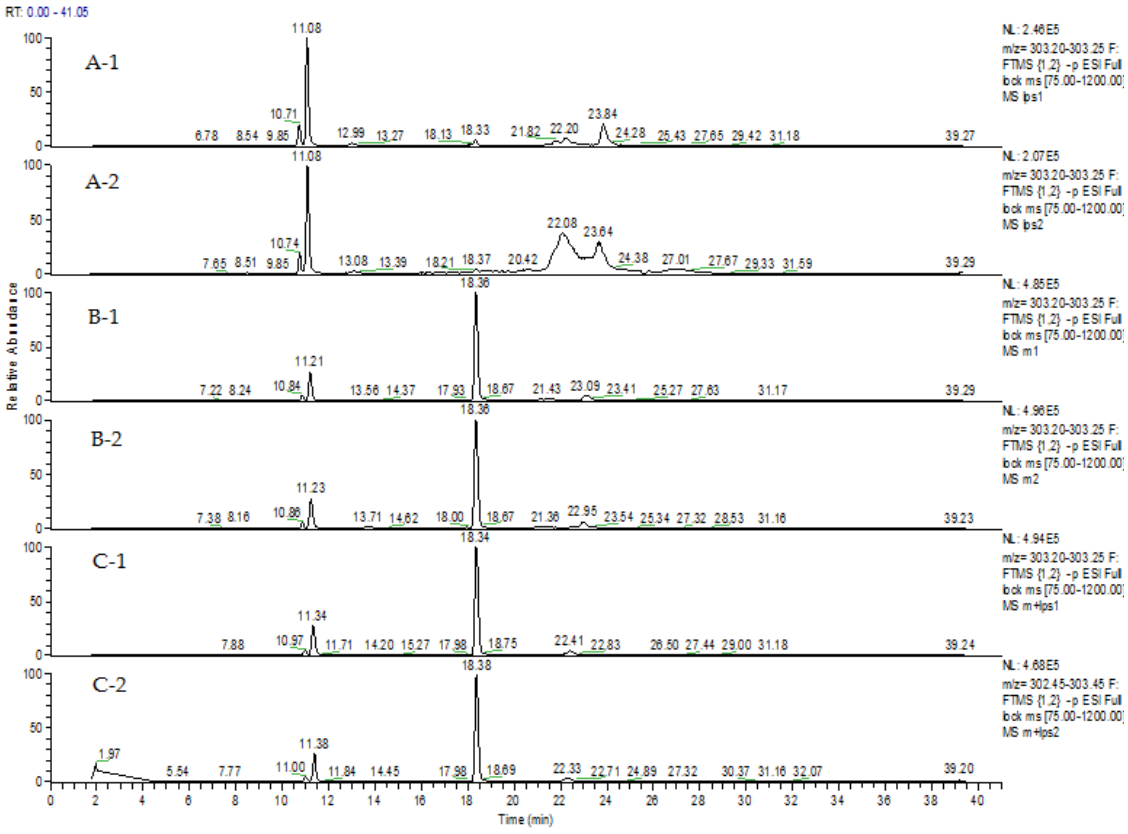

Figure S3.15: Extracted ion chromatograms for arachidonic acid in THP-1 cells after treated by LPS (A), melittin (B) and the combination of melittin and LPS (C). The level of the arachidonic acid elevated significantly by melittin alone or in combination with LPS. The biological samples were analysed using ACE C4 column.

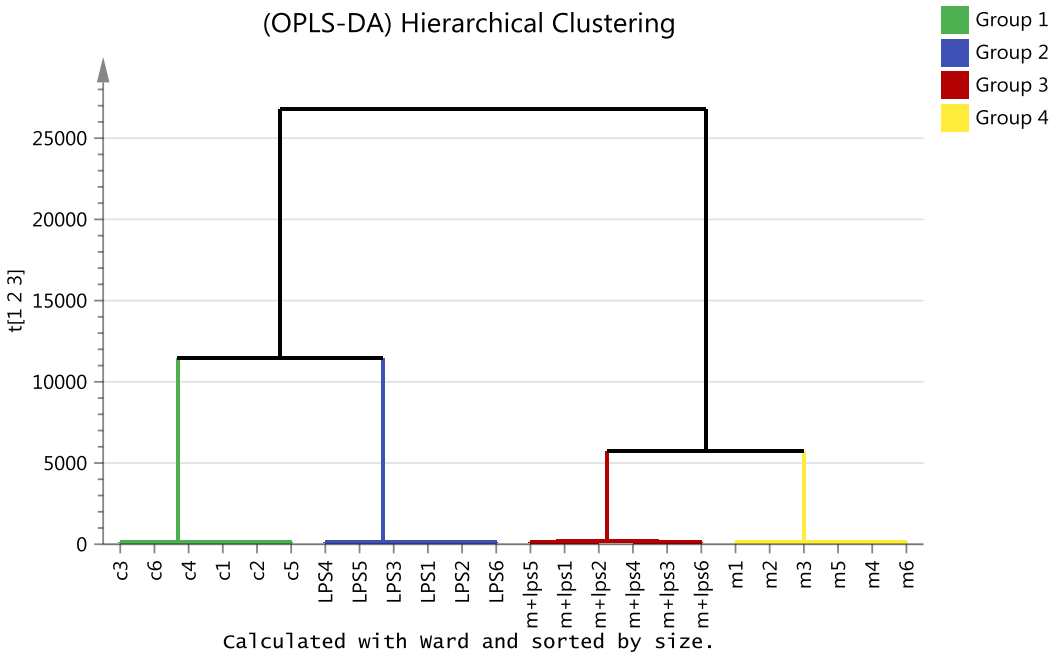

Figure S3.16: Hierarchical clustering analysis (HCA) of 24 THP-1 cells samples.

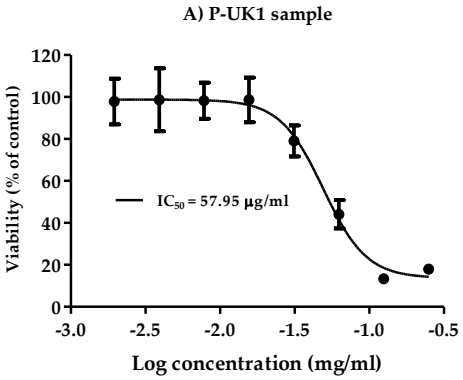
A) P-UK1 sample
Viability (% of control)
IC50 = 57.95 µg/ml
Log concentration (mg/ml)

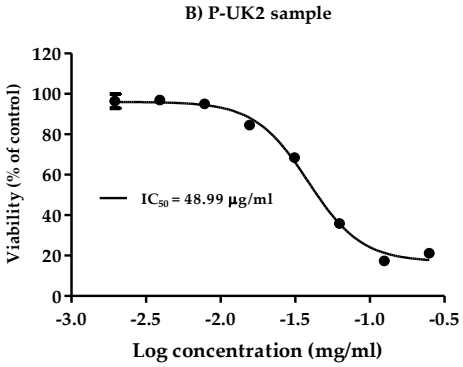
B) P-UK2 sample
Viability (% of control)
IC50 = 48.99 µg/ml
Log concentration (mg/ml)

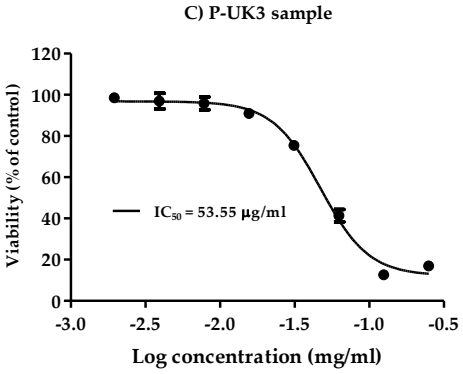
C) P-UK3 sample
Viability (% of control)
IC50 = 53.55 µg/ml
Log concentration (mg/ml)

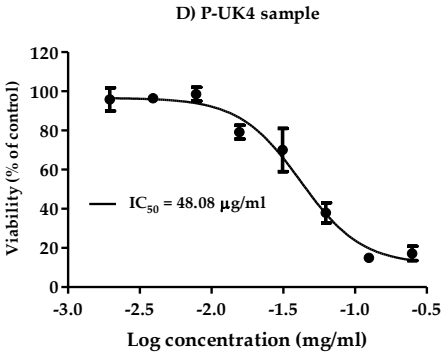
D) P-UK4 sample
Viability (% of control)
IC50 = 48.08 µg/ml
Log concentration (mg/ml)

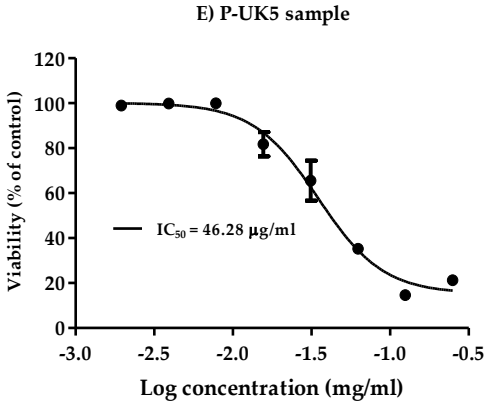
E) P-UK5 sample
Viability (% of control)
IC50 = 46.28 µg/ml
Log concentration (mg/ml)

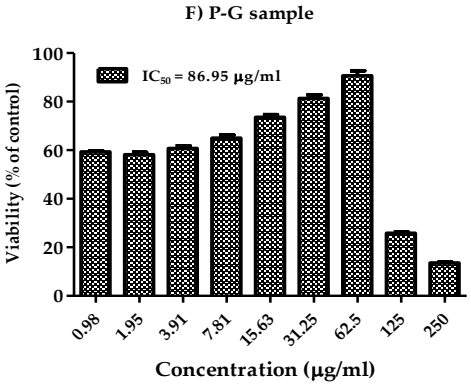
F) P-G sample
Viability (% of control)
IC50 = 86.95 µg/ml
0.98
1.95
3.91
7.81
15.63
31.25
62.5
125
250
Concentration (µg/ml)

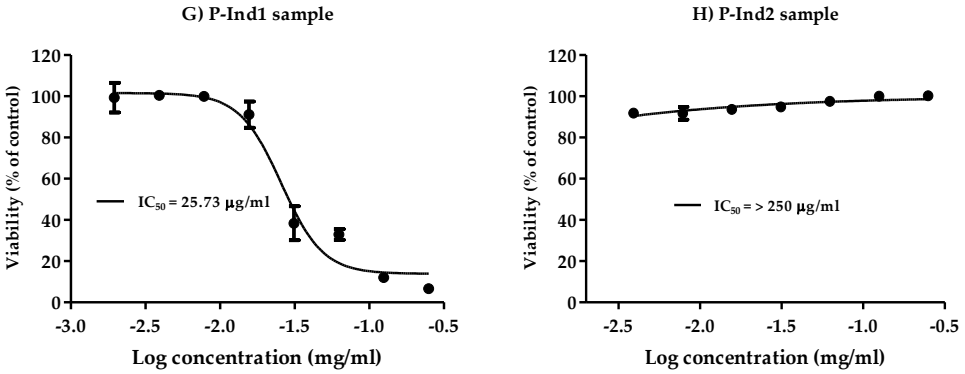

Figure S4.1: Cytotoxic effects of propolis extracts at varying doses on phorbol 12-myristate 13-acetate (PMA)-differentiated THP-1 cells. Each data point represents the mean ± SD (*n*=3).
P-UK (1-5): Five propolis extracts from the UK; P-G: Propolis from Ghana; P-Ind (1 and 2): Two Propolis extracts from Indonesia.

TNF-α production

Table S4.1: Effect of propolis extracts on the production of TNF-α cytokines in the presence and absence of LPS on PMA-differentiated THP-1 cells (n=3).

	TNF-α concentration (pg/ml)									
	Sample only					**Sample + LPS**				
Propolis Samples	n=1	n=2	n=3	Mean	RSD	n=1	n=2	n=3	Mean	RSD
P-UK1	21	2	94	39.00	124.54	981	1796	2093	1623.33	35.47
P-UK2	31	52	215	99.33	101.40	1526	1824	2112	1820.67	16.09
P-UK3	60	23	138	73.67	79.69	1304	1817	2089	1736.67	22.95
P-UK4	136	79	277	164.00	62.15	1573	1838	2121	1844.00	14.86
P-UK5	103	39	158	100.00	59.56	1519	1788	2136	1814.33	17.05
P-G	110	72	124	102.00	26.38	1218	1805	2104	1709.00	26.37
P-C	80	14	50	48.00	68.84	816	1813	2085	1571.33	42.52
P-Ind1	214	212	373	266.33	34.69	1237	1821	2141	1733.00	26.45
P-Ind2	<2.0	<2.0	<2.0	n/a	n/a	369	711	233	437.67	56.27
Media	113	132	196	147.00	29.58					
LPS	1521	1885	2183	1863.00	17.80					

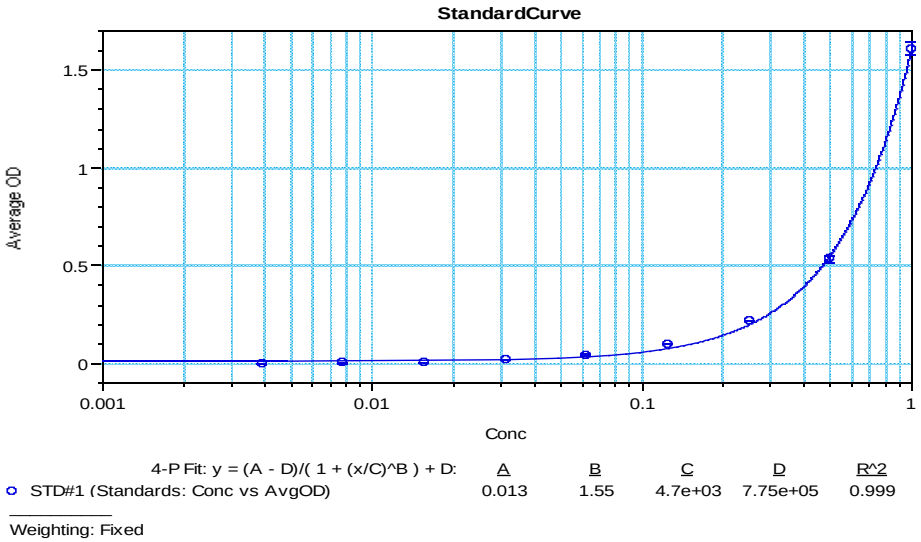

Figure S4.2: A representative 4-parameter logistic plot of TNF-α standard samples of 9 points showing the values of a, b, c, and d constants and the calibration equation with a best t fit (R2=0.999). The data represents the mean ± SD of optical density (OD) values for duplicate standard concentrations (n=2).

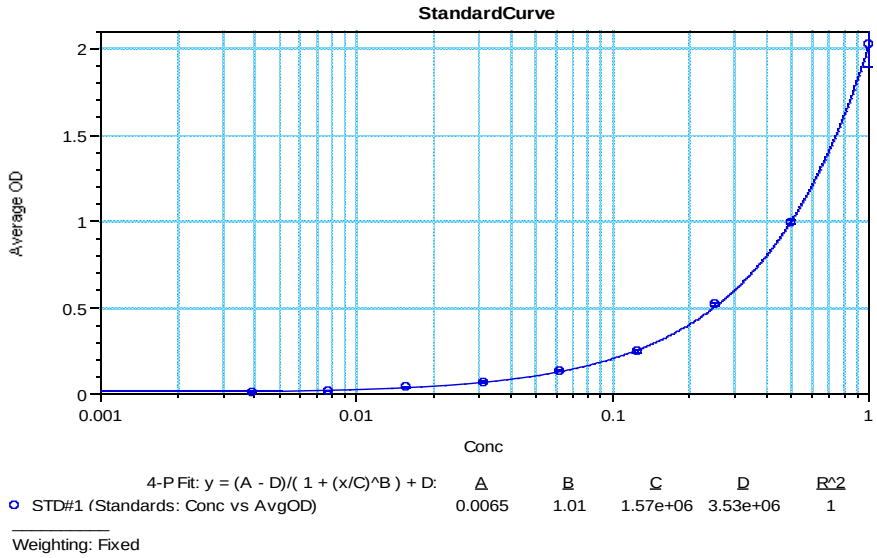

Figure S4.3: A representative 4-parameter logistic plot of TNF-α standard samples of 9 points showing the values of a, b, c, and d constants and the calibration equation with a best fit (R2=1.0). The data represents the mean ± SD of optical density (OD) values for duplicate standard concentrations (n=2).

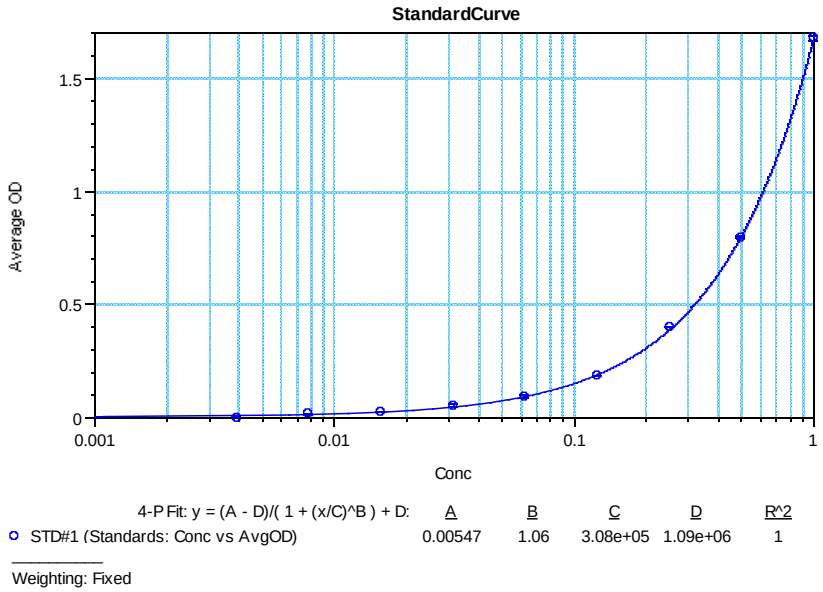

Figure S4.4: A representative 4-parameter logistic plot of TNF-α standard samples of 9 points showing the values of a, b, c, and d constants and the calibration equation with a best fit (R2=1.0). The data represents the mean ± SD of optical density (OD) values for duplicate standard concentrations (n=2).

IL-1β production

Table S4.2: Effect of propolis extracts on the production of IL-1β cytokines in the presence and absence of LPS on PMA-differentiated THP-1 cells (n=3).

	IL-1β concentration (pg/ml)									
	Sample only					**Sample + LPS**				
Propolis Samples	n=1	n=2	n=3	Mean	RSD	n=1	n=2	n=3	Mean	RSD
P-UK1	19.00	33.00	10.00	20.67	56.08	59.00	58.00	89.00	68.67	25.65
P-UK2	28.00	21.00	14.00	21.00	33.33	36.00	52.00	47.00	45.00	18.19
P-UK3	7.00	17.00	14.00	12.67	40.51	29.00	41.00	60.00	43.33	36.07
P-UK4	5.00	12.00	11.00	9.33	40.56	27.00	42.00	42.00	37.00	23.41
P-UK5	8.00	20.00	12.00	13.33	45.83	28.00	41.00	57.00	42.00	34.59
P-G	36.00	46.00	44.00	42.00	12.60	110.00	89.00	112.00	103.67	12.29
P-C	14.00	37.00	9.00	20.00	74.67	50.00	31.00	32.00	37.67	28.39
P-Ind1	9.00	18.00	12.00	13.00	35.25	79.00	77.00	120.00	92.00	26.38
P-Ind2	27.00	28.00	13.00	22.67	37.00	93.00	108.00	110.00	103.67	8.96
Media	6.00	10.00	16.00	10.67	5.03					
LPS	60.00	60.00	63.00	61.00	1.73					

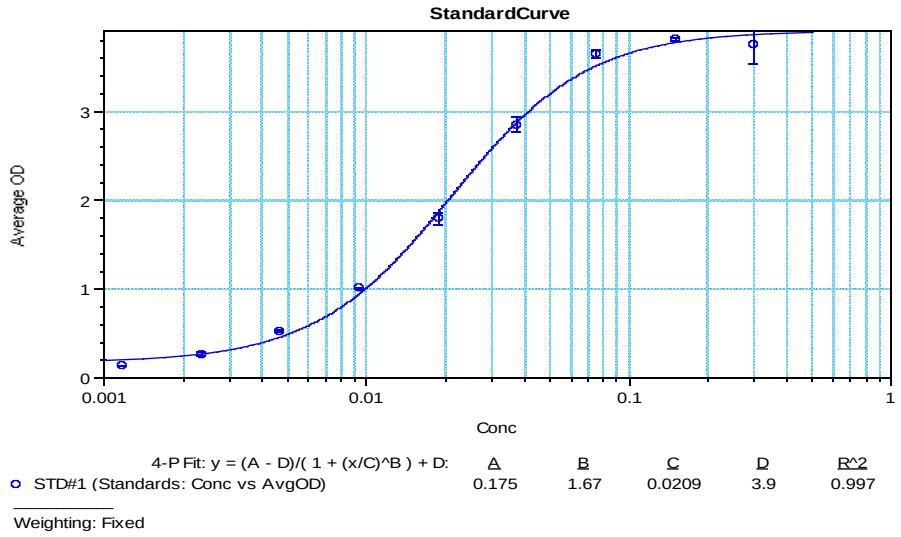

Figure S4.5: A representative 4-parameter logistic plot of IL-1β standard samples of 9 points showing the values of a, b, c, and d constants and the calibration equation with a best fit (R2=0.997). The data represents the mean ± SD of optical density (OD) values for duplicate standard concentrations (n=2).

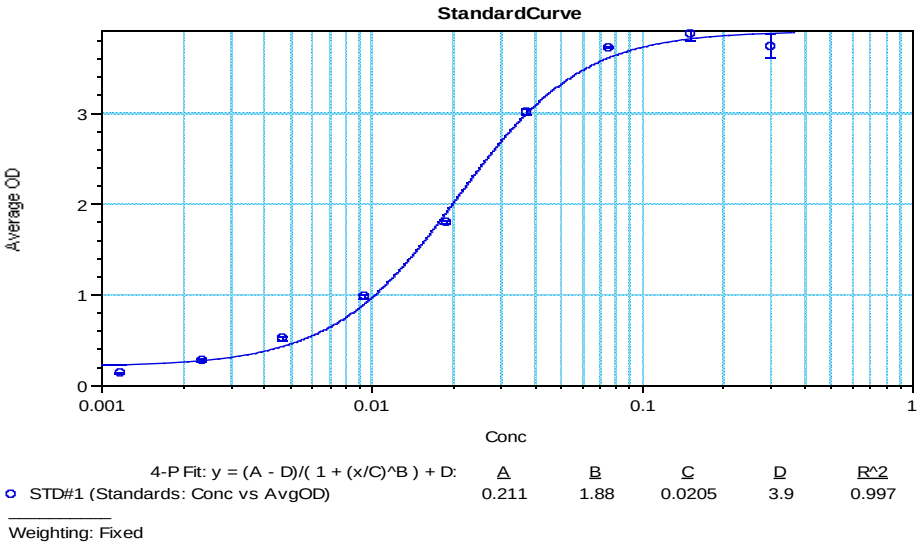

Figure S4.6: A representative 4-parameter logistic plot of IL-1β standard samples of 9 points showing the values of a, b, c, and d constants and the calibration equation with a best fit (R2=0.997). The data represents the mean ± SD of optical density (OD) values for duplicate standard concentrations (n=2).

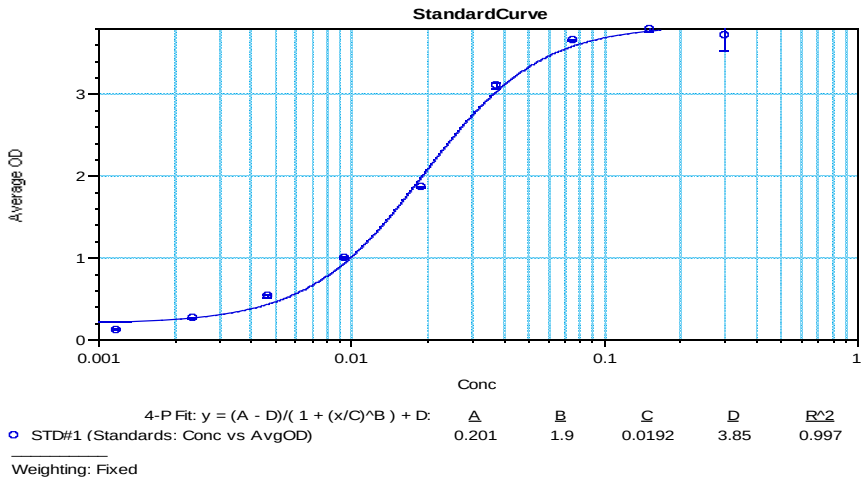

Figure S4.7: A representative 4-parameter logistic plot of IL-1β standard samples of 9 points showing the values of a, b, c, and d constants and the calibration equation with a best fit (R2=0.997). The data represents the mean ± SD of optical density (OD) values for duplicate standard concentrations (n=2).

IL-6 production

Table S4.3: Effect of propolis extracts on the production of IL-6 cytokines in the presence and absence of LPS on PMA-differentiated THP-1 cells (n=3).

	IL-6 concentration (pg/ml)									
	Sample only					**Sample + LPS**				
Propolis Samples	**n=1**	**n=2**	**n=3**	**Mean**	**RSD**	**n=1**	**n=2**	**n=3**	**Mean**	**RSD**
P-UK1	<2.0	<2.0	<2.0	n/a	n/a	13	11	12	12.00	8.33
P-UK2	<2.0	<2.0	<2.0	n/a	n/a	47	37	49	44.33	14.50
P-UK3	<2.0	<2.0	<2.0	n/a	n/a	46	34	49	43.00	18.46
P-UK4	<2.0	<2.0	<2.0	n/a	n/a	55	48	65	56.00	15.26
P-UK5	<2.0	<2.0	<2.0	n/a	n/a	53	45	49	49.00	8.16
P-G	<2.0	<2.0	<2.0	n/a	n/a	19	20	20	19.67	2.94
P-C	<2.0	<2.0	<2.0	n/a	n/a	26	25	20	23.67	13.58
P-Ind1	<2.0	<2.0	<2.0	n/a	n/a	50	39	41	43.33	13.52
P-Ind2	<2.0	<2.0	<2.0	n/a	n/a	1	<2.0	1	1	n/a
Media	<2.0	<2.0	<2.0	n/a	n/a					
LPS	111	113	82	102	17.01					

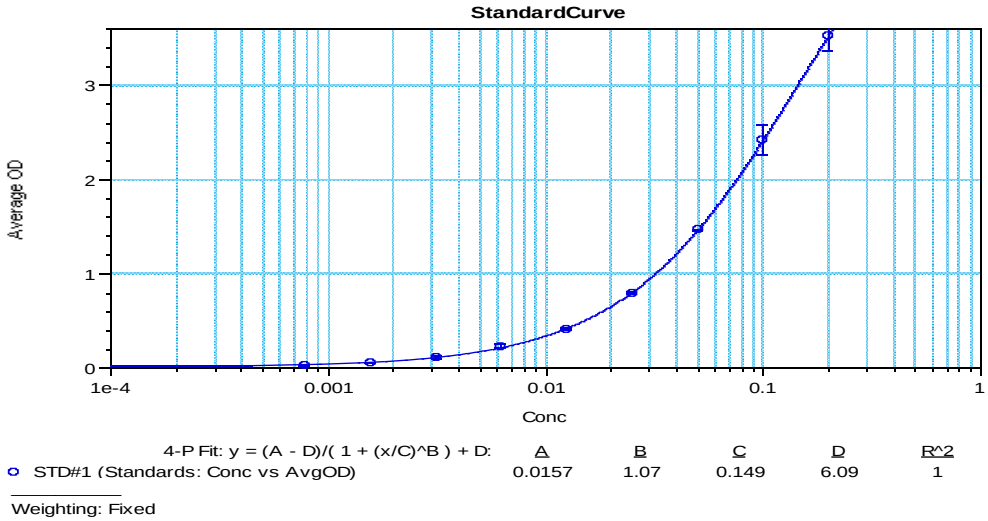

Figure S4.8: A representative 4-parameter logistic plot of IL-6 standard samples of 8 points showing the values of a, b, c, and d constants and the calibration equation with a best fit (R2=1). The data represents the mean ± SD of optical density (OD) values for duplicate standard concentrations (n=2).

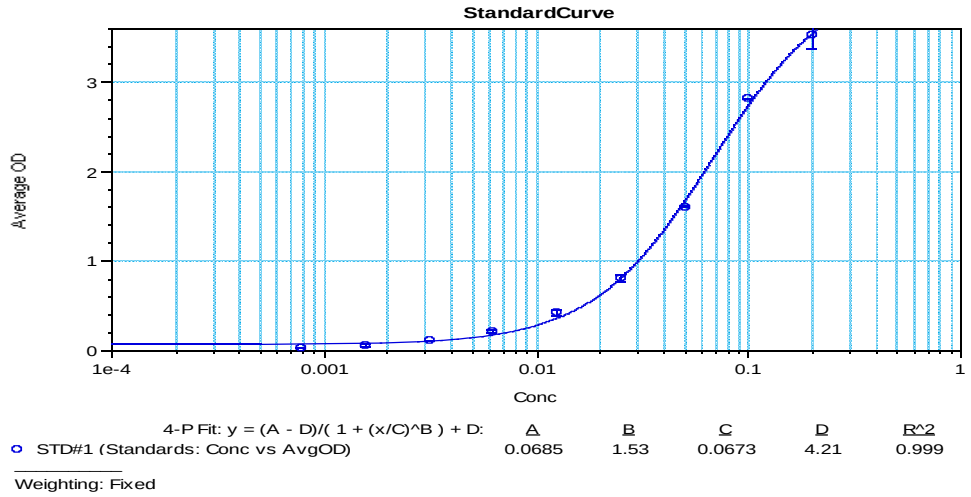

Figure S4.9: A representative 4-parameter logistic plot of IL-6 standard samples of 8 points showing the values of a, b, c, and d constants and the calibration equation with a best fit (R2=0.999). The data represents the mean ± SD of optical density (OD) values for duplicate standard concentrations (n=2).

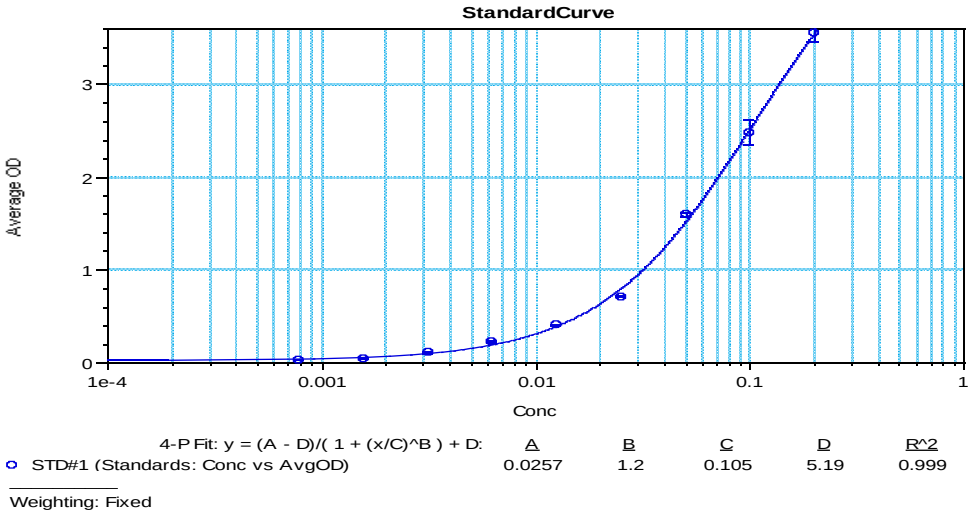

Figure S4.10: A representative 4-parameter logistic plot of IL-6 standard samples of 8 points showing the values of a, b, c, and d constants and the calibration equation with a best fit (R2=0.999). The data represents the mean ± SD of optical density (OD) values for duplicate standard concentrations (n=2).

IL-10 production

Table S4.4: Effect of propolis extracts on the production of IL-10 cytokines in the presence and absence of LPS on PMA-differentiated THP-1 cells (n=3).

	IL-10 concentration (pg/ml)									
	Sample only					**Sample + LPS**				
Propolis Samples	**n=1**	**n=2**	**n=3**	**Mean**	**RSD**	**n=1**	**n=2**	**n=3**	**Mean**	**RSD**
P-UK1	16	19	5	13.33	55.28	18	10	7	11.67	48.74
P-UK2	21	25	7	17.67	53.50	16	13	11	13.33	18.87
P-UK3	11	26	6	14.33	72.62	14	12	10	12.00	16.67
P-UK4	14	17	8	13.00	35.25	19	15	13	15.67	19.50
P-UK5	15	25	8	16.00	53.40	17	14	11	14.00	21.43
P-G	9	12	4	8.33	48.50	13	8	7	9.33	34.44
P-C	19	25	6	16.67	58.28	33	14	10	19.00	64.67
P-Ind1	14	18	5	12.33	53.99	31	17	11	19.67	52.19
P-Ind2	6	2	<2.0	4.00	70.71	<2.0	<2.0	<2.0	n/a	n/a
Media	15.00	14.00	10.00	13.00	20.35					
LPS	30.00	21.00	26.00	25.67	17.57					

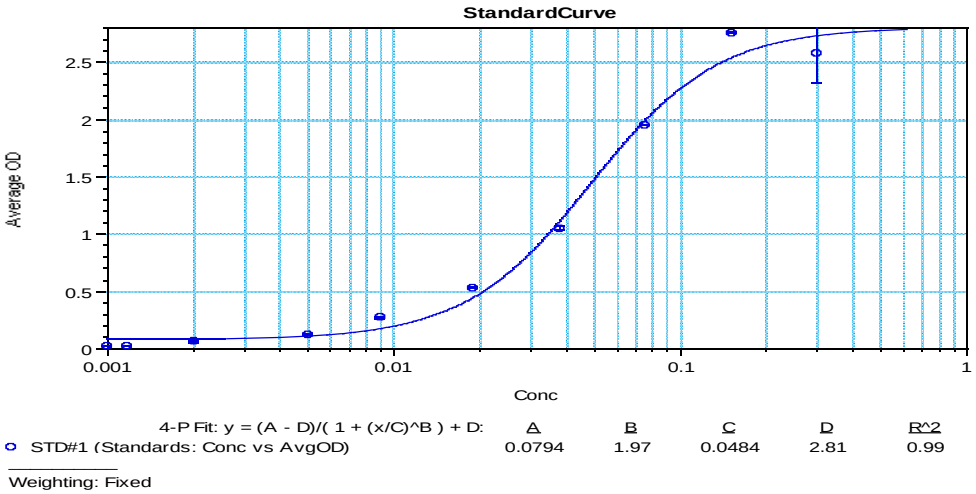

Figure S4.11: A representative 4-parameter logistic plot of IL-10 standard samples of 9 points showing the values of a, b, c, and d constants and the calibration equation with a best fit (R2=0.99). The data represents the mean ± SD of optical density (OD) values for duplicate standard concentrations (n=2).

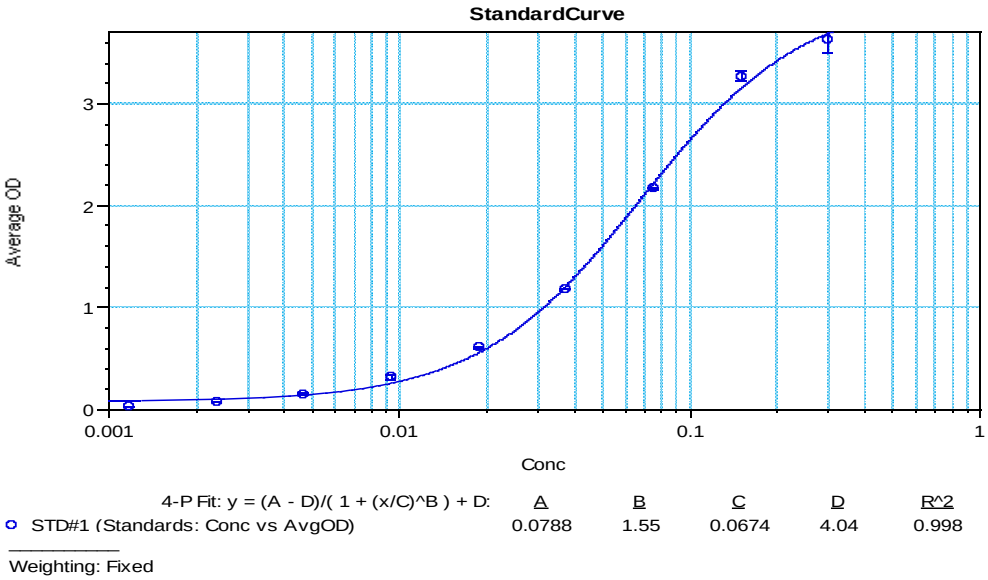

Figure S4.12: A representative 4-parameter logistic plot of IL-10 standard samples of 9 points showing the values of a, b, c, and d constants and the calibration equation with a best fit (R2=0.998). The data represents the mean ± SD of optical density (OD) values for duplicate standard concentrations (n=2).

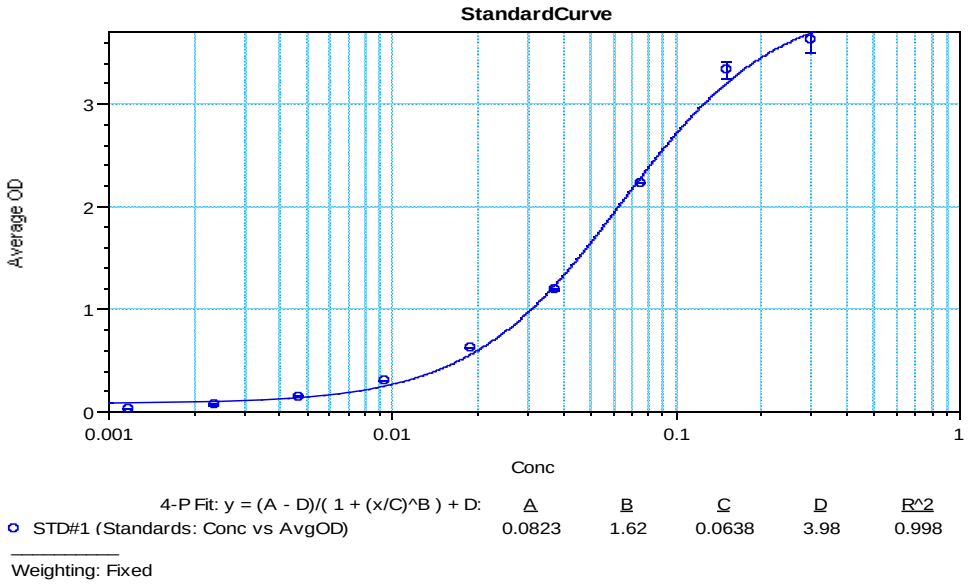

Figure S4.13: A representative 4-parameter logistic plot of IL-10 standard samples of 9 points showing the values of a, b, c, and d constants and the calibration equation with a best fit (R2=0.998). The data represents the mean ± SD of optical density (OD) values for duplicate standard concentrations (n=2).

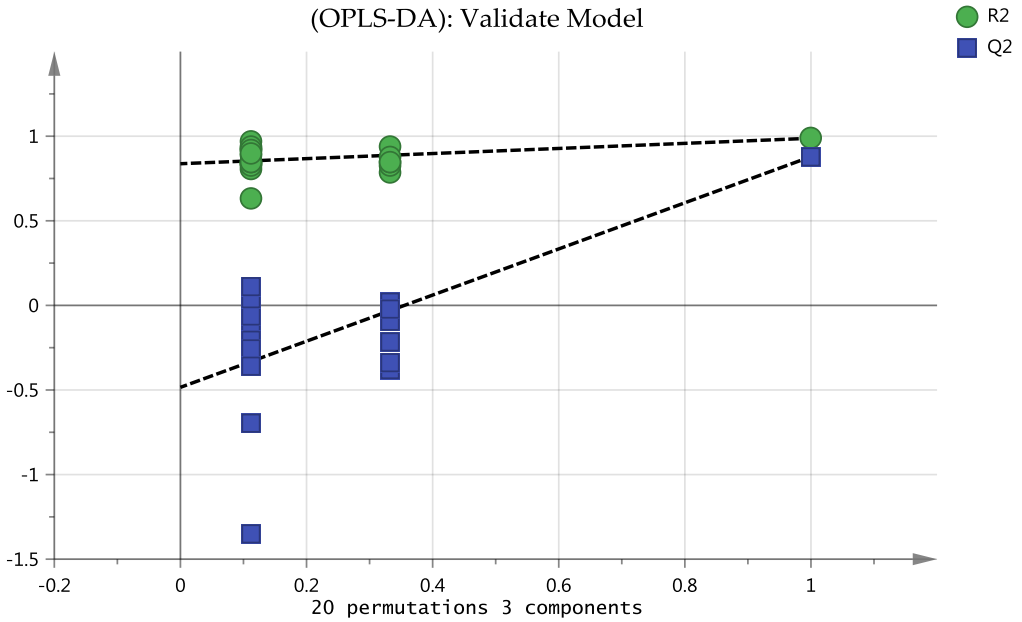

Figure S4.14: Validation of OPLS-DA by permutation test of THP-1 cells treated with LPS, P-C and P-C +LPS. The plot shows, the vertical axis gives the R2Y and Q2Y values of each model. The horizontal axis represents the correlation coefficient between the original Y (= 1.0), and the permuted Y.

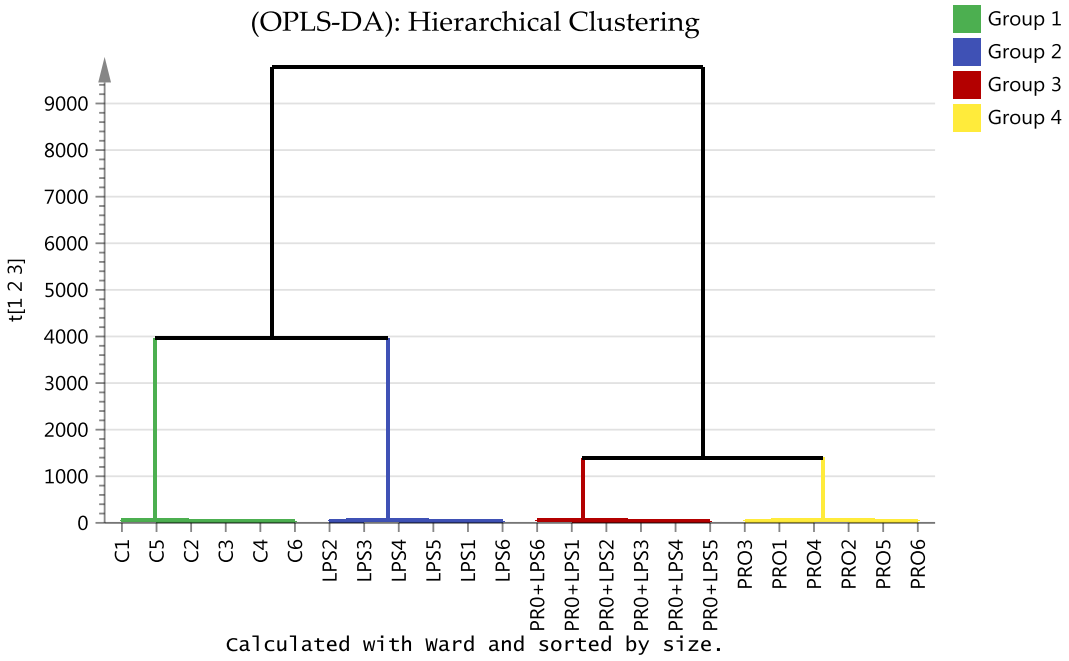

Figure S4.15: Hierarchical clustering analysis (HCA) of 24 THP-1 cells samples.

Chapter 5:

TNF-α production

Table S5.1: Effect of eicosenoid compounds on the production of TNF-α cytokines in the presence and absence of LPS on PMA-differentiated THP-1 cells (*n*=3).

	TNF-α concentration (pg/ml)									
	Sample only					**Sample + LPS**				
Eicosenoid compounds	n=1	n=2	n=3	Mean	RSD	n=1	n=2	n=3	Mean	RSD
(11E)-OH	422	375	273	356.67	21.36	592	586	595	591.00	0.78
(11E)-ester	52	29	4	28.33	84.73	537	578	581	565.33	4.35
(11E)-acid	182	155	37	124.67	61.85	599	615	604	606.00	1.35
Media	100	83	98	93.67	9.92					
LPS	572	572	587	577.00	1.50					

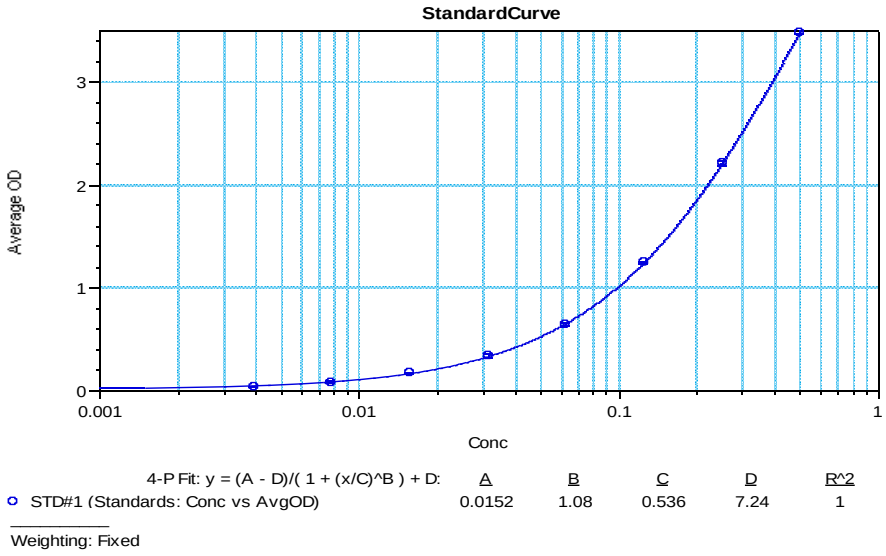

Figure S5.1: A representative 4-parameter logistic plot of TNF-α standard samples of 8 points showing the values of a, b, c, and d constants and the calibration equation with a bestt fit (R^2=1.0). The data represents the mean ± SD of optical density (OD) values for duplicate standard concentrations (*n*=2).

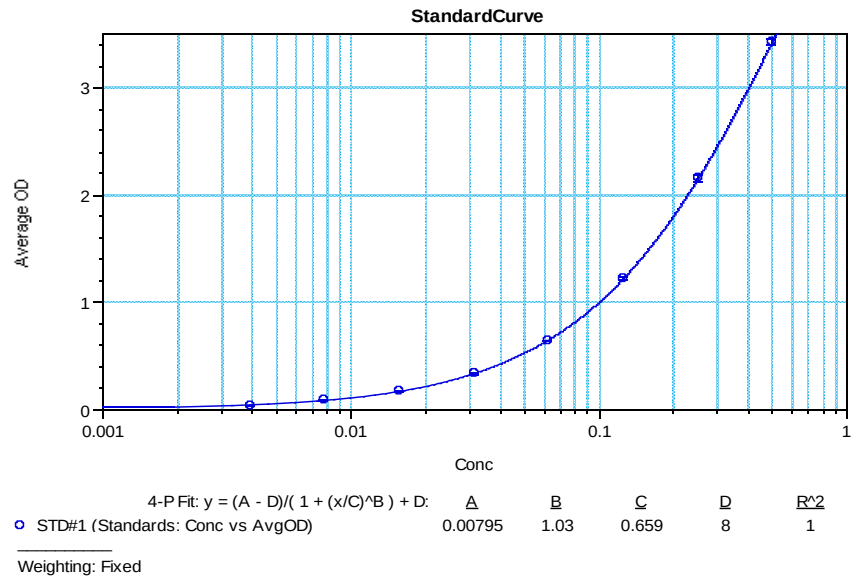

Figure S5.2: A representative 4-parameter logistic plot of TNF-α standard samples of 8 points showing the values of a, b, c, and d constants and the calibration equation with a best fit (R^2=1.0). The data represents the mean ± SD of optical density (OD) values for duplicate standard concentrations (*n*=2).

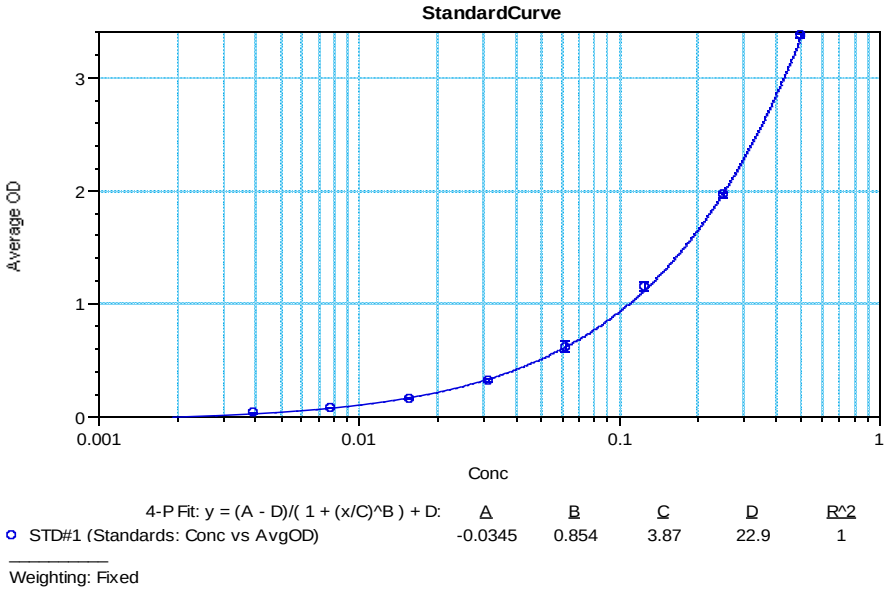

Figure S5.3: A representative 4-parameter logistic plot of TNF-α standard samples of 8 points showing the values of a, b, c, and d constants and the calibration equation with a best fit (R^2=1.0). The data represents the mean ± SD of optical density (OD) values for duplicate standard concentrations (*n*=2).

IL-1β production

Table S5.2: Effect of eicosenoid compounds on the production of IL-1β cytokines in the presence and absence of LPS on PMA-differentiated THP-1 cells (*n*=3).

	IL-1β concentration (pg/ml)									
	Sample only					**Sample + LPS**				
Eicosenoid compounds	n=1	n=2	n=3	Mean	RSD	n=1	n=2	n=3	Mean	RSD
(11E)-OH	90	86	26	67.33	53.24	158	110	85	117.67	31.53
(11E)-ester	73	22	10	35.00	95.58	152	129	135	138.67	8.60
(11E)-acid	124	83	35	80.67	55.22	181	123	120	141.33	24.33
Media	47	47	37	43.67	13.22					
LPS	82	78	68	76	9.48					

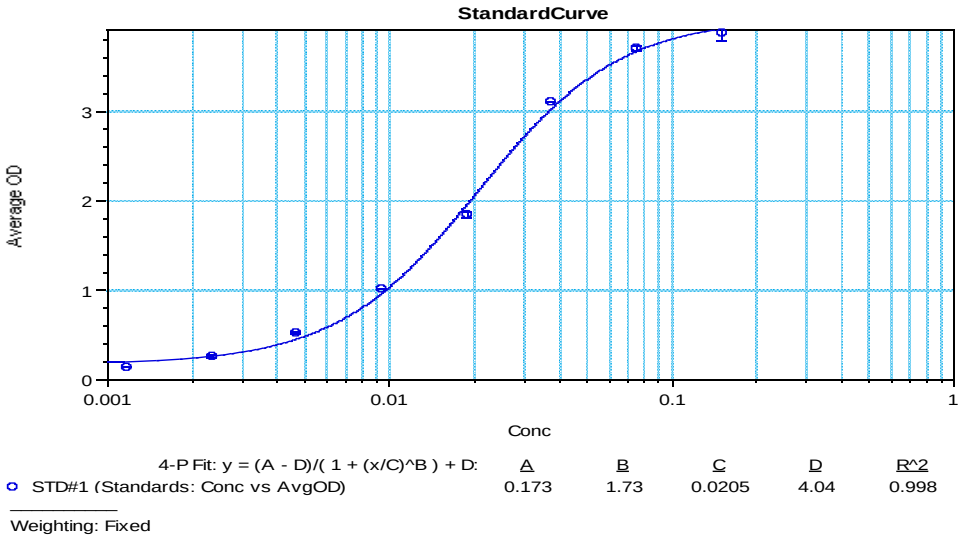

Figure S5.4: A representative 4-parameter logistic plot of IL-1β standard samples of 8 points showing the values of a, b, c, and d constants and the calibration equation with a best fit (R^2=0.998). The data represents the mean ± SD of optical density (OD) values for duplicate standard concentrations (*n*=2).

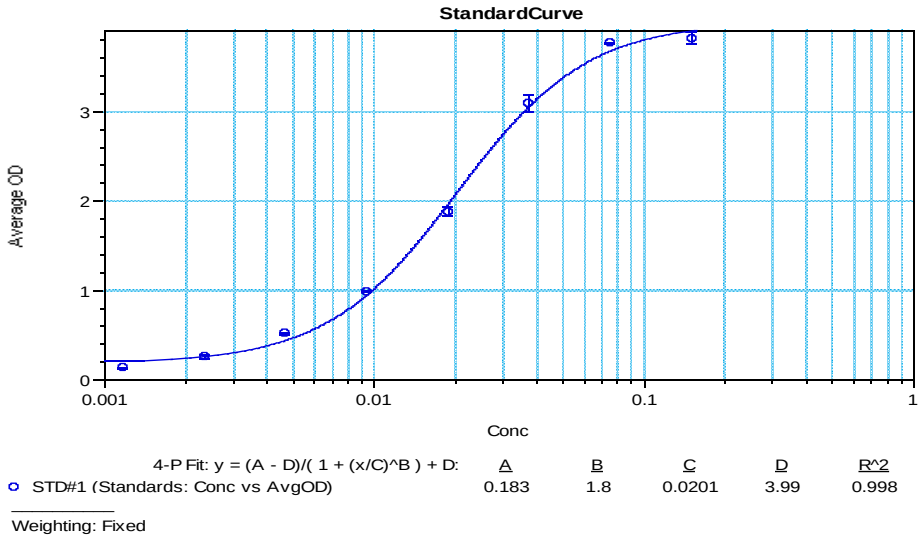

Figure S5.5: A representative 4-parameter logistic plot of IL-1β standard samples of 8 points showing the values of a, b, c, and d constants and the calibration equation with a best fit (R^2=0.998). The data represents the mean ± SD of optical density (OD) values for duplicate standard concentrations (*n*=2).

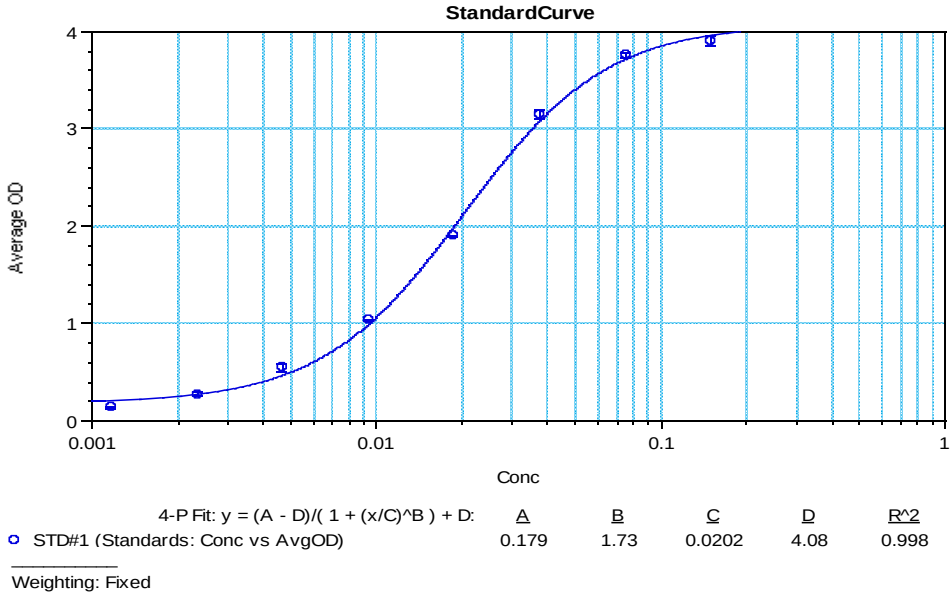

Figure S5.6: A representative 4-parameter logistic plot of IL-1β standard samples of 8 points showing the values of a, b, c, and d constants and the calibration equation with a best fit (R^2=0.998). The data represents the mean ± SD of optical density (OD) values for duplicate standard concentrations (*n*=2).

IL-6 production

Table S5.3: Effect of eicosenoid compounds on the production of IL-6 cytokines in the presence and absence of LPS on PMA-differentiated THP-1 cells (*n*=3).

	IL-6 *concentration (pg/ml)*									
	Sample only					**Sample + LPS**				
Eicosenoid compounds	n=1	n=2	n=3	Mean	RSD	n=1	n=2	n=3	Mean	RSD
(11E)-OH	<2.0	<2.0	<2.0	n/a	n/a	38	62	71	57	29.93
(11E)-ester	<2.0	<2.0	<2.0	n/a	n/a	<2.0	<2.0	<2.0	<2.0	n/a
(11E)-acid	<2.0	<2.0	<2.0	n/a	n/a	21.00	47.00	39.00	35.67	37.34
Media	<2.0	<2.0	<2.0	n/a	n/a					
LPS	88.00	104.00	114.00	102.00	12.86					

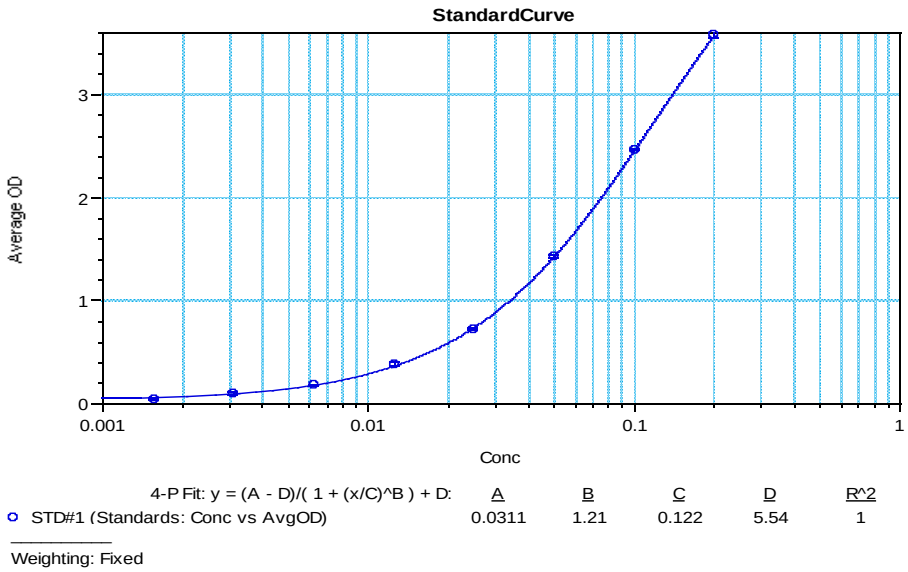

Figure S5.7: A representative 4-parameter logistic plot of IL-6 standard samples of 8 points showing the values of a, b, c, and d constants and the calibration equation with a best fit (R^2=1). The data represents the mean ± SD of optical density (OD) values for duplicate standard concentrations (*n*=2).

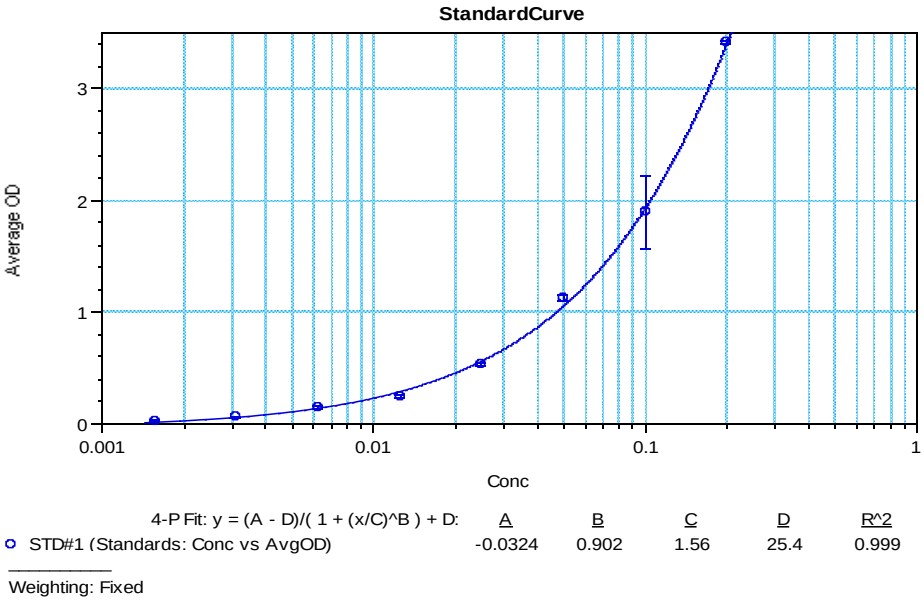

Figure S5.8: A representative 4-parameter logistic plot of IL-6 standard samples of 8 points showing the values of a, b, c, and d constants and the calibration equation with a bestfit (R^2=0.999). The data represents the mean ± SD of optical density (OD) values for duplicate standard concentrations (*n*=2).

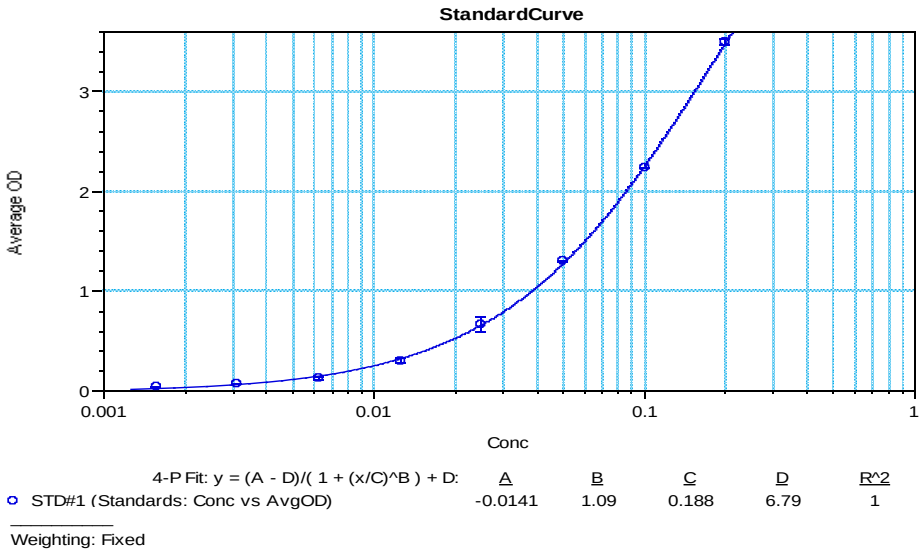

Figure S5.9: A representative 4-parameter logistic plot of IL-6 standard samples of 8 points showing the values of a, b, c, and d constants and the calibration equation with a best fit (R^2=1). The data represents the mean ± SD of optical density (OD) values for duplicate standard concentrations (*n*=2).

IL-10 production

Table S5.4: Effect of eicosenoid compounds on the production of IL-10 cytokines in the presence and absence of LPS on PMA-differentiated THP-1 cells (*n*=3).

	IL-10 *concentration (pg/ml)*									
	Sample only					**Sample + LPS**				
Eicosenoid compounds	n=1	n=2	n=3	Mean	RSD	n=1	n=2	n=3	Mean	RSD
(11E)-OH	10.0	10.0	6.00	8.67	26.65	14.00	15.00	17.00	15.33	9.96
(11E)-ester	3.00	<2.0	<2.0	3	n/a	<2.0	3.00	6.00	4.5	47.14
(11E)-acid	5.00	4.00	5.00	4.67	12.37	8.00	12.00	12.00	10.67	21.65
Media	5.00	2.00	9.00	5.33	65.85					
LPS	20.00	21.00	23.00	21.33	7.16					

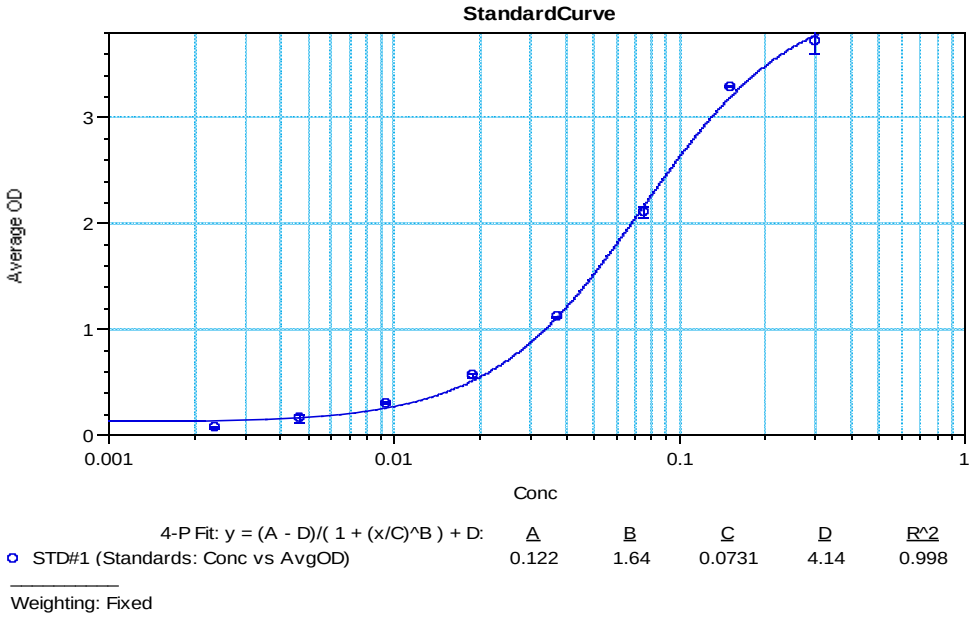

Figure S5.10: A representative 4-parameter logistic plot of IL-10 standard samples of 8 points showing the values of a, b, c, and d constants and the calibration equation with a best fit (R^2=0.998). The data represents the mean ± SD of optical density (OD) values for duplicate standard concentrations (*n*=2).

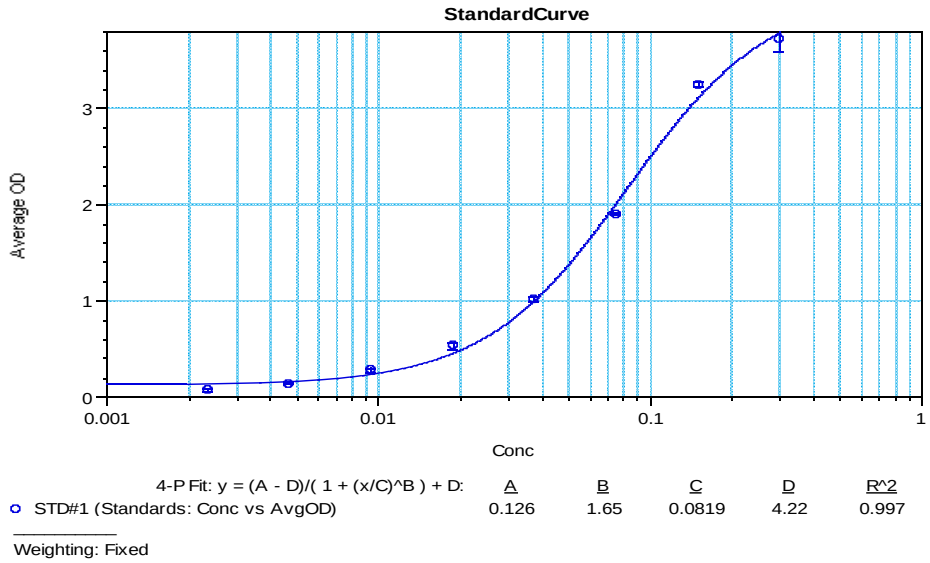

Figure S5.11: A representative 4-parameter logistic plot of IL-10 standard samples of 8 points showing the values of a, b, c, and d constants and the calibration equation with a best fit (R^2=0.997). The data represents the mean ± SD of optical density (OD) values for duplicate standard concentrations (*n*=2).

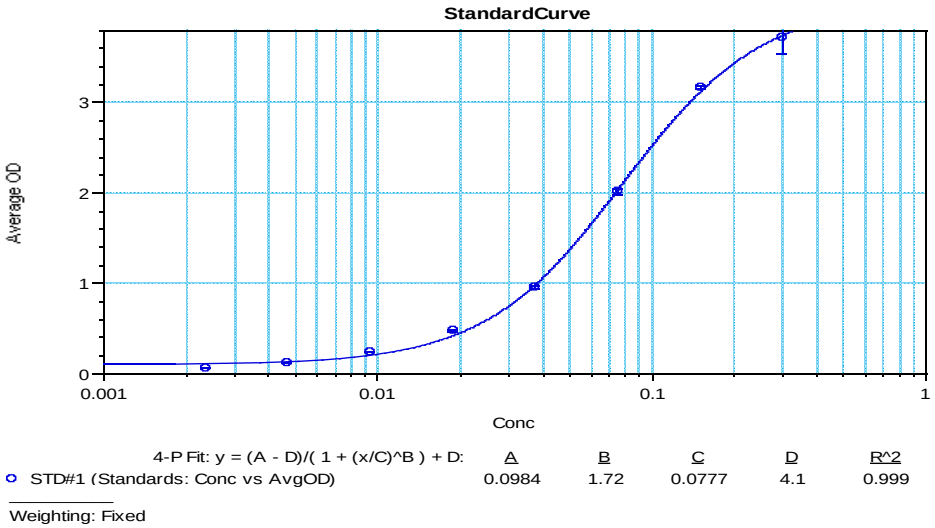

Figure S5.12: A representative 4-parameter logistic plot of IL-10 standard samples of 8 points showing the values of a, b, c, and d constants and the calibration equation with a best fit (R^2=0.999). The data represents the mean ± SD of optical density (OD) values for duplicate standard concentrations (*n*=2).

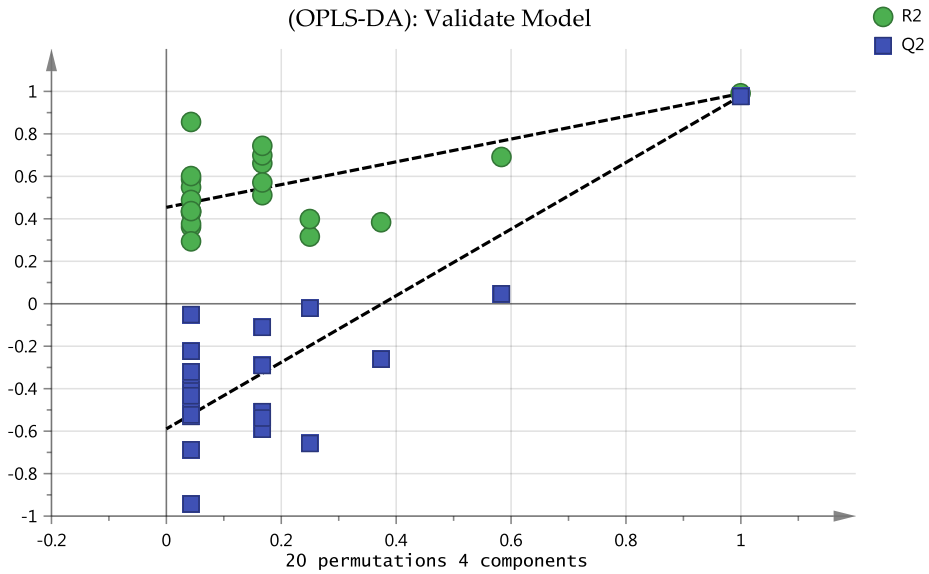

Figure S5.13: Validation of OPLS-DA by permutation test of THP-1 cells treated with LPS, eicosenoid and eicosenoid +LPS. The plot shows, the vertical axis gives the R2Y and Q2Y values of each model. The horizontal axis represents the correlation coefficient between the original Y (= 1.0), and the permuted Y.

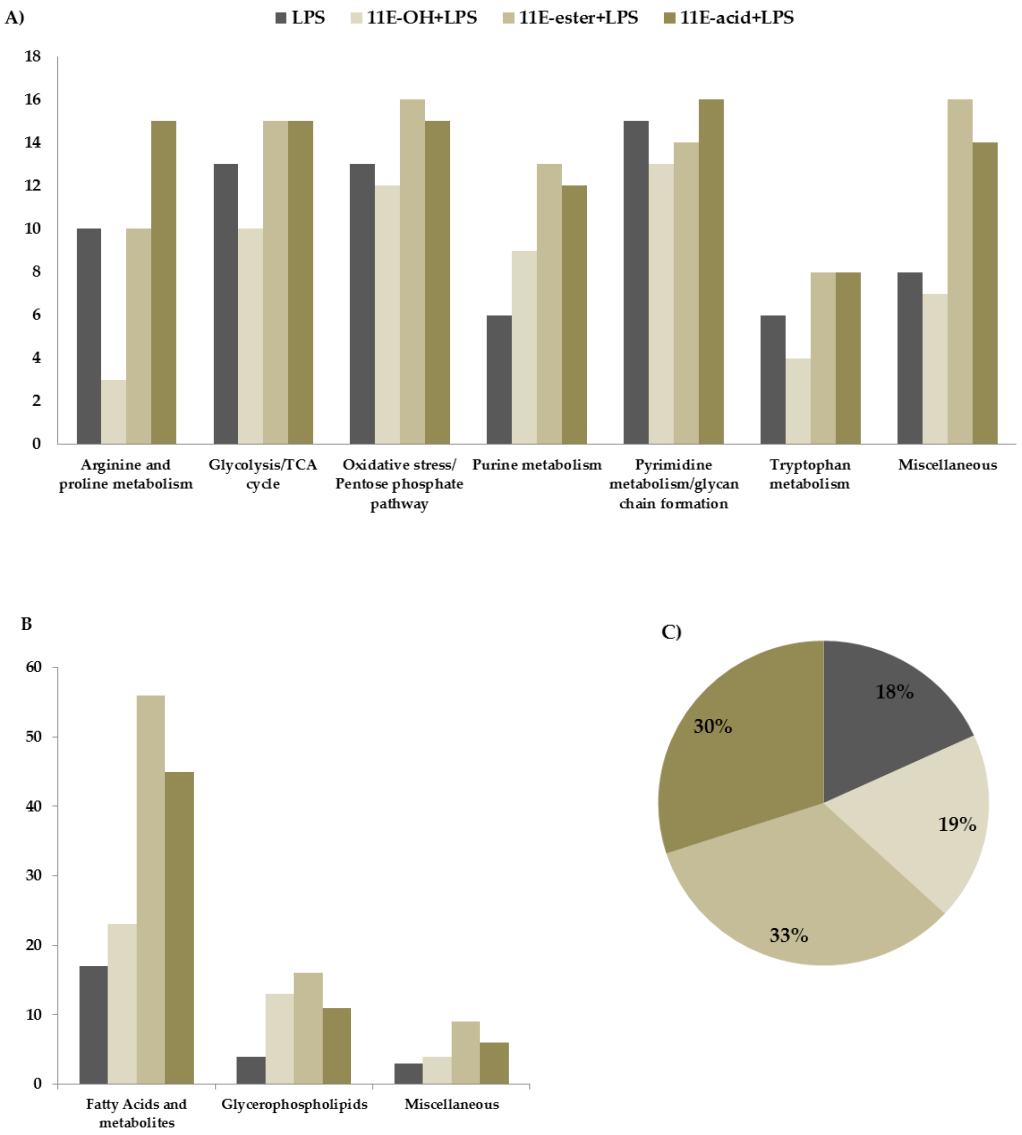

Figure S5.14: Changes in metabolites by treatment with LPS alone or in combination with one of three forms of eicosenoid derivatives when compared with untreated control cells. **(A)** Metabolites separated on a ZIC-pHILIC column and **(B)** on an ACE C4 column. **(C)** Percentage of significantly changed metabolites by treatments. (LPS: Lipopolysaccharide; (11E-OH): (Z)-11-eicosenol; (11E-ester): Eicosenoate; (11E-acid): Eicosenoic acid).

Table S5.5: Additional changed non-polar metabolites in THP-1 cells treated with lipopolysaccharide (LPS), alone or in combination with one of three synthetic forms of honey bee eicosenoids

Mass	Rt	Putative Metabolite	LPS/C		11E-OH + LPS/C		11E-ester + LPS/C		11E-acid + LPS/C	
			Ratio	p.value	Ratio	p.value	Ratio	p.value	Ratio	p.value
		Fatty acid and related metabolites								
270.220	15.12	3-oxo-hexadecanoic acid	1.018	ns	1.075	ns	1.154	0.003	1.141	0.006
244.167	6.55	Tridecanedioic acid	1.088	ns	1.268	ns	2.099	0.004	1.508	0.007
174.125	4.80	[FA hydroxy(9:0)] 2-hydroxy-nonanoic acid	1.241	ns	1.780	ns	2.082	0.017	1.813	0.012
342.277	21.13	Eicosanedioic acid*	0.979	ns	1.056	ns	1.118	0.034	1.167	0.010
396.397	29.61	hexacosanoic acid*	1.152	ns	1.070	ns	1.073	0.012	1.116	0.012
382.345	20.49	[FA hydroxy(24:0)] 2-hydroxy-15-tetracosenoic acid	0.981	ns	1.099	ns	1.176	0.001	1.148	0.013
244.204	11.64	2S-Hydroxytetradecanoic acid	0.740	<0.001	1.010	ns	0.920	ns	0.838	0.013
202.157	4.60	hydroxy-undecanoic acid	0.891	ns	4.096	<0.001	56.490	<0.001	2.130	0.032
270.256	20.57	heptadecanoic acid*	1.013	ns	1.043	ns	1.121	ns	1.087	0.044
156.079	25.56	5-oxo-7-octenoic acid	1.084	ns	1.156	ns	1.563	0.007	1.183	0.020
256.204	9.30	4-oxo-pentadecanoic acid	1.168	ns	1.262	ns	1.344	0.001	1.187	0.046
214.157	5.62	Oxododecanoic acid	1.072	ns	1.394	<0.001	1.465	<0.001	1.420	<0.001
354.313	20.75	10-oxo-docosanoic acid	1.013	ns	1.324	ns	8.329	<0.001	4.465	<0.001
346.235	12.85	9-hydroperoxy-12,13-dihydroxy-10-octadecenoic acid	0.935	ns	1.122	ns	100.996	0.010	1.858	ns
240.209	16.22	2,5-dimethyl-2E-tridecenoic acid	1.098	ns	1.029	ns	1.531	0.032	0.898	ns
340.298	17.05	2-oxo-heneicosanoic acid	1.007	ns	1.139	0.041	1.135	0.033	1.080	ns
426.371	26.35	Hexacosanedioic acid*	0.947	ns	1.035	ns	1.085	0.043	1.062	ns
216.172	8.55	Hydroxydodecanoic acid	0.564	0.001	0.946	ns	1.055	ns	0.904	ns
408.303	25.52	octacosaoctaenoic acid	2.604	0.029	1.653	ns	0.491	ns	1.717	ns
188.141	5.63	Hydroxydecanoic acid	0.747	0.040	1.334	ns	1.376	ns	1.173	ns

382.381	28.86	[FA (25:0)] pentacosanoic acid*	1.124	0.019	1.084	ns	1.106	0.011	1.128	0.001
389.260	9.17	N-(9Z-octadecenoyl)-taurine	0.924	ns	1.632	0.005	1.146	ns	1.143	ns
308.196	14.76	Trifluoro-11E-tetradecenyl acetate	1.599	0.007	1.524	0.027	2.133	0.004	1.484	0.017
300.266	14.33	9-methoxy-heptadecanoic acid	1.811	ns	1.328	ns	2.351	0.012	3.703	ns
268.204	7.94	3-oxo-2-pentyl-cyclopentanehexanoic acid	1.596	<0.001	1.155	ns	1.757	0.049	1.575	0.047
298.251	17.94	9-hydroxy-12Z-octadecenoic acid	1.059	ns	1.054	ns	1.080	0.011	1.100	0.037

Rt: Retention time (min); LPS: Lipopolysaccharides; *: Matches the analytical standard retention time; ns: Non-significant;

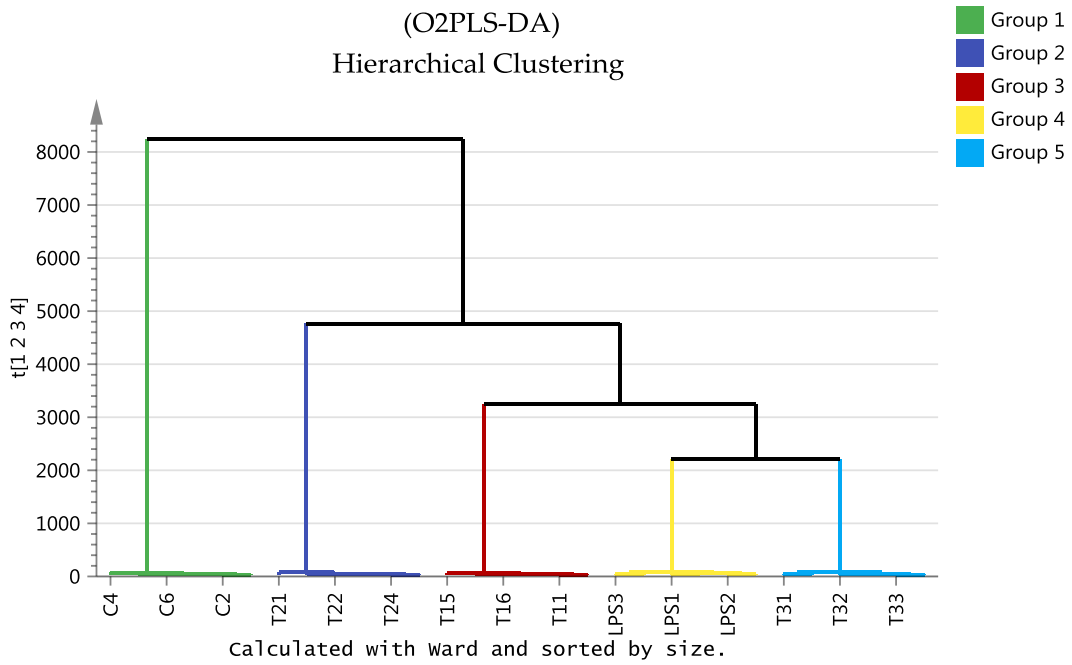

Figure S5.15: Hierarchical clustering analysis (HCA) of 30 THP-1 cells samples. The groups: T1: (Z)-11-eicosenol; T2: Eicosenoate and T3: Eicosenoic acid.

Chapter 6:

TNF-α production

Table S6.1: Effect of gypenoside compounds on the production of TNF-α cytokines in the presence and absence of LPS on PMA-differentiated THP-1 cells (*n*=3).

	TNF-α concentration (pg/ml)									
	Sample only					**Sample + LPS**				
Gyp conc.	n=1	n=2	n=3	Mean	RSD	n=1	n=2	n=3	Mean	RSD
Gyp 5	544	307	354	401.67	31.24	690.00	636.00	638.00	654.67	4.68
Gyp 25	238	185	259	227.33	16.78	685.00	636.00	634.00	651.67	4.43
Gyp 50	159	138	157	151.33	7.66	681.00	634.00	629.00	648.00	4.43
Gyp 75	228	152	254	211.33	25.08	682.00	646.00	633.00	653.67	3.88
Media	358	261	307	308.67	15.72					
LPS	723	704	696	707.67	1.96					

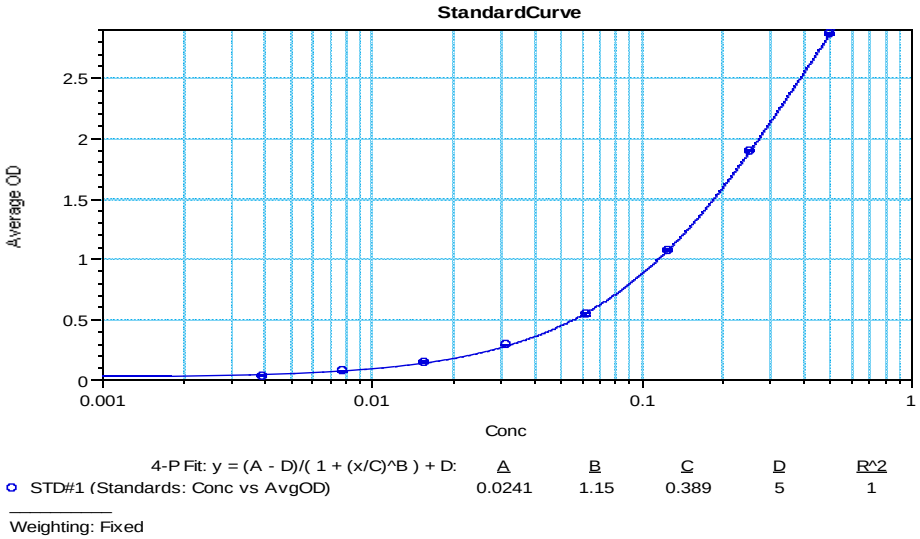

Figure S6.1: A representative 4-parameter logistic plot of TNF-α standard samples of 8 points showing the values of a, b, c, and d constants and the calibration equation with a best fit (R^2=1.0). The data represents the mean ± SD of optical density (OD) values for duplicate standard concentrations (*n*=2).

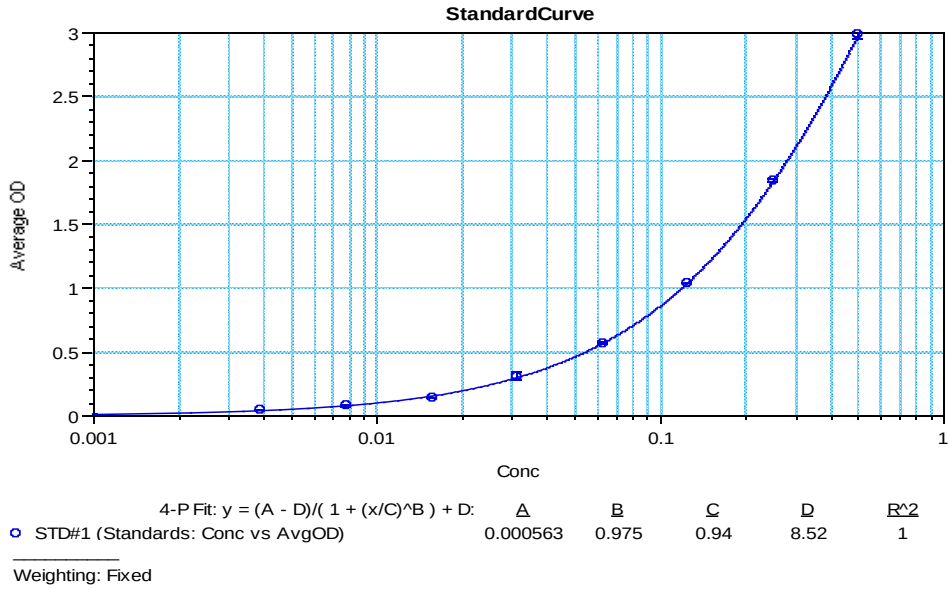

Figure S6.2: A representative 4-parameter logistic plot of TNF-α standard samples of 8 points showing the values of a, b, c, and d constants and the calibration equation with a best fit (R^2=1.0). The data represents the mean ± SD of optical density (OD) values for duplicate standard concentrations (*n*=2).

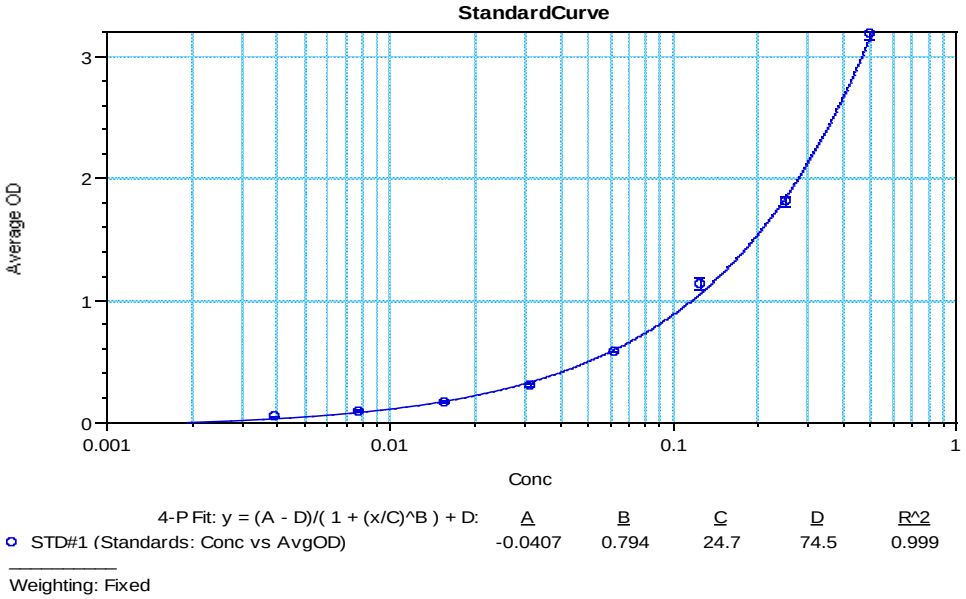

Figure S6.3: A representative 4-parameter logistic plot of TNF-α standard samples of 8 points showing the values of a, b, c, and d constants and the calibration equation with a best fit (R^2=0.999). The data represents the mean ± SD of optical density (OD) values for duplicate standard concentrations (*n*=2).

IL-1β production

Table S6.2: Effect of gypenoside compounds on the production of IL-1β cytokines in the presence and absence of LPS on PMA-differentiated THP-1 cells (*n*=3).

	IL-1β concentration (pg/ml)									
	Sample only					**Sample + LPS**				
Gyp conc.	n=1	n=2	n=3	Mean	RSD	n=1	n=2	n=3	Mean	RSD
Gyp 5	75	30	41	48.67	48.20	124	120	93	112.33	15.01
Gyp 25	46	35	53	44.67	20.31	123	110	102	111.67	9.49
Gyp 50	48	44	43	45.00	5.88	121	116	112	116.33	3.88
Gyp 75	87	74	81	80.67	8.07	122	92	102	105.33	14.50
Media	39	37	49	43.67	15.43					
LPS	124	143	142	136.33	7.84					

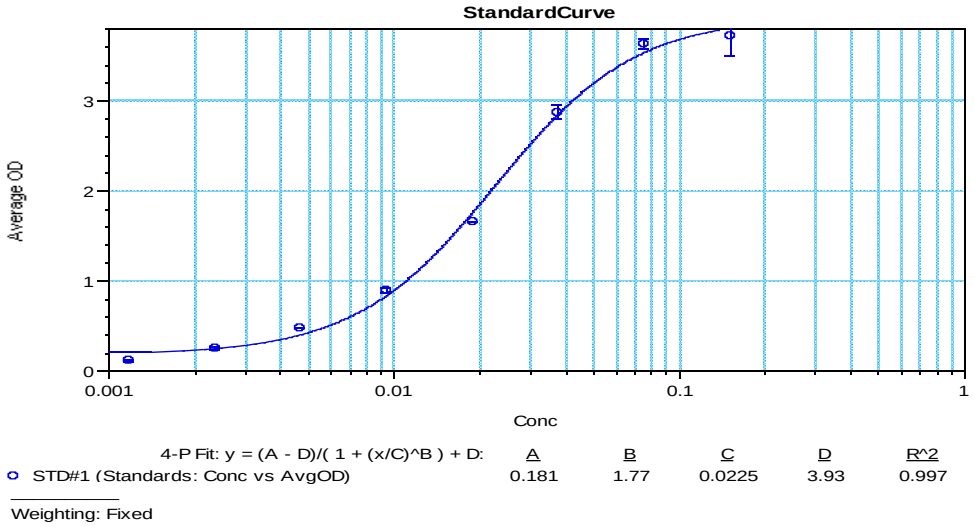

Figure S6.4: A representative 4-parameter logistic plot of IL-1β standard samples of 8 points showing the values of a, b, c, and d constants and the calibration equation with a best fit (R^2=0.997). The data represents the mean ± SD of optical density (OD) values for duplicate standard concentrations (*n*=2).

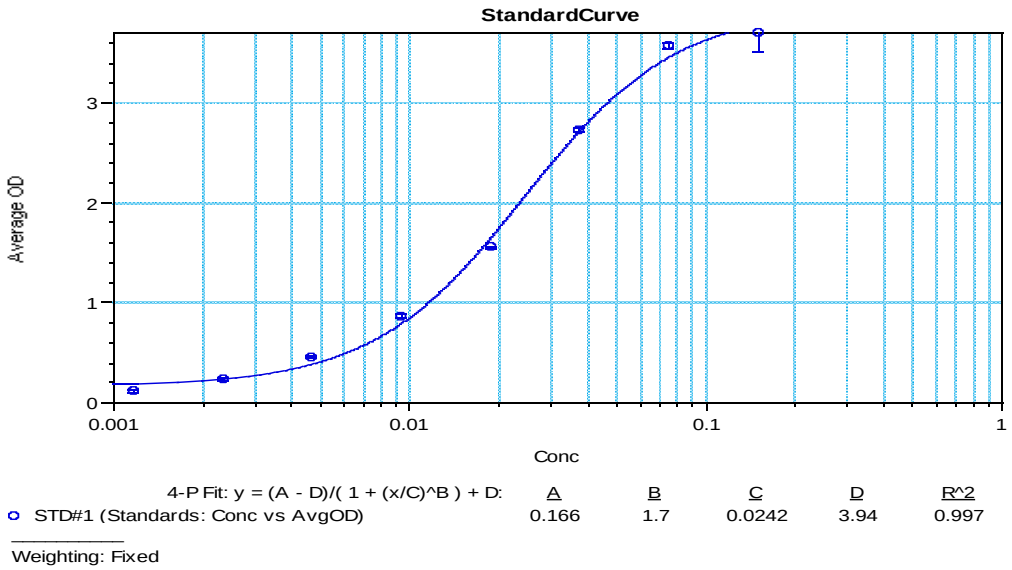

Figure S6.5: A representative 4-parameter logistic plot of IL-1β standard samples of 8 points showing the values of a, b, c, and d constants and the calibration equation with a best fit (R^2=0.997). The data represents the mean ± SD of optical density (OD) values for duplicate standard concentrations (*n*=2).

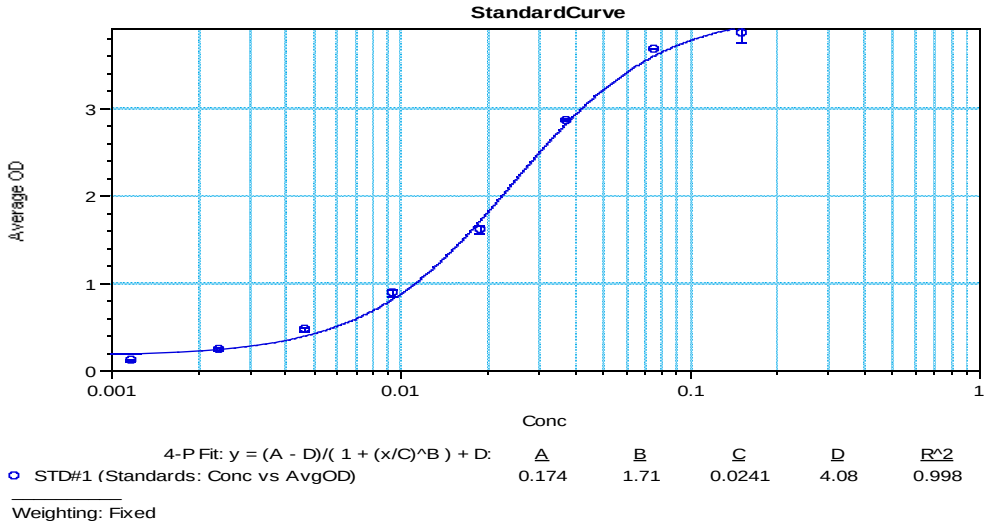

Figure S6.6: A representative 4-parameter logistic plot of IL-1β standard samples of 8 points showing the values of a, b, c, and d constants and the calibration equation with a best fit (R^2=0.998). The data represents the mean ± SD of optical density (OD) values for duplicate standard concentrations (*n*=2).

IL-6 production

Table S6.3: Effect of gypenoside compounds on the production of IL-6 cytokines in the presence and absence of LPS on PMA-differentiated THP-1 cells (*n*=3).

	IL-6 *concentration (pg/ml)*									
	Sample only					**Sample + LPS**				
Gyp conc.	n=1	n=2	n=3	Mean	RSD	n=1	n=2	n=3	Mean	RSD
Gyp 5	<2.0	<2.0	<2.0	n/a	n/a	65	77	89	77.00	15.58
Gyp 25	<2.0	<2.0	<2.0	n/a	n/a	49	45	51	48.33	6.32
Gyp 50	<2.0	<2.0	2	n/a	n/a	24	24	28	25.33	9.12
Gyp 75	2	<2.0	2	n/a	n/a	11	9	9	9.67	11.95
Media	<2.0	<2.0	<2.0	n/a	n/a					
LPS	79	84	100	87.67	12.51					

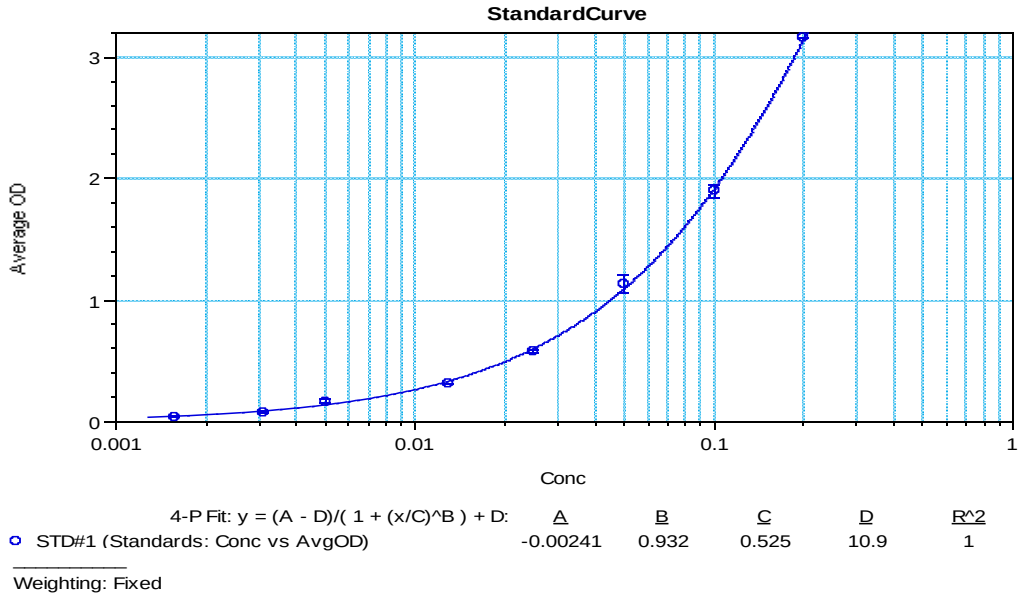

Figure S6.7: A representative 4-parameter logistic plot of IL-6 standard samples of 8 points showing the values of a, b, c, and d constants and the calibration equation with a best fit (R^2=1.0). The data represents the mean ± SD of optical density (OD) values for duplicate standard concentrations (*n*=2).

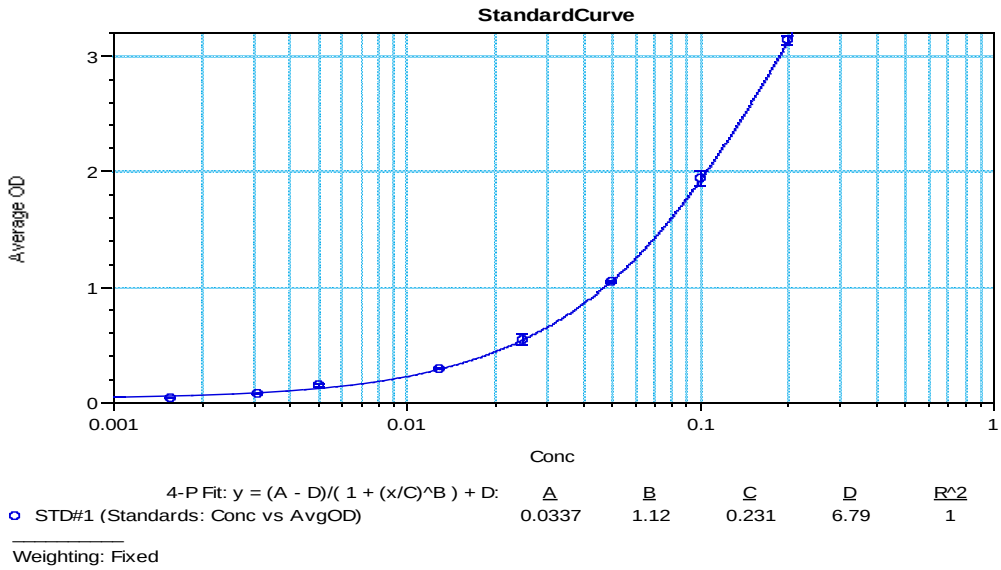

Figure S6.8: A representative 4-parameter logistic plot of IL-6 standard samples of 8 points showing the values of a, b, c, and d constants and the calibration equation with a best fit (R^2=1.0). The data represents the mean ± SD of optical density (OD) values for duplicate standard concentrations (*n*=2).

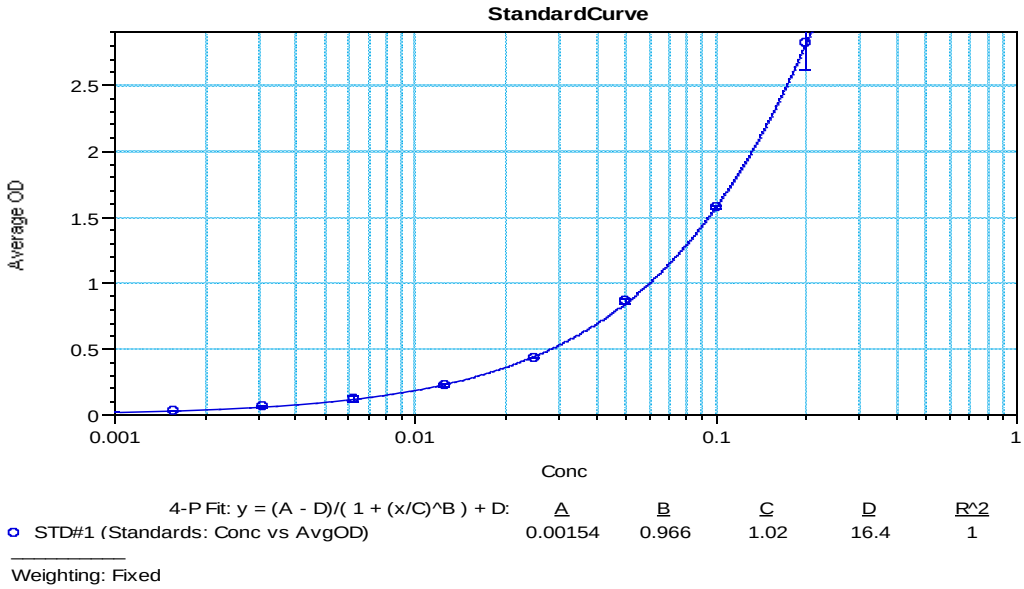

Figure S6.9: A representative 4-parameter logistic plot of IL-6 standard samples of 8 points showing the values of a, b, c, and d constants and the calibration equation with a best fit (R^2=1.0). The data represents the mean ± SD of optical density (OD) values for duplicate standard concentrations (*n*=2).

IL-10 production

Table S4: Effect of gypenoside compounds on the production of IL-10 cytokines in the presence and absence of LPS on PMA-differentiated THP-1 cells (*n*=3).

	IL-10 *concentration (pg/ml)*									
	Sample only					**Sample + LPS**				
Gyp conc.	n=1	n=2	n=3	Mean	RSD	n=1	n=2	n=3	Mean	RSD
Gyp 5	8	5	6	6.33	24.12	17	15	17	16.33	7.07
Gyp 25	4	<2.0	3	3.50	20.20	9	7	11	9.00	22.22
Gyp 50	2	<2.0	2	2.00	n/a	4	5	8	5.67	36.74
Gyp 75	6	<2.0	<2.0	n/a	n/a	3	2	2	2.33	24.74
Media	4.00	5.00	6.00	5.00	20					
LPS	16	15	17	16	6.25					

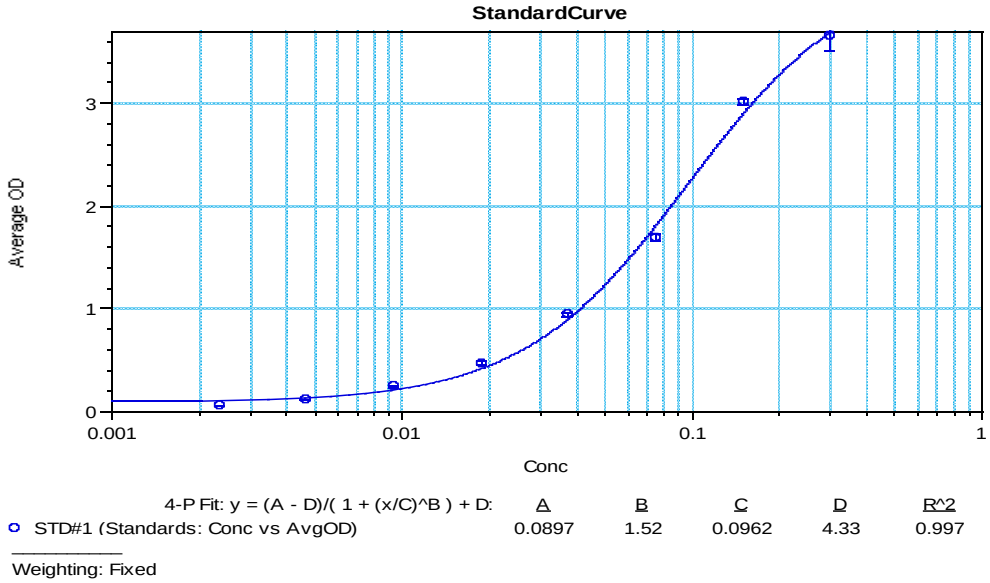

Figure S6.10: A representative 4-parameter logistic plot of IL-10 standard samples of 8 points showing the values of a, b, c, and d constants and the calibration equation with a best fit (R^2=0.997). The data represents the mean ± SD of optical density (OD) values for duplicate standard concentrations (*n*=2).

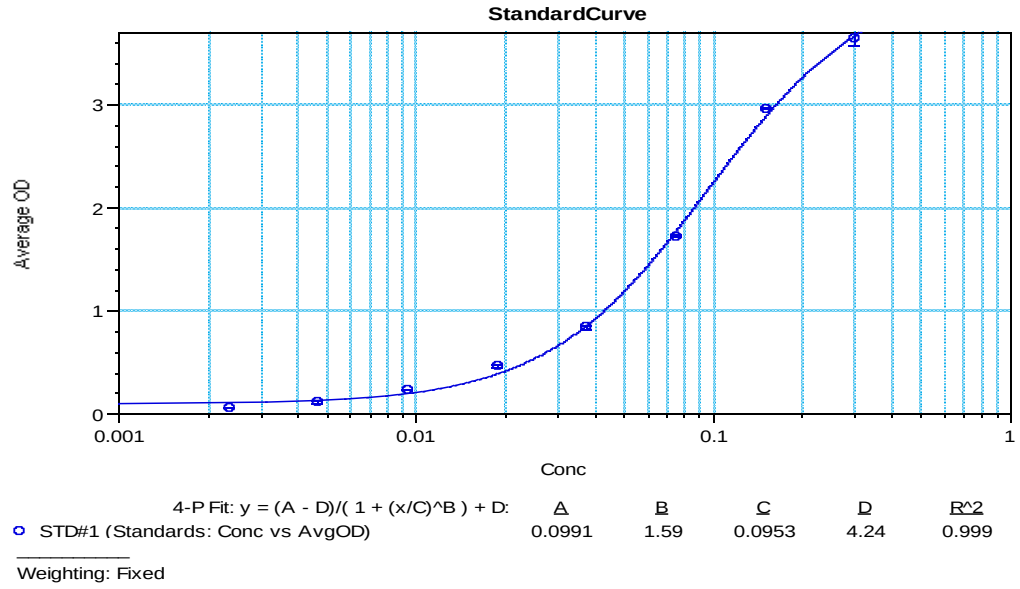

Figure S6.11: A representative 4-parameter logistic plot of IL-10 standard samples of 8 points showing the values of a, b, c, and d constants and the calibration equation with a best fit (R^2=0.999). The data represents the mean ± SD of optical density (OD) values for duplicate standard concentrations (*n*=2).

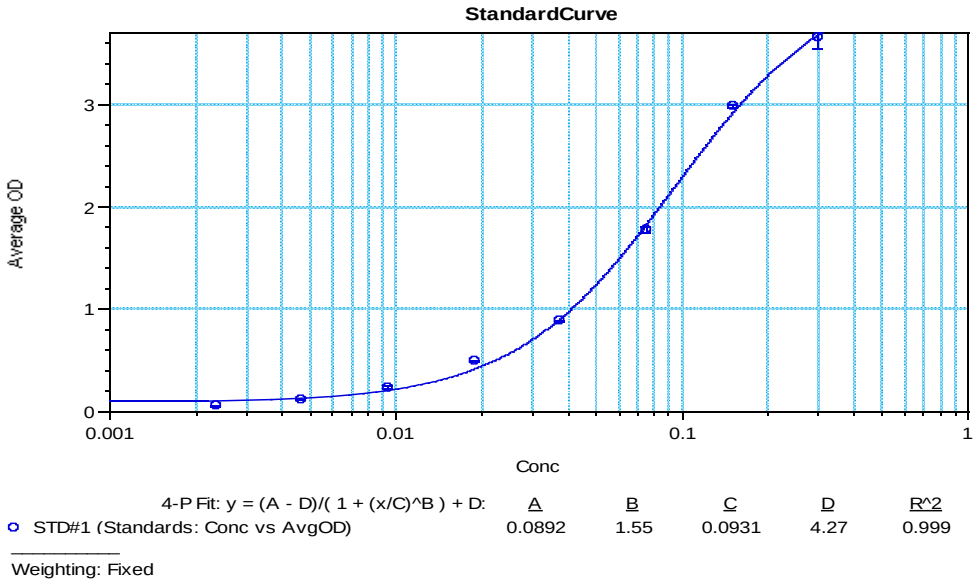

Figure S6.12: A representative 4-parameter logistic plot of IL-10 standard samples of 8 points showing the values of a, b, c, and d constants and the calibration equation with a best fit (R^2=0.999). The data represents the mean ± SD of optical density (OD) values for duplicate standard concentrations (*n*=2).

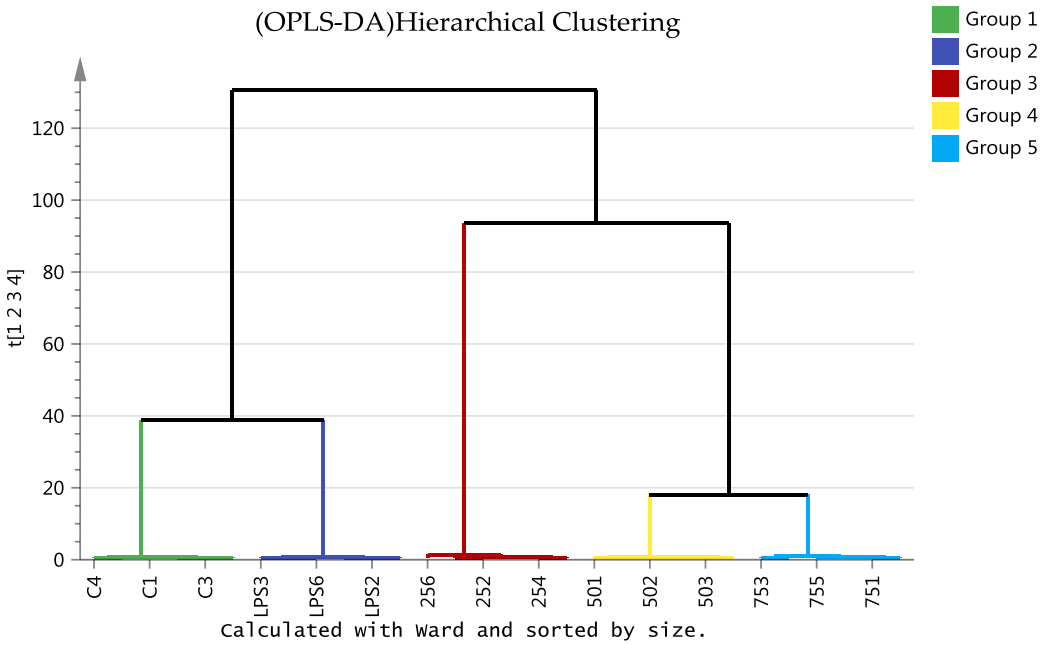

Figure S6.13: Hierarchical clustering analysis (HCA) of 30 THP-1 cells samples. The groups: 25, 50 and 75 µg/mL of Gyp at different concentrations.